Evaluation of the 1-37A Design Process for New and Rehabilitated JPCP and HMA Pavements

Final Report

The Michigan Department of Transportation
Contract & Technology Division
8885 Ricks Road
Lansing, MI 48909

By

Neeraj Buch, Ph.D. (PI) & Karim Chatti, Ph.D. (Co-PI)
Syed Waqar Haider, Ph.D., P.E., & Anshu Manik, Ph.D.

Michigan State University
Department of Civil and Environmental Engineering
3546 Engineering Building
East Lansing, MI 48824

October 2008

1. Report No. Research Report RC-1516	**2. Government Accession No.**	**3. MDOT Project Manager** Mike Eacker
4. Title and Subtitle Evaluation of the 1-37A Design Process for New and Rehabilitated JPCP and HMA Pavements		**5. Report Date** June 2008 **6. Performing Organization Code**
7. Author(s) Neeraj Buch, Karim Chatti, Syed W. Haider and Anshu Manik		**8. Performing Org. Report No.**
9. Performing Organization Name and Address Michigan State University Department of Civil and Environmental Engineering 3546 Engineering Building East Lansing, MI 48824 Tel: (517) 355-5107, Fax: (517) 432-1827		**10. Work Unit No. (TRAIS)** **11. Contract No.** **11(a). Authorization No.**
12. Sponsoring Agency Name and Address Michigan Department of Transportation Construction and Technology Division P.O. Box 30049, Lansing, MI 48909		**13. Type of Report & Period Covered** Final Report **14. Sponsoring Agency Code**
15. Supplementary Notes		

16. Abstract

Recognizing the limitations of the 1993 AASHTO design guide and the need for improvement in the pavement design process, the NCHRP project 1-37A was initiated to develop a pavement design guide for new and rehabilitated pavements based on mechanistic-empirical (M-E) approaches. Therefore, a need to evaluate the M-E PDG was realized in Michigan. This report highlights the evaluation of the current performance models for jointed plain concrete (JPC) and hot mix asphalt (HMA) concrete pavements for the state of Michigan. The results showed that effect of PCC slab thickness and edge support on performance were significant among design variables while CTE, MOR, base type and subgrade played an important role among material-related properties. Slab thickness interacts significantly with material properties—CTE and MOR, for cracking in JPCP. A lower MOR and a higher CTE combination is drastic for JPCP cracking. For faulting, the material properties—CTE and MOR interact significantly with site factors—subgrade soil type and climate. For roughness, the interactions — slab thickness by CTE and climate by subgrade soil types, play a significant role. The results for HMA pavements showed that eleven design and material variables were significant in affecting performance. These include AC layer thickness, AC mix characteristics, base, subbase and subgrade moduli, and base and subbase thickness. Binder grade was found to be the most critical parameter affecting transverse cracking. Significant interactions were found among several of the variables in affecting all the performance measures.

17. Key Words M-E PDG sensitivity, pavement analysis and design, design variables, rigid and flexible pavement performance.	**18. Distribution Statement** No restrictions. This document is available to the public through the Michigan Department of Transportation.

19. Security Classification - report Unclassified	**20. Security Classification - page** Unclassified	**21. No. of Pages**	**22. Price**

TABLE OF CONTENTS

SECTION – I: INTRODUCTION AND BACKGROUND

CHAPTER 1 - INTRODUCTION 1
1.1 BACKGROUND 1
1.2 RESEARCH OBJECTIVES 4
1.3 ORGANIZATION OF REPORT 6

CHAPTER 2 - LITERATURE REVIEW 7
2.1 EFFECT OF TRAFFIC INPUTS ON PAVEMENT PERFORMANCE 7
2.2 EFFECT OF MATERIAL CHARACTERIZATION ON PAVEMENT PERFORMANCE 8
2.3 EFFECT OF CLIMATE INPUTS ON PAVEMENT PERFORMANCE 10
2.4 EFFECT OF STRUCTURAL INPUTS ON PAVEMENT PERFORMANCE 10

SECTION – II: RIGID PAVEMENTS

CHAPTER 3 - PRELIMINARY SENSITIVITY ANALYSIS - RIGID 13
3.1 DESIGN INPUT LEVELS 13
3.2 INPUT VARIABLES IN M-E PDG AND MDOT CURRENT PRACTICE 13
3.2.1 Input Variable Ranges 18
3.2.2 Determination of Significance for Input Variables 25
3.2.3 Determination of Performance Threshold 25
3.3 PREPARATION OF INITIAL SENSITIVITY TEST MATRIX 28

CHAPTER 4 - DETAILED SENSITIVITY ANALYSIS - RIGID 38
4.1 EFFECT OF INPUT VARIABLES ON CRACKING 38
4.1.1 Descriptive Statistics 38
4.1.2 Statistical Analysis (ANOVA) 39
4.2 EFFECT OF INPUT VARIABLES ON FAULTING 47
4.2.1 Descriptive Statistics 47
4.2.2 Statistical Analysis (ANOVA) 48
4.3 EFFECT OF INPUT VARIABLES ON ROUGHNESS (IRI) 58
4.3.1 Descriptive Statistics 58
4.3.2 Statistical Analysis (ANOVA) 59
4.4 SUMMARY OF STATISTICAL ANALYSES RESULTS 66

CHAPTER 5 - SATELLITE SENSITIVITY ANALYSES - RIGID 69
5.1 SATELLITE SENSITIVITY STUDY — JOINT SPACING, CTE, AND SLAB THICKNESS 69
5.1.1 Effect of Input Variables on Cracking 71
5.1.1.1 Descriptive Statistics 71
5.1.1.2 Statistical Analysis (ANOVA) 72
5.1.2 Effect of Input Variables on Faulting 76
5.1.2.1 Descriptive Statistics 76
5.1.2.2 Statistical Analysis (ANOVA) 77
5.1.3 Effect of Input Variables on Roughness (IRI) 81
5.1.3.1 Descriptive Statistics 81

5.1.3.2 Statistical Analysis (ANOVA) 82
5.2 VERIFICATION OF M-E PDG PERFORMANCE PREDICTION IN MICHIGAN 86
5.2.1 LTPP SPS-2 Pavement Sections in Michigan 87
5.2.1.1 Traffic Inputs 88
5.2.1.2 Material Inputs— thickness, type and stiffness 88
5.2.1.3 Climate 88
5.2.1.4 Discussion of Results for SPS-2 Test Section—Predicted versus Observed 90
5.2.2 MDOT Rigid Pavement Sections 94
5.2.2.1 Traffic Inputs 94
5.2.2.2 Material Inputs 94
5.2.2.3 Climate 94
5.2.2.4 Discussion of Results for MDOT Sections—Predicted versus Observed Performance 98
5.3 SATELLITE SENSITIVITY ANALYSIS FOR TRAFFIC 100
5.3.1 MDOT Traffic Data Analysis Using TrafLoad Software 100
5.3.1.1 Traffic Volume Adjustment Factors 101
5.3.1.2 Axle Distribution Factors 109
5.3.1.3 General Traffic Inputs 110
5.3.2 Effect of Traffic Levels of Rigid Pavement Performance 114
5.4 NEEDS FOR LOCAL CALIBRATION OF PERFORMANCE MODELS 116

CHAPTER 6 - PAVEMENT DESIGN IMPLICATIONS - RIGID 119
6.1 QUANTIFYING EFFECT OF SIGNIFICANT VARIABLES ON RIGID PAVEMENT PERFORMANCE 119
6.1.1 Background 120
6.1.2 Simplified Regression Models — M-E PDG Performance Prediction 122
6.1.2.1 Transverse Cracking Model 123
6.1.2.2 Transverse Joint Faulting Model 129
6.1.2.3 Smoothness Model 136
6.1.2.4 Spalling Model 141
6.2 EFFECT OF TRAFFIC CHARACTERIZATION (ESALS VERSUS LOAD SPECTRA) ON RIGID PAVEMENT PERFORMANCE 143
6.2.1 Background 144
6.2.2 Problem Statement 150
6.2.3 Equivalent Axle Load Spectra 151
6.2.3.1 Axle Load Spectra with Equivalent ESALs 153
6.2.3.2 Equivalent ESALs for Different Axle Load Spectra 154
6.2.4 Performance Prediction using M-E PDG 155
6.2.4.1 Axle Load Spectra with Equivalent ESALs 155
6.2.4.2 Different Axle Load Spectra 157
6.2.5 Conclusions 159

CHAPTER 7 - CONCLUSIONS - RIGID 160
7.1 sensitivity analyses 160
7.1.1 Preliminary Sensitivity 160
7.1.2 Detail Sensitivity 161
7.1.2.1 Slab Cracking 161
7.1.2.2 Joint Faulting 162
7.1.2.3 Roughness (IRI) 164
7.2 SATELLITE SENSITIVITY ANALYSES 165

7.2.1 Effects of Joint Spacing, CTE and Slab Thickness on Pavement Performance 165
7.2.1.1 Slab Cracking..... 165
7.2.1.2 Joint Faulting 165
7.2.1.3 Roughness (IRI) 166
7.2.2 Preliminary Verification of M-E PDG Performance Prediction for Michigan.....166
7.2.3 Effect of Traffic on Pavement Performance.....167
7.3 PAVEMENT DESIGN IMPLICATIONS.....167
7.3.1 Quantification of Significant Variables Effects on Pavement Performance 167
7.3.2 Effects of Traffic Characterization on Pavement Performance 167
7.4 RECOMMENDATIONS.....167

SECTION – III: FLEXIBLE PAVEMENTS

CHAPTER 8 - PRELIMINARY SENSITIVITY ANALYSIS 168
8.1 INTRODUCTION 168
8.2 PREPARATION OF INITIAL SENSITIVITY MATRIX 168
8.3 INPUT VARIABLE RANGES FOR ROBUSTNESS.....176
8.4 IDENTIFICATION OF VARIABLES SIGNIFICANCE 180
8.5 CONCLUSION 190

CHAPTER 9 - DETAILED SENSITIVITY ANALYSES - FLEXIBLE.....191
9.1 INTRODUCTION 191
9.2 DEVELOPMENT OF SENSITIVITY MATRIX.....191
9.3 EFFECT OF INPUT VARIABLES ON FATIGUE CRACKING 193
9.3.1 Main Effects 194
9.3.2 Interaction Effects 197
9.4 EFFECT OF INPUT VARIABLES ON LONGITUDINAL CRACKING 200
9.4.1 Main Effects 200
9.4.2 Interaction Effects 201
9.5 EFFECT OF INPUT VARIABLES ON TRANSVERSE CRACKING 205
9.5.1 Main Effects 205
9.5.2 Interaction Effects 208
9.6 EFFECT OF INPUT VARIABLES ON RUTTING.....210
9.6.1 Main Effects 210
9.6.2 Interaction Effects 213
9.7 EFFECT OF INPUT VARIABLES ON IRI 214
9.7.1 Main Effects 214
9.7.2 Interaction Effects 218
9.8 CONCLUSION 220

CHAPTER 10 - THE SATELLITE STUDIES - FLEXIBLE 221
10.1 INTRODUCTION 221
10.2 THE THERMAL CRACKING MODEL 222
10.3 THERMAL CRACKING ANALYSIS 224
10.3.1 Asphalt Mixtures Selected for Thermal Cracking Analysis 224
10.3.2 Inputs for Analysis Runs 227
10.3.3 Thermal Cracking Analysis Results 228
10.4 COMPLEX MODULUS SATELLITE STUDY 231
10.4.1 The Projects and Their Performance 231

10.4.2 Effect of Asphalt Concrete Layer Modulus....234
10.5 VERIFICATION OF M-E PDG PERFORMANCE PREDICTION IN MICHIGAN....237
10.5.1 LTPP SPS-1 Pavement Sections in Michigan....238
10.5.2 MDOT Flexible Pavement Sections....248

CHAPTER 11 - FLEXIBLE PAVEMENT DESIGN IMPLICATIONS - FLEXIBLE....257
11.1 INTRODUCTION....257
11.2 ANALYZING PAVEMENT DESIGNS....257
11.2.1 Pavement Design Analysis Strategy....257
11.2.2 Pavement Design Analysis Examples....258
11.2.3 Results from Pavement Design Analysis....264
11.3 DESIGN BASED ON PERFORMANCE....267
11.3.1 Strategy for Design Based on Performance....267
11.3.2 Examples of Design Based on Performance....267
11.3.3 Advantages of Interpolation Method Used....271
11.4 CONCLUSION....273

CHAPTER 12 - CONCLUSIONS - FLEXIBLE....274
12.1 SENSITIVITY ANALYSES....274
12.1.1 Preliminary Sensitivity....274
12.1.2 Detail Sensitivity....275
12.2 SATELLITE STUDIES....278
12.2.1 Thermal Cracking Analysis....279
12.2.2 Complex Modulus Satellite Study....279
12.2.3 Verification (Preliminary) of M-E PDG Performance Prediction for Michigan....280
12.3 PAVEMENT DESIGN IMPLICATIONS....281
12.4 RECOMMENDATIONS....281

SECTION – IV: RECOMMENDATIONS

CHAPTER 13 - RECOMMENDATIONS....282
13.1 THE 1993 AASHTO GUIDE VERSUS THE M-E PDG DESIGN PROCESS....282
13.2 NEED FOR ADOPTING THE M-E PDG DESIGN PROCESS....283
13.3 ADOPTION of THE M-E PDG IN MICHIGAN....283
8.3.1 Short-term Plan....283
8.3.2 Long-term Plan....284
13.4 RECOMMENDATIONS FOR THE FUTURE RESEARCH....285

REFERENCES

APPENDIX A – RIGID PAVEMENTS
APPENDIX B – FLEXIBLE PAVEMENTS

EXECUTIVE SUMMARY

Recognizing the limitations of the 1993 AASHTO design guide and the need for improvement in the pavement design process, the NCHRP project 1-37A was initiated to develop a pavement design guide for new and rehabilitated pavements based on mechanistic-empirical (M-E) approaches. The initial step in adopting the new Mechanistic-Empirical Pavement Design Guide (M-E PDG) by state highway agencies (SHAs) requires a comprehensive evaluation of the M-E PDG for both rigid and flexible pavements. The findings from such evaluation will determine the impact of the various inputs (material, traffic, construction and climatic) on pavement performance prediction. Identifying the list of input variables that have a significant impact on pavement performance will assist in determining the amount of "new" data collection that state highway agencies (SHAs) will have to engage in. Guidance with respect to practical ranges of significant inputs will demonstrate to pavement engineers the viability and robustness of the performance models. Therefore, a need to evaluate the M-E PDG was realized by Michigan Department of Transportation (MDOT) and a study was conducted at Michigan State University (MSU). The objectives of this study were to: (a) evaluate the M-E PDG rigid pavement design procedure for Michigan conditions; (b) verify the relationship between predicted and observed pavement performance for selected pavement sections in Michigan, and; (c) discuss the needs for calibration of performance models. The accomplishment of these objectives will pave the way in the prospective adoption and implementation of this new pavement design procedure in Michigan.

The adoption and implementation of the M-E PDG by various SHAs requires validation and calibration of its performance models. However, to facilitate the use of the guide, sensitivity analyses are warranted as a preliminary step. Such an analysis will identify significant input variables required for the design process. The results from the sensitivity analysis will also highlight the needs for resources required to quantify the input variables. Subsequently, the calibration of performance models will assist the SHAs to customize the design process to reflect local practices. This report highlights the evaluation of the current performance models for jointed plain concrete (JPC) and hot mix asphalt (HMA) concrete pavements for the state of Michigan. The sensitivity analyses involved: (a) preliminary sensitivity—one variable at a time, (b) detailed analysis—full factorial. Both analyses reflect the local design and construction practices in Michigan. The purpose of the preliminary sensitivity investigation was to prepare a short-list of significant variables. The abbreviated variables were further refined based on engineering judgment and local practices while levels of the significant variables were selected based on the local design practices. In the detailed analysis, the full factorial multivariate analyses were conducted to highlight both main and interaction effects between input variables on rigid pavement performance. Finally, it is highlighted that the interactions among input variables play an important role while interpreting the pavement performance from the design perspective.

The predicted and observed pavement performances on a sample of JPC and HMA sections in Michigan were compared to verify the applicability of national calibrated performance models. As a result of this comparison, the needs for local calibration of performance models are highlighted. The verification of current performance models, in M-E PDG, for the selected

pavements in Michigan warranted a need for local calibration. The local calibration of the performance models should reflect the local materials and construction practices to encompass the particular pavement performance in Michigan.

The results showed that effect of PCC slab thickness and edge support on performance were significant among design variables while CTE, MOR, base type and subgrade played an important role among material-related properties. In addition, to effectively capture the interaction effects between variables a full factorial experiment was designed and analyzed. Statistical analyses results identified significant main and interactions effects of input variables. It was found that slab thickness interacts significantly with material properties—CTE and MOR, for cracking in JPCP. From the design perspective, increasing slab thickness for a higher CTE or a higher MOR may not help in achieving better cracking performance. On the other hand, increasing slab thickness for a lower CTE and a lower MOR may improve cracking performance. A lower MOR and a higher CTE combination is drastic for JPCP cracking. For faulting, the material properties—CTE and MOR interact significantly with site factors—subgrade soil type and climate. For roughness, the interactions — slab thickness by CTE and climate by subgrade soil types, play a significant role.

In order to determine the effects of traffic levels on various rigid pavement performance measures, the M-E PDG software was used to analyze selected Michigan sites (observed traffic characteristics). All other variables were kept constant in this analysis except traffic. Therefore, the effects on performance are mainly due to traffic-related inputs. The results show that traffic levels (low, medium and high) significantly affect the rigid pavement performance. Also within a traffic level, due to variations in truck volumes and loadings, the predicted performance can vary considerably. This implies that the default traffic values (respective truck traffic classification, TTC) in M-E PDG may not be representative for the actual traffic of a particular site. Therefore, traffic data plays a key role in the new design process using M-E PDG.

Since performance prediction process in M-E PDG is very complex due to a large number of variables. The simplified M-E PDG regression models involving only a few important design variables were developed. Four important design and material-related variables (slab thickness, joint spacing, flexural strength, and coefficient of thermal expansion) affecting rigid pavement performance in the M-E PDG design process were selected in the regression model development. While these models are limited in scope, they can facilitate in the preliminary design process especially with regards to economic decisions for selecting appropriate materials and slab thickness. The simplified models can also help in quantifying the effects of several significant design variables.

The use of two types of load characterizations (equivalent axle load versus axle load spectra) in mechanistic analysis and design procedures were evaluated. The results showed that the concept of equivalent axle load spectra can be used in mechanistic procedures to achieve similar performance prediction as achieved by using an axle load spectra. The equivalent axle load spectra for each axle configuration can be developed by using site-specific loadings. The number of repetitions (ADTT) can be adjusted to achieve desired level of ESALs during the design life. However, it is important to determine the design ESALs from a site-specific axle load spectra. On the other hand, assuming axle load spectra which are not site-specific and achieving desired

level of ESALs by changing number of repetitions may not give reliable estimates of expected pavement performance as compared to site-specific axle load spectra.

The results for HMA pavements showed that eleven design and material variables were significant in affecting performance. These include AC layer thickness, AC mix characteristics, base, subbase and subgrade moduli, and base and subbase thickness. Binder grade was found to be the most critical parameter affecting transverse cracking. Also, it was found that 20% reduction in AC complex modulus could lead to a 4-fold increase in fatigue cracking. Significant interactions were found among several of the variables in affecting all the performance measures.

It was also demonstrated that M-E PDG can be used efficiently as a pavement analysis and design tool by using n-dimensional response surfaces. Once the response surfaces are developed for the desired variables the analysis and design can be significantly simplified and the computational time is reduced to practically zero. Development of the original response surfaces and interpolated response surfaces and extracting distresses for design and analysis cases was done though a set of programs written in MATLAB.

The verification of current performance models, in M-E PDG, for the selected pavements in Michigan warranted a need for local calibration. The local calibration of the performance models should reflect the local materials and construction practices to encompass the particular pavement performance in Michigan.

CHAPTER 1 - INTRODUCTION

1.1 BACKGROUND

In the late 1950s, the AASHO road test was constructed in Ottawa, Illinois for the primary purpose of developing a fair tax scheme for different vehicle types based on fuel consumption. Its use later evolved to serve as the basis for the AASHTO design guides. The design data from the test sections and their performance histories were used as the foundation of developing the 1972 AASHTO design guide, which was later refined to develop the 1986 and the 1993 AASHTO Guide for the design of pavement structures. These design guides are adopted by the majority of State DOT's in addition to other countries. Today, the 1993 AASHTO Design Guide for Pavement Structures is the most widely used design guide in the United States and around the world. It is estimated that 26 State DOT's are currently using the 1993 Guide (*1*).

The design equations that are incorporated in the current 1993 design guide have evolved over time. These equations are empirical in nature, strictly built using statistical regression models, performance observations rather than using fundamental material properties and/or constitutive engineering relationships (*1*). The original conditions of the AASHO road test are represented by the single climatic condition and single subgrade type of Ottawa city, the local Illinois materials and specifications that were used to construct the test sections, the mixture design procedures of the 1950s, and the typical traffic inputs of the 1950s' (number of traffic applications, traffic loading, axle configurations and tire pressure). Nowadays, pavement engineers design roads that would be constructed over different subgrade conditions, using new mixture design procedures, and a range of materials specifications. Additionally, those pavements are expected to perform under a spectrum of traffic levels and conditions, in addition to a diverse variety of climatic conditions. These conditions depart significantly from those that prevailed at the AASHO road test. Recognizing the limitation of the 1993 AASHTO design guide and the need for improvement in the pavement design process, the NCHRP project 1-37A was initiated to develop a new pavement design guide for new and rehabilitated pavements based on mechanistic-empirical (M-E) approaches that incorporate specific conditions prevalent at the road site and relate to the fundamental material properties to be used in construction.

There are apprehensions on the part of State Highway Agencies (SHAs) towards the adoption of the new M-E PDG because of the (a) complex nature of the design software (numerous inputs and hierarchical nature of the inputs); (b) perceived need to collect more data (laboratory and/or field); (c) possible necessary redesign of the pavement management system to accommodate data germane to the design guide; (d) need to calibrate the performance equations to local conditions; (e) need to employ or train pavement professionals at the district or region level; (f) shrinking manpower and funds; and (g) lack of evidence that adoption of the M-E PDG would improve design procedures over existing practices.

The terms empirical, mechanistic, and mechanistic-empirical designs are frequently used to identify general approaches for pavement design. An empirical design approach is based exclusively on the results of experiments (empirical evidence). Observations are used to establish

associations between the inputs and the outcomes of the process—pavement design inputs and expected performance in terms of various distresses. Generally, these relationships do not have a firm scientific basis, but are often used as surrogate measures to define theoretically the precise cause-and-effect relationships of a phenomenon (*2*). The primary disadvantage of the empirical approach is the limited validity of the relationships to the conditions other than observed in the data used to develop those relationships. Consequently, new materials, construction procedures, and changed traffic characteristics cannot be readily incorporated into empirical design procedures.

On the other hand, the mechanistic design approach represents the other end of the gamut. The mechanistic design approach is based on the theories of mechanics to relate pavement structural behavior and performance to traffic loading and environmental changes. A key element of the mechanistic design approach is the determination of the response of the pavement materials and thus of the pavement system. The elasticity-based solutions by Boussinesq, Burmister, and Westergaard were important first steps toward a theoretical description of the pavement response under load (*2*). However, the linearly elastic material behavior assumption adopted for these solutions is incompatible with the nonlinear and inelastic material behaviors. In order to capture this material response, more complicated material models and analytical tools are needed. Some progress has been made in recent years on isolated pieces of the mechanistic performance prediction problem. Nonetheless, in reality a fully mechanistic design approach for practical pavement design does not yet exist. Typically, some empirical information and relationships are still required to relate theory to the real world of pavement performance.

The combination of theory with empirical evidence is the definition of the mechanistic-empirical approach to pavement design. The mechanistic constituent deals with theoretical determination of pavement responses such as stresses, strains, and deflections due to loading and environmental effects. The calculated responses at critical locations in pavement system are then related to the performance of the pavement via empirical distress models. For example, a linearly elastic mechanics model can be used to compute the tensile strains at the bottom of the asphalt layer due to an applied load; this strain is then related empirically to the accumulation of fatigue cracking distress. In other words, an empirical relationship links the mechanistic response of the pavement to an observed distress.

The various versions of the AASHTO Design Guide (1972, 1986, and 1993) have served well for several decades. However, as mentioned above, the low traffic volumes, antiquated vehicle characteristics, short test duration, limited material types and climate conditions, and other deficiencies of the original AASHO road test limits the continued use of the AASHTO Design Guide. These perceived deficiencies of the empirical design approach were the motivation for the development of the mechanistic-empirical methodology in NCHRP 1-37A (M-E PDG). In this new analysis and design approach structural responses such as stresses, strains, and deflections are mechanistically calculated using multilayer elastic theory or finite element methods based on material properties, environmental conditions, and loading characteristics. Thermal and moisture distributions are also mechanistically determined using the Enhanced Integrated Climate Model (EICM). These computed pavement layer responses are used as inputs in empirical models to individually predict permanent deformation, fatigue cracking (bottom-up and top-down), thermal

cracking, and roughness. The performance models were calibrated using data from the LTPP database for conditions representative of the entire United States.

The interaction between geometrics, material properties, traffic, and environmental conditions in the NCHRP 1-37A approach is more pronounced than in the AASHTO Guide. As illustrated in Figure 1.1, layer thicknesses are obtained through an iterative process in which predicted performance is compared against the design criteria for the multiple predicted distresses until all design criteria are satisfied to the specified reliability level (*2*).

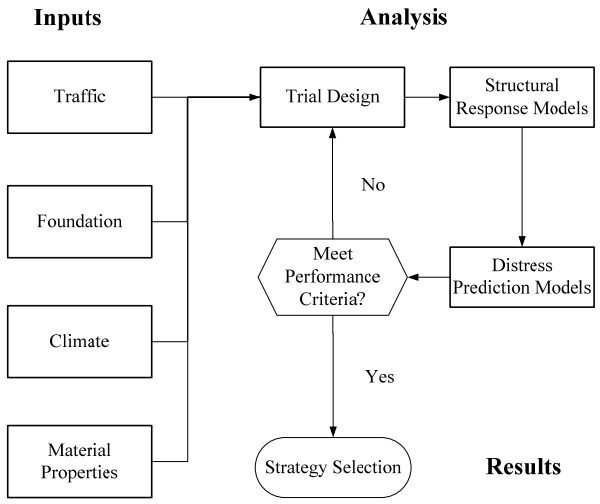

Figure 1.1 Flow chart for M-E PDG design process

In addition to conceptual differences between empirical and mechanistic-empirical design approaches, there are several important operational differences between 1993 AASHTO and M-E PDG procedures. The most important differences include (*2*):

- The 1993 AASHTO Guide designs pavements to a single performance criterion, PSI, while the M-E PDG approach simultaneously considers multiple performance criteria (e.g., rutting, cracking, and roughness for flexible pavements). Appropriate design limits must be specified for each performance measure.
- Many more variables are required in the M-E PDG procedure, especially environmental and material properties. It also employs a hierarchical concept in which one may choose different input quality levels, depending upon the level of information, resources available, and the importance of the project.
- The 1993 AASHTO guide was developed based on limited field test data from only one location (Ottawa, IL). Seasonal adjustment of subgrade resilient modulus and selection of appropriate layer drainage coefficients are the only ways for incorporating environmental influences on pavement deterioration. The M-E PDG procedure utilizes a set of project-specific climate data (i.e., air temperature, precipitation, wind speed, relative humidity, etc.) and the Enhanced Integrated Climate Model (EICM) to determining the material properties for different environmental condition throughout the year (i.e., temperature-adjusted asphalt concrete dynamic modulus and moisture-adjusted resilient modulus of unbound materials).

- The 1993 AASHTO guide uses the concept of equivalent single axle load (ESAL) to define traffic levels, while the M-E PDG approach uses traffic in terms of axle load spectra.

All of these differences between the design procedures make a direct comparison more intricate. Most of the evaluations of the M-E PDG procedure to date have focused on sensitivity studies and tests of "engineering reasonableness." However, direct comparisons are essential to gain confidence in the newer mechanistic-empirical approach as a potential replacement for the existing empirical procedure. At the very least, the mechanistic-empirical approach should give designs and/or predicted performance that are broadly better or similar to those from the 1993 AASHTO Guide for "standard" types of design scenarios.

A comprehensive evaluation of the 1-37A performance models for new design of jointed plain concrete (JPCP) and flexible (HMA) pavements is warranted prior to the universal adoption of the new Mechanistic-Empirical Pavement Design Guide (M-E PDG). The findings from this evaluation will lead to the determination of (a) practical ranges for inputs over which the performance models are mathematically viable and reasonable, and (b) the impact of the various inputs (material, traffic, construction and climatic) on the magnitude of the performance measures (fatigue, transverse and longitudinal cracking, rutting, spalling, faulting and roughness).

Such research will help in reducing some of the uncertainties associated with the M-E PDG. An extensive test of the software will add evidence on the viability and correctness of the software. Identifying the list of input variables that have a significant (versus those that do not) impact on performance will assist in determining the amount of "new" data collection that the Michigan Department of Transportation (MDOT) will have to engage in. Guidance with respect to practical ranges of significant inputs will demonstrate to MDOT pavement engineers the viability and robustness of the performance models. In addition, the study will identify the needs and resources required in the existing MDOT practices for adoption of the new design procedure.

1.2 RESEARCH OBJECTIVES

The overall goal of this study is to evaluate the NCHRP 1-37A flexible and rigid pavement performance models as they relate to the set of MDOT design inputs proposed for use in the Mechanistic-Empirical (M-E) Design Guide for New and Rehabilitated Pavements. The scope of work for this project includes:

- Documenting the relevant literature and necessary software to evaluate the NCHRP 1-37A flexible and rigid pavement performance models and their application to the new M-E Design Guide.
- Determining the mathematical viability of the models and sensitivity of independent variables, in terms of a given model's ability to estimate in-service pavement damage and performance.
- Developing a viable plan to study the impact of typical MDOT input parameters on HMA and JPCP performance measures.

- Determining the ranges of input parameters over which performance prediction is realistic.
- Developing a technology transfer package and demonstrate the viability of various performance models using typical MDOT inputs.

Figure 1.2 shows a general flow chart for the execution of this research.

1.3 ORGANIZATION OF REPORT

The report is divided into three sections. Section I covers introduction and literature review in Chapter 1 and Chapter 2, respectively.

Section II entails the analyses and results for rigid pavements. It contains five chapters. Chapter 3 presents the methodology adopted for evaluation of M-E PDG and results of preliminary sensitivity. Chapter 4 contains analyses and results of detailed sensitivity. Chapter 5 includes satellite studies on (a) CTE, slab thickness and joint spacing, (b) Effect of traffic inputs on rigid pavement performance, and (c) verification of the M-E PDG in Michigan. Chapter 6 covers design implications using regression analyses and different traffic characterizations in M-E PDG. Finally, Chapter 7 includes summary of findings and conclusions regarding rigid pavements from this study.

Section III includes the analyses and results for flexible pavements. It contains five chapters. Chapter 8 presents the results of preliminary sensitivity. Chapter 9 contains analyses and results of detailed sensitivity. Chapter 10 includes satellite studies on (a) Thermal cracking inputs, (b) Effect of E* on flexible pavement performance, and (c) verification of the M-E PDG in Michigan. Chapter 11 covers design implications using response surfaces and interpolation techniques. Strategies have been described for analyses and design of flexible pavements. Finally, Chapter 12 includes summary of findings and conclusions regarding flexible pavements from this study.

Section IV contains the recommendations identifying the needs and the potential benefits of implementing the M-E PDG in Michigan. A systematic approach for the implementation of the M-E PDG along with the required resources to accomplish a successful adoption is also discussed.

There are two appendices with this report. Appendix A includes results from the analyses of rigid pavements while Appendix B contains the same for flexible pavements.
.

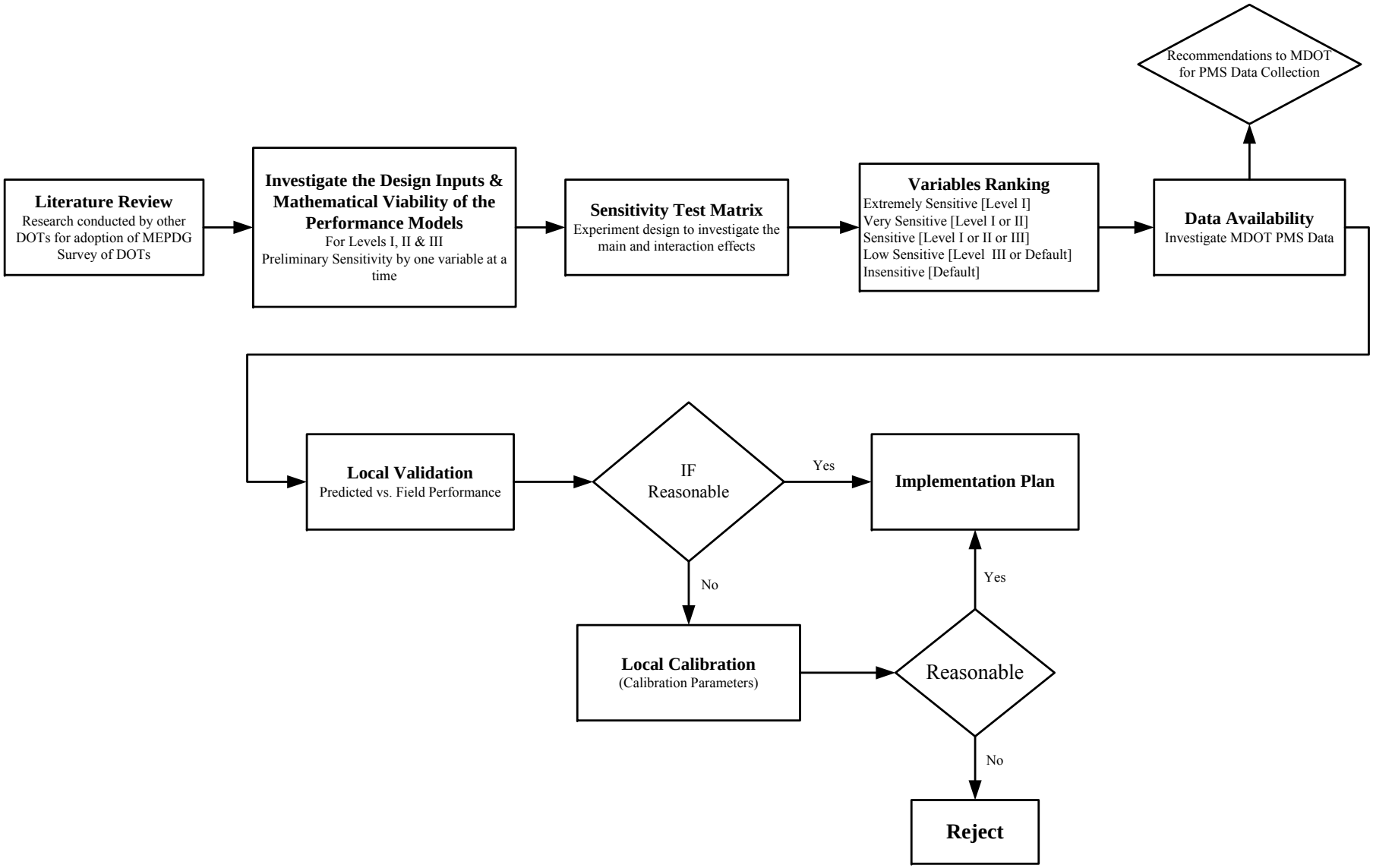

Figure 1.2 Research approach

CHAPTER 2 - LITERATURE REVIEW

The M-E PDG Software was made public in mid 2004. Since that time many SHAs are working to explore various aspects of this new design and analysis procedure (*3-8*). This ongoing research effort generally involves: input variable sensitivity to determine the most important inputs, local calibration of performance models and implementation issues. The following sections will summarize some of the recent efforts by various SHAs.

2.1 EFFECT OF TRAFFIC INPUTS ON PAVEMENT PERFORMANCE

Indiana DOT conducted a study for implementation initiatives of the Mechanistic-Empirical Pavement Design Guides (*9*). The conclusion of this study indicate that in the traffic load spectra, the default values in Level 3 design input are too general to achieve design accuracy. The existing empirical design method may give a better result since many state agencies already have databases about performance of pavement in ESALs that are comparable to that of Level 3 traffic load.

The study emphasized that loads and load distribution are very important in both flexible and rigid pavement performance. Therefore, strength parameters on both types of pavement are very sensitive to the design accuracy. At least a traffic design input Level 2 has to be implemented in the State Route and higher road classifications. The same study also indicates that the relationship between AADTT and the amount of distress is linear for all distresses, where increase in traffic leads to a direct increase in the distresses (*3*). In addition, thermal cracking is independent of traffic level. They also found that the effect of Level 1 data compared to the default values (Level 3) yields less than 0.03% difference in fatigue damage after 20 years.

Another study in Arkansas (*10*) concluded that the state-specific class distribution factors have a significant effect on predicted pavement performance, compared to predictions generated using default distribution values. However, the effect of using state-specific monthly and hourly distribution factors on predicted pavement performance, compared to using default values, was not significant. Therefore, it was recommended that the state-specific class distribution factors be used with the default monthly and hourly distribution factors in the M-E PDG. In addition, it was recommended to periodically review and update statewide class distribution factors as necessary. A sensitivity analysis related to the axle load spectra (*11*) showed a significant difference in predicted pavement performance resulting from the statewide and M-E PDG default axle load spectra. Therefore, the state-specific axle load spectra were recommended for implementation of the M-E PDG in Arkansas and updated periodically unless no significant changes are observed in the future.

2.2 EFFECT OF MATERIAL CHARACTERIZATION ON PAVEMENT PERFORMANCE

The Indiana study indicated that in the hot mix asphalt pavement, longitudinal cracking model is very sensitive to the HMA layer thickness, air voids (AV), and asphalt binder type (*9*). Also, the thermal cracking model in the HMA design module is very sensitive to mixture creep compliance, indirect tensile strength, and coefficient of thermal contraction parameters. Since these parameters are in the hierarchical design input modules, moving from Level 3 to Level 1 makes very significant differences in terms of design accuracy.

The as-constructed AV effect has a significant impact on pavement performance. All types of distresses increased with increased AV content, with the most impact seen in longitudinal cracking. Selection of the appropriate binder grade significantly reduces the rutting and cracking potential in HMA pavements constructed in hot and cold regions respectively. Additionally, accurate characterization of the aged asphalt binder results in significant performance changes. It is evident that thermal cracking is mixture and binder related. Mixture properties (dynamic modulus, creep compliance, and indirect tensile strength) and binder properties (shear modulus and phase angle, aging characteristics) significantly impact the thermal cracking potential of the HMA. The selection of the appropriate low temperature binder grade is critical in minimizing the thermal cracking especially in cold regions (*3*).

The unbound material design input module depends on “completeness” of soil testing data to determine the hierarchical design input levels. For an agency that has already adopted resilient modulus testing, the more complete testing parameters, in terms of frequency of testing during the season, the higher the design accuracy that can be achieved by moving to higher design input levels. Therefore, moving from design input Level 3 to Level 1 will have significant differences in terms of design accuracy (*9*).

Softer subgrade negatively impacts both rutting and fatigue distresses of HMA pavements. This can be attributed to the high compressive stresses generated on the top of the subgrade and higher tensile strain generated at the bottom of the HMA layer, respectively (*3*).

A sensitivity study for input parameters was conducted by Iowa State University (*12, 13*) by considering five M-E PDG performance measures for flexible pavement. The five performance models for flexible pavements in the M-E PDG were: (1) longitudinal cracking, (2) fatigue cracking, (3) transverse cracking, (4) alligator cracking, (5) rutting (total and AC), and (5) IRI. In this research, a total of 20 input parameters were investigated. An overall summary of the sensitivity analysis results are presented in Table 2.1. In general, the sensitivity of design input variables listed in each cell of the table applies to both thick (Interstate) and thin (US Road) pavement structures. The table shows that most of the investigated input parameters were found to be sensitive to longitudinal cracking while most were listed as insensitive for alligator cracking. Out of the 20 input parameters, 15 were listed as sensitive for longitudinal cracking while only 2 inputs were listed as sensitive for alligator cracking and 3 input parameters related to AC material properties and climate were found sensitive for transverse cracking. Total rutting in the pavement was found to be sensitive to 11 of the 20 input parameters. All the 11 input variables were listed as sensitive for AC surface layer rutting while almost all of them were listed

as insensitive for permanent deformation in the AC base, unbound subbase and subgrade layers. This may be due to the relatively thick AC layers considered in this study. Only 4 out of 20 input parameters were listed as sensitive for IRI. This may be due to the nature of the IRI model included in the M-E PDG, which is based on the accumulation of IRI due to four factors: initial IRI, IRI due to distress, frost heave, and subgrade swelling. Among the distresses, rut depth standard deviation, transverse cracking and fatigue cracking were the most significant distresses that influenced smoothness and were therefore included in the IRI model.

Table 2.1 Overall summary of sensitivity analysis results (flexible pavements)

Flexible Pavement Input	Performance Model								
	Cracking			Rutting					IRI
	Long.	Allig.	Trans.	AC Surface	AC Base	Subbase	Subgrade	Total	
AC layer thickness↑	↑	↔	↔	↔	↔	↔	↔	↔	↔
Nominal Max. Size↑	↑	↔	↔	↔	↔	↔	↔	↔	↔
PG Grade↑	↓↓	↔	↑↑	↓	↔	↔	↔	↓	↑
AC Volumetric↑	↑	↔	↑↑	↑	↔	↔	↔	↑	↑
AC Unit Weight↑	↔	↔	↔	↔	↔	↔	↔	↔	↔
AC Poissons's Ratio↑	↓	↔	↔	↓	↔	↔	↔	↓	↔
AC Thermal Cond. ↑	↔	↔	↔	↔	↔	↔	↔	↔	↔
AC Heat Capacity↑	↓	↔	↔	↓	↔	↔	↔	↓	↔
AADTT↑	↑↑	↔	↔	↑↑		↔	↑	↑↑	↔
Tire Pressure↑	↑↑	↔	↔	↑	↔	↔	↔	↑	↔
Traffic Distribution↑	↑	↔	↔	↑	↔	↔	↔	↑	↔
Traffic Speed↑	↓	↔	↔	↓	↔	↔	↔	↓	↔
Traffic Wander↑	↓	↔	↔	↔	↔	↔	↔	↔	↔
Climate (MAAT) ↑	↑	↔	↓↓	↑	↔	↔	↔	↑	↓
Base Thickness↑	↑	↓↓	↔	↓	↔	↔	↔	↓	↔
Base M_r↑	↔	↓↓	↔	↔		↔	↔	↔	↓
Subbase Thickness↑	↑	↔	↔	↔	↔	↔	↔	↔	↔
Subbase M_r↑	↔	↔	↔	↔	↔	↔	↔	↔	↔
Subgrade M_r↑	↑↑	↔	↔	↔	↔	↔	↓	↓	↔
Agg. Thermal Coeff. ↑	↔	↔	↔	↔	↔	↔	↔	↔	↔

↓↓/↑↑ - very sensitive to changes in input values
↓/↑ - sensitive to changes in input values
↔ - insensitive to change in input values

Zeghal et al. conducted a study, at National Research Council Canada, to review the new M-E PDG from a material characterization perspective (*14*). In this study, a comparison was made between the correlations (Level II) and the laboratory test results for AC dynamic modulus and resilient modulus for unbound materials (Level I). The following are conclusions based on the results of the study:

- The flexible pavement performance models reflected sensitivity to variation in asphalt concrete mix types with unique physical and mechanical properties. Performance predictions produced using the new M-E PDG while implementing laboratory measured

dynamic modulus values (input Level 1) are in agreement with performance patterns established in the current practice and reported in the literature.

- However, AC dynamic modulus estimated using the predictive equation incorporated in the guide proved to be substantially different from measured values. The error in estimating the modulus (input Level 3) led to underestimates of accumulated damage, which will consequently result in undersigning the road structure.
- Similarly, input Level 3 for unbound materials, mainly based on correlation between physical properties (including AASHTO classification) and the resilient modulus, produced unreliable values when compared with actual measurements made in the laboratory. Applications based on a modulus estimated using the guide proposed values to run the software resulted in substantially different performance predictions compared with those produced using measured modulus values.

2.3 EFFECT OF CLIMATE INPUTS ON PAVEMENT PERFORMANCE

The Indiana DOT study indicated that in jointed plain concrete pavement, all parameters related to concrete strength and curling stresses are very sensitive to the performance parameter, especially the mid-panel cracking (*9*). Temperature differential between top and bottom of the slab, joint spacing, and coefficient of thermal expansion significantly impact the amount of percent slabs cracked. Failure to recognize these parameters by using the default values may result in a pavement design that indicates it is excessively over-designed while in fact it is not. Since temperature differential, joint spacing, and layer thicknesses are not in the hierarchical input design modules, moving from design input Level 3 to Level 1 will not have significant differences in terms of design accuracy.

For flexible pavement, the same study concluded that in warm regions, rutting increases due to the reduced stiffness of the HMA, and longitudinal (top-down) cracking increases due to increased shear strain at the surface of the HMA. In colder regions, low air temperature causes tensile stresses to develop at the surface of the HMA due to shrinkage which generates thermal cracking. The impact of climate on fatigue cracking is minimized due to the nature of the thick structure of this pavement section (*3*).

2.4 EFFECT OF STRUCTURAL INPUTS ON PAVEMENT PERFORMANCE

It was reported in Indiana DOT study that thicker surface course and overall increase in the HMA total layer thickness provide better fatigue resistance. However, longitudinal cracking is increased with the increase of the surface course thickness and the total HMA layer thickness. Increasing both the surface course thickness and overall HMA layer thickness provides the most resistance to both rutting and fatigue (*3*).

A sensitivity analysis was conducted by Iowa State University for rigid pavement systems using M-E PDG. A number of conclusions drawn from this study are shown in Table 2.2.

A study was performed to assess the relative sensitivity of the performance models used in the M-E Design Guide to inputs relating to Portland Cement Concrete (PCC) materials in the analysis of jointed plain concrete pavements (JPCP) at the University of Arkansas (*5, 15*). A total

of 29 inputs were evaluated by analyzing a standard pavement section and changing the value of each input individually (see Table 2.3). The three pavement distress models (cracking, faulting, and roughness) were not sensitive to 17 of the 29 inputs. All three models were sensitive to 6 of 29 inputs. Combinations of only one or two of the distress models were sensitive to 6 of 29 inputs. These results may aid designers in focusing on those inputs having the most effect on desired pavement performance.

Table 2.2 Sensitivity analysis results from Iowa study (rigid pavements)

Performance Measure	Extremely Sensitive	Very Sensitive
Transverse cracking	• Curl/warp effective temperature difference (built-in) • Coefficient of thermal expansion • Thermal conductivity • PCC layer thickness • PCC strength properties • Joint spacing	• Edge support • Mean wheel location (traffic wander) • Unit weight • Poisson's ratio • Climate • Surface shortwave absorptivity • Annual average daily truck traffic (AADTT)
Faulting	• Curl/warp effective temperature difference (built-in) • Doweled transverse joints (load transfer mechanism, doweled or un-doweled)	• Coefficient of thermal expansion • Thermal conductivity • Annual average daily truck traffic (AADTT) • Mean wheel location (traffic wander) • Unbound layer modulus • Cement content • Water to cement ratio
Smoothness	• Curl/warp effective temperature difference • Coefficient of thermal expansion • Thermal conductivity	• Annual average daily truck traffic (AADTT) • Doweled transverse joints (load transfer mechanism, doweled or un-doweled) • Mean wheel location (traffic wander) • Joint spacing • PCC layer thickness • PCC strength properties • Poisson's ratio • Surface shortwave absorptivity • Unbound layer modulus • Cement content • Water to cement ratio

A study was conducted at University of California Davis to understand reasonableness of the model predictions for California conditions; a detailed sensitivity study was undertaken. The reasonableness of the model predictions was checked using a full factorial considering traffic volume, axle load distribution, climate zones, thickness, design features, PCC strength, and unbound layers. Satellite sensitivity studies were performed to study the effects of surface absorptivity (*16*) and coefficient of thermal expansion which were not included in the primary sensitivity analysis (*6, 17*).

The cracking model was found to be sensitive to the coefficient of thermal expansion, surface absorptivity, joint spacing, shoulder type, PCC thickness, climate zone, and traffic volume. The faulting values are sensitive to dowels, shoulder type, climate zone, PCC thickness, and traffic volume. Though on average both the cracking and faulting models show trends that agree with prevailing knowledge in pavement engineering and California experience, there were some cases

where results were counter-intuitive. These include thinner sections performing better than thicker sections, asphalt shoulders performing better than tied and widened lanes. It was also found that the models fail to capture the effect of soil type, erodibility index and that the cracking model is very sensitive to surface absorption.

Table 2.3 Summary of results of sensitivity analysis

JPCP Concrete Material Characteristics	Performance Models		
	Faulting	Cracking	Smoothness
Curl/wrap Effective Temperature Difference	S	S	S
Joint Spacing	S	S	S
Sealant Type	I	I	I
Dowel Diameter	S	I	S
Dowel Spacing	I	I	I
Edge Support	S	S	S
PCC-Base Interface	I	I	I
Erodibility Index	I	I	I
Surface Shortwave Absorptivity	I	S	I
Infiltration of Surface Water	I	I	I
Drainage Path Length	I	I	I
Pavement Cross-slope	I	I	I
PCC Layer Thickness	S	S	S
Unit Weight	S	S	S
Poisson's Ratio	I	S	I
Coefficient of Thermal Expansion	S	S	S
Thermal Conductivity	I	S	I
Heat Capacity	I	I	I
Cement Type	I	I	I
Cement Content	I	I	I
Water/cement Ratio	I	I	I
Aggregate Type	I	I	I
PCC Set Temperature	I	I	I
Ultimate Shrinkage at 40% RH	I	I	I
Reversible Shrinkage	I	I	I
Time to Develop 50% of Ultimate Shrinkage	I	I	I
Curling Method	I	I	I
28-day PCC Modulus of Rupture	I	S	S
28-day PCC Compressive Strength	I	S	S

S = sensitive to change in the input value
I = insensitive to change in the input value

CHAPTER 3 - PRELIMINARY SENSITIVITY ANALYSIS - RIGID

To determine the mathematical viability of the performance models for new and rehabilitated HMA and JPC pavements, models "reasonableness" and boundaries of the equations, various input variables need some practical ranges. The mathematically viability of performance models can be conducted within these practical ranges. The details regarding the selection of these input ranges are presented in this chapter.

3.1 DESIGN INPUT LEVELS

The major sub-systems in the M-E PDG include the input system, mechanistic pavement analysis model, transfer functions, and output system which consist of predicted pavement distresses. A new feature in the M-E PDG, which is not available in the existing versions of the AASHTO 1993 Design Guide, is the *hierarchical approach* to design inputs. Depending on the desired level of accuracy of input parameter, three levels of input are provided from Level 1 (highest level of accuracy) to level 3 (lowest level of accuracy). Based on the criticality of the project and the available resources, the designer has the flexibility to choose any one of the input levels for the design as well as use a mix of levels. However, irrespective of the input design levels, the computational algorithm used to predict distresses and smoothness remains the same. It is important that a designer has sufficient knowledge of how a particular input parameter will affect pavement distresses to decide on a suitable input level. Figures 3.1 and 3.2 illustrate the general input modules for flexible and rigid pavement types in the M-E PDG software.

3.2 INPUT VARIABLES IN M-E PDG AND MDOT CURRENT PRACTICE

Unlike the AASHTO 1993 Design Guide, which requires very limited information for design of flexible and rigid pavements, to analyze and design a pavement using new M-E PDG, a large number of design inputs related to layer materials, environment, traffic, drainage, and pavement shoulders need to be considered. While the main objective of this research is to evaluate the new M-E PDG, it will also incorporate the current state-of-the-practice in terms of required inputs for AASHTO 1993 Design Guide. For adopting the new M-E PDG, it is essential to fill the gap between the available and the required input variables. Hence, to accomplish this objective a series of tables which include all required input (at various levels) variables for M-E PDG were prepared. These tables include traffic data requirements (see Table 3.1), structural and material inputs for rigid (see Table 3.2), and flexible pavements (see Table 3.3), respectively. These tables show tentative inputs that are being currently used by MDOT for pavement design practices, the variables that can be measured, and the inputs which are practically difficult to measure.

Since 2004, when the new M-E PDG become available, many state highway agencies (SHAs) have conducted research on evaluation and implementation of this new design and analysis procedure. This relevant literature search will further assist the research team to identify the most important variables in the pavement design process.

It should be noted that all of variables shown in Tables 3.1 through 3.3 will be used in the sensitivity analysis to identify the most important input variables that need to be measured or used due to their significant influence on the pavement performance. The importance of variables in light of the MDOT needs and their input data ranges are also considered while studying these input variables.

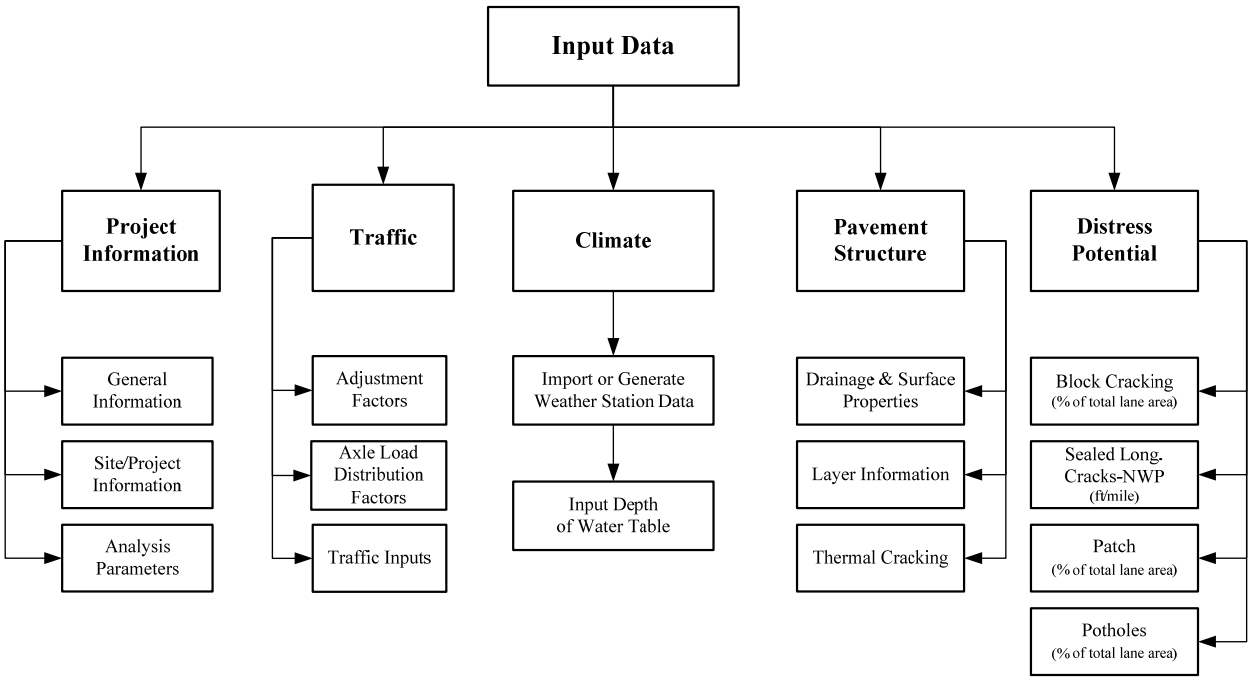

Figure 3.1 M-E PDG data input modules—Flexible pavements

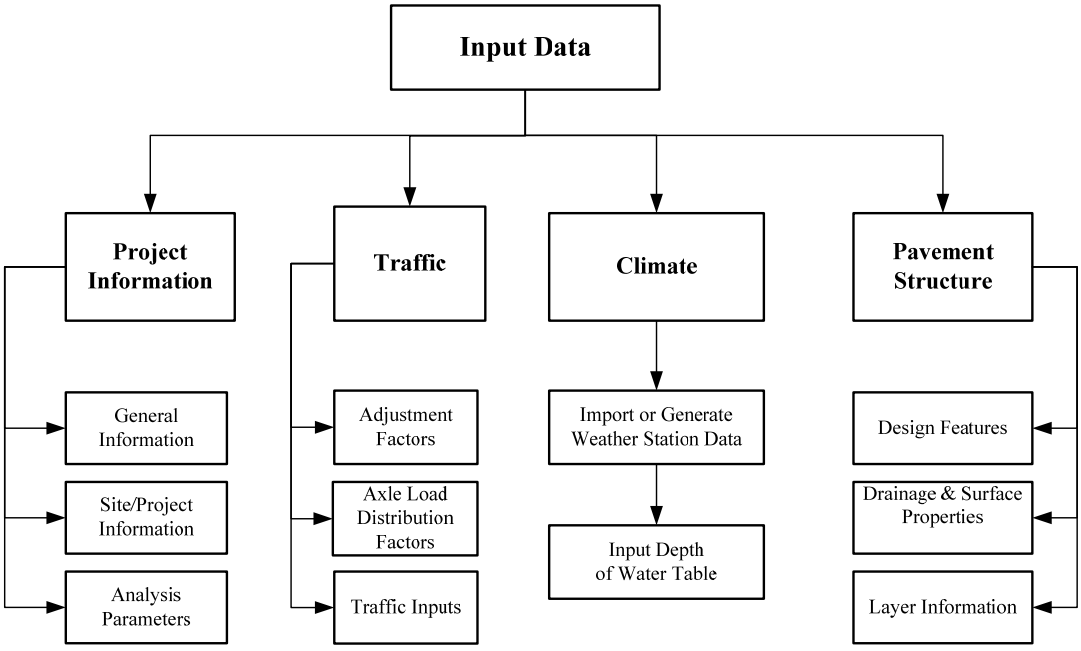

Figure 3.2 M-E PDG data input modules—Rigid pavements

Table 3.1 M-E PDG input variables —Traffic

Inputs		Data	Being Used by MDOT	Can be Measured	Hard to Measure
Main		Initial two-way AADTT	✓		
		Number of lanes in design direction	✓		
		Percent of trucks in design direction (%)	✓		
		Percent of trucks in design lane (%)	✓		
Traffic Volume Adjustment Factors	Monthly Adjustment	Load monthly adjustment factors (MAF) (sum of the MAF of all months for each class must equal 12)		✓	
		Level 1: Site specific distribution		✓	
		Level 2: Regional Distribution		✓	
		Level 3: Default Distribution (National Avg.)		✓	
	Vehicle Class Distribution	AADTT distribution by vehicle class (%)		✓	
		Level 1: Site specific distribution		✓	
		Level 2: Regional Distribution		✓	
		Level 3: Default Distribution (National Avg.)		✓	
	Hourly Distribution	Hourly truck traffic distribution by period beginning		✓	
		Level 1: Site specific distribution		✓	
		Level 2: Regional Distribution		✓	
		Level 3: Default Distribution (National Avg.)		✓	
	Traffic Growth Factors	Vehicle-class specific traffic growth in percent or Default growth function (all classes) (no growth, linear growth, compound growth)		✓	
Axle Load Distribution Factors		Axle factors by axle type (percent of axles (single, tandem, tridem, and quad) in weight categories for each vehicle class for each month) Level 1: Site specific distribution Level 2: Regional Distribution Level 3: Default Distribution (National Avg.)		✓	
General Traffic Inputs	Lateral Traffic Wander	Mean wheel location (inches from the lane marking)		?[1]	
		Traffic wander standard deviation (in.)		?[2]	
		Design lane width (ft)	✓		
	Number Axles/Truck	Average number of single, tandem, tridem and quad axles per truck	✓		
		Level 1: Site specific distribution		✓	
		Level 2: Regional Distribution		✓	
		Level 3: Default Distribution (National Avg.)		✓	
	Axle Configuration	Average axle width (edge-to-edge) outside dimension (ft)		✓	
		Dual tire spacing (in.)		✓	
		Tire pressure for single and dual tires (psi)		✓	
		Axle spacing (in.) for tandem, tridem, and quad axles		✓	
	Wheelbase	Average axle spacing (ft) for short, medium, and long trucks		✓	
		Percents of truck for shot, medium, and long trucks		✓	

[1] It is the mean wheel location for wander from the edge of outer lane marking.

[2] Generally, a normal distribution is assumed from wheel wander. This distribution is defined by two parameters: mean and standard deviation. This is the standard deviation of the lateral traffic wander is used to estimate the number of axle load repetitions over a single point in a probabilistic manner for predicting distress and performance.

Table 3.2 M-E PDG input variables —Structure for rigid pavement

Inputs		Data	Being Used by MDOT	Can be Measured	Hard to Measure
Design Feature		Permanent curl/warp effective temperature difference (^oF)		✓	
		Joint spacing (ft)	✓		
		Sealant type (None, Liquid, Silicone, or Preformed)	✓		
		Dowel diameter (in.) and spacing (in.)	✓		
		Edge support (Tied PCC shoulder and/or Widened slab)	✓		
		PCC-Base Interface (bonded or unbounded)			✓
		Erodibility Index[Extremely resistant (1) through Very Erodible (5)]		?[3]	
		Loss of bond age (months)			✓
Drainage and Surface Properties		Surface shortwave absorptivity			✓
		Infiltration (Negligible (0%) through Extreme (100%))		?[4]	
		Drainage path length (ft) (not for Negligible infiltration)	✓		
		Pavement cross slope (%) (not for Negligible infiltration)	✓		
Layers - PCC Material Properties	Thermal	PCC material		?	
		Layer thickness (in.)	✓		
		Unit weight (pcf)	✓		
		Poisson's ratio		✓	
		CTE (per ^oF x 10-6)		✓	
		Thermal conductivity (BTU/hr-ft-^oF)		?[5]	
		Heat capacity (BTU/lb-^oF)		?[6]	
	Mix	Cement type (Type I, Type II or Type III)	✓		
		Cementitious material content (lb/yd^3)	✓		
		Water/cement ratio	✓		
		Aggregate type	✓		
		PCC zero-stress temperature (^oF)		✓	
		Ultimate shrinkage at 40% R.H. (micro-strain)		✓	
		Reversible shrinkage (% of ultimate shrinkage)		✓	
		Time to develop 50% of ultimate shrinkage (days)		✓	
		Curing method (curing compound or wet curing)	✓		
	Strength	Level 1 - Elastic modulus (psi) and Modulus of rupture (psi) at 7-, 14-, 28-, and 90-day and the ratio 20 Year/28 Day	✓		
		Level 2 - Compressive strength (psi) at 7-, 14-, 28-, and 90-day and the ratio 20 Year/28 Day	✓		
		Level 3 - 28-day PCC compressive strength (psi)	✓		
Layers- Chemically Stabilized Material		Material type		✓	
		Layer thickness (in.)		✓	
		Unit weight (pcf)		✓	
		Poisson's ratio		✓	
		Elastic/resilient modulus (psi)		✓	
		Minimum elastic/relilient modulus (psi)		✓	
		Modulus of rupture (psi)		✓	
		Thermal conductivity (BTU/hr-ft-oF)		?[5]	
		Heat capacity (BTU/lb-oF)		?[6]	

[3] This is an index on a scale of 1 to 5 to rate the potential for erodibility of the base material. The potential for base or subbase erosion (layer directly beneath the PCC layer) has a significant impact on the initiation and propagation of pavement distress.

[4] This parameter defines the net infiltration potential of the pavement over its design life. In the Design Guide approach, infiltration can assume four values – none, minor (10 percent of the precipitation enters the pavement), moderate (50 percent of the precipitation enters the pavement), and extreme (100 percent of the precipitation enters the pavement). Based on this input, the EICM determines the amount of water available on top of the first unbound layer.

[5] Thermal conductivity is a measure of the ability of the material to uniformly conduct heat through its mass when two faces of the material are under a temperature differential. It is defined as the ratio of heat flux to temperature gradient. The value is determined using laboratory testing in accordance with ASTM E 1952.

[6] Heat capacity parameter is defined as the amount of heat required to raise a unit mass of material by a unit temperature. This is estimated using laboratory testing in accordance with ASTM D 2766.

Table 3.2 M-E PDG input variables —Structure for rigid pavement (continued…)

Inputs		Data	Being Used by MDOT	Can be Measured	Hard to Measure
Layers - Unbound Layer	General	Unbound Material	✓		
		Thickness (in.)	✓		
	Strength Properties	Poisson's ratio		✓	
		Coefficient of lateral pressure, Ko		?[7]	
		Level 2 (Seasonal or Representative Input) - Modulus (psi), CBR, R-value, Layer Coefficient (ai), Penetration (DCP), or Based upon PI and Gradation		✓	
		Level 3 (Representative Input only) - Modulus (psi)	✓		
	EICM	Plasticity Index	✓		
		Passing #200 sieve (%)	✓		
		Passing #4 sieve (%)	✓		
		D60 (mm)	✓		
		Compacted unbound material or Uncompacted/natural unbound material	✓		

Table 3.3 M-E PDG input variables —Structure for flexible pavement

Inputs	Data		Being Used by MDOT	Can be Measured	Hard to Measure
Drainage	Same as Rigid Pavement		Same as Rigid Pavement		
Layers - Asphalt Material Properties	General	Asphalt material type	✓		
		Layer thickness (in.)	✓		
	Asphalt Mix	Modulus of asphalt material at different temperatures and different frequencies - Level 1 (site)		✓	
		Cumulative percent retained 3/4-in. sieve - Level 2 (regional) and Level 3 (default)		✓	
		Cumulative percent retained 3/8-in. sieve - Level 2 (regional) and Level 3 (default)		✓	
		Cumulative percent retained #4 sieve - Level 2 (regional) and Level 3 (default)		✓	
		Percent passing #200 sieve - Level 2 (regional) and Level 3 (default)		✓	
	Asphalt Binder	Superpave binder test data (G and Delta at 10 rad/sec at different temperatures for Level 1 (site) and Level 2 (regional) or Superpave binder grade for Level 3 (default))		✓	
		Conventional binder test data (Softening point, Absolute viscosity, Kinematic viscosity, Specific gravity for Level 1 (site) and Level 2 (regional) or Viscosity grade or Penetration grade)	✓		
	Asphalt General	Reference temperature		✓	
		Effective binder content (%)	✓		
		Air voids (%)	✓		
		Total unit weight (pcf)	✓		
		Poisson's ratio		✓	
		Thermal conductivity (BTU/hr-ft-oF)			✓
		Heat capacity (BTU/lb-oF)			✓
Layers - Unbound Layer	Same as Rigid Pavement		Same as Rigid Pavement		
Thermal Cracking	Average tensile strength at 14 ^{o}F (psi)			✓	
	Creep test duration (sec)				✓
	Creep Compliance (1/psi) at -4, 14 and 32 1oF (for Level 1 (site) and Level 3 (default)) at only 14 oF (for Level 2 (regional))				✓
	VMA (%)		✓		
	Aggregate coefficient of thermal contraction			?[8]	
	Mix coefficient of thermal contraction			?[9]	

[7] Estimate the at-rest earth pressure coefficient, k_o, for the soil stratum for which the resilient modulus is needed.

[8] This is the coefficient of thermal contraction of the aggregate used in the mix design, and is expressed as the change in volume per unit volume for unit decrease in temperature. The typical values range from 21 to 37 /^{o}C.

[9] This is the coefficient of thermal contraction of the AC mix, and is expressed as the change in length per unit length for unit decrease in temperature. The typical values range from 2.2 to 3.4 /oC

Table 3.3 M-E PDG input variables —Structure for flexible pavement (continued...)

Inputs	Data		Being Used by MDOT	Can be Measured	Hard to Measure
Asphalt Binder	Level III: SuperPave Binder Grading Conventional Viscosity Grade Conventional Penetration Grade	 Specify PG Binder Grade Specify Binder Viscosity Specify Binder Penetration Grade	✓		
	Level II: Superpave Binder Test Data	 Specify relationship between temperature and G*, phase angle		✓	
	Conventional Binder Test Data	Specify Softening Point Specify Absolute Viscosity Specify kinematic Viscosity Specific Gravity Penetration at different temperatures Specify Brookfield Viscosity at different temperatures			
	Level I: Superpave Binder Test Data	 Specify relationship between temperature and G*, phase angle		✓	
	Conventional Binder Test Data	Specify Softening Point Specify Absolute Viscosity Specify kinematic Viscosity Specific Gravity Penetration at different temperatures Specify Brookfield Viscosity at different temperatures			

3.2.1 Input Variable Ranges

To conduct the robustness and sensitivity analyses of the input variables, it is essential to determine practical ranges of these variables. The primary sources for the magnitudes of input parameters are (i) General pavement sections — GPS-1, GPS-2, GPS-3, GPS-6, GPS-7 experiments, Specific pavement sections — SPS-1 and SPS-2 experiments in the Long Term Pavement Performance (LTPP) database, these pavement sections are located in various climatic regions in the US and (ii) typical design inputs used by MDOT in designing their mainline flexible and concrete pavements.

A series of frequency histograms were plotted for each input variable for which the data was available in the Release 19.0 of DataPave. From these histograms (frequency distributions) the modal values (most frequently occurring range) were identified. The distributions also provide information about "extreme" values ($\mu \pm 2\sigma$) for each input variable (see Figure 3.3). For non-normal distributions, the 25th and 75^{th} percentile values were used instead (see Appendix A). These extreme values will be used to conduct the sensitivity of the M-E PDG software while the mean values for input variable distributions will be used as a base design. For example, the mean PCC slab thickness within the GPS-3 experiment is 8-9-inches and the extreme values are 7- and 14-inch (see Figure 3.4). It should be noted that not all required input variables data are available in the LTPP DataPave. Therefore, in those cases, the recommended input variable ranges provided in the M-E PDG software were used. Tables 3.4 and 3.5 show the ranges for each input

variables for rigid pavement (JPCP) to be used in the preliminary sensitivity analysis. The LTPP data distributions for available input variables are shown in Appendix A.

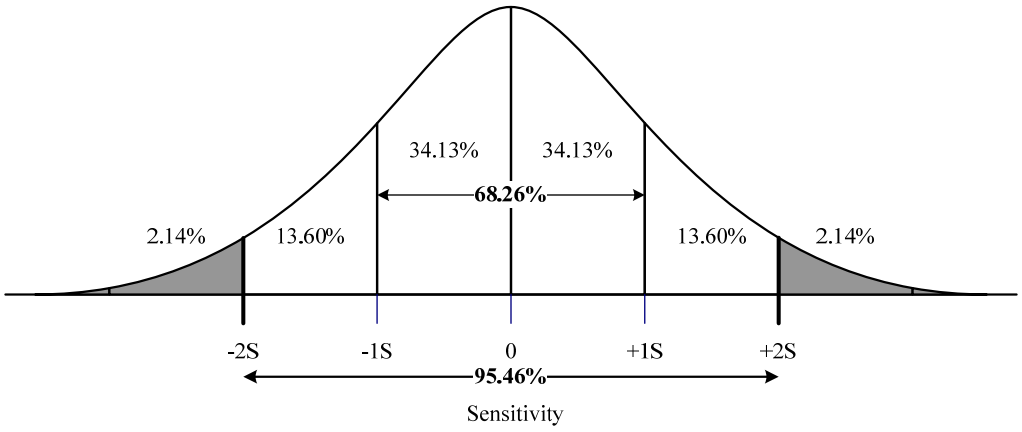

Figure 3.3 Extreme values for normal distribution

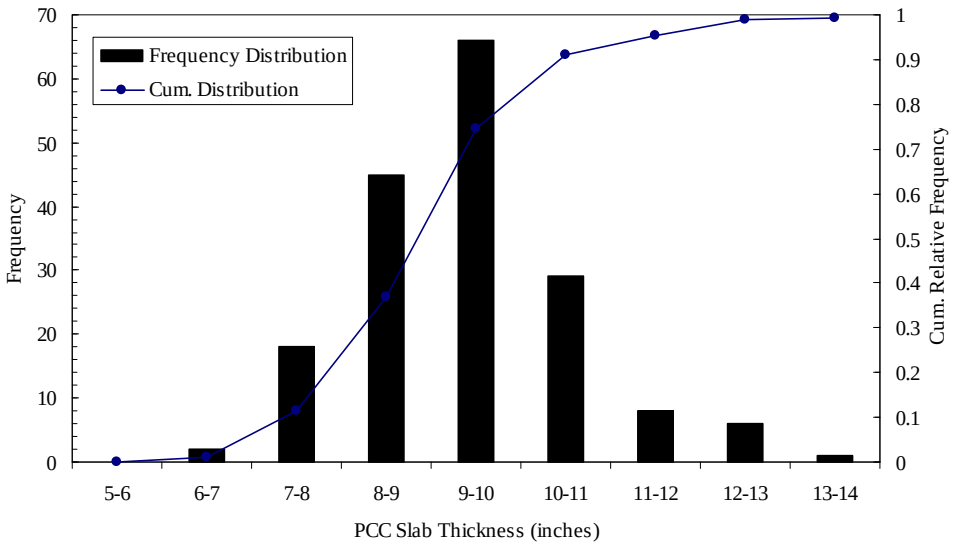

Figure 3.4 Distribution of slab thickness in GPS-3 experiment pavements

Table 3.4 M-E PDG input variables— Traffic data

Inputs		Data	Mean, μ	Std, σ	μ–2σ	μ–1σ	μ	μ+1σ	μ+2σ
Main		Initial two-way AADTT			100		12000		25000
		Number of lanes in design direction					2		
		Percent of trucks in design direction (%)					50		
		Percent of trucks in design lane (%)					90		
Traffic Volume Adjustment Factors	Monthly Adjustment	Load monthly adjustment factors (MAF) (sum of the MAF of all months for each class must equal 12)					1		
		Level 1: Site specific distribution					1		
		Level 2: Regional Distribution					1		
		Level 3: Default Distribution (National Avg.)					1		
	Vehicle Class Distribution	AADTT distribution by vehicle class (%)					TTC 1		
		Level 1: Site specific distribution					TTC 1		
		Level 2: Regional Distribution					TTC 1		
		Level 3: Default Distribution (National Avg.)					TTC 1		
	Hourly Distribution	Hourly truck traffic distribution by period beginning	National Average						
		Level 1: Site specific distribution							
		Level 2: Regional Distribution							
		Level 3: Default Distribution (National Avg.)							
	Traffic Growth Factors	Vehicle-class specific traffic growth in percent or Default growth function (all classes) (no growth, linear growth, compound growth)					5		
Axle Load Distribution Factors		Axle factors by axle type (percent of axles (single, tandem, tridem, and quad) in weight categories for each vehicle class for each month) Level 1: Site specific distribution Level 2: Regional Distribution Level 3: Default Distribution (National Avg.)	National Average						

Table 3.4 M-E PDG input variables— Traffic data (continued…)

Inputs		Data	Mean, μ	Std, σ	μ–2σ	μ–1σ	μ	μ+1σ	μ+2σ
General Traffic Inputs	Lateral Traffic Wander	Mean wheel location (inches from the lane marking)			0		18		36
		Traffic wander standard deviation (in.)			7		10		13
		Design lane width (ft) ***Software Range: 10 to 13]***			10		12		13
	Number Axles/Truck	Average number of single, tandem, tridem and quad axles per truck	National Average						
		Level 1: Site specific distribution							
		Level 2: Regional Distribution							
		Level 3: Default Distribution (National Avg.)							
	Axle Configuration	Average axle width (edge-to-edge) outside dimension (ft)			8		9		10
		Dual tire spacing (in.)			0		12		24
		Tire Pressure for single and dual tires (psi) ***[Software Range: 120]***			80		120		140
		Axle spacing (in.) for: Tandem Tridem Quad			 24 24 24		 51 51 51		 144 144 144
	Wheelbase	Average axle spacing (ft) for: Short trucks Medium trucks Long trucks			 10 12 15		 12 15 18		 15 18 22
		Percents of truck for: Short trucks Medium trucks Long trucks					 33 33 34		

Table 3.5 M-E PDG input variables— Structure data for rigid pavement

Inputs		Data	Mean, μ Median	Std, σ Range	μ–2σ 25th	μ–1σ 37.5 th	μ 50 th	μ+1σ 62.5 th	μ+2σ 75 th
Design Feature		Permanent curl/warp effective temperature difference (°F)[10] ***[Software Range: -30 to 0]***	-	-	-	-	-10	-	-
		Joint spacing (ft) ***[Software Range: 10 to 20]***	15	3.5	10		15		30
		Sealant type (None, Liquid, Silicone, or Preformed)			None	Liquid	Silicone	Preformed	
		Dowel diameter (in.) and spacing (in.) ***[Software Range: 1 to1.75 [Software Range: 10 to 14]]***	1.2 12	0.2 2	1 10		1.25 12		1.5 20
		Edge support (Tied PCC shoulder and/or Widened slab) LTE	-	-	Tied 80%		Asphalt 40%		Widened 14 ft
		PCC-Base Interface (bonded or unbounded)	-	-		-	Un-bonded	-	Bonded
		Erodibility index (Extremely resistant (1) through Very erodable (5))	-	-	Very Erodible		Erosion Resistant		Extremely Resistant
		Loss of bond age (months) ***[Software Range: 0 to120]***	-	-	0		60		120
Drainage and Surface Properties		Surface shortwave absorptivity ***[Software Range: 0.5 to 1]***	-	-	0.5		0.7		1
		Infiltration (Negligible (0%) through Extreme (100%))	-	-	0		50		100
		Drainage path length (ft) (not for Negligible infiltration) ***[Software Range: 5 to 25]***	-	-	5		15		25
		Pavement cross slope (%) (not for Negligible infiltration) ***[Software Range: 0 to 5]***	-	-	0		2		5
Layers - PCC Material Properties	Thermal	PCC material	-	-	-	-	JPCP	-	-
		Layer thickness (in.) ***[Software Range: 1 to 20]***	9	1	7	8	9	11	14
		Unit weight (pcf) ***[Software Range: 140 to 160]***	139	14			140		
		Poisson's ratio ***[Software Range: 0.1 to 0.3]***	0.18	0.07			0.2		
		CTE (per °F x 10-6) ***[Software Range: $2*10^{-6}$ to $10*10^{-6}$]***	5.56×10^{-6}	8.03×10^{-7}	4×10^{-6}		5.56×10^{-6}		7.18×10^{-6}
		Thermal conductivity (BTU/hr-ft-°F) ***[Software Range: 0.2 to 2]***	-	-	-	0.2	1.25	2	-
		Heat capacity (BTU/lb-°F)	-	-	-	0.1	0.28	0.5	-
	Mix	Cement type (Type I, Type II or Type III)	-	-	-	-	Type I	-	-
		Cementitious material content (lb/yd^3) ***[Software Range: 400 to800]***	544	71	402		544		686
		Water/cement ratio ***[Software Range: 0.3 to 0.7]***	0.47	0.12	0.22		0.47		0.72
		Aggregate type					Limestone		
		PCC zero-stress temperature (°F) ***[Software Range: 50 to 125]***			50		98		125
		Ultimate shrinkage at 40% R.H. (microstrain) ***[Software Range: 300 to 1000]***			300		639		1000
		Reversible shrinkage (% of ultimate shrinkage) ***[Software Range: 30 to 80]***			30		50		80
		Time to develop 50% of ultimate shrinkage (days) ***[Software Range: 30 to 50]***			30		35		50
		Curing method (curing compound or wet curing)					Curing Compound		

[10] Default value

Table 3.5 M-E PDG input variables— Structure data for rigid pavement (continued...)

Inputs		Data	Mean, μ	Std, σ	μ–2σ	μ–1σ	μ	μ+1σ	μ+2σ
Layers - PCC Material Properties	Strength	Level 1 - Elastic Modulus (psi) and Modulus of Rupture (psi) at 7 – days ***[Software Range: 1 to 7x10^6] [Software Range: 300 to 1000]***			$1x10^6$		$3.8x10^6$		$7x10^6$
			662	98	465		662		858
		14 – days *[Same as above]*					$4x10^6$		
			663	115	433		663		894
		28 – days *[Same as above]*					$5.1x10^6$		
			632	153	327		632		937
		90 – days *[Same as above]*					$5.2x10^6$		
					300		650		1000
		Ratio 20 Year/28 Day ***[Software Range: 0 to10] [Software Range: 0 to 10]***			1		1.2		10
		Level 2 - Compressive strength (psi) at 7 – days ***[Software Range: 2000 to 10000]***	3671	5284	2000		3671		10000
		14 – days ***[Software Range: 2000 to 10000]***	3240	4446	2000		3240		10000
		28 – days ***[Software Range: 2000 to 10000]***	4837	817	2000		4837		10000
		90 – days ***[Software Range: 2000 to 10000]***			2000		6000		10000
		Ratio 20 Year/28 Day ***[Software Range: 0 to10]***			1		1.2		10
		Level 3 28-day PCC Compressive Strength (psi) ***[Software Range: 3000 to 8000]***	5370	13000	3000		5370		8000
		28-day PCC Modulus of Rupture (psi) ***[Software Range: 450 to 1200]***	730	9220	450		730		1200
		28-day PCC Elastic Modulus (psi)	4.6E+06	1.1E+06	2.4E+06		4.6E+06		6.8E+06
Layers- Chemically Stabilized Material		Material type			Cement Stabilized		Lime Cement Fly Ash		Lime Stabilized
		Layer thickness (in.) ***[Software Range: 2 to 24]***	4.6	1.2	0		5		8
		Unit weight (pcf) ***[Software Range:50 to 200]***			50		125		200
		Poisson's ratio ***[Software Range:0.15 to 0.45]***			0.15		0.3		0.45
		Elastic/Resilient Modulus (psi) ***[Software Range: 0.5 to 4x10^6]***			$0.5x10^6$		$2x10^6$		$4x10^6$
		Minimum Elastic/Resilient Modulus (psi)							
		Modulus of rupture (psi)							
		Thermal conductivity (BTU/hr-ft-oF) ***[Software Range: 0.1 to 4]***			0.1		2		4
		Heat capacity (BTU/lb-oF) ***[Software Range: 0 to 1]***			0		0.5		1

Table 3.5 M-E PDG input variables— Structure data for rigid pavement (continued...)

Inputs		Data	Mean, μ	Std, σ	μ–2σ	μ–1σ	μ	μ+1σ	μ+2σ
Layers - Unbound Layer **Base/Subbase**	General	Unbound Material					Crush Stone		
		Thickness (in.) ***[Software Range: 1 to 100]***	7	4	2		7		10
	Strength Properties	Poisson's ratio ***[Software Range: 0.1 to 0.4]***			0.25		0.35		0.4
		Coefficient of lateral pressure, Ko ***[Software Range: 0.2 to 3]***					0.5		
		Level 2 (Seasonal or Representative Input) – Modulus (psi) ***[Software Range: 38,500 to 42,000]***			38,500		40,000		42,000
		Level 3 (Representative Input only) - Modulus (psi) ***[Software Range: 38,500 to 42,000]***			38,500		40,000		42,000
	ICM	Plasticity Index ***[Software Range: 0 to 6]***			0		3		6
		Passing #200 sieve (%)***[Software Range: 0 to15]***			0		8		15
		Passing #4 sieve (%)***[Software Range: 0 to 100]***			0		50		100
		D60 (mm) ***[Software Range: 2 to 25]***			2		13		25
		Compacted unbound material or Uncompacted/Natural unbound material							
Layers - Unbound Layer **Subgrade**	General	Unbound Material M_R (psi)			A-7-6 8,000		A-4 15,000		A-1-a 40,000
		Thickness (in.) ***[Software Range: 1 to 100]***							
	Strength Properties	Poisson's ratio ***[Software Range: 0.1 to 0.4]***			0.3		.4		0.5
		Coefficient of lateral pressure, Ko ***[Software Range: 0.2 to 3]***					0.5		
		Level 3 (Representative Input only) - Modulus (psi) ***[Software Range: 38,500 to 42,000]***			3,500		15,000		29,000
	ICM	Plasticity Index ***[Software Range: 0 to 10]***[11]			0		5		10
		Passing #200 sieve (%)***[Software Range: 36 to100]***			36		68		100
		Passing #4 sieve (%)***[Software Range: 0 to 100]***			0		50		100
		D60 (mm) ***[Software Range: 0.001 to 25]***			.001		12		25
		Compacted unbound material or Uncompacted/Natural unbound material							

[11] Default range depends on the soil type

3.2.2 Determination of Significance for Input Variables

To evaluate the significance of input variables from both practical and statistical point of view, there is a need to assess the effect more rationally based on some performance criteria which are more acceptable by the pavement community. Therefore, to determine the consequence of various levels of input variable, rather than using subjective criteria purely based on the visual inspection of the performance curves, in this study a more coherent criteria was adopted. In this research two different approaches were used to determine the significant effects:

- Performance threshold, and
- Age threshold

For performance threshold, acceptable failure criteria at national/local (MDOT) levels were considered for various performance measures. As shown in Figure 3.5, performance(s) threshold can be used to determine ages for each input level for the same variable. From these ages significance (statistical as well as practical) will be determined. For example, if the difference in ages is more than 5 years, one can consider this variable has a significant effect. On the other hand if the difference is less than 5 years, one can assume insignificant effect.

For the age threshold, the performance for each input level of a variable can be determined based on age as shown in Figure 3.6. The difference in performances at a particular age (10, 15 or 20 years) can be compared to the national common characteristics or good and poorly performing pavements (*18, 19*). Based on the project technical advisory group (TAG) feedback in order to accommodate the local needs, age threshold criterion was adopted in this research to identify the significance of an effect.

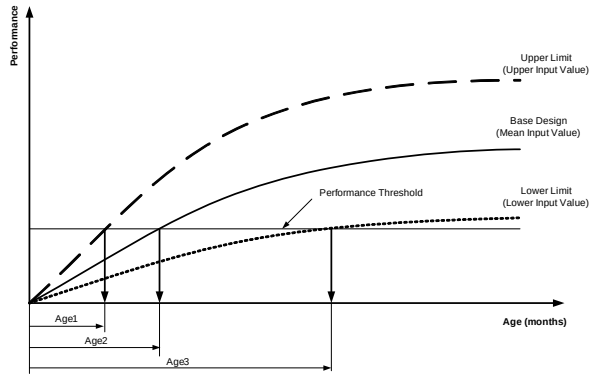

Figure 3.5 Effect of input variables on pavement performance — Performance threshold

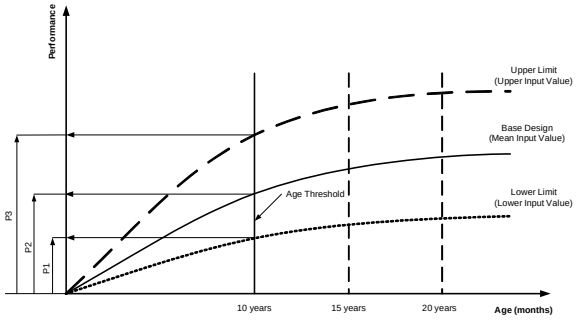

Figure 3.6 Effect of input variables on pavement performance — Age threshold

3.2.3 Determination of Performance Threshold

In this investigation, performance criteria developed by the FHWA (*18*), based on age threshold were modified to reflect MDOT practices and were used to ascertain the practical significance of an effect on cracking, faulting, and IRI. Figure 3.7 shows the performance criteria for various performance indicators while Table 3.6 presents the good-normal and normal-poor performance

thresholds to assess the practical significance of an effect. Also, to ascertain practical significance, one can compare the change in slope along the performance curve for a particular performance measure.

Therefore, two methods are proposed to establish the practical significance of an effect:

- If the performance difference at a particular age is greater than the mean difference for variable levels, then the effect of that variable is practical. For example, if the mean difference for cracking between 9- and 14-inches slab thicknesses at 30 years is greater than the difference between performance threshold (Δ_4, see Figure 3.8), the effect of slab thickness is of practical significance.
- One can also determine the change in slope for various ages to calculate the increase in distress per year (see Figure 3.8) and this increase per year can be used to identify the practical significance of an effect. If the slope is variable between various ages, a weighted average of the slope can be determined to ascertain an on average effect.

Table 3.6 shows both of the above criteria thresholds for percent slabs cracked, faulting and roughness in JPCP.

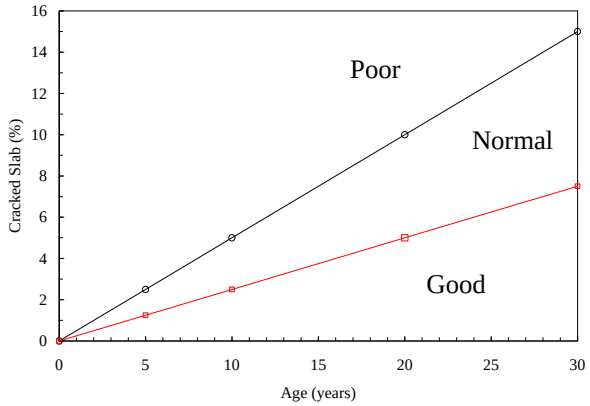

(a) Percent slab cracked

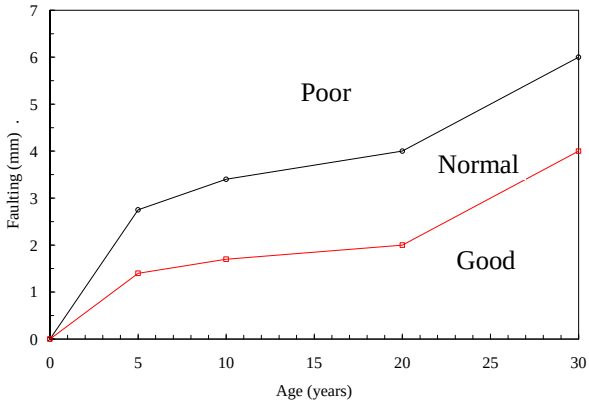

(b) Joint or crack faulting

(c) Roughness in terms of IRI

Figure 3.7 Adopted performance criteria for JPCP

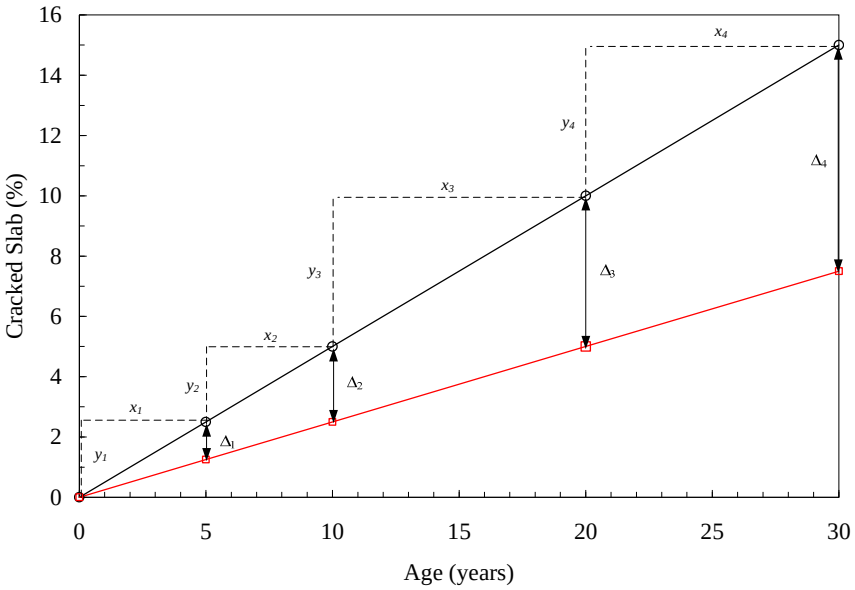

Figure 3.8 An example of estimating practical significance for % slab cracked in JPCP

Table 3.6 FHWA performance criteria at different ages− Rigid pavements

Performance Measure	Criteria	Pavement Age (years)				
		0	*5*	*10*	*20*	*30*
Cracking (% Slabs cracked)	Good-Normal	0	1.25	2.5	5	7.5
	Normal-Poor	0	2.5	5	10	15
	Δ	*0*	*1.25*	*2.5*	*5*	*7.5*
	Increase/year		0.5	0.5	0.5	0.5
	Weighted Avg. (Increase/year)	0.5				
Faulting (mm)	Good-Normal	0	1.4	1.7	2	4
	Normal-Poor	0	2.75	3.4	4	6
	Δ	*0*	*1.35*	*1.7*	*2*	*2*
	Increase/year		0.55	0.13	0.06	0.2
	Weighted Avg. (Increase/year)	0.2				
IRI (m/km)	Good-Normal	0.7	0.9	1.2	1.9	2.2
	Normal-Poor	1.2	1.75	2.1	3	3.45
	Δ	*0.5*	*0.85*	*0.9*	*1.1*	*1.25*
	Increase/year		0.11	0.07	0.09	0.045
	Weighted Avg. (Increase/year)	0.075				

The following section highlights the methodology and steps involved in preparation of a refined input variables matrix based on preliminary sensitivity and typical MDOT input ranges.

3.3 PREPARATION OF INITIAL SENSITIVITY TEST MATRIX

Trends and sensitivity of the models of the M-E PDG design software to the various input variables was addressed first. The output includes estimates as a function of design life of performance from cracking, faulting, and roughness models. Tables 3.4 and 3.5 show the final input variable ranges used for preliminary sensitivity analysis. This sensitivity was based on running M-E PDG software for one variable at a time. The results for three levels for each variable were plotted on the same graph to determine their effects on various performance measures (cracking, faulting, and IRI in case of rigid pavements). Visual inspection and engineering judgment were employed to identify the sensitive variables. For example Figures 3.9 and 3.10 show two of the very sensitive variables. Tables 3.7 and 3.8 present the summary of results of the preliminary sensitivity analysis.

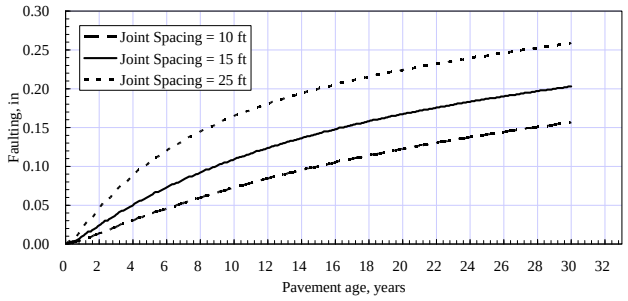

(a) Faulting

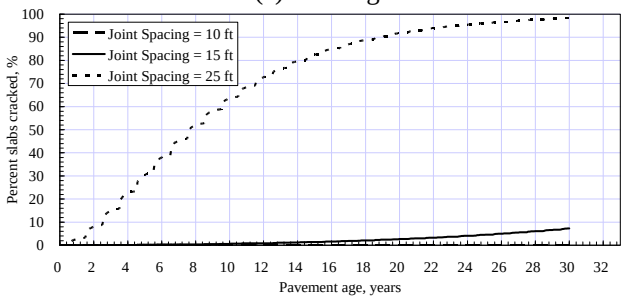

(b) Transverse cracking

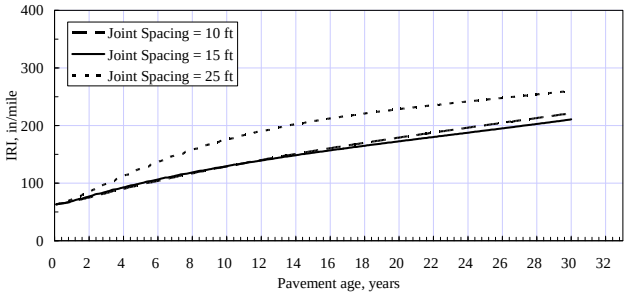

(c) IRI

Figure 3.9 Effect of joint spacing on performance – Example of very sensitive variable

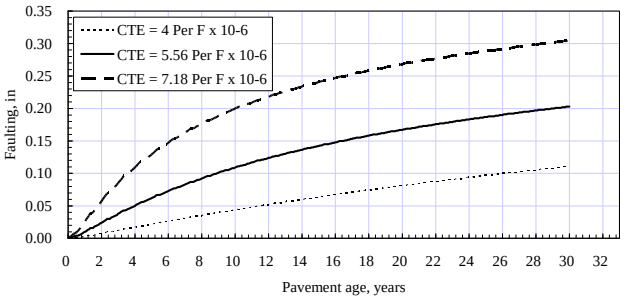

(a) Faulting

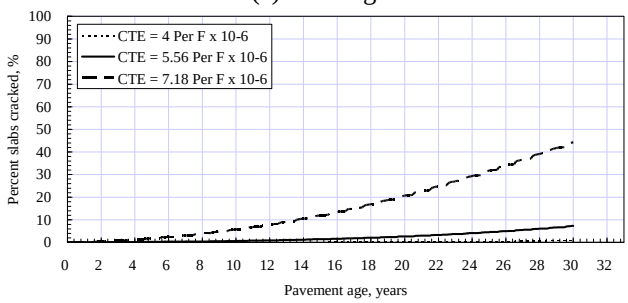

(b) Transverse cracking

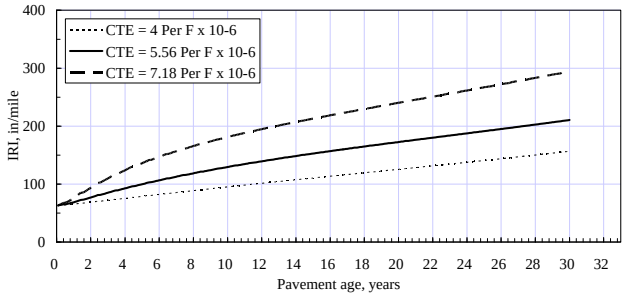

(c) IRI

Figure 3.10 Effect of CTE on performance – Example of very sensitive variable

Table 3.7 Results of preliminary sensitivity analysis — Traffic data

Inputs		Data	Faulting	IRI	Cracking
Main		Initial two-way AADTT	I	I	I
		Number of lanes in design direction	-	-	-
		Percent of trucks in design direction (%)	-	-	-
		Percent of trucks in design lane (%)	-	-	-
Traffic Volume Adjustment Factors	Monthly Adjustment	Load monthly adjustment factors (MAF) (sum of the MAF of all months for each class must equal 12)	-	-	-
		Level 1: Site specific distribution	-	-	-
		Level 2: Regional Distribution	-	-	-
		Level 3: Default Distribution (National Avg.)	-	-	-
	Vehicle Class Distribution	AADTT distribution by vehicle class (%)	-	-	-
		Level 1: Site specific distribution	-	-	-
		Level 2: Regional Distribution	-	-	-
		Level 3: Default Distribution (National Avg.)	-	-	-
	Hourly Distribution	Hourly truck traffic distribution by period beginning	National Average		
		Level 1: Site specific distribution			
		Level 2: Regional Distribution			
		Level 3: National Avg.-Default			
	Traffic Growth Factors	Vehicle-class specific traffic growth in percent or Default growth function (all classes) (no growth, linear growth, compound growth)	5		
Axle Load Distribution Factors		Axle factors by axle type (percent of axles (single, tandem, tridem, and quad) in weight categories for each vehicle class for each month) Level 1: Site specific distribution Level 2: Regional Distribution Level 3: Default Distribution (National Avg.)	National Average		

Note: I: Very Sensitive, II: Sensitive, III: Insensitive

Table 3.7 Results of preliminary sensitivity analysis — Traffic data (continued…)

Inputs		Data	Faulting	IRI	Cracking
General Traffic Inputs	Lateral Traffic Wander	Mean wheel location (inches from the lane marking)	I	I	I
		Traffic wander standard deviation (in.)	II	II	II
		Design lane width (ft) ***Software Range: 10 to 13]***	III	III	III
	Number Axles/Truck	Average number of single, tandem, tridem and quad axles per truck	National Average		
		Level 1: Site specific distribution			
		Level 2: Regional Distribution			
		Level 3: Default Distribution (National Avg.)			
	Axle Configuration	Average axle width (edge-to-edge) outside dimension (ft)	III	III	III
		Dual tire spacing (in.)	III	III	I
		Tire Pressure for single and dual tires (psi) ***[Software Range: 120]***	III	III	II
		Axle spacing (in.) for: Tandem Tridem Quad	- 	- 	-
	Wheelbase	Average axle spacing (ft) for: Short trucks Medium trucks Long trucks	 III III III	 III III III	 III III III
		Percents of truck for: Short trucks Medium trucks Long trucks	- 	- 	-

Note: I: Very Sensitive, II: Sensitive, III: Insensitive

Table 3.8 Results of preliminary sensitivity analysis — Structure data for rigid pavement

Inputs		Data	Faulting	IRI	Cracking
Design Feature		Permanent curl/warp effective temperature difference (^oF)[12] ***[Software Range: -30 to 0]***	-	-	-
		Joint spacing (ft) ***[Software Range: 10 to 20]***	I	I	I
		Sealant type (None, Liquid, Silicone, or Preformed)			
		Dowel diameter (in.) and spacing (in.) ***[Software Range: 1 to1.75 [Software Range: 10 to 14]]***	I III	I III	I III
		Edge support (Tied PCC shoulder and/or Widened slab) LTE	I	I	III
		PCC-Base Interface (bonded or unbounded)	III	III	III
		Erodibility index (Extremely resistant (1) through Very erodable (5))	I	II	III
		Loss of bond age (months) ***[Software Range: 0 to120]***	III	III	III
Drainage and Surface Properties		Surface shortwave absorptivity ***[Software Range: 0.5 to 1]***	I	I	I
		Infiltration (Negligible (0%) through Extreme (100%))	III	III	III
		Drainage path length (ft) (not for Negligible infiltration) ***[Software Range: 5 to 25]***	III	III	III
		Pavement cross slope (%) (not for Negligible infiltration) ***[Software Range: 0 to 5]***	III	III	III
Layers - PCC Material Properties	Thermal	PCC material	-	-	-
		Layer thickness (in.) ***[Software Range: 1 to 20]***	I	I	I
		Unit weight (pcf) ***[Software Range: 140 to 160]***	III	III	III
		Poisson's ratio ***[Software Range: 0.1 to 0.3]***	-	-	-
		CTE (per ^oF x 10-6) ***[Software Range: $2*10^{-6}$ to $10*10^{-6}$]***	I	I	I
		Thermal conductivity (BTU/hr-ft-^oF) ***[Software Range: 0.2 to 2]***	I	I	I
		Heat capacity (BTU/lb-^oF)	II	II	I
	Mix	Cement type (Type I, Type II or Type III)	-	-	-
		Cementitious material content (lb/yd^3) ***[Software Range: 400 to800]***	III	III	III
		Water/cement ratio ***[Software Range: 0.3 to 0.7]***	III	III	III
		Aggregate type	-	-	-
		PCC zero-stress temperature (^oF) ***[Software Range: 50 to 125]***	I	I	III
		Ultimate shrinkage at 40% R.H. (microstrain) ***[Software Range: 300 to 1000]***	III	III	III
		Reversible shrinkage (% of ultimate shrinkage) ***[Software Range: 30 to 80]***	III	III	II
		Time to develop 50% of ultimate shrinkage (days) ***[Software Range: 30 to 50]***	III	III	III
		Curing method (curing compound or wet curing)	-	-	-

Note: I: Very Sensitive, II: Sensitive, III: Insensitive

[12] Default value

Table 3.8 Results of preliminary sensitivity analysis — Structure data for rigid pavement (continued...)

Inputs		Data	Faulting	IRI	Cracking
Layers - PCC Material Properties	Strength	Level 1 - Elastic Modulus (psi) and Modulus of Rupture (psi) at 7 – days ***[Software Range: 1 to 7x10^6] [Software Range: 300 to 1000]***	-	-	-
			-	-	-
		14 – days *[Same as above]*	-	-	-
			-	-	-
		28 – days *[Same as above]*	-	-	-
			-	-	-
		90 – days *[Same as above]*	-	-	-
			-	-	-
		Ratio 20 Year/28 Day ***[Software Range: 0 to10] [Software Range: 0 to 10]***	-	-	-
		Level 2 - Compressive strength (psi) at 7 – days ***[Software Range: 2000 to 10000]***	-	-	-
		14 – days ***[Software Range: 2000 to 10000]***	-	-	-
		28 – days ***[Software Range: 2000 to 10000]***	-	-	-
		90 – days ***[Software Range: 2000 to 10000]***	-	-	-
		Ratio 20 Year/28 Day ***[Software Range: 0 to10]***	-	-	-
		Level 3 28-day PCC Compressive Strength (psi) ***[Software Range: 3000 to 8000]***	I	I	I
		28-day PCC Modulus of Rupture (psi) ***[Software Range: 450 to 1200]***	I	I	I
		28-day PCC Elastic Modulus (psi)	I	I	I
Layers- Chemically Stabilized Material		Material type	-	-	-
		Layer thickness (in.) ***[Software Range: 2 to 24]***	-	-	-
		Unit weight (pcf) ***[Software Range:50 to 200]***	-	-	-
		Poisson's ratio ***[Software Range:0.15 to 0.45]***	-	-	-
		Elastic/Resilient Modulus (psi) ***[Software Range: 0.5 to 4x10^6]***	-	-	-
		Minimum Elastic/Resilient Modulus (psi)			
		Modulus of rupture (psi)			
		Thermal conductivity (BTU/hr-ft-oF) ***[Software Range: 0.1 to 4]***	-	-	-
		Heat capacity (BTU/lb-oF) ***[Software Range: 0 to 1]***	-	-	-

Note: I: Very Sensitive, II: Sensitive, III: Insensitive

Table 3.8 Results of preliminary sensitivity analysis — Structure data for rigid pavement (continued.)

Inputs		Data	Faulting	IRI	Cracking
Layers - Unbound Layer Base/ Subbase	General	Unbound Material	-	-	-
		Thickness (in.) ***[Software Range: 1 to 100]***	II	II	II
	Strength Properties	Poisson's ratio ***[Software Range: 0.1 to 0.4]***	III	III	III
		Coefficient of lateral pressure, Ko ***[Software Range: 0.2 to 3]***	-	-	-
		Level 2 (Seasonal or Representative Input) – Modulus (psi) ***[Software Range: 15,000 to 40,000]***	III	III	III
		Level 3 (Representative Input only) - Modulus (psi) ***[Software Range: 15,000 to 40,000]***	III	III	III
	ICM	Plasticity Index ***[Software Range: 0 to 6]***	II	II	II
		Passing #200 sieve (%)***[Software Range: 0 to15]***	II	II	II
		Passing #4 sieve (%)***[Software Range: 0 to 100]***	III	III	III
		D60 (mm) ***[Software Range: 2 to 25]***	III	III	II
		Compacted unbound material or Un-compacted/Natural unbound material	-	-	-
Layers - Unbound Layer Subgrade	General	Unbound Material	I	I	I
		Thickness (in.) ***[Software Range: 1 to 100]***	-	-	-
	Strength Properties	Poisson's ratio ***[Software Range: 0.1 to 0.4]***	III	III	II
		Coefficient of lateral pressure, Ko ***[Software Range: 0.2 to 3]***	-	-	-
		Level 3 (Representative Input only) - Modulus (psi) ***[Software Range: 5,000 to 25,000]***	II	II	II
	ICM	Plasticity Index ***[Software Range: 0 to 10]***[13]	III	III	I
		Passing #200 sieve (%)***[Software Range: 36 to100]***	II	II	II
		Passing #4 sieve (%)***[Software Range: 0 to 100]***	III	III	III
		D60 (mm) ***[Software Range: 0.001 to 25]***	III	III	III
		Compacted unbound material or Un-compacted/Natural unbound material	-	-	-

Note: I: Very Sensitive, II: Sensitive, III: Insensitive

[13] Default range depends on the soil type

Based on the results summarized in Tables 3.7 and 3.8, a list of sensitive (significant) variables was prepared. There are 23 input variables characterizing environment, traffic loading, pavement section materials, etc (see Table 3.9). As a benchmark, for a full factorial experiment design, a complete test of 23 variables, each at three levels, requires $3^{23} = 9.41 \times 10^{10}$ tests (runs), which is an impossible task. In addition, the analyses will be impracticable given the time and the financial constraints. Therefore, the project team decided to reduce the number of variables and their levels to decrease the runs within an achievable practical limit. This was accomplished by adopting the following strategies:

- By conducting separate satellite sensitivity for certain important variables such as traffic.
- By considering the variables, that can be controlled at the design stage, such as joint spacing, edge support and slab thickness. It is important to note that some variables such as subgrade type and traffic are site dependent, the designer may not have a choice to vary them; however, design variables can be selected to fulfill the requirements for a particular site.
- By considering only surrogated variables. For example, *fc'* is correlated with MOR, hence MOR was only considered in the analysis.

Based on the latter two strategies and MDOT's state-of-practice for rigid pavements and discussions with the project TAG, the list of input variables was further refined. For example, in practice (Michigan), the dowel diameter and dowel spacing are generally not varied. Table 3.10 shows the final input variables along with their levels for detailed sensitivity analysis. Six variables have two levels while climate has three levels which make the full factorial with 192 runs ($2^6 \times 3$). Table 3.11 shows the full factorial design matrix for the detailed sensitivity analysis. Figure 3.11 present the typical pavement cross-section for rigid pavements adopted in this sensitivity.

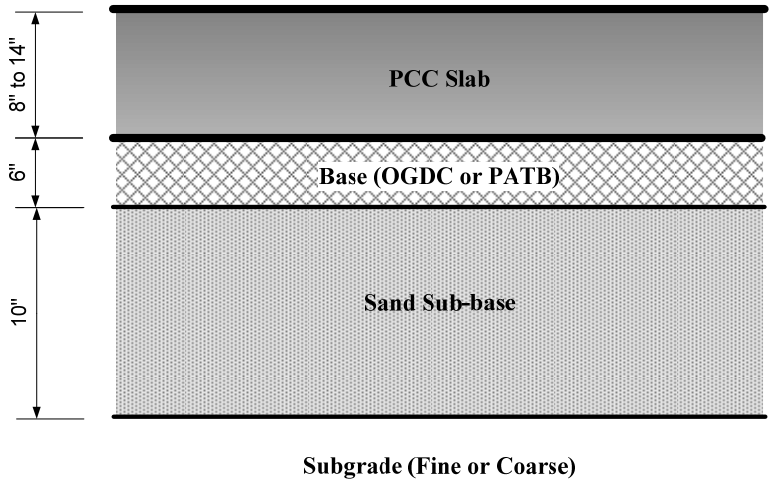

Figure 3.11 Rigid pavement cross-section used for analysis

Table 3.9 List of sensitive input variables from preliminary sensitivity

Category		Input variable	Levels
Traffic		AADTT	Low, Medium and High
		Axle Load Spectra	Low, Medium and High
		Monthly Adjustment Factors	Low, Medium and High
		Hourly Adjustment Factors	Low, Medium and High
Design		Permanent Curl/Warp Effective Temperature Difference	-10
		Joint Spacing (ft)	10, 15 and 25
		Edge Support	Tied, Asphalt and Widened
		Dowel Diameter (in)	1, 1.25 and 1.5
		Dowel Spacing (in)	10, 12 and 15
Surface Properties		Surface Shortwave Absorptivity	0.85
Materials	PCC	PCC Slab Thickness	7, 9 and 14
		CTE (per ^{o}F)	4×10^{-6}, 5.5×10^{-6} and 7×10^{-6}
		Thermal Conductivity (BTU/hr-ft-^{o}F)	0.2, 1.25 and 2
		PCC Zero-stress Temperature (^{o}F)	70, 98 and 125
		fc' (Compressive Strength, psi)	3000, 5000 and 8000
		MOR (Modulus of Rupture, psi)	450, 750 and 1200
		Elastic Modulus (psi)	2×10^{6}, 4×10^{6} and 6×10^{6}
	Base/Subbase	Base Type	Granular Base and Asphalt Treated
		Base Thickness (in)	2, 6 and 10
		Passing # 200	0, 8 and 15
		Plasticity Index	0, 3 and 6
	Subgrade	Soil Type	A-7-6, A-4 and A-1-a
		Passing # 200	30, 60 and 90
		Plasticity Index	0, 5 and 10
Environmental		Different Climatic Regions	Extreme and Moderate

Note: Excluding two variables—Permanent curl/warp effective temperature difference and surface shortwave absorptivity, there are remaining 23 variables in the above list to be considered for further analysis.

Table 3.10 Final variable list for JPCP incorporating Michigan state-of-the-practice

Category		Surrogate Variable	Levels	Remarks
Design		Edge Support	12 ft tied shoulder *versus* 14 ft asphalt shoulder	2 Levels[14]
		PCC Slab Thickness	9 inches (Joint Spacing = 14 ft) (Dowel Diameter = 1.25 in) (Dowel Spacing = 12 in) *versus* 14 inches (Joint Spacing = 16 ft) (Dowel Diameter = 1.5 in) (Dowel Spacing = 12 in)	2 Levels[15]
Materials	PCC	CTE (per ^{o}F)	4×10^{-6} *versus* 6.5×10^{-6}	2 Levels[16]
		MOR (Modulus of Rupture, psi)	450 *versus* 900	2 Levels[17]
	Base/Subbase	Base Type	Granular Base *versus* Asphalt Treated	2 Levels[18]
	Subgrade	Soil Type	A-7-6 (fine) *versus* A-1-a (Coarse)	2 Levels[19]
Environmental		Different Climatic Regions	Lansing Pellston Detroit	3 Levels[20]

[14] Edge support is dependent lane width and shoulder type (MDOT practice)
[15] Slab thickness is tied with joint spacing, dowel diameter and dowel spacing (MDOT practice)
[16] Based on aggregate types
[17] *fc'* and *E* is correlated with *MOR*
[18] Asphalt treated base is permeable asphalt treated base
[19] Change strength and material properties according to soil type
[20] Represents three different climatic regions within Michigan

Table 3.11 Matrix for JPCP sensitivity analyses

Slab Thickness	Edge Support	Base Type	CTE	MOR	Soil Type/Climate						Total
					Coarse			Fine			
					Detroit	Lansing	Pellston	Detroit	Lansing	Pellston	
9	Asphalt	DGAB	4	450	1	2	3	4	5	6	6
				900	7	8	9	10	11	12	6
			6.5	450	13	14	15	16	17	18	6
				900	19	20	21	22	23	24	6
		PATB	4	450	25	26	27	28	29	30	6
				900	31	32	33	34	35	36	6
			6.5	450	37	38	39	40	41	42	6
				900	43	44	45	46	47	48	6
	Tied	DGAB	4	450	49	50	51	52	53	54	6
				900	55	56	57	58	59	60	6
			6.5	450	61	62	63	64	65	66	6
				900	67	68	69	70	71	72	6
		PATB	4	450	73	74	75	76	77	78	6
				900	79	80	81	82	83	84	6
			6.5	450	85	86	87	88	89	90	6
				900	91	92	93	94	95	96	6
14	Asphalt	DGAB	4	450	97	98	99	100	101	102	6
				900	103	104	105	106	107	108	6
			6.5	450	109	110	111	112	113	114	6
				900	115	116	117	118	119	120	6
		PATB	4	450	121	122	123	124	125	126	6
				900	127	128	129	130	131	132	6
			6.5	450	133	134	135	136	137	138	6
				900	139	140	141	142	143	144	6
	Tied	DGAB	4	450	145	146	147	148	149	150	6
				900	151	152	153	154	155	156	6
			6.5	450	157	158	159	160	161	162	6
				900	163	164	165	166	167	168	6
		PATB	4	450	169	170	171	172	173	174	6
				900	175	176	177	178	179	180	6
			6.5	450	181	182	183	184	185	186	6
				900	187	188	189	190	191	192	6
Total					32	32	32	32	32	32	192

CHAPTER 4 - DETAILED SENSITIVITY ANALYSIS - RIGID

In Chapter 3, a sensitivity matrix was developed through preliminary sensitivity analyses and was used to execute the M-E PDG software. Table 4.1 summarizes the runs required within each cell of the full-factorial matrix. These runs were executed to capture pavement performance curves (cracking, faulting, and IRI). The performance magnitudes at 5, 10, 20 and 30 years were used to conduct Analysis of Variance (ANOVA). In this analysis all main effects and all possible two-way interactions were considered between seven variables. Once all the desired runs were accomplished, a database was prepared to study the input variables and various pavement performance measures. Using this database, detailed statistical analyses were conducted for each predicted performance measure. The results of these are discussed next.

4.1 EFFECT OF INPUT VARIABLES ON CRACKING

The detailed analyses were performed in two steps. Initially, the descriptive statistics such as mean performance for each input variable was summarized. However, as the differences in the means might not ascertain a significant difference, essentially due to uncertainty (variability) associated with means. Therefore, statistically analyses using ANOVA were performed for all performance measures.

4.1.1 Descriptive Statistics

Table 4.2 shows the cracking performance within each cell of the full-factorial design matrix at 30 years life. Also, the row and column averages are presented in the same table. The row averages can be used to investigate the main effects of input variables ignoring various subgrade types and climates within the state of Michigan. Furthermore, the column averages can be utilized to study the effects of subgrade types and climate, ignoring other input variables. Similar tables were generated for cracking at 5, 10, 15 and 20 years and are presented in Appendix A.

Also to investigate the descriptive or average effects of all input variables on cracking, time series averages were plotted for the various input variables levels. Figure 1 presents the input variables effects on percent slabs cracked in rigid pavements. These effects are summarized below:

Slab Thickness: Figure 4.1 (a) shows the percent slabs cracked for 9- and 14-inches thick slabs. It is evident, that effect of slab thickness is very significant on cracking. Rigid pavement with thin slab thickness showed higher cracking than those with thick slabs. Also, the results show that this effect is more pronounced over a longer life of a pavement.

Edge Support: In general, rigid pavements with asphalt shoulders (untied) showed higher cracking than those with tied shoulders, as shown by Figure 4.1 (b). However, the effect of edge support is not as significant as of slab thicknesses.

Base Type: Two types of bases were used in this analysis; a dense graded aggregate base (DGAB) and a permeable asphalt treated base (PATB). The base thickness was fixed at 6-inches and a 10-inch thick sand subbase (see Chapter 3), according to MDOT practice, was considered in all the runs. The results of the predicted cracking show that at early age, rigid pavements with PATB base performed marginally better than those with DGAB base. However, over the long-term (after 30 years) the effect of base type diminishes for cracking [see Figure 4.1 (c)].

Coefficient of Thermal Expansion (CTE): A significant effect of CTE was observed for cracking performance. The pavements with higher CTE showed much higher cracking than those with a lower CTE value. This effect is consistent throughout the life span of a rigid pavement as presented in Figure 4.1 (d).

Modulus of Rupture (MOR): Similarly, MOR effect on cracking performance of rigid pavement seems to be the most significant. Pavements slab having a higher MOR exhibited little or no cracking as compared to those with lower MOR, which showed a very high level of cracking; see Figure 1 (e). This effect is also consistent over the life span of rigid pavements.

Subgrade Type: Marginal to insignificant effects were noticed for subgrade types, see Figure 4.1 (f). The pavements constructed on fine subgrade showed slightly higher cracking than those constructed on coarse subgrade.

Climate: In order to investigate the effects of climate on cracking performance of rigid pavements within Michigan, three locations were selected in this analysis. Figure 4.1 (g) shows that on average, the climate seems to have a slight effect on cracking in Michigan. Rigid pavements located in Pellston exhibited a higher amount of cracking than those located in Detroit and Lansing area. The effect of location seems to be consistent with time.

It should be noted that the above discussion of the results is simply based on the average performance. To ascertain the real effects of input variables on the predicted cracking of rigid pavements, statistical analyses (ANOVA) is warranted. Also, the above simple analyses only assisted in the interpretation of the main effects of input variables, while interaction between input variables still needs to be explored. Therefore, detailed statistical analyses were executed to address the above mentioned short-comings. The outcomes of such type of analyses are described next.

4.1.2 Statistical Analysis (ANOVA)

The main objectives of the statistical analyses are to: (a) obtain the real effects with some level of confidence, (b) explore the interactive effects between various input variables, and (c) attain definite conclusions. Typically, a full-factorial experiments design such as considered in this study can be analyzed using fixed-effect models employing analysis of variance (ANOVA). This type of statistical analyses can help in identifying the main and the interactive effects between considered variables. However, it should be noted that if certain variables are interacting with each other, their main effect should not be considered while making a conclusion. Therefore, conclusions in this case should be based on the cell means rather than marginal means. For example, the summary results from ANOVA are given in Table 4.6 at 30 years. A *p-value* less

than 0.05 (i.e. a confidence level of 95%) is used as a threshold to identify a statistical significant effect. The results are presented below according to main and interaction.

Main Effects

The results in Table 4.3 confirm that input variables such as PCC slab thickness, CTE of the concrete mixture and MOR have a statistically significant effect on the cracking performance. The mean values for all variables are presented in Table 4.4. The interpretation of only statistically significant effects is presented below:

Slab Thickness: Rigid pavements with thicker PCC slabs out perform those with thinner PCC slab thickness. The practical significance of this effect can be assessed using criteria mentioned in Chapter 3 and comparing differences in the cracking performance between 9- and 14-inch slab thicknesses (see Table 3.6). Applying this criterion, one can easily identify that effect of slab thickness on cracking is practically significant as well.

CTE: Pavement concrete having a higher CTE value has shown higher amount of cracking than those which have a lower CTE value. This effect is also of practical significance.

MOR: The flexure strength of the concrete has the most significant effect on the cracking performance. Concrete pavements having a higher strength have exhibited negligible cracking even after 30 years as compared to those having low strength concrete, which showed enormous amount of cracking at the same age. This effect is also of practical significance.

Interaction Effects

Table 3 also shows the significant interactions between input variables. The interactions between CTE and slab thickness, MOR and slab thickness, and CTE and MOR were found to be of statistically significance (*p-value* < 0.05). Table 4.5 shows the summary of cell means for these interactions, which can be used to explain these effects. While results were summarized above for the significant main effects, if certain variables are interacting with each other, their main effect should not be considered while making a conclusion. The following findings can be drawn from these results:

CTE by Slab Thickness: This interaction shows that for a lower level of CTE, slab thickness has a significant effect on the cracking. This effect is of both practical and statistical significance. On the other hand, for higher level of CTE, the slab thickness did not show a very significant difference in cracking performance. From the design perspective, the results of this interactive effect imply that if the CTE for a concrete is higher, increasing slab thickness will not help in achieving better cracking performance.

MOR by Slab Thickness: This interaction demonstrates that effect of slab thickness on cracking is more prominent for lower MOR than for higher MOR concrete. This means that for cracking, change in thickness is more important for lower MOR values in designing rigid pavements. These effects are of both statistical and practical significance.

CTE by MOR: The interaction between CTE and MOR was found to be the most important for rigid pavements. The combination of higher CTE with lower MOR is drastic for cracking. This also means that higher flexural strength of concrete can compensate for a higher CTE value. These effects are of both statistical and practical significance.

Table 4.1 Matrix for JPCP sensitivity runs

Slab Thickness	Edge Support	Base Type	CTE	MOR	Soil Type/Climate						Total
					Coarse			Fine			
					Detroit	Lansing	Pellston	Detroit	Lansing	Pellston	
9	Asphalt	DGAB	4	450	1	2	3	4	5	6	6
				900	7	8	9	10	11	12	6
			6.5	450	13	14	15	16	17	18	6
				900	19	20	21	22	23	24	6
		PATB	4	450	25	26	27	28	29	30	6
				900	31	32	33	34	35	36	6
			6.5	450	37	38	39	40	41	42	6
				900	43	44	45	46	47	48	6
	Tied	DGAB	4	450	49	50	51	52	53	54	6
				900	55	56	57	58	59	60	6
			6.5	450	61	62	63	64	65	66	6
				900	67	68	69	70	71	72	6
		PATB	4	450	73	74	75	76	77	78	6
				900	79	80	81	82	83	84	6
			6.5	450	85	86	87	88	89	90	6
				900	91	92	93	94	95	96	6
14	Asphalt	DGAB	4	450	97	98	99	100	101	102	6
				900	103	104	105	106	107	108	6
			6.5	450	109	110	111	112	113	114	6
				900	115	116	117	118	119	120	6
		PATB	4	450	121	122	123	124	125	126	6
				900	127	128	129	130	131	132	6
			6.5	450	133	134	135	136	137	138	6
				900	139	140	141	142	143	144	6
	Tied	DGAB	4	450	145	146	147	148	149	150	6
				900	151	152	153	154	155	156	6
			6.5	450	157	158	159	160	161	162	6
				900	163	164	165	166	167	168	6
		PATB	4	450	169	170	171	172	173	174	6
				900	175	176	177	178	179	180	6
			6.5	450	181	182	183	184	185	186	6
				900	187	188	189	190	191	192	6
Total					32	32	32	32	32	32	192

Table 4.2 Fatigue cracking in rigid pavements after 30 years - % slab cracked

Slab Thickness	Edge Support	Base Type	CTE	MOR	Soil Type						Average
					Coarse			Fine			
					Detroit	Lansing	Pellston	Detroit	Lansing	Pellston	
9	Asphalt	DGAB	4	450	93.2	80.6	96.9	99	96.7	99.3	94.3
				900	0	0	0	0	0	0	0.0
			6.5	450	100	100	100	100	100	100	100.0
				900	1.2	0.3	2.7	0.7	0.2	1.6	1.1
		PATB	4	450	89.2	67.8	93.6	98.5	94.7	98.7	90.4
				900	0	0	0	0	0	0	0.0
			6.5	450	100	100	100	100	100	100	100.0
				900	1.3	0.3	2.8	0.8	0.2	1.5	1.2
	Tied	DGAB	4	450	69.1	42.5	83.9	92.5	80.7	94.3	77.2
				900	0	0	0	0	0	0	0.0
			6.5	450	100	99.9	100	100	99.9	100	100.0
				900	0.3	0.1	0.6	0.2	0.1	0.5	0.3
		PATB	4	450	61.4	31.7	72	88.9	71.7	90.5	69.4
				900	0	0	0	0	0	0	0.0
			6.5	450	100	99.8	100	100	99.8	100	99.9
				900	0.3	0.1	0.6	0.3	0.1	0.6	0.3
14	Asphalt	DGAB	4	450	0.9	0.1	1	0.2	0	0.3	0.4
				900	0	0	0	0	0	0	0.0
			6.5	450	97.6	95.6	99	91.5	82.1	96.7	93.8
				900	0	0	0	0	0	0	0.0
		PATB	4	450	1	0.2	0.9	0.4	0	0.3	0.5
				900	0	0	0	0	0	0	0.0
			6.5	450	98.2	95.9	99.2	93	82.7	97	94.3
				900	0	0	0	0	0	0	0.0
	Tied	DGAB	4	450	0.3	0	0.4	0.1	0	0.1	0.2
				900	0	0	0	0	0	0	0.0
			6.5	450	95.1	91	98.1	84.4	70.4	94.3	88.9
				900	0	0	0	0	0	0	0.0
		PATB	4	450	0.4	0.1	0.5	0.1	0	0.1	0.2
				900	0	0	0	0	0	0	0.0
			6.5	450	96.2	91.1	98.4	87.1	70.8	94.8	89.7
				900	0	0	0	0	0	0	0.0
Total					34.6	31.2	36.0	35.6	32.8	36.6	34.4

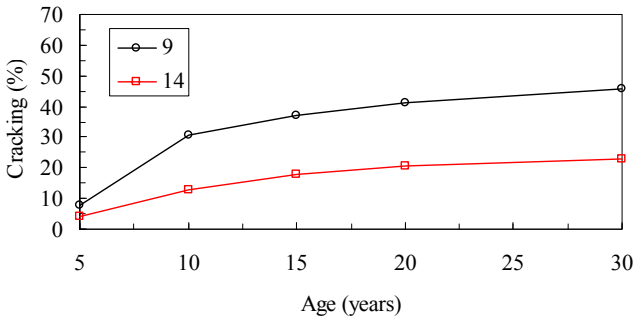

(a) Effect of *slab thickness* on cracking

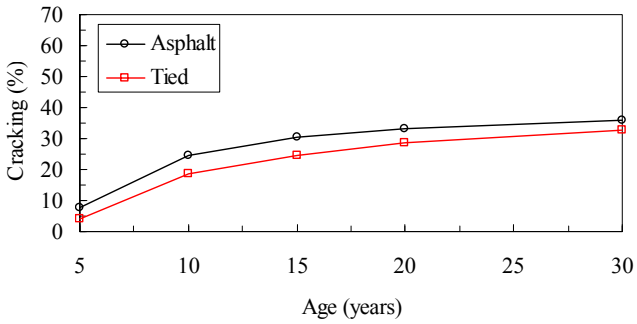

(b) Effect of *edge support* on cracking

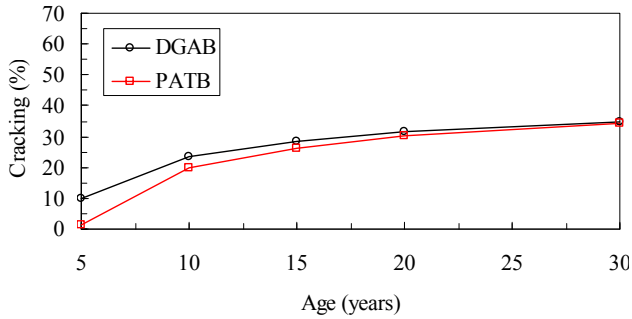

(c) Effect of *base type* on cracking

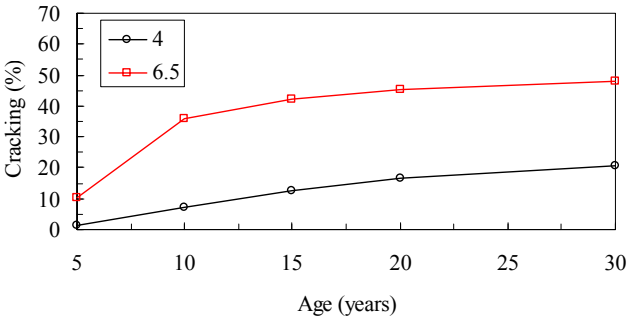

(d) Effect of *CTE* on cracking

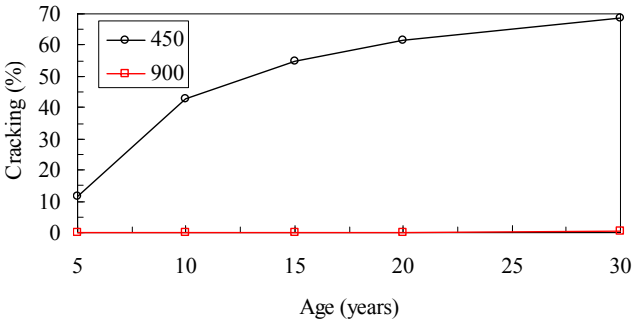

(e) Effect of *MOR* on cracking

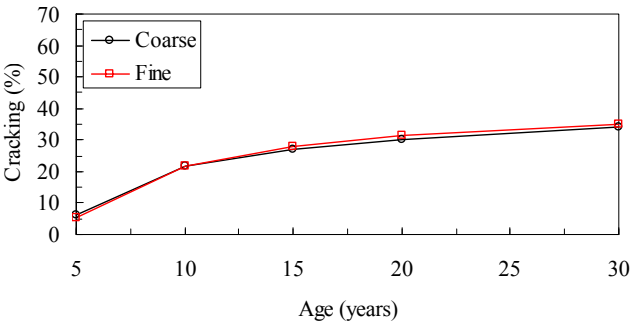

(f) Effect of *subgrade type* on cracking

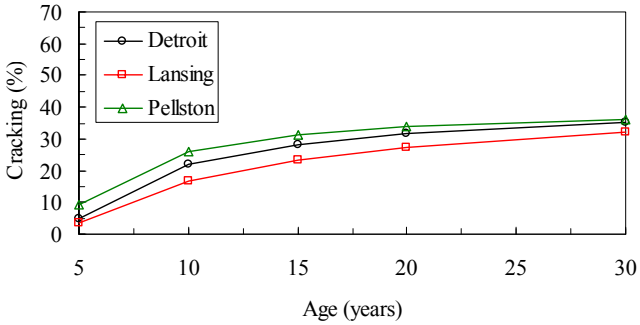

(g) Effect of *climate* on cracking

Figure 4.1 Main effects of the most sensitive input variables on JPCP cracking

Table 4.3 ANOVA results for fatigue cracking in rigid pavements after 30 years

Source	Type III Sum of Squares	df	Mean Square	F	Sig.
Corrected Model	1710.206[(a)]	35	48.863	40.457	.000
Intercept	55.610	1	55.610	46.044	.000
PCCThick	166.899	1	166.899	138.188	.000
EdgeSupp	3.567	1	3.567	2.953	.088
BaseType	.016	1	.016	.013	.910
CTE	178.622	1	178.622	147.894	.000
MOR	1167.769	1	1167.769	966.886	.000
SoilType	.813	1	.813	.673	.413
Climate	6.633	2	3.317	2.746	.067
PCCThick * EdgeSupp	.324	1	.324	.268	.605
PCCThick * BaseType	.026	1	.026	.021	.884
PCCThick * CTE	55.352	1	55.352	45.830	.000
PCCThick * MOR	60.290	1	60.290	49.918	.000
PCCThick * SoilType	.724	1	.724	.599	.440
PCCThick * Climate	.510	2	.255	.211	.810
EdgeSupp * BaseType	.005	1	.005	.004	.951
EdgeSupp * CTE	.041	1	.041	.034	.855
EdgeSupp * MOR	.010	1	.010	.008	.928
EdgeSupp * SoilType	.071	1	.071	.059	.809
EdgeSupp * Climate	.111	2	.056	.046	.955
BaseType * CTE	4.69E-006	1	4.69E-006	.000	.998
BaseType * MOR	.000	1	.000	.000	.992
BaseType * SoilType	.002	1	.002	.002	.967
BaseType * Climate	.023	2	.012	.010	.990
CTE * MOR	67.415	1	67.415	55.818	.000
CTE * SoilType	.041	1	.041	.034	.854
CTE * Climate	.287	2	.144	.119	.888
MOR * SoilType	.149	1	.149	.123	.726
MOR * Climate	.165	2	.082	.068	.934
SoilType * Climate	.343	2	.171	.142	.868
Error	188.411	156	1.208		
Total	1954.227	192			
Corrected Total	1898.617	191			

a R Squared = .901 (Adjusted R Squared = .878)

Table 4.4 Main effects of input variables on cracking

Input Variable	Levels	Mean % Slabs Cracked					Mean Differences				
		5 years	10 years	15 years	20 years	30 years	Δ_5	Δ_{10}	Δ_{15}	Δ_{20}	Δ_{30}
Slab Thickness (inches)	9	7.60	30.44	37.28	41.33	45.90	3.54	17.77	19.63	20.92	22.85
	14	4.06	12.68	17.65	20.41	23.05					
Edge Support	Asphalt	7.74	24.71	30.36	33.32	36.04	3.83	6.29	5.79	4.89	3.12
	Tied	3.92	18.41	24.57	28.43	32.92					
Base Type	DGAB	10.15	23.32	28.53	31.57	34.79	8.64	3.51	2.13	1.40	0.63
	PATB	1.51	19.80	26.40	30.17	34.16					
CTE	4	1.38	7.20	12.57	16.39	20.83	-8.90	-28.72	-29.79	-28.96	-27.28
	6.5	10.28	35.92	42.36	45.35	48.12					
MOR (psi)	450	11.56	43.02	54.82	61.60	68.70	11.46	42.92	54.71	61.47	68.44
	900	0.10	0.10	0.11	0.14	0.26					
Soil Type	Coarse	6.13	21.56	26.98	30.21	33.93	0.60	-0.01	-0.97	-1.32	-1.10
	Fine	5.53	21.56	27.95	31.53	35.03					
Climate	Detroit	5.05	21.87	28.04	31.56	35.09	-5.83	-8.91	-7.81	-6.56	-4.27
	Lansing	3.31	16.95	23.27	27.24	32.03					
	Pellston	9.13	25.86	31.08	33.81	36.31					

Table 4.5 Interaction effects of input variables on cracking

Input Variables		Levels1	Levels2	Mean % Slabs Cracked				Mean Differences			
1	2			5 years	10 years	20 years	30 years	Δ_5	Δ_{10}	Δ_{20}	Δ_{30}
CTE	Slab Thickness	4	9	2.66	14.30	32.66	41.45	2.56	14.20	32.54	41.24
			14	0.10	0.10	0.12	0.21				
		6.5	9	12.54	46.58	50.00	50.35	4.52	21.33	9.30	4.46
			14	8.02	25.25	40.70	45.89				
MOR	Slab Thickness	450	9	15.10	60.79	82.49	91.39	7.08	35.53	41.76	45.39
			14	8.02	25.25	40.72	46.00				
		900	9	0.10	0.10	0.18	0.41	0.00	0.00	0.08	0.31
			14	0.10	0.10	0.10	0.10				
CTE	MOR	4	450	2.66	14.30	32.68	41.57	2.56	14.20	32.58	41.47
			900	0.10	0.10	0.10	0.10				
		6.5	450	20.46	71.74	90.53	95.83	20.36	71.64	90.35	95.41
			900	0.10	0.10	0.18	0.41				

4.2 EFFECT OF INPUT VARIABLES ON FAULTING

Again, the detailed analyses were performed in two steps. Initially, the descriptive statistics such as mean performance for each input variable was summarized. However, as the differences in the means might not ascertain a significant difference, essentially due to uncertainty (variability) associated with means. Therefore, statistically analyses using ANOVA were performed for predicted joint faulting.

4.2.1 Descriptive Statistics

Table 4.6 shows the faulting performance within each cell of the full-factorial design matrix at 30 years life. Also, the row and column averages are presented in the same table. The row averages can be used to investigate the main effects of input variables ignoring various subgrade types and climates within the state of Michigan. Furthermore, the column averages can be utilized to study the effects of subgrade types and climate ignoring other input variables. Similar tables were generated for faulting at 5, 10, 15 and 20 years and are attached in Appendix A.

Also to investigate the average effects of all input variables on faulting, time series averages were plotted for each input variables levels. Figure 2 presents the input variables effects on joint faulting in rigid pavements. These effects are summarized below:

Slab Thickness: Figure 4.2 (a) shows the joint faulting for 9- and 14-inches thick slabs. It is evident, that the effect of slab thickness is very significant on faulting. Rigid pavement with thin slab thickness showed higher faulting than those with thick slabs. Also, the results show that this effect is more pronounced at a latter life of a pavement.

Edge Support: In general, rigid pavements with asphalt shoulders (untied) showed higher faulting than those with tied shoulders, as shown by Figure 4.2 (b). However, the effect of edge support is not as significant as of slab thicknesses.

Base Type: Two types of bases were used in this analysis; a dense graded aggregate base (DGAB) and a permeable asphalt treated base (PATB). The base thickness was fixed at 6-inches and 10-inch thick sand subbase (see Chapter 3) was considered in all the runs. The results of the predicted faulting show that at an early age, rigid pavements with PATB base performed slightly better than those with DGAB base. However, in the long-term (after 30 years) the effect of base type increases for faulting [see Figure 4.2 (c)].

Coefficient of Thermal Expansion (CTE): A significant effect of CTE was observed on faulting performance. The pavement slabs with higher CTE showed much higher faulting than those with a lower CTE value. This effect is consistent and increases throughout the life span of a rigid pavement as presented in Figure 4.2 (d).

Modulus of Rupture (MOR): MOR effect on faulting performance of rigid pavement seems to be the least significant. Pavement slabs having a higher MOR exhibited less faulting as compared to those with lower MOR, which showed slightly higher level of faulting; see Figure 4.2 (e). This effect increases over the life span of rigid pavements.

Subgrade Type: A significant effect was noticed for subgrade type, see Figure 4.2 (f). The pavements constructed on fine subgrade exhibited higher amount of faulting than those constructed on coarse subgrade. The effect of subgrade type is more pronounced in the long-term.

Climate: In order to investigate the effects of climate on joint faulting for rigid pavements within Michigan, three locations were selected in this analysis. Figure 4.2 (g) shows that on average, the climate seems to have a very low effect on faulting. Rigid pavements located in Detroit exhibited higher amount of faulting than those located in Pellston and Lansing area. The effect of location seems to be consistent with time.

It should be noted that above discussion of the results is simply based on the average performance. To ascertain the real effects of input variables on the predicted faulting of rigid pavements, statistical analyses (ANOVA) is warranted. Also, the above simple analyses only helped in the interpretations of the main effects of input variables, while interaction between input variables still needs to be explored. Therefore, detailed statistical analyses were executed to address above mentioned short-comings. The outcomes of such type of analyses are described next.

4.2.2 Statistical Analysis (ANOVA)

Typically, a full-factorial experiments design such as considered in this study can be analyzed using fixed-effect models employing analysis of variance (ANOVA). This type of statistical analyses can help in identifying the main and the interactive effects between input variables. However, it should be noted that if certain variables are interacting with each other, their main effect should not be considered while making conclusion. Therefore, conclusions in this case should be based on the cell means rather than marginal means.

As an example, the summary results from ANOVA are given in Table 4.7 at 30 years. A *p-value* less than 0.05 (i.e. a confidence level of 95%) is used as a threshold to identify a statistically significant effect. The results are presented below according to main and interaction effects.

Main Effects

The results in Table 4.7 confirm that all input variables have a statistically significant effect on the joint faulting. The mean values for all variables are presented in Table 8. While all input variables effect joint faulting significantly, the difference for input levels of each variable should pass the test of practical significance. The interpretation of only statistical and practical significant effects is presented below:

Slab Thickness: Rigid pavements with thicker PCC slabs out performed those with thinner PCC slab thickness. The practical significance of this effect can be assessed using criteria mentioned in Table 3.6 and comparing the difference in the faulting performance between 9- and 14-inch slab thicknesses (see Table 4.8). Applying this criterion, one can easily identify that the effect of slab thickness on faulting is of practical significance.

CTE: Concrete having a higher CTE value has shown a higher amount of faulting than those which have a lower CTE value. This effect is also of practical significance.

Interaction Effects

Table 4.7 also shows the significant interactions between input variables. The interactions between several input variables were found to be of statistically significance (*p-value* < 0.05). Table 4.9 shows the summary of cell means for these interactions, which can be used to explain these effects. While results were summarized above for the significant main effects, if certain variables are interacting with each other, their main effect should not be considered while making conclusions. Due to low predicted values of faulting, the effects can be statistically significant for very low mean differences between various levels of input variables. However, a practical significance may help explain some of these effects. The following findings can be drawn from these results:

CTE by Slab Thickness: This interaction shows that for a higher level of CTE, slab thickness has a significant effect on the faulting. This effect is of both practical and statistical significance. On the other hand, for lower level of CTE, the slab thickness did not show a very significant difference in faulting performance. From the design perspective, the results of this interactive effect imply that if the CTE for a concrete is higher, increasing slab thickness will help in achieving better faulting performance.

MOR by Slab Thickness: This interaction demonstrates that effect of slab thickness on faulting is more prominent for higher MOR than for lower MOR concrete. This means that for faulting, change in thickness is more important for higher MOR values in designing rigid pavements. These effects are of both statistical and practical significance.

Soil Type by CTE: The interaction between soil type and CTE was found to be the most important for rigid pavements. The combination of higher CTE with fine subgrade soil is drastic for faulting. This also means that a lower CTE value of concrete can compensate for pavements constructed on fine grained subgrade soils. These effects are of both statistical and practical significance.

Climate by CTE: The interaction between climate and CTE was both statistically and practically significant. Therefore, it is very important to consider CTE values while designing a pavement in a particular climate even within the state of Michigan. Results show that rigid pavements in Detroit region are more prone to faulting while Lansing and Pellston showed slight lower levels of predicted faulting. Therefore, for pavement design, a lower CTE value will help in better joint faulting performance.

It should be noted that the level of faulting in all main and interaction effects, in the above analyses, were well below the MDOT acceptable threshold. This is mainly because of considering doweled joints in the analyses. Therefore, the results can only be used for making comparisons to study the relative effects of inputs on faulting. The results also indicate that if proper design is adopted, faulting may not be a problem in Michigan.

Table 4.6 Faulting in rigid pavements after 30 years

Slab Thickness	Edge Support	Base Type	CTE	MOR	Soil Type						Average
					Coarse			Fine			
					Detroit	Lansing	Pellston	Detroit	Lansing	Pellston	
9	Asphalt	DGAB	4	450	1.17	0.99	0.97	1.98	1.75	1.65	1.418
				900	1.63	1.40	1.37	2.26	2.01	1.91	1.761
			6.5	450	3.71	3.71	3.66	4.75	4.39	4.57	4.132
				900	4.52	4.19	4.47	5.31	4.95	5.16	4.767
		PATB	4	450	0.81	0.64	0.64	1.55	1.30	1.24	1.029
				900	1.17	0.91	0.97	1.73	1.42	1.40	1.266
			6.5	450	3.23	2.82	3.10	4.29	3.86	4.04	3.556
				900	4.06	3.63	3.91	4.78	4.32	4.57	4.212
	Tied	DGAB	4	450	0.99	0.84	0.81	1.78	1.55	1.45	1.236
				900	1.42	1.22	1.14	2.03	1.78	1.68	1.545
			6.5	450	3.40	3.07	3.25	4.47	4.11	4.22	3.755
				900	4.14	3.81	3.94	4.98	4.60	4.70	4.360
		PATB	4	450	0.71	0.56	0.51	1.37	1.12	1.04	0.885
				900	0.99	0.76	0.76	1.50	1.22	1.17	1.067
			6.5	450	2.92	2.51	2.67	3.99	3.53	3.63	3.209
				900	3.61	3.15	3.33	4.39	3.91	4.06	3.742
14	Asphalt	DGAB	4	450	0.79	0.69	0.61	1.30	1.17	1.07	0.936
				900	0.71	0.61	0.56	1.12	1.02	0.91	0.821
			6.5	450	2.41	2.21	2.18	3.20	3.00	2.95	2.659
				900	2.41	2.18	2.13	3.10	2.90	2.79	2.587
		PATB	4	450	0.46	0.38	0.41	0.84	0.74	0.66	0.580
				900	0.43	0.38	0.38	0.74	0.66	0.64	0.538
			6.5	450	1.91	1.65	1.60	2.64	2.36	2.26	2.070
				900	1.88	1.63	1.63	2.49	2.24	2.16	2.002
	Tied	DGAB	4	450	0.66	0.58	0.51	1.14	1.04	0.94	0.813
				900	0.61	0.53	0.46	0.99	0.89	0.79	0.711
			6.5	450	2.18	1.98	1.93	2.97	2.77	2.72	2.426
				900	2.16	1.96	1.85	2.87	2.67	2.54	2.341
		PATB	4	450	0.38	0.30	0.28	0.74	0.64	0.56	0.483
				900	0.36	0.30	0.30	0.64	0.56	0.53	0.449
			6.5	450	1.68	1.45	1.35	2.41	2.13	2.01	1.837
				900	1.63	1.42	1.40	2.26	2.01	1.91	1.770
Average					1.848	1.640	1.658	2.519	2.269	2.247	2.030

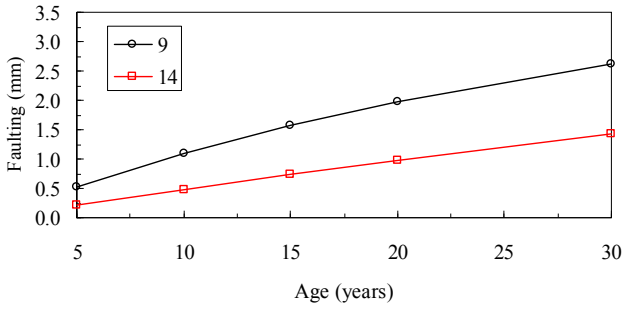

(a) Effect of *slab thickness* on faulting

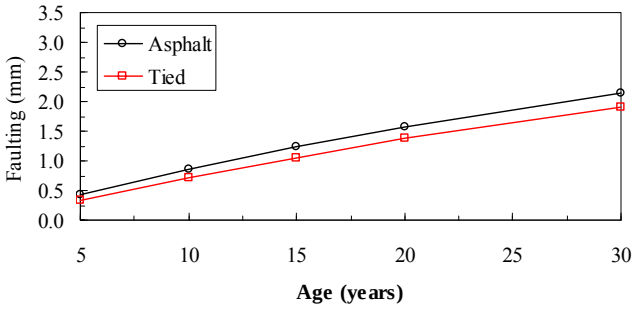

(b) Effect of *edge support* on faulting

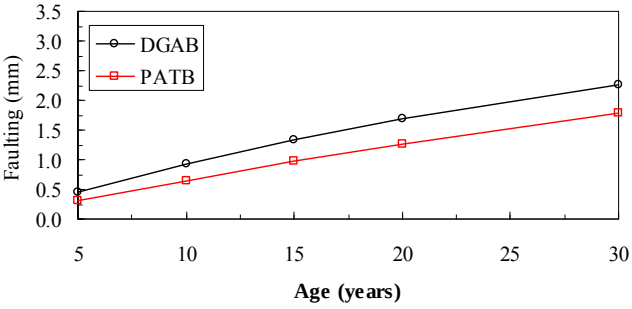

(c) Effect of *base type* on faulting

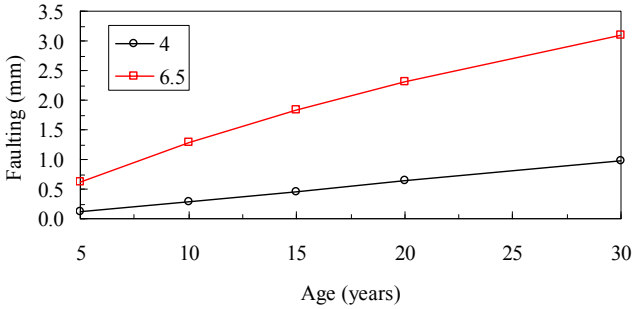

(d) Effect of *CTE* on faulting

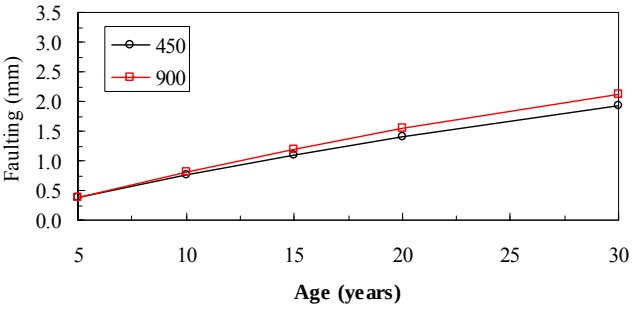

(e) Effect of *MOR* on faulting

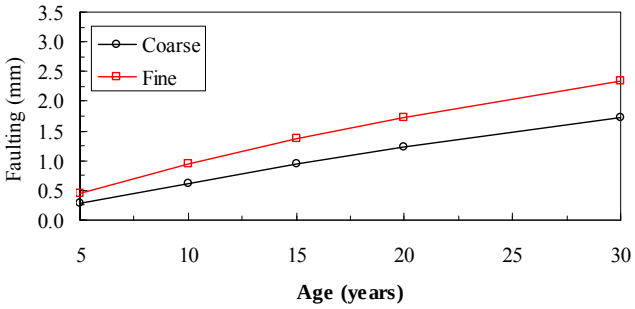

(f) Effect of *subgrade type* on faulting

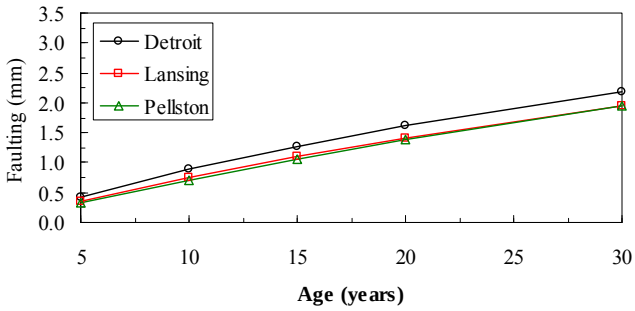

(g) Effect of *climate* on faulting

Figure 4.2 Main effects of the most sensitive input variables on JPCP faulting

Table 4.7 ANOVA results for faulting in rigid pavements after 30 years

Source	Type III Sum of Squares	df	Mean Square	F	Sig.
Corrected Model	107.315[(a)]	35	3.066	2058.609	.000
Intercept	40.333	1	40.333	27079.836	.000
PCCThick	19.013	1	19.013	12765.627	.000
EdgeSupp	.880	1	.880	590.973	.000
BaseType	4.713	1	4.713	3163.999	.000
CTE	70.859	1	70.859	47574.662	.000
MOR	.231	1	.231	155.106	.000
SoilType	7.809	1	7.809	5242.656	.000
Climate	.896	2	.448	300.810	.000
PCCThick * EdgeSupp	.002	1	.002	1.523	.219
PCCThick * BaseType	.181	1	.181	121.726	.000
PCCThick * CTE	.058	1	.058	39.010	.000
PCCThick * MOR	.811	1	.811	544.640	.000
PCCThick * SoilType	.064	1	.064	42.837	.000
PCCThick * Climate	.030	2	.015	9.983	.000
EdgeSupp * BaseType	.011	1	.011	7.251	.008
EdgeSupp * CTE	.036	1	.036	24.372	.000
EdgeSupp * MOR	1.87E-005	1	1.87E-005	.013	.911
EdgeSupp * SoilType	.023	1	.023	15.129	.000
EdgeSupp * Climate	.012	2	.006	4.172	.017
BaseType * CTE	.513	1	.513	344.115	.000
BaseType * MOR	.004	1	.004	2.351	.127
BaseType * SoilType	.041	1	.041	27.416	.000
BaseType * Climate	.021	2	.010	6.883	.001
CTE * MOR	.001	1	.001	.740	.391
CTE * SoilType	.827	1	.827	555.165	.000
CTE * Climate	.120	2	.060	40.351	.000
MOR * SoilType	.151	1	.151	101.215	.000
MOR * Climate	.002	2	.001	.760	.470
SoilType * Climate	.007	2	.004	2.444	.090
Error	.232	156	.001		
Total	147.881	192			
Corrected Total	107.547	191			

a R Squared = .998 (Adjusted R Squared = .997)

Table 4.8 Main effects of input variables on faulting

Input Variable	Levels	Mean faulting (mm)				Mean Differences			
		5 years	10 years	20 years	30 years	Δ_5	Δ_{10}	Δ_{20}	Δ_{30}
Slab Thickness (inches)	9	0.53	1.09	1.97	2.62	0.32	0.61	0.98	1.18
	14	0.22	0.48	0.98	1.44				
Edge Support	Asphalt	0.42	0.85	1.58	2.15	0.08	0.15	0.21	0.23
	Tied	0.33	0.71	1.37	1.91				
Base Type	DGAB	0.45	0.92	1.68	2.27	0.15	0.28	0.41	0.47
	PATB	0.30	0.64	1.27	1.79				
CTE	4	0.13	0.29	0.63	0.97	-0.50	-0.99	-1.69	-2.12
	6.5	0.62	1.28	2.32	3.09				
MOR (psi)	450	0.37	0.76	1.41	1.94	0.00	-0.05	-0.13	-0.18
	900	0.38	0.81	1.54	2.12				
Soil Type	Coarse	0.29	0.63	1.22	1.72	-0.17	-0.31	-0.51	-0.63
	Fine	0.46	0.94	1.73	2.34				
Climate	Detroit	0.43	0.88	1.62	2.18	0.02	0.03	0.03	0.00
	Lansing	0.36	0.75	1.42	1.95				
	Pellston	0.34	0.71	1.39	1.95				

Table 4.9 Interactions effects of input variables on faulting

Input Variables		Levels1	Levels2	Mean faulting (mm)				Mean Differences			
1	2			5 years	10 years	20 years	30 years	Δ_5	Δ_{10}	Δ_{20}	Δ_{30}
Base Type	Slab Thickness	DGAB	9	0.63	1.26	2.20	2.87	0.37	0.68	1.04	1.21
			14	0.27	0.58	1.16	1.66				
		PATB	9	0.43	0.91	1.74	2.37	0.26	0.54	0.93	1.15
			14	0.17	0.37	0.80	1.22				
CTE	Slab Thickness	4	9	0.17	0.40	0.85	1.28	0.10	0.22	0.43	0.61
			14	0.08	0.18	0.41	0.67				
		6.5	9	0.89	1.78	3.09	3.97	0.53	1.00	1.54	1.76
			14	0.36	0.78	1.55	2.21				
MOR	Slab Thickness	450	9	0.50	1.00	1.80	2.40	0.26	0.49	0.78	0.93
			14	0.24	0.51	1.02	1.48				
		900	9	0.56	1.17	2.14	2.84	0.37	0.73	1.19	1.44
			14	0.19	0.44	0.94	1.40				
Soil Type	Slab Thickness	Coarse	9	0.42	0.88	1.66	2.25	0.25	0.51	0.87	1.08
			14	0.16	0.37	0.79	1.18				
		Fine	9	0.65	1.29	2.28	2.99	0.38	0.70	1.10	1.29
			14	0.27	0.59	1.18	1.70				
Climate	Slab Thickness	Detroit	9	0.61	1.23	2.15	2.80	0.37	0.69	1.05	1.24
			14	0.25	0.54	1.09	1.57				
		Lansing	9	0.50	1.02	1.87	2.50	0.29	0.55	0.91	1.09
			14	0.21	0.47	0.96	1.41				
		Pellston	9	0.48	1.00	1.89	2.56	0.29	0.58	0.99	1.22
			14	0.19	0.42	0.90	1.34				

Table 4.9 Interactions effects of input variables on faulting (continued…)

Input Variables		Levels1	Levels2	Mean faulting (mm)				Mean Differences			
1	2			5 years	10 years	20 years	30 years	Δ_5	Δ_{10}	Δ_{20}	Δ_{30}
Base Type	Edge Support	DGAB	Asphalt	0.50	1.00	1.79	2.38	0.10	0.16	0.22	0.24
			Tied	0.40	0.84	1.57	2.15				
		PATB	Asphalt	0.33	0.71	1.37	1.91	0.07	0.13	0.20	0.23
			Tied	0.26	0.58	1.17	1.68				
CTE	Edge Support	4	Asphalt	0.14	0.32	0.69	1.04	0.03	0.06	0.11	0.14
			Tied	0.11	0.26	0.58	0.90				
		6.5	Asphalt	0.69	1.39	2.47	3.25	0.14	0.23	0.30	0.32
			Tied	0.55	1.16	2.17	2.93				
Soil Type	Edge Support	Coarse	Asphalt	0.33	0.69	1.32	1.83	0.08	0.13	0.20	0.23
			Tied	0.25	0.56	1.12	1.60				
		Fine	Asphalt	0.50	1.02	1.84	2.46	0.09	0.16	0.21	0.23
			Tied	0.41	0.86	1.63	2.23				
Climate	Edge Support	Detroit	Asphalt	0.47	0.96	1.72	2.29	0.09	0.15	0.20	0.22
			Tied	0.39	0.81	1.52	2.07				
		Lansing	Asphalt	0.40	0.82	1.52	2.07	0.08	0.14	0.20	0.22
			Tied	0.32	0.68	1.32	1.84				
		Pellston	Asphalt	0.38	0.79	1.50	2.08	0.08	0.15	0.22	0.25
			Tied	0.29	0.64	1.28	1.83				

Table 4.9 Interactions effects of input variables on faulting (continued…)

Input Variables		Levels1	Levels2	Mean faulting (mm)				Mean Differences			
1	2			5 years	10 years	20 years	30 years	Δ_5	Δ_{10}	Δ_{20}	Δ_{30}
CTE	Base Type	4	DGAB	0.16	0.36	0.77	1.16	0.07	0.14	0.27	0.37
			PATB	0.09	0.22	0.49	0.79				
		6.5	DGAB	0.74	1.48	2.60	3.38	0.24	0.41	0.55	0.58
			PATB	0.50	1.07	2.05	2.80				
Soil Type	Base Type	Coarse	DGAB	0.35	0.74	1.40	1.93	0.12	0.23	0.36	0.43
			PATB	0.23	0.51	1.04	1.50				
		Fine	DGAB	0.55	1.10	1.96	2.60	0.18	0.32	0.46	0.51
			PATB	0.37	0.78	1.50	2.09				
Climate	Base Type	Detroit	DGAB	0.51	1.03	1.82	2.41	0.16	0.28	0.41	0.46
			PATB	0.35	0.74	1.41	1.96				
		Lansing	DGAB	0.44	0.89	1.64	2.21	0.16	0.29	0.44	0.50
			PATB	0.28	0.60	1.20	1.70				
		Pellston	DGAB	0.40	0.84	1.59	2.18	0.13	0.25	0.39	0.46
			PATB	0.27	0.59	1.20	1.72				

Table 4.9 Interactions effects of input variables on faulting (continued…)

Input Variables		Levels1	Levels2	Mean faulting (mm)				Mean Differences			
1	2			5 years	10 years	20 years	30 years	Δ_5	Δ_{10}	Δ_{20}	Δ_{30}
MOR	Soil Type	450	Coarse	0.28	0.58	1.13	1.59	-0.20	-0.36	-0.57	-0.70
			Fine	0.47	0.94	1.70	2.29				
		900	Coarse	0.31	0.68	1.32	1.84	-0.14	-0.26	-0.45	-0.56
			Fine	0.44	0.94	1.76	2.40				
Soil Type	CTE	Coarse	4	0.08	0.20	0.46	0.73	-0.41	-0.86	-1.53	-1.97
			6.5	0.50	1.05	1.99	2.70				
		Fine	4	0.17	0.38	0.81	1.21	-0.58	-1.12	-1.85	-2.27
			6.5	0.75	1.50	2.66	3.48				
Climate	CTE	Detroit	4	0.15	0.34	0.72	1.09	-0.57	-1.09	-1.79	-2.18
			6.5	0.71	1.43	2.51	3.27				
		Lansing	4	0.12	0.27	0.61	0.94	-0.47	-0.95	-1.62	-2.04
			6.5	0.59	1.22	2.23	2.97				
		Pellston	4	0.11	0.25	0.56	0.88	-0.45	-0.93	-1.66	-2.14
			6.5	0.56	1.18	2.22	3.02				

4.3 EFFECT OF INPUT VARIABLES ON ROUGHNESS (IRI)

The detailed analyses were performed in two steps. Initially, the descriptive statistics such as mean performance for each input variable was summarized. However, as the differences in the means might not ascertain a significant difference, essentially due to uncertainty (variability) associated with means. Therefore, statistically analyses using ANOVA were performed for predicted pavement roughness.

4.3.1 Descriptive Statistics

Table 4.10 shows predicted roughness performance within each cell of the full-factorial design matrix at 30 years. Also, the row and column averages are presented in the same table. The row averages can be used to investigate the main effects of input variables ignoring various subgrade types and climates within the state of Michigan. Furthermore, the column averages can be utilized to study the effects of subgrade types and climate ignoring other input variables. Similar tables were generated for roughness at 5, 10, 15 and 20 years and are attached in Appendix A.

Also to investigate the average effects of all input variables on roughness, time series averages were plotted for input variable levels. Figure 3 presents the input variables effects on surface roughness in rigid pavements. These effects are summarized below:

Slab Thickness: Figure 4.3 (a) shows the roughness development for 9- and 14-inches thick slabs. It is evident, that effect of slab thickness is very significant on roughness. Rigid pavement with thin slabs developed higher roughness than those with thick slabs. Also, the results show that this effect is more pronounced over a longer life of a pavement.

Edge Support: In general, rigid pavements with asphalt shoulders (untied) showed higher roughness than those with tied shoulders, as shown by Figure 4.3 (b). However, the effect of edge support is not significant.

Base Type: Two types of bases were used in this analysis; a dense graded aggregate base (DGAB) and a permeable asphalt treated base (PATB). The results of the predicted roughness show that rigid pavements with PATB base developed slightly less roughness than those with DGAB base. However, the effect of base type is consistent on roughness development (see Figure 4.3 (c)).

Coefficient of Thermal Expansion (CTE): A significant effect of CTE was observed for roughness development. The pavements with higher CTE showed much higher roughness than those with a lower CTE value. This effect is consistent and increases throughout the life span of a rigid pavement as presented in Figure 4.3 (d).

Modulus of Rupture (MOR): Similarly, MOR effect on roughness development of rigid pavement seems to be the most significant. Pavements slab having a higher MOR exhibited much less roughness as compared to those with lower MOR, which showed a very high level of roughness; see Figure 4.3 (e). This effect is also consistent over the life span of rigid pavements. This effect

can be explained from the cracking magnitude as well i.e., roughness prediction model is a function of slab cracking.

Subgrade Type: A significant effect was noticed for subgrade type, see Figure 4.3 (f). For longer service lives, the pavements constructed on fine subgrade showed higher roughness than those constructed on coarse subgrade.

Climate: In order to investigate the effects of climate on roughness development of rigid pavements within Michigan, three locations were selected in this analysis. Figure 4.3 (g) shows that on average, the climate seems to have a marginal effect on roughness development within Michigan. Rigid pavements located in Pellston exhibited higher amount of roughness than those located in Detroit and Lansing area. The effect of location seems to be consistent with time.

It should be noted that above discussion of the results is simply based on the average performance. To ascertain the real effects of input variables on the predicted roughness of rigid pavements, statistical analyses (ANOVA) is warranted. Also, the above simple analyses only helped in the interpretations of the main effects of input variables, while interaction between input variables still needs to be explored. Therefore, detailed statistical analyses were executed to address above mentioned short-comings. The outcomes of such type of analyses are described next.

4.3.2 Statistical Analysis (ANOVA)

Typically, a full-factorial experiments design such as considered in this study can be analyzed using fixed-effect models employing analysis of variance (ANOVA). This type of statistical analyses can help in identifying the main and the interactive effects between considered variables. However, it should be noted that if certain variables are interacting with each other, their main effect should not be considered while making conclusions. Therefore, conclusions in this case should be based on the cell means rather than marginal means.

As an example, the summary results from ANOVA are given in Table 4.11 at 30 years. A *p-value* less than 0.05 (i.e. a confidence level of 95%) is used as a threshold to identify a statistical significant effect. The results are presented below according to main and interaction.

Main Effects

The results in Table 4.11 confirm that all input variables except edge support have a statistically significant effect on the roughness development. The mean values for all variables are presented in Table 4.12. The interpretation of only statistically significant effects is presented below:

Slab Thickness: Rigid pavements with thicker PCC slabs out perform those with thinner PCC slab thickness. The practical significance of this effect can be assessed using criteria mentioned in Table 3.6 and comparing difference in the roughness performance between 9- and 14-inch slab thicknesses (see Table 4.12). Applying this criteria, one can easily identify that effect of slab thickness on roughness is not practical significant.

CTE: Pavement concrete having a higher CTE value has shown higher amount of roughness than those which have a lower CTE value. This effect is marginal with regards to practical significance.

MOR: The flexure strength of the concrete has the most significant effect on the roughness development. Concrete pavements having a high strength concrete have exhibited negligible roughness even after 30 years as compared to those having low strength concrete, which showed higher amount of roughness development at the same age. The practical significance of this effect is marginal.

Interaction Effects

Table 4.11 also shows the significant interactions between input variables. The interactions between CTE by slab thickness, CTE by soil type, and soil type by climate were found to be of statistical significance (*p-value* < 0.05). Table 4.13 shows the summary of cell means for these interactions, which can be used to explain these effects. While results were summarized above for the significant main effects, if certain variables are interacting with each other, their main effect should not be considered while making conclusions. The following findings can be drawn from these results:

CTE by Slab Thickness: This interaction shows that for a lower level of CTE, slab thickness has a significant effect on the roughness. This effect is marginal for a practical significance. On the other hand, for higher level of CTE, the slab thickness did not show a very significant difference in roughness development. This higher value of CTE is masking the effect of slab thickness because pavement with thin and thick slabs exhibited a high roughness. From the design perspective, the results of this interactive effect imply that if the CTE for a concrete is higher, increasing slab thickness will not help in achieving better roughness performance.

Soil Type by CTE: This interaction demonstrates that effect of soil types (site conditions) on roughness is more prominent for lower CTE value than for higher CTE value. This means that for roughness, change in CTE is more important for pavement to be constructed on fine soil types. These effects are of both statistical and of marginal practical significance.

Climate and Soil Types: The interaction between climate (location) and subgrade type (site conditions) was found to be important for rigid pavements. The combination of fine subgrade soils with location like Pellston is drastic for roughness development. This also means that higher slab thicknesses and lower CTE values can compensate for such critical site conditions and weather. These effects are of both statistical and of marginal practical significance.

Table 4.10 Roughness development (IRI, m/km) in rigid pavements after 30 years

Slab Thickness	Edge Support	Base Type	CTE	MOR	Soil Type						Average
					Coarse			Fine			
					Detroit	Lansing	Pellston	Detroit	Lansing	Pellston	
9	Asphalt	DGAB	4	450	2.90	2.79	3.11	3.54	3.65	4.05	3.34
				900	1.61	1.56	1.60	2.11	2.14	2.45	1.91
			6.5	450	2.58	2.58	2.80	3.23	4.62	3.78	3.26
				900	2.64	2.53	2.71	3.19	3.18	3.60	2.98
		PATB	4	450	2.72	2.50	2.95	3.39	3.46	3.90	3.15
				900	1.45	1.39	1.46	1.93	1.94	2.27	1.74
			6.5	450	2.41	3.69	2.60	3.07	4.42	3.60	3.30
				900	2.48	2.34	2.52	3.01	2.95	3.40	2.78
	Tied	DGAB	4	450	2.53	2.25	2.89	3.38	3.37	3.91	3.06
				900	1.54	1.49	1.52	2.04	2.07	2.37	1.84
			6.5	450	3.77	3.77	2.66	4.42	4.52	4.95	4.01
				900	2.50	2.40	2.50	3.07	3.06	3.43	2.83
		PATB	4	450	2.33	2.01	2.63	3.19	3.10	3.72	2.83
				900	1.39	1.34	1.39	1.85	1.88	2.19	1.67
			6.5	450	3.60	3.58	3.75	4.25	4.31	4.75	4.04
				900	2.31	2.17	2.29	2.87	2.81	3.21	2.61
14	Asphalt	DGAB	4	450	1.40	1.44	1.54	1.82	1.97	2.33	1.75
				900	1.26	1.24	1.26	1.66	1.74	2.04	1.53
			6.5	450	3.15	3.15	3.28	3.59	3.59	4.16	3.49
				900	1.78	1.72	1.75	2.27	2.32	2.62	2.07
		PATB	4	450	1.30	1.35	1.47	1.69	1.83	2.21	1.64
				900	1.17	1.17	1.21	1.55	1.63	1.95	1.45
			6.5	450	3.00	2.98	3.11	3.44	3.40	3.95	3.31
				900	1.61	1.55	1.60	2.08	2.12	2.42	1.90
	Tied	DGAB	4	450	1.36	1.41	1.50	1.78	1.93	2.29	1.71
				900	1.23	1.22	1.24	1.62	1.70	2.01	1.50
			6.5	450	3.05	3.02	3.19	3.43	3.37	4.05	3.35
				900	1.70	1.65	1.67	2.19	2.25	2.54	2.00
		PATB	4	450	1.27	1.33	1.43	1.65	1.80	2.18	1.61
				900	1.15	1.15	1.19	1.52	1.60	1.93	1.42
			6.5	450	2.90	2.85	3.02	3.29	3.18	3.84	3.18
				900	1.54	1.49	1.52	2.01	2.05	2.34	1.82
Total					2.11	2.10	2.17	2.63	2.75	3.08	2.47

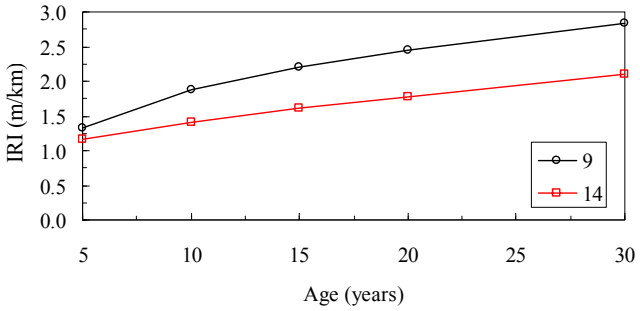

(a) Effect of *slab thickness* on IRI

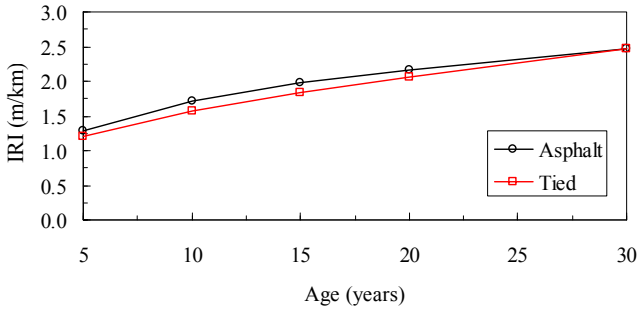

(b) Effect of *edge support* on IRI

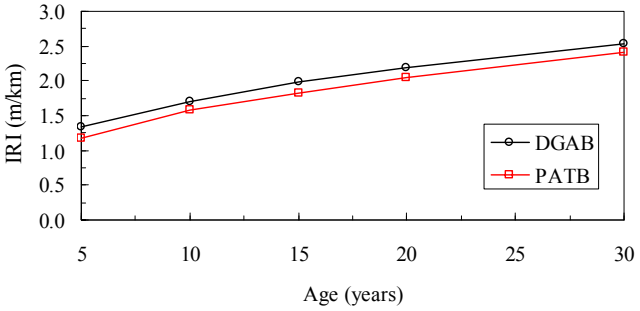

(c) Effect of *base type* on IRI

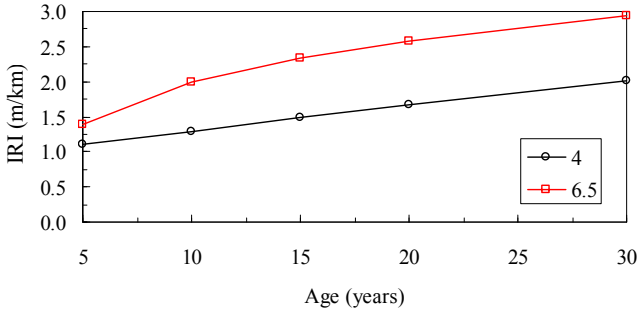

(d) Effect of *CTE* on IRI

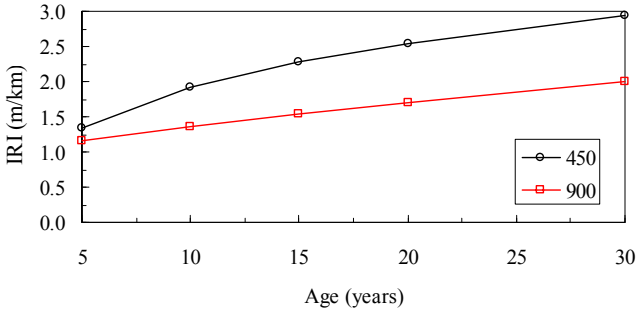

(e) Effect of *MOR* on IRI

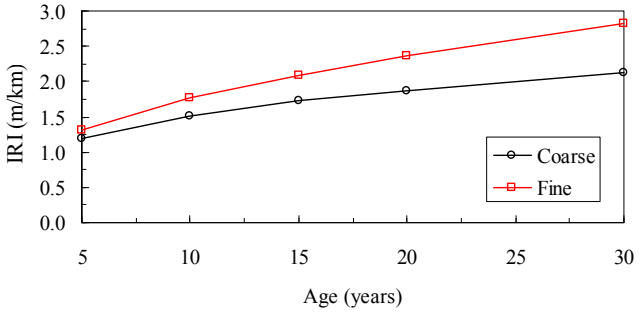

(f) Effect of *subgrade type* on IRI

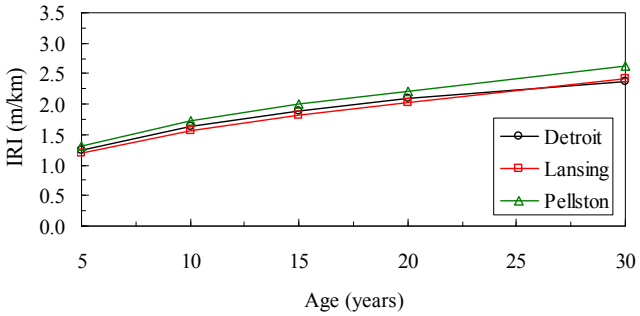

(g) Effect of *climate* on IRI

Figure 4.3 Main effects of the most sensitive input variables on JPCP IRI

Table 4.11 ANOVA results for IRI in rigid pavements after 30 years

Source	Type III Sum of Squares	df	Mean Square	F	Sig.
Corrected Model	24.667[(a)]	35	.705	46.950	.000
Intercept	134.216	1	134.216	8941.034	.000
PCCThick	4.701	1	4.701	313.161	.000
EdgeSupp	.009	1	.009	.620	.432
BaseType	.178	1	.178	11.854	.001
CTE	7.632	1	7.632	508.449	.000
MOR	6.568	1	6.568	437.529	.000
SoilType	4.234	1	4.234	282.037	.000
Climate	.356	2	.178	11.857	.000
PCCThick * EdgeSupp	.012	1	.012	.824	.365
PCCThick * BaseType	.001	1	.001	.082	.776
PCCThick * CTE	.402	1	.402	26.802	.000
PCCThick * MOR	.048	1	.048	3.183	.076
PCCThick * SoilType	4.38E-006	1	4.38E-006	.000	.986
PCCThick * Climate	.016	2	.008	.550	.578
EdgeSupp * BaseType	7.88E-005	1	7.88E-005	.005	.942
EdgeSupp * CTE	.053	1	.053	3.542	.062
EdgeSupp * MOR	.031	1	.031	2.067	.152
EdgeSupp * SoilType	.001	1	.001	.082	.776
EdgeSupp * Climate	.015	2	.008	.514	.599
BaseType * CTE	.005	1	.005	.360	.549
BaseType * MOR	.017	1	.017	1.120	.291
BaseType * SoilType	.001	1	.001	.044	.835
BaseType * Climate	.003	2	.002	.108	.897
CTE * MOR	.045	1	.045	2.981	.086
CTE * SoilType	.080	1	.080	5.345	.022
CTE * Climate	.050	2	.025	1.653	.195
MOR * SoilType	.034	1	.034	2.251	.136
MOR * Climate	.017	2	.008	.553	.576
SoilType * Climate	.157	2	.078	5.222	.006
Error	2.342	156	.015		
Total	161.226	192			
Corrected Total	27.009	191			

a R Squared = .913 (Adjusted R Squared = .894)

Table 4.12 Main effects of input variables on Roughness (IRI)

Input Variable	Levels	Mean IRI (m/km)				Mean Differences			
		5 years	10 years	20 years	30 years	Δ_5	Δ_{10}	Δ_{20}	Δ_{30}
Slab Thickness (inches)	9	1.33	1.88	2.46	2.83	0.17	0.48	0.68	0.73
	14	1.16	1.41	1.78	2.11				
Edge Support	Asphalt	1.29	1.71	2.17	2.48	0.08	0.13	0.10	0.01
	Tied	1.21	1.58	2.07	2.47				
Base Type	DGAB	1.33	1.71	2.18	2.54	0.16	0.14	0.13	0.14
	PATB	1.17	1.58	2.05	2.40				
CTE	4	1.11	1.29	1.66	2.01	-0.28	-0.70	-0.91	-0.92
	6.5	1.39	2.00	2.57	2.93				
MOR (psi)	450	1.33	1.93	2.53	2.94	0.16	0.57	0.83	0.94
	900	1.17	1.36	1.70	2.00				
Soil Type	Coarse	1.19	1.52	1.88	2.13	-0.12	-0.25	-0.48	-0.69
	Fine	1.31	1.77	2.36	2.82				
Climate	Detroit	1.24	1.65	2.10	2.37	-0.10	-0.17	-0.17	-0.20
	Lansing	1.20	1.56	2.04	2.42				
	Pellston	1.30	1.73	2.21	2.62				

Table 4.13 Main effects of input variables on Roughness (IRI)

Input Variables		Levels1	Levels2	Mean IRI (m/km)				Mean Differences			
1	2			5 years	10 years	20 years	30 years	Δ_5	Δ_{10}	Δ_{20}	Δ_{30}
CTE	Slab Thickness	4	9	1.15	1.44	1.98	2.44	0.08	0.28	0.64	0.87
			14	1.07	1.15	1.34	1.58				
		6.5	9	1.52	2.33	2.93	3.23	0.26	0.67	0.72	0.59
			14	1.26	1.66	2.22	2.64				
Soil Type	CTE	Coarse	4	1.05	1.15	1.41	1.68	-0.28	-0.74	-0.93	-0.89
			6.5	1.33	1.89	2.34	2.57				
		Fine	4	1.17	1.44	1.91	2.34	-0.28	-0.67	-0.89	-0.96
			6.5	1.45	2.10	2.80	3.30				
Climate	Soil Type	Detroit	Coarse	1.18	1.54	1.91	2.11	-0.12	-0.22	-0.39	-0.52
			Fine	1.30	1.76	2.30	2.63				
		Lansing	Coarse	1.15	1.45	1.82	2.10	-0.10	-0.22	-0.44	-0.65
			Fine	1.25	1.67	2.25	2.75				
		Pellston	Coarse	1.23	1.57	1.90	2.17	-0.14	-0.32	-0.61	-0.91
			Fine	1.37	1.89	2.52	3.08				

Figure 4.4 presents the average climatic properties (temperature, rainfall, and number of freeze/thaw cycles) for three locations considered with the state of Michigan. It can be observed that higher cracking potential is associated with locations having higher freeze index and number of freeze/thaw cycles.

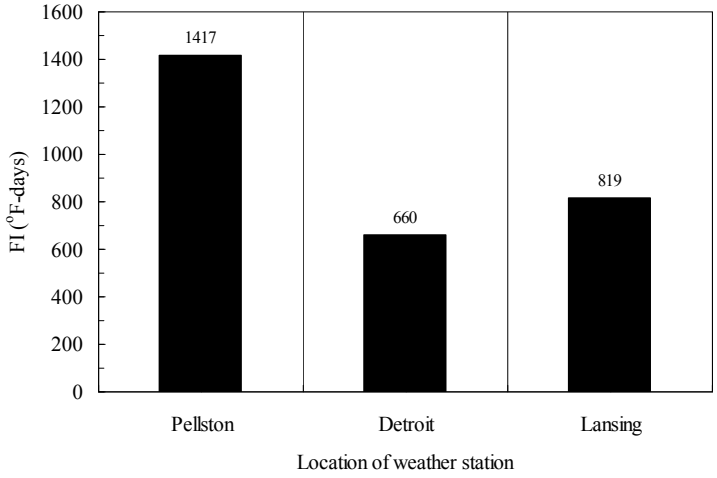

(a) Average Freezing index by location

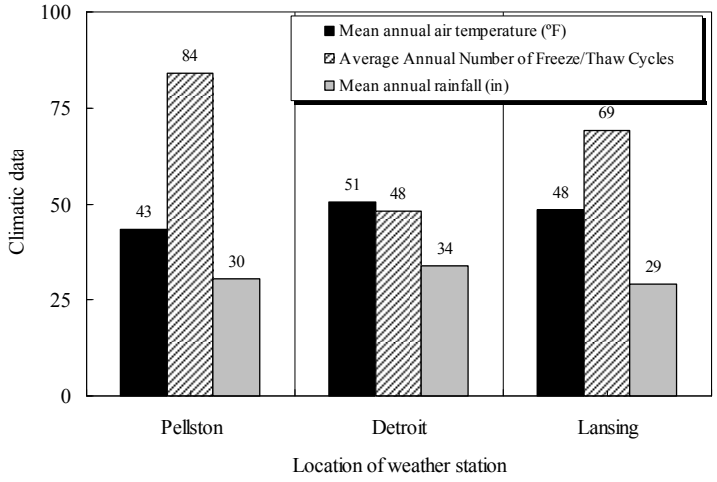

(b) Mean annual air temperature, number of F/T cycles and average precipitation by location

Figure 4.4 Summary of climatic properties by location within Michigan

4.4 SUMMARY OF STATISTICAL ANALYSES RESULTS

The summary results, at 30 years, from ANOVA are given in Table 4.14. As an example, the results for transverse cracking for statistically and practically significant interactions between variables are presented below.

Table 4.14 also shows the significant interaction effects between input variables on various performance measures. The interactions between CTE and slab thickness, MOR and slab thickness, and CTE and MOR were found to be statistically significant (p-value < 0.05). Table 4.5 shows the summary of cell means for these interactions, which can be used to explain the practical significance of these effects.

Table 4.14 Summary of results for statistical and practical significance

Transverse cracking (% slab cracked)								
Variable	Main effect	Interaction effect						
		Slab thickness	Edge support	CTE	MOR	Base type	Subgrade soil type	Climate
Slab thickness	*S*	-		**S**	**S**			
Edge support			-					
CTE	*S*	**S**		-	**S**			
MOR	*S*	**S**		**S**	-			
Base type						-		
Subgrade soil type							-	
Climate								-
Joint faulting (mm)								
Variable	Main effect	Interaction effect						
		Slab thickness	Edge support	CTE	MOR	Base type	Subgrade soil type	Climate
Slab thickness	*S*	-		**S**	**S**	S	S	S
Edge support	*S*		-	S		S	S	
CTE	*S*	**S**	S	-			**S**	**S**
MOR	*S*	**S**			-		S	
Base type	*S*	S	S			-		
Subgrade soil type	*S*	S	S	**S**	S		-	
Climate	*S*	S		**S**				-
Roughness, IRI (in/mile)								
Variable	Main effect	Interaction effect						
		Slab thickness	Edge support	CTE	MOR	Base type	Subgrade soil type	Climate
Slab thickness	*S*	-		**S**				
Edge support			-					
CTE	*S*	**S**		-			**S**	
MOR	*S*				-			
Base type	*S*					-		
Subgrade soil type	*S*			**S**			-	**S**
Climate	*S*						**S**	-

Note: *S* implies statistical significance of main effects
S implies statistical significance of interaction effects
S and **S** imply both statistical and practical significance of main and interactive effects, respectively.

The following findings can be drawn from these results:

The analyses highlight the critical steps for conducting M-E PDG sensitivity analyses. A preliminary sensitivity, considering one variable at a time, was used to determine the most important input variables affecting JPCP performance. In order to customize the use of the software to the local needs, it is essential to consider the state-of-the-practice and local experience in such analyses to reduce the number of input variables and their levels. The results showed that effect of PCC slab thickness and edge support on performance were significant among design variables while CTE, MOR, base type and subgrade played an important role among material-related properties. In addition, to effectively capture the interaction effects between variables a full factorial experiment was designed and analyzed. Statistical analyses results identified significant main and interactions effects of input variables. It was found that slab thickness interacts significantly with material properties—CTE and MOR, for cracking in JPCP. From the design perspective, increasing slab thickness for a higher CTE or a higher MOR may not help in achieving better cracking performance. On the other hand, increasing slab thickness for a lower CTE and a lower MOR may improve cracking performance. A lower MOR and a higher CTE combination is drastic for JPCP cracking. For faulting, the material properties—CTE and MOR interact significantly with site factors—subgrade soil type and climate. For roughness, the interactions between slab thickness by CTE and climate by subgrade soil types play a significant role.

CHAPTER 5 - SATELLITE STUDIES - RIGID

In this chapter analyses and results of the following activities are presented:

1. Satellite study to investigate the effects of joint spacing, CTE and slab thickness on rigid pavement performance;
2. Verification of M-E PDG predicted and observed rigid pavement performance for the SPS-2 pavements in Michigan;
3. Verification of M-E PDG for selected MDOT rigid (JPCP) pavement sections;
4. Satellite sensitivity analysis to assess the effects of traffic-related inputs on rigid pavement performance.

The details of above mentioned activities are presented next.

5.1 SATELLITE SENSITIVITY STUDY — JOINT SPACING, CTE, AND SLAB THICKNESS

The detailed sensitivity analysis results for rigid pavements were reported in Chapter 4. However, it was decided to conduct satellite sensitivity for the following three important design inputs for JPCP:

- Joint spacing (12-, 16- and 20-feet)
- CTE (4, 5 and 6.5 in/in/^{o}F)
- PCC slab thickness (9-, 12- and 14-inch)

The reasons for conducting the sensitivity include:

1. Considering CTE and PCC slab thickness interactions, the effect of joint spacing on performance is hidden due to MDOT practice of tying joint spacing with the PCC slab thickness. Therefore, it was decided to initiate separate satellite sensitivity by considering three levels of joint spacing (12-, 16- and 20-feet). This sensitivity analysis will determine the importance of these three variables on the rigid pavement performance and interactions between them (if any).
2. While the results of the sensitivity are purely an academic exercise, the practical aspects of the results will be useful in providing guidance to the designer.
3. At present MDOT uses DARWIN software (based on AASHTO 1993 Pavement Design Guide); however, the old AASHTO design procedure does not completely account for concrete material properties for example CTE. Therefore, this new design procedure will help the designer to incorporate the actual material properties, thus providing a better guidance of the expected pavement performance at the design stage.

Figure 5.1 illustrates the typical MDOT pavement cross-section for a jointed plain concrete pavement (JPCP). This pavement cross-section was used in this analysis. It should be noted that open graded base course (OGDC) material option is not available in the M-E PDG; instead a

crushed stone material option was used in this analysis. The selection of base material will not impact the results of this sensitivity as these analyses are relative in nature and type of base is not considered as a variable.

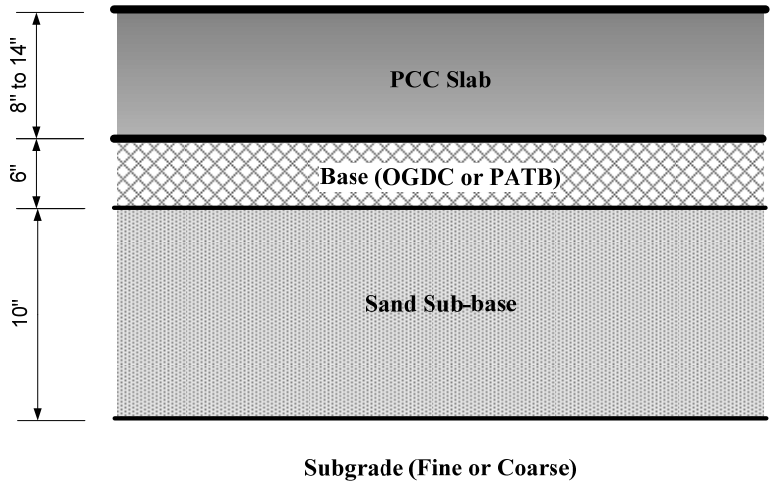

Figure 5.1 Typical MDOT pavement cross-section — JPCP

Table 5.1 shows the summary of variables along with their different levels considered in this analysis. This table also presents the full factorial matrix considered in this sensitivity study.

Table 5.1 Sensitivity design matrix (Slab thickness, CTE and Joint spacing)

Slab Thickness (inches)	CTE per ^{o}F	Joint Spacing (feet)			Total
		12	16	20	
9	4	1	2	3	3
	5	4	5	6	3
	6.5	7	8	9	3
12	4	10	11	12	3
	5	13	14	15	3
	6.5	16	17	18	3
14	4	19	20	21	3
	5	22	23	24	3
	6.5	25	26	27	3
Total		9	9	9	27

Table 5.1 also summarizes the number of runs required within each cell of the full-factorial matrix. These runs were executed to capture pavement performance in terms of cracking, faulting, and IRI. Similar to the detailed sensitivity, the performance magnitudes at 5, 10, 20 and 30 years were used to conduct Analysis of Variance (ANOVA). In this analysis all main effects and all possible two-way interactions were considered between the three variables. Once all the

desired runs were accomplished, a database was prepared to study the input variables and various pavement performance measures. Using this database detailed statistical analyses were conducted for each rigid pavement predicted performance measure. The results of these are discussed next.

5.1.1 Effect of Input Variables on Cracking

The detailed analyses were performed in two steps. Initially, the descriptive statistics such as mean performance for each input variable was summarized. However, as the differences in the means might not ascertain a significant difference, essentially due to uncertainty (variability) associated with means. Therefore, statistical analyses using ANOVA were performed for all performance measures (cracking, faulting, and IRI).

5.1.1.1 Descriptive Statistics

Table 5.2 shows the cracking predicted by the M-E PDG within each cell of the full-factorial design matrix at 30 years life. Also, the row and column averages are presented in the same table. The row averages can be used to investigate the main effects of input variables by ignoring joint spacing. Furthermore, the column averages can be utilized to study the effects of joint spacing on cracking by ignoring other input variables. Similar tables were generated for cracking at 5, 10, 15 and 20 years and are attached in Appendix A.

Also to investigate the descriptive or average effects of all input variables on cracking, time series averages were plotted for input variables levels. Figure 5.2 presents the input variables effects on percent slab cracked in rigid pavements. These effects are summarized below:

Joint Spacing: Rigid pavements with longer joint spacing showed higher cracking than those with shorter joint spacing, as shown by Figure 5.2(a). This effect of joint spacing is very significant and is consistent over pavement age.

Slab Thickness: Figure 5.2(b) shows the percent slabs cracked for 9-, 12- and 14-inches thick slabs. It is evident, that effect of slab thickness is very significant on cracking. Rigid pavement with thin slab thickness showed higher levels of cracking than those with thick slabs. Also, the results show that this effect is more pronounced over a longer life of a pavement.

Coefficient of Thermal Expansion (CTE): A significant effect of CTE was observed for cracking. The pavements with higher CTE showed much higher cracking than those with a lower CTE value. This effect is consistent throughout the life span of a rigid pavement as presented in Figure 5.2(c).

It should be noted that above discussion of the results is simply based on the average performance over time. To ascertain the real effects of input variables on the predicted cracking of rigid pavements, statistical analyses (ANOVA) is warranted. Also, the above simple analyses only helped in the interpretation of the main effects of input variables, while interaction between input variables still needs to be explored. Therefore, detailed statistical analyses were executed to address above mentioned concerns. The outcomes of such type of analyses are described next.

5.1.1.2 Statistical Analysis (ANOVA)

The main objectives of the statistical analyses are to: (a) obtain the real effects with some level of confidence, (b) explore the interactive effects between various input variables, and (c) attain definite conclusions. Typically, a full-factorial experiment design such as considered in this satellite study can be analyzed using fixed-effect models by employing analysis of variance (ANOVA). This type of statistical analyses can help in identifying the main and the interactive effects between variables. In addition, it should be noted that if certain variables are interacting with each other, their main effect should not be considered while making conclusion. Therefore, conclusions in this case are based on the cell means rather than marginal means.

As an example, the summary results from ANOVA are given in Table 5.3 at 30 years. A *p-value* less than 0.05 (i.e. a confidence level of 95%) is used as a threshold to identify a statistically significant effect. The results are presented below according to main and interaction.

Main Effects

The results in Table 5.3 confirm that input variables; PCC slab thickness, CTE and joint spacing have a statistically significant effect on the cracking performance. The mean values for all variables are presented in Table 5.4. The interpretation of these effects is presented below:

Joint Spacing: The joint spacing of rigid pavement slab has a significant effect on the cracking performance. Concrete pavements having a higher joint spacing have exhibited more cracking as compared to those having lower joint spacing. This effect is also of practical significance.

Slab Thickness: Rigid pavements with thicker PCC slabs out perform those with thinner PCC slab thickness. The practical significance of this effect can be assessed using criteria mentioned in Table 3.5 and comparing difference in the cracking performance between 9- and 14-inch slab thicknesses (see Table 5.3). Applying this criteria, one can easily identify that effect of slab thickness on cracking is practical significant as well.

CTE: Pavement concrete having a higher CTE value has shown higher amount of cracking than those which have a lower CTE value. This effect is also of practically significance.

Interaction Effects

Table 5.3 also shows the significant interactions between input variables. The interaction between joint spacing and slab thickness was found to be of statistically significance (*p-value* < 0.05). Table 5.5 shows the summary of cell means, which can be used to explain these effects. While results were summarized above for the significant main effects, if certain variables are interacting with each other, their main effect should not be considered while making conclusions. The following findings can be drawn from these results:

Joint Spacing by Slab Thickness: This interaction shows that for a lower level of slab thickness, joint spacing has a significant effect on the cracking. This effect is of both practical and statistical significance. On the other hand, for higher level of slab thickness, the joint spacing did

not show a very significant difference in cracking performance, especially for thick slabs (12- and 14-inch). This is because thinner slabs are prone to cracking irrespective of joint spacing at the later ages. Joint spacing has a very significant effect for thinner slabs at early ages. From the design perspective, the results of this interactive effect imply that if the joint spacing for a concrete slab is larger, increasing slab thickness will only help in achieving improved cracking performance to a certain extent.

Table 5.2 Fatigue cracking (% slab cracked) for rigid pavements after 30 years

Slab Thickness (inch)	CTE per ^{o}F	Joint Spacing (feet)			Average
		12	16	20	
9	4	88.2	99.3	100.0	95.8
	5	95.4	100.0	100.0	98.5
	6.5	99.8	100.0	100.0	99.9
12	4	0.0	2.4	59.8	20.7
	5	0.2	39.8	99.3	46.4
	6.5	12.9	98.3	100.0	70.4
14	4	0.0	0.0	6.9	2.3
	5	0.0	2.1	88.7	30.3
	6.5	0.8	78.2	99.9	59.6
Average		33.0	57.8	83.8	58.2

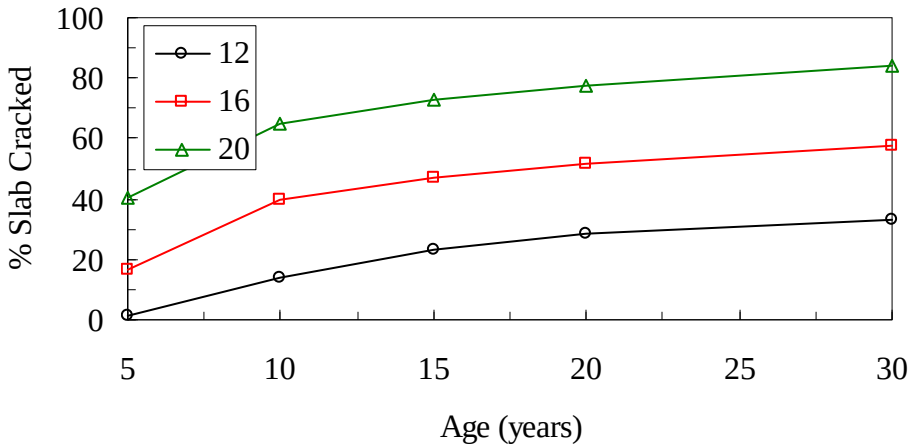

(a) Effect of joint spacing

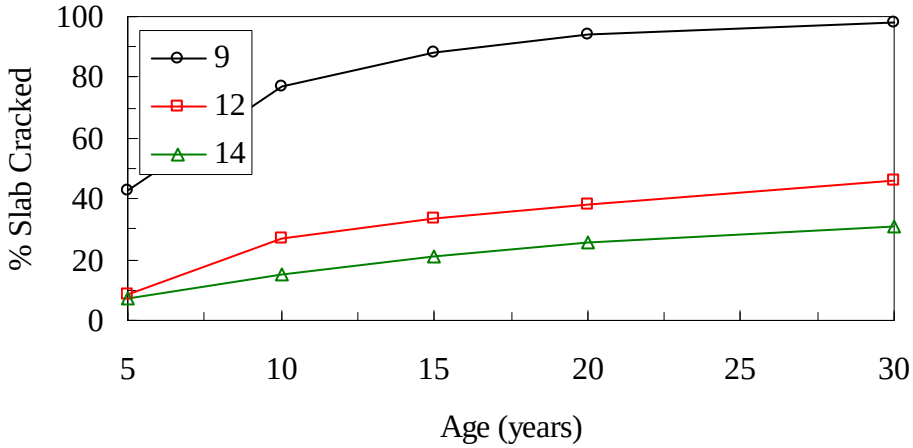

(b) Effect of slab thickness

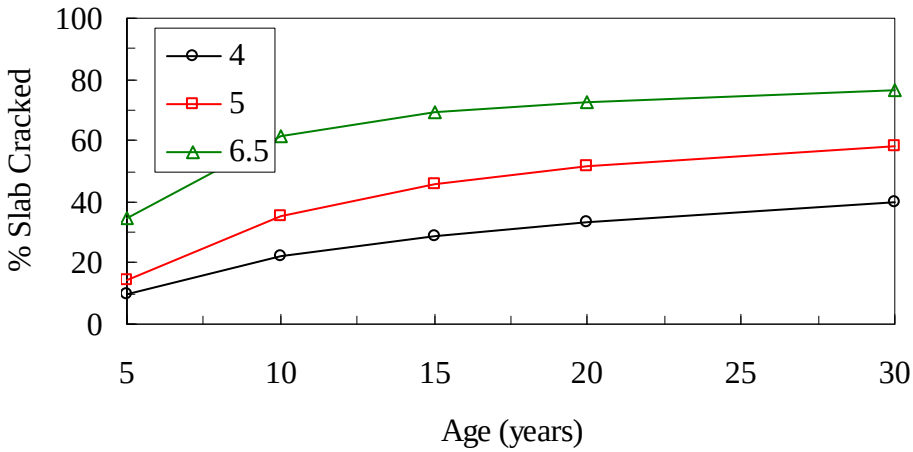

(c) Effect of CTE

Figure 5.2 Effect of input variables on cracking performance of JPCP

Table 5.3 ANOVA results for cracking

Source	Type III Sum of Squares	df	Mean Square	F	Sig.
Corrected Model	181.085[(a)]	18	10.060	8.866	.002
Intercept	188.512	1	188.512	166.134	.000
Joint spacing	52.918	2	26.459	23.318	.000
Slab thickness	59.076	2	29.538	26.031	.000
CTE	23.675	2	11.838	10.433	.006
Joint spacing * Slab thickness	26.985	4	6.746	5.945	.016
Joint spacing * CTE	6.564	4	1.641	1.446	.304
Slab thickness * CTE	11.867	4	2.967	2.615	.115
Error	9.078	8	1.135		
Total	378.675	27			
Corrected Total	190.163	26			

a R Squared = .952 (Adjusted R Squared = .845)

Table 5.4 Main effect of input variables on cracking

Input Variable	Level	Mean % Slabs Cracked				Mean Differences			
		5 years	10 years	20 years	30 years	Δ_5	Δ_{10}	Δ_{20}	Δ_{30}
Joint Spacing (ft)	12	1.62	14.22	28.23	33.07	38.93	50.97	49.28	50.78
	16	16.56	39.57	51.61	57.80				
	20	40.56	65.19	77.51	83.84				
Slab Thickness (inch)	9	42.94	76.72	93.87	98.08	-35.66	-61.53	-68.40	-67.31
	12	8.50	27.07	38.02	45.87				
	14	7.29	15.19	25.47	30.77				
CTE (in/in/^{o}F)	4	9.74	22.16	33.07	39.66	25.02	39.10	39.49	37.00
	5	14.22	35.57	51.73	58.40				
	6.5	34.77	61.26	72.56	76.66				

Table 5.5 Interaction effect of input variables on cracking

Input Variables		Level 1	Level 2	Mean % Slabs Cracked			
1	2			5 years	10 years	20 years	30 years
Joint Spacing	Slab Thickness	12	9	4.67	42.27	82.87	94.47
			12	0.10	0.30	1.67	4.40
			14	0.10	0.10	0.17	0.33
		16	9	47.13	90.23	98.83	99.77
			12	1.50	22.60	37.30	46.83
			14	1.03	5.87	18.70	26.80
		20	9	77.03	97.67	99.90	100.00
			12	23.90	58.30	75.10	86.37
			14	20.73	39.60	57.53	65.17

5.1.2 Effect of Input Variables on Faulting

Again, the detailed analyses were performed in two steps. Initially, the descriptive statistics such as mean performance for each input variable was summarized. However, as the differences in the means might not ascertain a significant difference, essentially due to uncertainty (variability) associated with means. Therefore, statistically analyses using ANOVA were performed for predicted joint faulting.

5.1.2.1 Descriptive Statistics

Table 5.6 shows the predicted faulting magnitudes within each cell of the full-factorial design matrix at 30 years life. Also, the row and column averages are presented in the same table. The row averages can be used to investigate the main effects of input variables by ignoring joint spacing. In addition, the column averages can be utilized to study the effects of joint spacing on cracking by ignoring other input variables. Similar tables were generated for cracking at 5, 10, 15 and 20 years and are attached in Appendix A.

Also to investigate the average effects of all input variables on faulting, time series averages were plotted for each input variables levels. Figure 5.3 presents the effects of input variables on joint faulting in rigid pavements. These effects are summarized below:

Joint Spacing: Rigid pavements with longer joint spacing show significantly higher magnitudes of faulting at joints than those with shorter joint spacing, as shown by Figure 5.3(b). This effect is consistent over the life of the pavements.

Slab Thickness: Figure 5.3(b) shows the joint faulting for 9-, 12- and 14-inches thick slabs. It is evident, that effect of slab thickness is very significant on faulting. It should be noted that a reverse trend is exhibited in this analysis i.e. the pavement with thinner slab has shown less faulting. This unexpected performance can be explained by the fact that in this analysis the dowel diameter was fixed at 1.25 inches; therefore, increased bearing stress in thicker slabs due

to smaller dowel diameter will cause this anomaly. However, by increasing the dowel diameter to 1.5 inch for thicker slab (i.e. the MDOT practice) will rectify this predicted trend. Nonetheless, one can comprehend that rigid pavement with thin slab thickness will exhibit higher faulting than those with thick slabs if dowel diameter is adjusted according to PCC slab thickness.

Coefficient of Thermal Expansion (CTE): A significant effect of CTE was observed on faulting magnitudes. The pavement slabs constructed with higher CTE concrete exhibited much higher faulting than those with a lower CTE value. This effect is consistent and increases throughout the life span of a rigid pavement as presented in Figure 5.3(c).

To ascertain the real effects of input variables on the predicted faulting of rigid pavements, statistical analyses (ANOVA) is warranted. Also, the above simple analyses only helped in the interpretations of the main effects of input variables, while interaction between input variables still needs to be explored. Therefore, detailed statistical analyses were executed and the results of the analyses are described next.

5.1.2.2 Statistical Analysis (ANOVA)

Again a fixed-effect models employing analysis of variance (ANOVA) was considered for this analysis. This statistical analysis can help in identifying the main and the interactive effects between input variables. However, it should be noted that if certain variables are interacting with each other, their main effect should not be considered while making conclusions. Therefore, conclusions in this case are based on the cell means rather than marginal means.

As an example, the summary results from ANOVA are given in Table 5.7 for 30 years. A *p-value* less than 0.05 (i.e. a confidence level of 95%) is used as a threshold to identify a statistically significant effect. The results are presented below according to main and interaction effects.

Main Effects

The results in Table 5.7 confirm that all input variables have a statistically significant effect on the joint faulting. The mean values for all variables are presented in Table 5.8. While all input variables effect joint faulting significantly, the difference for input levels of each variable should pass the test of practical significance. The interpretation of only statistical and practical significant effects is presented below:

Joint Spacing: Rigid pavements with higher joint spacing show significantly higher faulting at joints than those with lower joint spacing. This effect is consistent over the life span of the pavements. However, the effect is of practical significance between 20 to 30 years of service life.

Slab Thickness: Rigid pavements with thicker PCC slabs out performed those with thinner PCC slab thickness. The practical significance of this effect can be assessed using criteria mentioned in Table 3.6 and by comparing difference in the faulting performance between 9- and 14-inch slab thicknesses (see Table 5.8). Applying this criterion, one can easily identify that effect of slab

thickness on faulting is of practical significance if higher dowel diameter is used for thicker slabs.

CTE: Pavement concrete having a higher CTE value has shown higher amount of faulting than those which have a lower CTE value. This effect is also of practical significance.

Interaction Effects

Table 5.7 also shows the significant interactions between input variables. The interactions between all the input variables (joint spacing by slab thickness and slab thickness by CTE) were found to be of statistical significance (*p-value* < 0.05). Tables 5.9 and 5.10 show the cell means for these interactive effects which can be used to explain these effects. While results were summarized above for the significant main effects, if certain variables are interacting with each other, their main effect should not be considered while making conclusions. Due to low predicted values of faulting, the effects can be statistical significant for a very low mean differences between various levels of input variables. However, a practical significance may help explain some of these effects. Following findings can be drawn from these results:

Joint Spacing by Slab Thickness: This interaction demonstrates that effect of slab thickness on faulting is more prominent for higher joint spacing. This means that for faulting, change in thickness is more important for higher joint spacing in designing rigid pavements. These effects are of both statistical and practical significance at older age.

CTE by Slab Thickness: This interaction shows that for a higher level of CTE, slab thickness has a significant effect on the faulting. This effect is of both practical and statistical significance. On the other hand, for lower level of CTE, the slab thickness did not show a very significant difference in faulting performance. From the design perspective, the results of this interactive effect imply that if the CTE for a concrete is higher, increasing slab thickness will help in achieving better faulting performance.

Table 5.6 Faulting in rigid pavements after 30 years

Slab Thickness	CTE	Joint Spacing			Average
		12	16	20	
9	4	1.37	1.91	2.06	1.78
	5	2.16	2.97	3.28	2.80
	6.5	3.56	4.85	5.49	4.63
12	4	1.70	2.74	3.33	2.59
	5	2.49	3.73	4.52	3.58
	6.5	3.71	5.31	6.50	5.17
14	4	1.55	3.07	4.09	2.90
	5	2.39	4.06	5.26	3.90
	6.5	3.63	5.54	7.16	5.44
Average		2.51	3.80	4.63	3.65

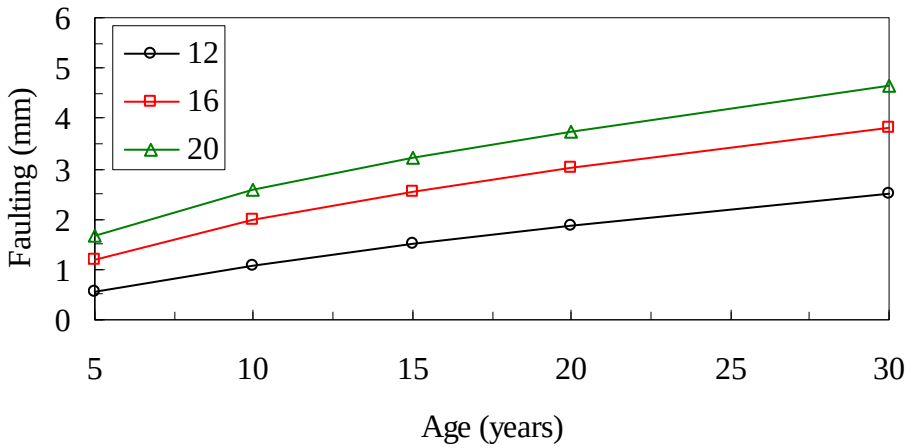

(a) Effect of joint spacing

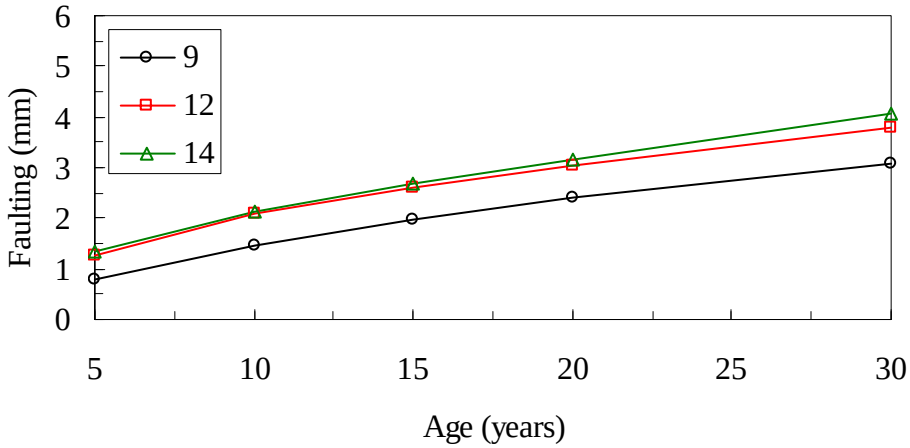

(b) Effect of slab thickness

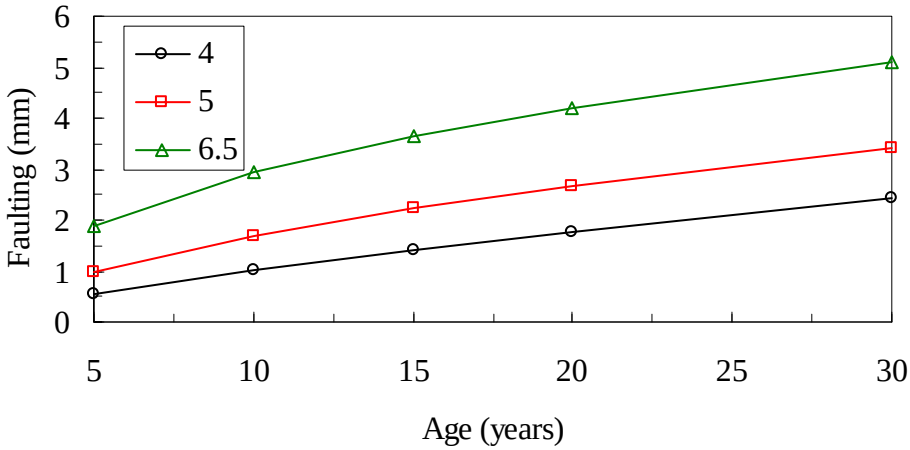

(c) Effect of CTE

Figure 5.3 Effect of input variables on faulting performance of JPCP

Table 5.7 ANOVA results for faulting

Source	Type III Sum of Squares	df	Mean Square	F	Sig.
Corrected Model	5.115[(a)]	18	.284	159.078	.000
Intercept	39.078	1	39.078	21877.8	.000
Joint spacing	1.781	2	.891	498.607	.000
Slab thickness	.416	2	.208	116.558	.000
CTE	2.708	2	1.354	757.932	.000
Joint spacing * Slab thickness	.118	4	.029	16.490	.001
Joint spacing * CTE	.017	4	.004	2.378	.138
Slab thickness * CTE	.075	4	.019	10.436	.003
Error	.014	8	.002		
Total	44.207	27			
Corrected Total	5.129	26			

a R Squared = .997 (Adjusted R Squared = .991)

Table 5.8 Main effect of input variables on faulting

Input Variable	Levels	Mean Faulting (mm)				Mean Differences			
		5 years	10 years	20 years	30 years	Δ_5	Δ_{10}	Δ_{20}	Δ_{30}
Joint Spacing (ft)	12	0.56	1.09	1.88	2.51	1.12	1.51	1.84	2.13
	16	1.18	1.98	3.01	3.80				
	20	1.68	2.60	3.72	4.63				
Slab Thickness (inch)	9	0.79	1.46	2.41	3.07	0.55	0.68	0.75	1.01
	12	1.28	2.08	3.05	3.78				
	14	1.34	2.14	3.16	4.08				
CTE (in/in/^{o}F)	4	0.54	1.02	1.77	2.42	1.35	1.94	2.42	2.66
	5	0.98	1.69	2.66	3.43				
	6.5	1.89	2.96	4.19	5.08				

Table 5.9 Interaction effect of joint spacing by slab thickness on faulting

Input Variables		Level 1	Level 2	Mean Faulting (mm)			
1	2			5 years	10 years	20 years	30 years
Joint Spacing	Slab Thickness	12	9	0.49	0.98	1.76	2.36
			12	0.64	1.20	2.01	2.63
			14	0.54	1.08	1.88	2.52
		16	9	0.85	1.55	2.57	3.24
			12	1.33	2.18	3.19	3.93
			14	1.37	2.23	3.29	4.22
		20	9	1.03	1.84	2.90	3.61
			12	1.88	2.85	3.95	4.78
			14	2.12	3.11	4.31	5.50

Table 5.10 Interaction effect of CTE by slab thickness on faulting

Input Variables		Level 1	Level 2	Mean Faulting (mm)			
1	2			5 years	10 years	20 years	30 years
CTE	Slab Thickness	4	9	0.32	0.66	1.26	1.78
			12	0.63	1.15	1.94	2.59
			14	0.69	1.24	2.10	2.90
		5	9	0.64	1.23	2.14	2.80
			12	1.11	1.88	2.84	3.58
			14	1.19	1.96	2.99	3.90
		6.5	9	1.41	2.48	3.83	4.63
			12	2.11	3.20	4.36	5.17
			14	2.16	3.20	4.39	5.44

Note: The unexpected trend of less faulting for thinner slab and vice versa is due to fixing the dowel diameter to 1.25 inches. The increased bearing stress in thicker slabs due to smaller dowel diameter will cause this anomaly. By increasing the dowel diameter to 1.5 inch for thicker slab (i.e. the MDOT practice) will rectify this predicted trend.

5.1.3 Effect of Input Variables on Roughness (IRI)

Initially, the descriptive statistics such as mean performance for each input variable was summarized. However, as the differences in the means might not ascertain a significant difference, essentially due to uncertainty (variability) associated with means. Therefore, statistically analyses using ANOVA were performed for predicted pavement roughness.

5.1.3.1 Descriptive Statistics

Table 5.11 shows predicted roughness performance within each cell of the full-factorial design matrix at 30 years. Also, the row and column averages are presented in the same table. The row

averages can be used to investigate the main effects of input variables by ignoring joint spacing. In addition, the column averages can be utilized to study the effects of joint spacing on cracking by ignoring other input variables. Similar tables were generated for cracking at 5, 10, 15 and 20 years and are attached in Appendix A

Also to investigate the average effects of all input variables on roughness, time series averages were plotted for input variable levels. Figure 5.4 presents the input variables effects on surface roughness in rigid pavements. These effects are summarized below:

Joint Spacing: In general, rigid pavements with higher joint spacing showed higher roughness than those with lower joint spacing, as shown by Figure 5.4(a). The effect of joint spacing seems to be consistent over the pavement service life.

Slab Thickness: Figure 5.4(b) shows the roughness development for 9-, 12- and 14-inches thick slabs. It is evident, that effect of slab thickness is significant on roughness. Rigid pavement with thin slabs developed higher roughness than those with thick slabs. Also, the results show that this effect is more pronounced over a longer life of a pavement.

Coefficient of Thermal Expansion (CTE): A significant effect of CTE was observed for roughness development. The pavements with higher CTE showed much higher roughness than those with a lower CTE value. This effect is consistent and increases throughout the life span of a rigid pavement as presented in Figure 5.4(c).

The above simple analyses only helped in the interpretations of the main effects of input variables, while interaction between input variables still needs to be explored. Therefore, detailed statistical analyses were executed to address above mentioned short-comings. The outcomes of such type of analyses are described next.

5.1.3.2 Statistical Analysis (ANOVA)

Typically, a full-factorial experiments design such as considered in this study can be analyzed using fixed-effect models employing analysis of variance (ANOVA). This type of statistical analyses can help in identifying the main and the interactive effects between considered variables. However, it should be noted that if certain variables are interacting with each other, their main effect should not be considered while making conclusions. Therefore, conclusions in this case should be based on the cell means rather than marginal means.

As an example, the summary results from ANOVA are given in Table 5.12 at 30 years. A *p-value* less than 0.05 (i.e. a confidence level of 95%) is used as a threshold to identify a statistically significant effect. The results are presented below according to main and interaction.

Main Effects

The results in Table 5.12 confirm that only CTE has a statistically significant effect on the roughness development. The mean values for all variables are presented in Table 5.13. The interpretation of only statistically significant effects is presented below:

CTE: Pavement concrete having a higher CTE value has shown a higher amount of roughness than those which have a lower CTE value. This effect is marginal with regards to practical significance.

Interaction Effects

No statistical significant interaction was found between the input variables for roughness development.

Table 5.11 Roughness in rigid pavements after 30 years

Slab Thickness	CTE	Joint Spacing			Average
		12	16	20	
9	4	3.48	3.65	3.58	3.57
	5	3.90	3.99	2.58	3.49
	6.5	4.52	3.27	3.13	3.64
12	4	2.36	2.55	3.26	2.72
	5	2.69	3.33	4.06	3.36
	6.5	3.36	4.57	3.27	3.73
14	4	2.25	2.55	2.70	2.50
	5	2.59	2.88	4.05	3.17
	6.5	3.10	4.32	4.65	4.02
Average		3.14	3.46	3.48	3.36

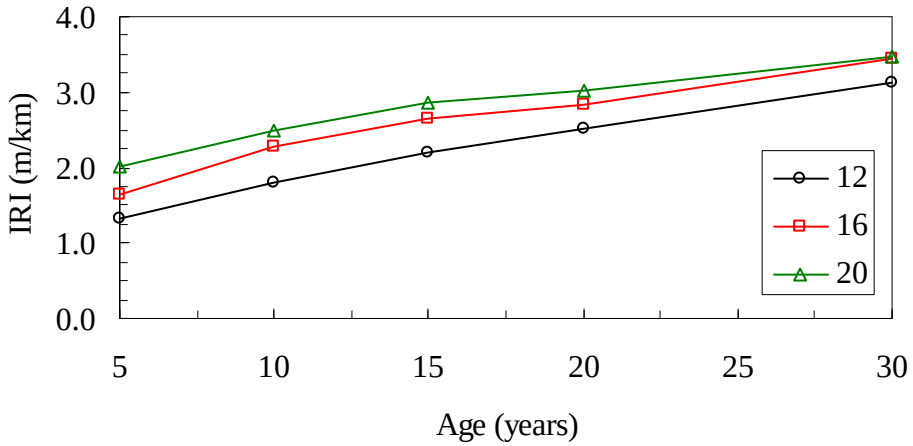

(a) Effect of joint spacing

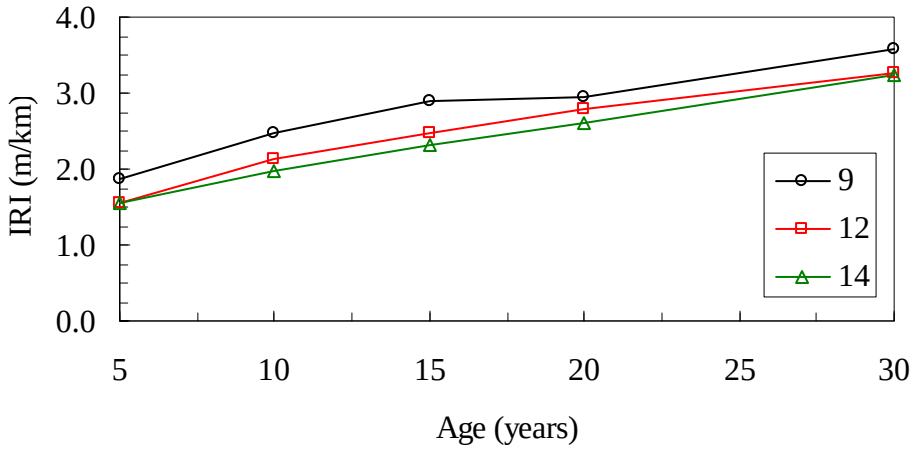

(b) Effect of slab thickness

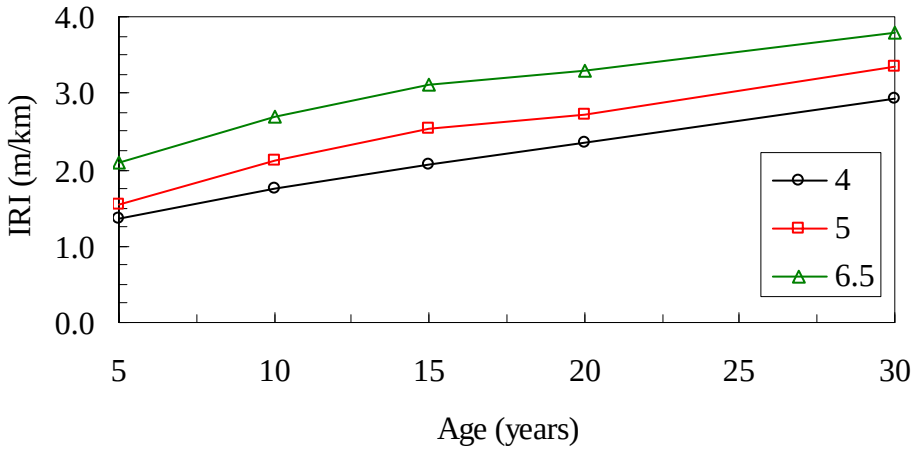

(c) Effect of CTE

Figure 5.4 Effect of input variables on roughness performance of JPCP

Table 5.12 ANOVA results for roughness (IRI)

Source	Type III Sum of Squares	df	Mean Square	F	Sig.
Corrected Model	.963[(a)]	18	.054	1.932	.172
Intercept	38.177	1	38.177	1378.29	.000
Joint spacing	.067	2	.034	1.213	.347
Slab thickness	.071	2	.036	1.286	.328
CTE	.306	2	.153	5.518	.031
Joint spacing * Slab thickness	.307	4	.077	2.770	.103
Joint spacing * CTE	.039	4	.010	.348	.839
Slab thickness * CTE	.174	4	.043	1.569	.272
Error	.222	8	.028		
Total	39.362	27			
Corrected Total	1.185	26			

a R Squared = .813 (Adjusted R Squared = .392)

Table 5.13 Main effect of input variables on roughness

Input Variable	Levels	Mean IRI (m/km)				Mean Differences			
		5 years	10 years	20 years	30 years	Δ_5	Δ_{10}	Δ_{20}	Δ_{30}
Joint Spacing (ft)	12	1.33	1.80	2.52	3.14	0.69	0.71	0.49	0.34
	16	1.65	2.29	2.83	3.46				
	20	2.01	2.50	3.01	3.48				
Slab Thickness (inch)	9	1.88	2.48	2.96	3.57	0.33	0.50	0.34	0.34
	12	1.56	2.13	2.79	3.27				
	14	1.55	1.98	2.62	3.23				
CTE (in/in/^{o}C)	4	1.36	1.75	2.34	2.93	0.72	0.95	0.96	0.87
	5	1.55	2.13	2.71	3.34				
	6.5	2.08	2.70	3.31	3.80				

5.2 VERIFICATION OF M-E PDG PERFORMANCE PREDICTION IN MICHIGAN

The study also entails *preliminary* evaluation and validation of M-E PDG software performance prediction and the comparison with in-service pavement sections in Michigan. In order to accomplish the objectives of research, the availability of following data elements are essential for both rigid and flexible pavement types:

- Pavement material-related data inputs
- Pavement layers cross-sectional information
- Traffic in terms of truck volumes and axle load spectrum
- Pavement performance (time series with age) data (cracking, faulting, rutting, and IRI etc,)

The state of Wisconsin is working on the regional calibration of the M-E PDG performance models. For this purpose, MDOT had provided them with above mentioned pavement data for five rigid and five flexible pavement sections. The particular requirements for this data were:

- Pavement sections should be old enough to exhibit some level of distresses;
- Pavement sections should include a mix of good and poor performing pavements; and
- Only AADTT and estimated growth rates were desired by Wisconsin study as this study is using national average for truck loadings and classifications

The research team used the same data for conducting performance prediction validation. However, there are some issues pertaining to the detailed traffic requirements, especially WIM data for those exact five locations each for rigid and flexible sections. MDOT provided an estimated percentage of vehicle classification by considering the WIM stations in vicinity of those locations. This data included the mix of traffic for all these specific sites based on the available truck volume and loading data from the nearby WIM stations. However, it was also pointed out that three or more years old MDOT WIM data have certain accuracy issues:

- Data older than 3 years were collected based on the piezo-sensor technology, which had serious calibration issues;
- Temperature dependency of piezo-sensors;
- Based on above reasons, this data contains an error of about ± 20 – 25% in GVWs.

Nonetheless, in the past 3 years the WIM data collected by MDOT is more accurate with an error of ± 3 – 5% in GVWs. The accuracy of the newer MDOT WIM data was improved because of following reasons:

- Use of quartz-sensors and bending plate technology
- Adoption of improved calibration procedures

In order to increase the number of sections in this exercise, it was also decided that the research team will also look at the rigid and flexible pavement sections in the SPS-2 (US-23) and SPS-1 (US-127) experiments. The required data for these sections were extracted from the LTPP

database. Next, the results from the SPS-2 (in Michigan) and the MDOT pavement sections are presented.

5.2.1 LTPP SPS-2 Pavement Sections in Michigan

The main advantages and motivations for using the SPS-2 rigid pavement sections in this research include:

- Availability of traffic, materials and pavement cross-sectional data in the LTPP database
- Accessibility of at least 5 to 10 years of performance data (cracking, faulting and roughness in terms of IRI)
- Pavement performance under local traffic and environment in Michigan.

The only limitation in using the SPS-2 pavements is that the pavement design does not reflect the typical MDOT practice. In addition, these pavements were used in the global calibration of M-E PDG performance models. The same pavement design for these test sections was repeated in several sites to populate the SPS-2 experiment design. Nevertheless, these pavement sections have undergone more than 10 years of unique truck traffic and Michigan climate. A brief introduction to the SPS-2 experiment is given below.

The primary objective of the SPS-2 experiment is to determine the relative influence and long-term effectiveness of design features and the impact of site conditions on the performance of doweled-jointed plain concrete pavement (JPCP) sections with transverse joints and uniform 4.6 m (15 ft.) joint spacing (*20*). As the test sections in the experiment have been monitored since construction, the experiment provides an opportunity to better estimate the relative influence of design and site-related factors affecting pavement performance.

The overall experiment consists of 192 factor-level combinations comprised of eight site-related (subgrade soil type and climate) combinations and 24 pavement-structure combinations (design factors). The experiment was developed such that 12 sections were built, with only half of the possible combinations of design factors, at each of 14 sites. The original plan was that 48 test sections representing all structural factor and subgrade type combinations in the experiment are to be constructed in each of the climatic zones, with 24 test sections to be constructed on fine-grained soil and 24 test sections to be constructed on coarse-grained soil. Moreover, for each climatic zone and soil type combination, 12 sections were to be constructed at one site and the other 12 sections at another (*21*). The structural (design) factors included in the experiment are:

- drainage—presence or lack of drainage;
- base type—dense-graded aggregate (DGAB), lean concrete (LCB), and permeable asphalt-treated (PATB);
- PCC slab thickness—8- and 11-inch;
- PCC flexural strength—550- and 900-psi at 14-day; and
- lane width—12- and 14-ft.

The SPS-2 site factors include climatic zones and subgrade types. At each site, six sections have a target PCC slab thickness of 203 mm and the remaining six have a target PCC slab thickness of

279 mm. The 76 mm difference was believed to be necessary to demonstrate the effect of PCC slab thickness and its interaction with other factors on performance (*22*). The other factors with two levels (PCC flexural strength and lane width) each have six test sections corresponding to each level. In terms of base type, four test sections have DGAB, four have LCB, and four have PATB over DGAB. In-pavement drainage is provided only for the sections with PATB as the base.

Though a major factor, traffic is not addressed like other design factors, in that only a lower limit was originally specified in terms of ESALs per year. SPS-2 test sites must have a minimum estimated traffic loading of 200,000 ESALs per year in the design lanes. Based on the average annual precipitation and the Freezing Index, the sites in the experiment have been classified into different climatic zones using the thresholds defined in the LTPP program.

5.2.1.1 Traffic Inputs

All the SPS-2 pavement sections are located sequentially on US-23 (North bound) in Michigan. Therefore, essentially the design lane of these sections has experienced the same amount of traffic in terms of loading and repetitions. The axle load spectra and AADTT along with the truck classification data were extracted from the LTPP database (Release 21). The truck classification and AADTT for these sections is shown in Table 5.14. The axle load spectra for different axle configurations were also imported in the M-E PDG software, however, due to limited space, that is not presented in this report.

5.2.1.2 Material Inputs— thickness, type and stiffness

Several material related inputs are required for various pavement layers, all the related material data including; (a) layer thicknesses, (b) layer material types, (c) strength and index properties and (d) other structural details, were extracted from the LTPP database if available. In cases, where material-related input was not available in the LTPP database, level 3 inputs were assumed. Table 5.14 also presents the summary of important inputs used in the M-E PDG software (version 1.0).

5.2.1.3 Climate

To simulate the specific environment close to the SPS-2 site, a weather station was used to incorporate the environment-related inputs in the M-E PDG software. The weather station in Adrian, Michigan which is a few miles away from the SPS-2 site on US-23 was utilized to extract specific climate-related inputs.

Table 5.14 Data Inputs for M-E PDG — SPS-2 Michigan Sections

Traffic		SPS-2 Experiment Pavement Sections											
		26-0213	26-0214	26-0215	26-0216	26-0217	26-0218	26-0219	26-0220	26-0221	26-0222	26-0223	26-0224
AADTT		3,295	3,295	3,295	3,295	3,295	3,295	3,295	3,295	3,295	3,295	3,295	3,295
FHWA Class	4	1.3%	1.3%	1.3%	1.3%	1.3%	1.3%	1.3%	1.3%	1.3%	1.3%	1.3%	1.3%
	5	12.1%	12.1%	12.1%	12.1%	12.1%	12.1%	12.1%	12.1%	12.1%	12.1%	12.1%	12.1%
	6	2.3%	2.3%	2.3%	2.3%	2.3%	2.3%	2.3%	2.3%	2.3%	2.3%	2.3%	2.3%
	7	0.3%	0.3%	0.3%	0.3%	0.3%	0.3%	0.3%	0.3%	0.3%	0.3%	0.3%	0.3%
	8	4.5%	4.5%	4.5%	4.5%	4.5%	4.5%	4.5%	4.5%	4.5%	4.5%	4.5%	4.5%
	9	67.2%	67.2%	67.2%	67.2%	67.2%	67.2%	67.2%	67.2%	67.2%	67.2%	67.2%	67.2%
	10	2.4%	2.4%	2.4%	2.4%	2.4%	2.4%	2.4%	2.4%	2.4%	2.4%	2.4%	2.4%
	11	3.0%	3.0%	3.0%	3.0%	3.0%	3.0%	3.0%	3.0%	3.0%	3.0%	3.0%	3.0%
	12	0.7%	0.7%	0.7%	0.7%	0.7%	0.7%	0.7%	0.7%	0.7%	0.7%	0.7%	0.7%
	13	6.2%	6.2%	6.2%	6.2%	6.2%	6.2%	6.2%	6.2%	6.2%	6.2%	6.2%	6.2%
Climate													
Latitude (degrees.minutes):		41.75	41.75	41.75	41.75	41.75	41.75	41.75	41.75	41.75	41.75	41.75	41.75
Longitude (degrees.minutes):		-83.7	-83.7	-83.7	-83.7	-83.7	-83.7	-83.7	-83.7	-83.7	-83.7	-83.7	-83.7
Elevation (ft):		677	677	677	677	677	677	677	677	677	677	677	677
Structure--Design Features													
Permanent curl/warp effective temperature difference (°F):		-10	-10	-10	-10	-10	-10	-10	-10	-10	-10	-10	-10
Joint Design													
Joint spacing (ft):		15	15	15	15	15	15	15	15	15	15	15	15
Sealant type:		Liquid											
Dowel diameter (in):		1.25											
Dowel bar spacing (in):		12											
Edge Support		AC Shoulder											
Widened Slab (ft):		14	12	12	14	14	12	12	14	14	12	12	14
Base Properties													
Base type:		Granular											
Erodibility index:		Fairly Erodable (4)											
PCC-Base Interface		Full friction contact											
Structure--ICM Properties													
Surface shortwave absorptivity:		0.85											
Structure - Layers													
Layer 1 - PCC													
PCC material		JPCP											
Layer thickness (in):		8.6	8.9	11.2	11.4	8.5	7.1	10.9	11.1	8.2	8.4	11	11.2
Unit weight (pcf):		150											
Poisson's ratio		0.2											
Thermal Properties													
Coefficient of thermal expansion (per F° x 10- 6):		5.5											
Thermal conductivity (BTU/hr-ft-F°) :		1.25											
Heat capacity (BTU/lb-F°):		0.28											
Mix Properties													
Cement type:		Type I											
Cementitious material content (lb/yd^3):		556											
Water/cement ratio:		0.42											
Aggregate type:		Dolomite											
PCC zero-stress temperature (F°)		Derived											
Ultimate shrinkage at 40% R.H (microstrain)		Derived											
Reversible shrinkage (% of ultimate shrinkage):		50											
Time to 50% of ultimate shrinkage (days):		35											
Curing method:		Curing compound											
Strength Properties													
Input level:		Level 3											
28-day PCC modulus of rupture (psi):		700	975	585	900	550	900	620	970	550	900	550	850
Layer 2 - Base													
Material:		GB	GB	GB	GB	LCB	LCB	LCB	LCB	PATB	PATB	PATB	PATB
Thickness(in):		6.1	5.8	6.2	5.9	6.2	7.1	6.3	5.8	4.2	4.2	4.1	4.3
Strength Properties													
Input Level:		Level 3											
Analysis Type:		ICM Calculated Modulus											
Poisson's ratio:		0.35											
Coefficient of lateral pressure,Ko:		0.5											
Modulus (input) (psi):		30,000	30,000	30,000	30,000	200,000	200,000	200,000	200,000	n/a	n/a	n/a	n/a
Layer 3 - Sand Subbase													
Unbound Material:		A-6	A-6	A-6	A-6	A-6	A-6	A-6	A-6	CS	CS	CS	CS
Thickness(in):		18.5	18.5	15.5	15.5	18.5	18.5	15.5	15.5	4.4	4.2	4.3	4
Strength Properties													
Input Level:		Level 3											
Analysis Type:		ICM Calculated Modulus											
Poisson's ratio:		0.35											
Coefficient of lateral pressure,Ko:		0.5											
Modulus (input) (psi):		14,000	14,000	14,000	14,000	14,000	14,000	14,000	14,000	30,000	30,000	30,000	30,000
Layer 4 - Subgrade													
Unbound Material:		A-6											
Thickness(in):		Semi-infinite											
Strength Properties													
Input Level:		Level 3											
Analysis Type:		ICM Calculated Modulus											
Poisson's ratio:		0.35											
Coefficient of lateral pressure,Ko:		0.5											
Modulus (input) (psi):		14,000	14,000	14,000	14,000	14,000	14,000	14,000	14,000	14,000	14,000	14,000	14,000
Data Source		LTPP DataPave (Release 21)											

5.2.1.4 Discussion of Results for SPS-2 Test Section—Predicted versus Observed Performance

As mentioned before, the main objectives of this task are to (a) verify the M-E PDG performance predictions in Michigan, and (b) identify the suitability needs for implementing M-E PDG design procedure in Michigan. To accomplish these objectives, the rigid pavement sections in Michigan were analyzed using M-E PDG software (version 1.0). These sections are distributed in different regions in the state of Michigan. Two sources of data were utilized to analyze these pavements and accordingly these pavements were considered separately in this task. These pavements included: (a) the LTPP SPS-2 experiment, and (b) the rigid pavements provided by Michigan DOT. In this section, the results for SPS-2 test sections are presented while the analysis of MDOT pavements is described in the next section of this report.

Table 5.14 shows all the M-E PDG required inputs used for analyzing the SPS-2 test sections. The comparison of predicted and observed performance was made by plotting the cracking, faulting, and roughness (IRI) with age of these test sections. Figures 5.5 through 5.7 present the examples of these plots for good, fair, and poor matches, respectively between observed and predicted performance. Similar plots for each distress types were prepared and are attached in Appendix B of this report.

Table 5.15 presents the summary of this comparison. It can be seen that most of the observed distresses in several sections match reasonably with the M-E PDG predictions. One of the reasons for these matches is that the performance models in the M-E PDG were calibrated using the LTPP data. However, the predicted performance is different for some of these sections. The plausible causes of such discrepancies in such could be construction-related issues which can not be explained by the mechanistic-empirical design procedures.

Table 5.15 Comparison of predicted and observed JPCP performance — SPS-2 Sections

Section	Fatigue (% slab cracked)	Joint faulting	Roughness (IRI)
26-0213	R	R	R
26-0214	U	R	R
26-0215	R	R	R
26-0216	R	R	R
26-0217	O	R	O
26-0218	U	R	U
26-0219	R	R	O
26-0220	R	R	R
26-0221	R	R	R
26-0222	R	R	O
26-0223	R	O	U
26-0224	R	R	R

R = Reasonable match between predicted and observed performance
O = Overestimate predicted performance
U = Underestimate predicted performance
Note: This comparison is based on visual trend assessment. The subjective approach is based on general trend matching between predicted and observed performance.

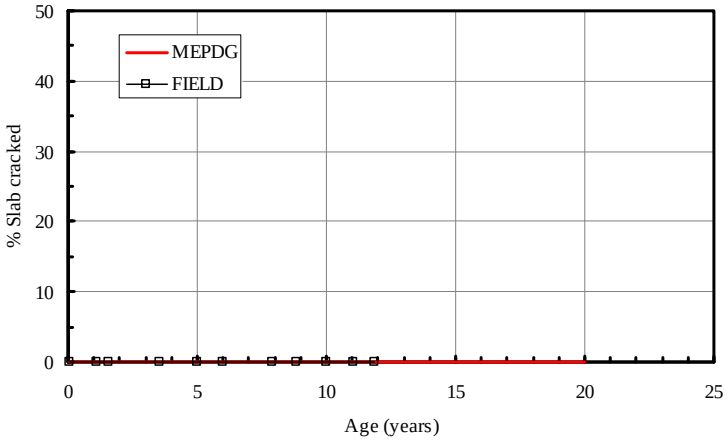

(a) Cracking (% slab cracked)

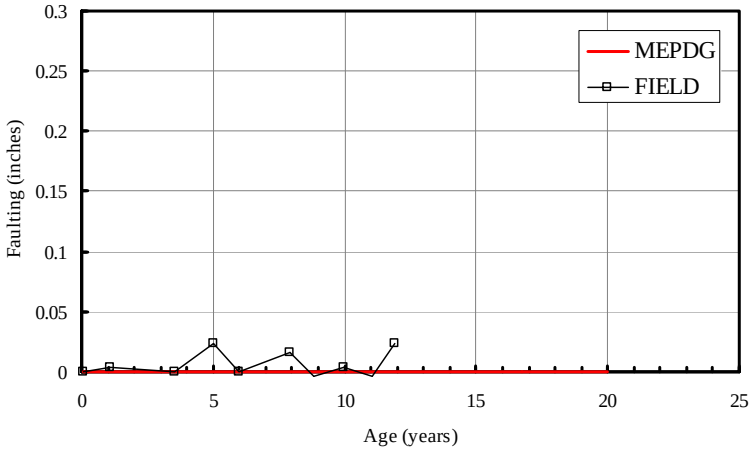

(b) Joint faulting (mm)

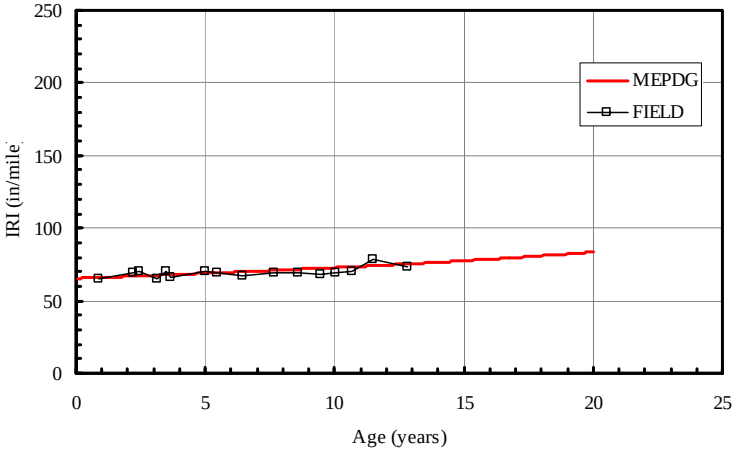

(c) Roughness in terms of IRI (inch/mile)

Figure 5.5 Observed versus predicted performance for section 26-0221— Good match

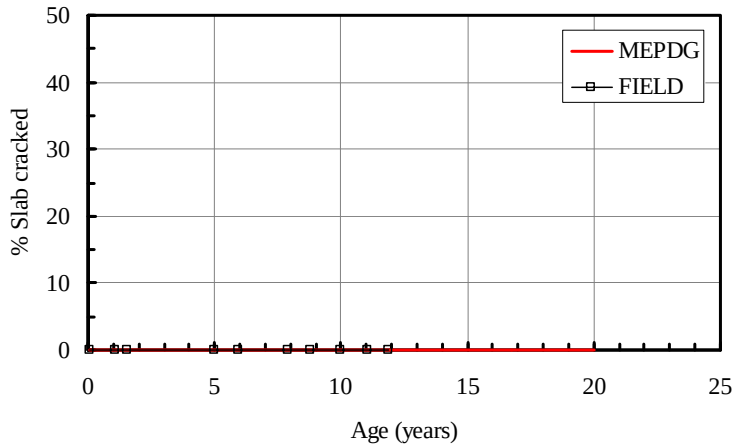

(a) Cracking (% slab cracked)

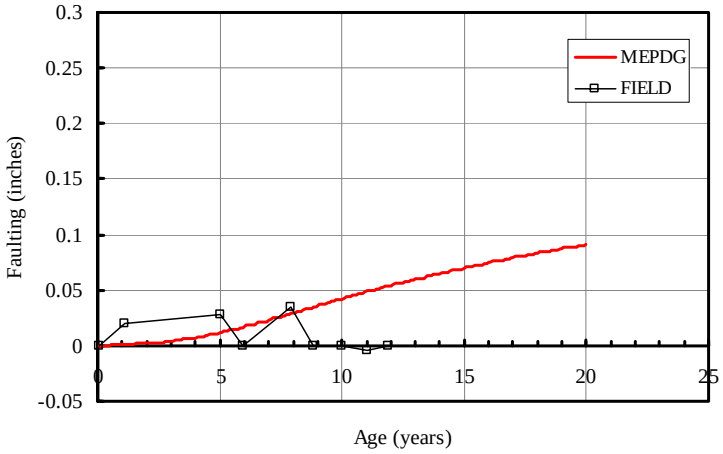

(b) Joint faulting (mm)

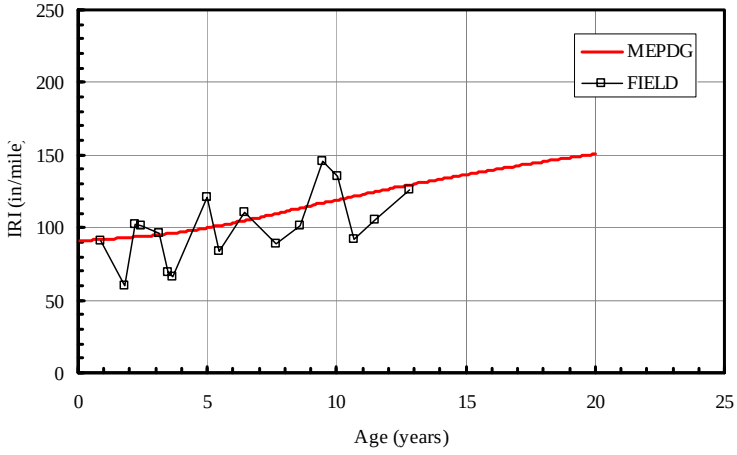

(c) Roughness in terms of IRI (inch/mile)

Figure 5.6 Observed versus predicted performance of section 26-0216 — Fair match

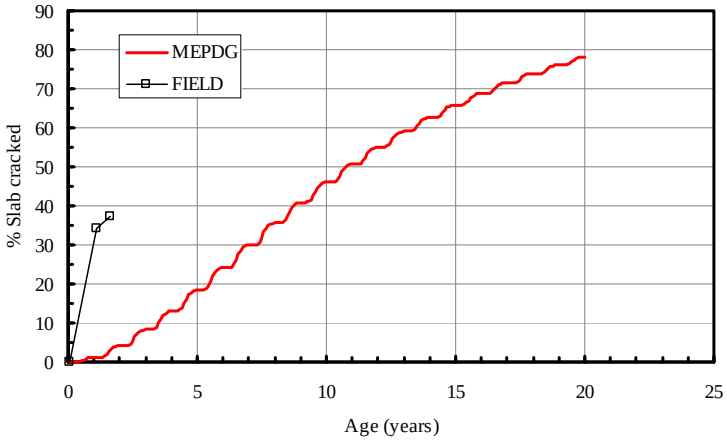

(a) Cracking (% slab cracked)

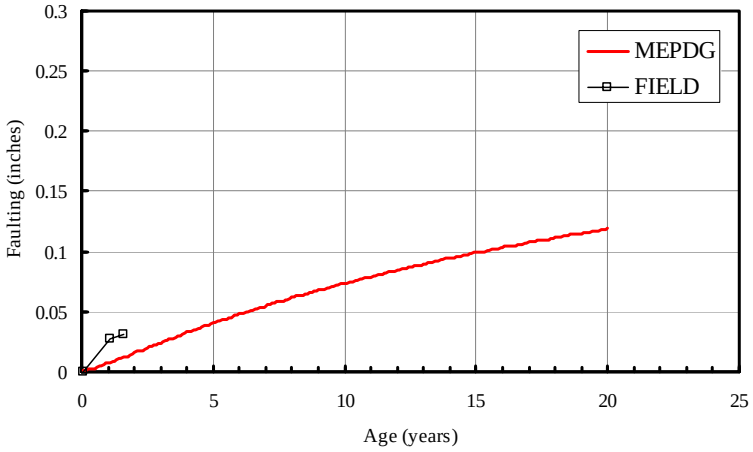

(b) Joint faulting (mm)

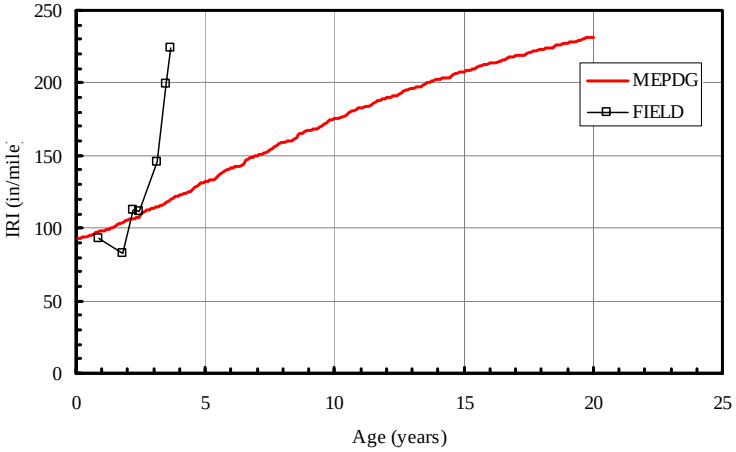

(c) Roughness in terms of IRI (inch/mile)

Figure 5.7 Observed versus predicted performance of section 26-0218 — Poor match

5.2.2 MDOT Rigid Pavement Sections

As mentioned above, five JPCP sections were provided by MDOT. These were the five oldest projects since MDOT began experimenting with JPCP construction in mid 90's. These pavements were selected based on the service life i.e. at least 10 years of age so that sufficient distresses are manifested on these pavements. The available pavement data required to execute M-E PDG was provided by MDOT. Level 3 input levels were adopted if appropriate or sufficient input data was unavailable. The respective weigh-in-motion (WIM) weigh station data was also used in the analyses to characterize the traffic loadings and repetitions for all these pavement sites. The traffic data used for the analysis is presented next.

5.2.2.1 Traffic Inputs

The closest WIM station to the pavement sites was used to acquire necessary traffic data. However, it may be possible that due to unavailability of WIM station close to selected project sites, some of the WIM data may not be exactly representative of the selected project site. Classification (Card 4) and truck weight (Card 7) data, for selected locations were analyzed using TrafLoad software to extract required traffic-related M-E PDG input data. It should be noted that both Card 4 and Card 7 traffic data included all days in each month spanning April 2006 to March 2007. Some of the weigh station sites have Piezo WIM sensors (see Table 5.17), which might have some concerns regarding temperatures variations and calibration. However, the available traffic data was used in this analysis as no other representative information was available for these sites.

Figure 5.8 shows the average annual daily truck traffic (AADTT) and truck distribution in the design lane for the four WIM sites. It can be seen from these results that WIM site 11-7179 (used for site 32516) has the highest truck traffic while WIM site 47-8219 (used for 2815) has the lowest truck volumes among four WIM sites (see Figure 8a). The truck distributions by class are shown in Figure 8b, which shows that class 9 has the highest share among all sites.

In order to consider the monthly and the hourly distribution of truck traffic, monthly and hourly adjustment factors were determined (using TrafLoad). These adjustment factors for all sites are presented in Figure 9. The respective adjustment factors for each site were used as an input in the M-E PDG.

5.2.2.2 Material Inputs

Several material related inputs are required for various pavement layers, all the related material data including; (a) layer thicknesses, (b) layer material types, (c) strength and index properties and (d) other structural details, were provided by MDOT and were used in this analysis if available. When material-related input was not available, level 3 inputs were assumed. Table 5.16 also presents the summary of important inputs, for all sections, used in the M-E PDG software (version 1.0).

5.2.2.3 Climate

To simulate the specific environment close to the MDOT site, weather stations were used to incorporate the environment-related inputs in the M-E PDG software. The weather stations at Detroit Airport, Lansing, and Kalamazoo which are a few miles away from the MDOT sites on respective highways (see Table 5.17) were utilized to extract specific climate-related inputs.

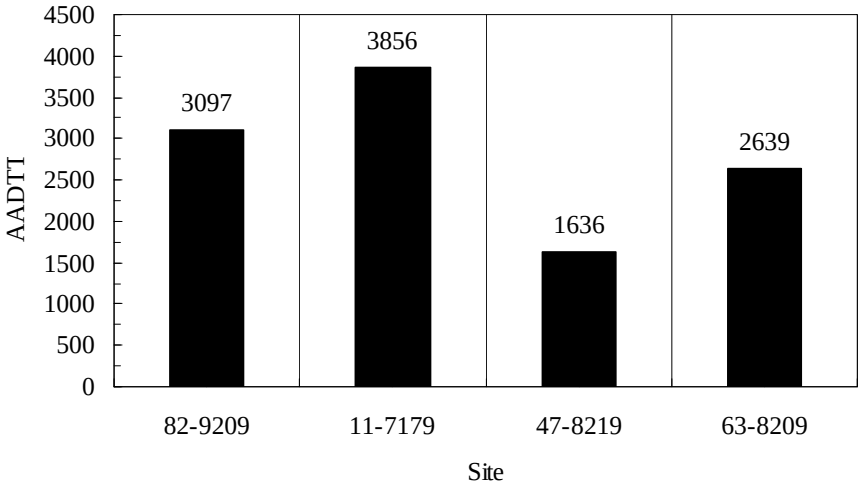

(a) Average annual truck traffic in the design lane

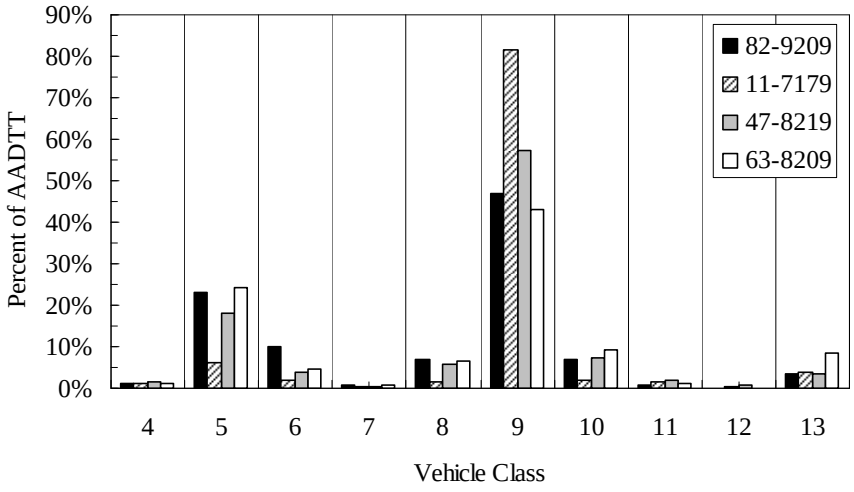

(b) Truck traffic distribution

Figure 5.8 Traffic inputs for MDOT JPCP sections

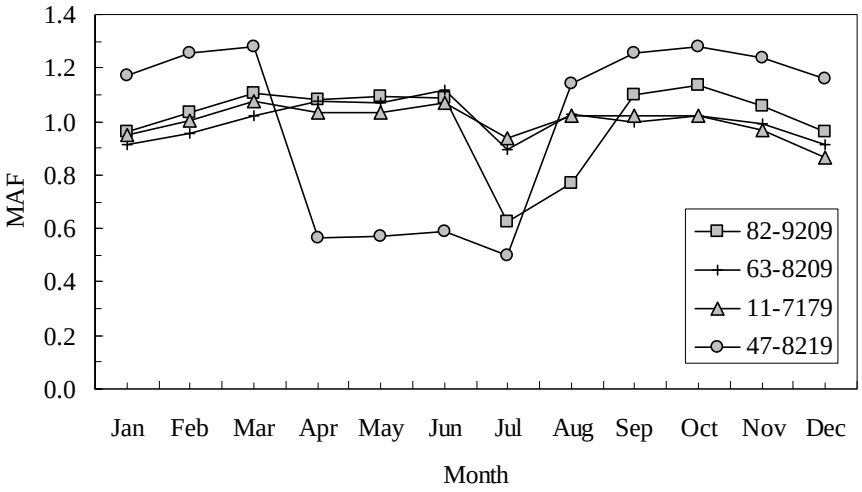

(a) Monthly adjustment factors

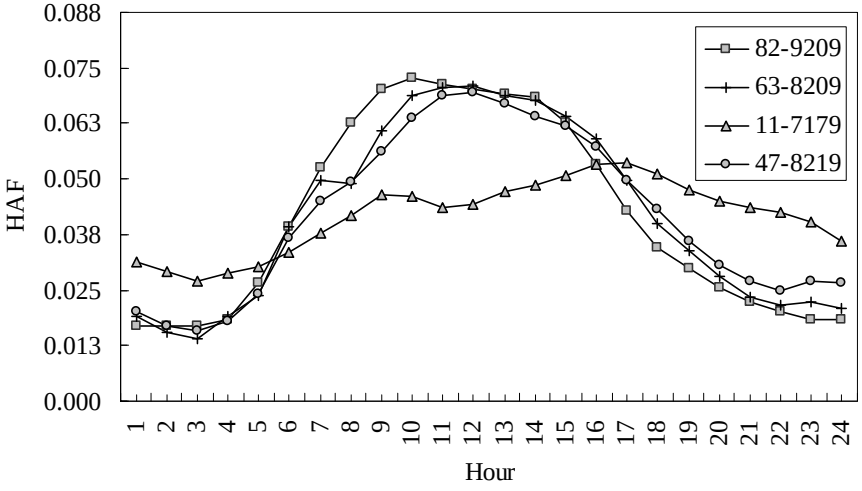

(a) Hourly adjustment factors

Figure 5.9 Monthly and hourly traffic variations for MDOT JPCP sections

Table 5.16 Data Inputs for M-E PDG —Michigan DOT Sections

Traffic		MDOT Pavement Sections				
		36003E	32516E	32516W	28215E	28215W
AADTT		3,097	3,856	3,856	1,636	1,636
FHWA Class	4	1.3%	1.2%	1.2%	1.4%	1.4%
	5	23.1%	6.2%	6.2%	18.1%	18.1%
	6	9.9%	2.1%	2.1%	3.7%	3.7%
	7	0.9%	0.2%	0.2%	0.5%	0.5%
	8	7.0%	1.5%	1.5%	5.9%	5.9%
	9	46.8%	81.5%	81.5%	57.3%	57.3%
	10	6.7%	1.8%	1.8%	7.2%	7.2%
	11	0.8%	1.4%	1.4%	2.0%	2.0%
	12	0.1%	0.4%	0.4%	0.6%	0.6%
	13	3.4%	3.8%	3.8%	3.3%	3.3%
Climate						
Latitude (degrees.minutes):		42.25	42.14	42.14	42.47	42.47
Longitude (degrees.minutes):		-83.01	-85.33	-85.33	-84.35	-84.35
Elevation (ft):		628	895	895	882	882
Structure--Design Features						
Permanent curl/warp effective temperature difference (°F):		-10	-10	-10	-10	-10
Joint Design						
Joint spacing (ft):		16	16	16	15	15
Sealant type:				Preformed		
Dowel diameter (in):				1.25		
Dowel bar spacing (in):				12		
Edge Support		Tied PCC shoulder	Widened Slab	Widened Slab	Tied PCC shoulder	Tied PCC shoulder
Long-term LTE(%):		40	40	40	40	40
Widened Slab (ft):		n/a	n/a	n/a	n/a	n/a
Base Properties						
Base type:				Granular		
Erodibility index:				Fairly Erodable (4)		
PCC-Base Interface		Full friction contact	Full friction contact	Full friction contact	Full friction contact	Full friction contact
Loss of full friction (age in months):		0	0	0	0	0
Structure--ICM Properties						
Surface shortwave absorptivity:				0.85		
Structure - Layers						
Layer 1 - PCC						
PCC material				JPCP		
Layer thickness (in):		12	12	12	10	10
Unit weight (pcf):				150		
Poisson's ratio				0.2		
Thermal Properties						
Coefficient of thermal expansion (per F° x 10- 6):		4.8	6	6	4.8	4.8
Thermal conductivity (BTU/hr-ft-F°) :				1.25		
Heat capacity (BTU/lb-F°):				0.28		
Mix Properties						
Cement type:				Type I		
Cementitious material content (lb/yd^3):				564		
Water/cement ratio:		0.42	0.42	0.42	0.42	0.42
Aggregate type:		Limestone	Limestone	Blast Furnace Slag	Blast Furnace Slag	Limestone
PCC zero-stress temperature (F°)				Derived		
Ultimate shrinkage at 40% R.H (microstrain)				Derived		
Reversible shrinkage (% of ultimate shrinkage):				50		
Time to50% of ultimate shrinkage (days):				35		
Curing method:				Curing compound		
Strength Properties						
Input level:				Level 3		
28-day PCC modulus of rupture (psi):				n/a		
28-day PCC compressive strength (psi):		5000	4500	5200	5000	5000
Layer 2 - Base						
Unbound Material:				Crushed gravel		
Thickness(in):		4	4	4	4	4
Strength Properties						
Input Level:				Level 3		
Analysis Type:				ICM Calculated Modulus		
Poisson's ratio:				0.35		
Coefficient of lateral pressure,Ko:				0.5		
Modulus (input) (psi):				25000		
Layer 3 - Sand Subbase						
Unbound Material:				A-3		
Thickness(in):		10	8	8	10	10
Strength Properties						
Input Level:				Level 3		
Analysis Type:				ICM Calculated Modulus		
Poisson's ratio:				0.35		
Coefficient of lateral pressure,Ko:				0.5		
Modulus (input) (psi):		13500	13500	13500	13500	13500
Layer 4 - Subgrade						
Unbound Material:		A-6	A-6	A-6	A-6	A-6
Thickness(in):				Semi-infinite		
Strength Properties						
Input Level:				Level 3		
Analysis Type:				ICM Calculated Modulus		
Poisson's ratio:				0.35		
Coefficient of lateral pressure,Ko:				0.5		
Modulus (input) (psi):		3500	3700	3700	4500	4500
Data Source				MDOT		

5.2.2.4 Discussion of Results for MDOT Sections—Predicted versus Observed Performance

In this section, the results for MDOT pavement sections are presented. Table 16 shows all the M-E PDG required inputs used for analyzing the MDOT pavement sections. The comparison of predicted and observed performance was made by plotting the faulting and the roughness (IRI) with age of these pavements. Figures 10 and 11 present the examples of these plots for good and poor matches, respectively between observed and predicted performance.

Table 17 presents the summary of this comparison. It can be seen that most of the observed distresses in several sections do not match reasonably with the M-E PDG predictions. One of the reasons for these matches is that the performance models in the M-E PDG were calibrated using the LTPP data. The plausible causes of such discrepancies could be construction-related issues which can not be explained by the mechanistic-empirical design procedures. In fact, the pavement section on I-94 in Berrien county have shown extensive cracking (see Figure 11) mainly due to negative built in curl as reported by Hansen and Smiley (*23*).

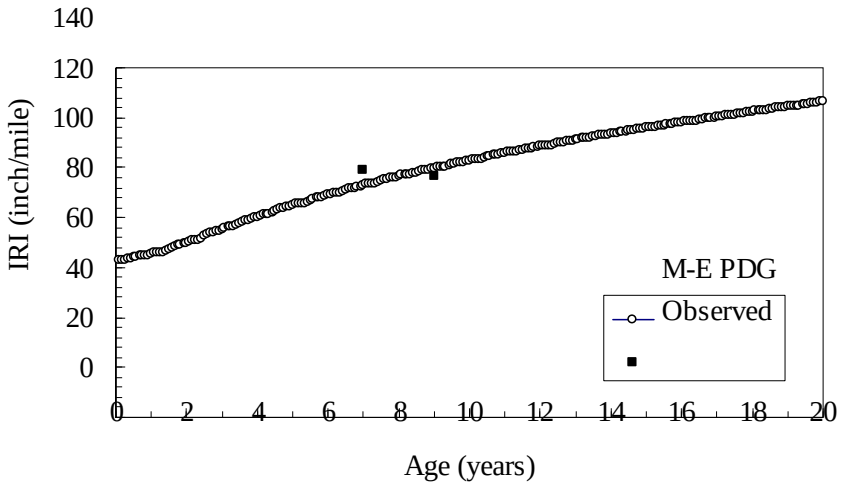

Figure 5.10 Predicted versus observed IRI for section 36003E— Good match

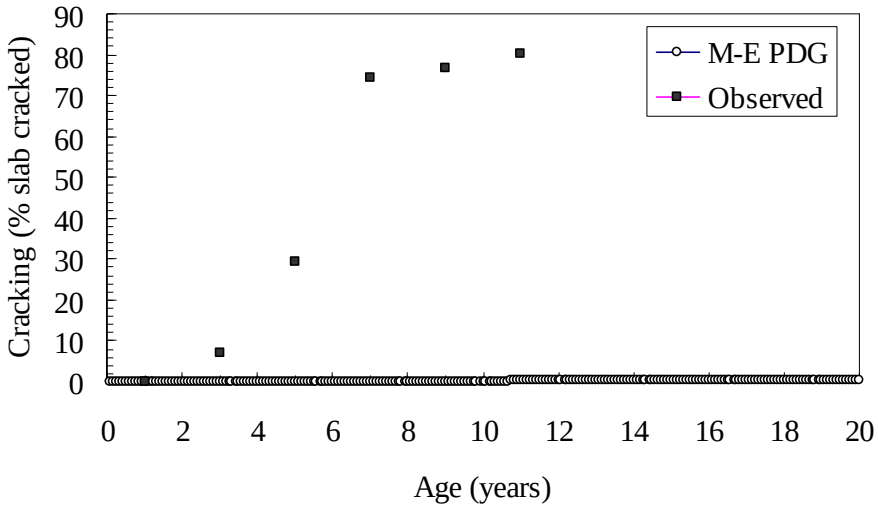

Figure 5.11 Observed versus predicted performance for section 32516E— Poor match

Table 5.17 Comparison of predicted and observed JPCP performance — MDOT sections

Section	County	Description of location	Fatigue (% slab cracked)	Roughness (IRI)
36003E	Oakland	I-96 WB/I-275 NB[1]	R	R
32516E	Berrien	I-94 EB East of I-96[2]	U	R
32516W	Berrien	I-94 WB East of I-96[2]	U	O
28215E	Livingston	I-96 EB East of Howell[3]	U	U
28215W	Livingston	I-96 WB East of Howell[3]	U	R

R = Reasonable match between predicted and observed performance
O = Overestimate predicted performance
U = Underestimate predicted performance
Note: This comparison is based on visual trend assessment. The subjective approach is based on general trend matching between predicted and observed performance.

[1] Closest WIM site 82-9201 (Quartz sensor)
[2] Closest WIM site 11-7179 (Piezo sensor)
[3] Closest WIM site 47-8219 (Quartz sensor)

5.3 SATELLITE SENSITIVITY ANALYSIS FOR TRAFFIC

This section will present the MDOT traffic data analysis using TrafLoad software. The output of TrafLoad is a direct input for traffic in M-E PDG software. The MDOT provided for characterizing the low, medium, and high traffic levels within the state of Michigan. The main objectives of the traffic data analyses are to:

- Use of TrafLoad software for traffic analyses to determine required traffic-related input in M-E PDG software and compare TrafLoad results with MDOT estimates,
- Compare traffic characteristics within various levels (low, medium and high) of traffic demands in Michigan,
- Evaluate traffic input requirements for M-E PDG software,
- Investigate the effects of various levels of traffic on rigid pavement performance.

The next section describes the traffic data used for these analyses.

5.3.1 MDOT Traffic Data Analysis Using TrafLoad Software

As mentioned before, a separate sensitivity was conducted for traffic-related inputs in M-E PDG. Four different locations were considered within each traffic level in this study (Data provided by MDOT traffic office). These twelve locations include a diversified traffic demand within the state of Michigan and cover several counties on the state highways representing low, medium, and high traffic, respectively, as shown in Table 5.18.

Table 5.18 MDOT Traffic Data for M-E PDG Project

Site Name	Traffic Level	Site ID	Site Description	Vehicle Class Scheme	Dates for Data
Hillsdale County	Low	308129	US-12	FHWA	Jan , 2005 to Dec, 2005
Arenac County		064249	US-23		Oct, 2005 to Sep, 2006
Sanilac County		746019	M-46		Oct, 2005 to Sep, 2006
Ingham County		338029	US-127		Oct, 2005 to Sep, 2006
Ionia County	Medium	345299	I-96	FHWA	Jan , 2005 to Dec, 2005
Clair County		776369	I-69		Oct, 2005 to Sep, 2006
Ottawa County		705059	I-196		Oct, 2005 to Sep, 2006
Kent County		419759	M-6		Oct, 2005 to Sep, 2006
Jackson County	High	387029	I-94	FHWA	Jan , 2005 to Dec, 2005
Brach County		127269	I-69		Oct, 2005 to Sep, 2006
Monroe County		588729	US-23		Oct, 2005 to Sep, 2006
Oakland County		638209	I-96		Oct, 2005 to Sep, 2006

The data provided by MDOT in FHWA ASCII format were analyzed using TrafLoad Software to calculate the required input for M-E PDG Software. Two types of data were required to generate these input traffic-related data:

- Card 4 for vehicle classification
- Card 7 for axle load spectra

All sites mentioned in Table 5.18 were analyzed using TrafLoad Software. It should be noted that the results of these analyses only show the traffic in the design lane in one direction. The direction of traffic used for the analyses was recommended by MDOT. The results from these analyses are presented in the next section according to M-E PDG required format:

1. Traffic Volume Adjustment Factors
   - Vehicle Class Distribution
     - Average annual daily truck traffic (AADTT)
     - AADTT distribution by vehicle class
   - Monthly Adjustment
     - Level 1 monthly adjustment factors (MAFs) by vehicle class
   - Hourly Traffic Distribution
     - Hourly truck traffic distribution i.e., hourly adjust factors (HAFs)

2. Axle Distribution Factors (Level 1 axle load distributions by axle configurations)
   - Single axle,
   - Tandem axle,
   - Tridem axle, and
   - Quad axle

3. General Traffic Inputs
   - Average Number of Axle per Vehicle Class
   - Axle configurations
   - Wheelbase

The traffic volume-related results are presented next.

5.3.1.1 Traffic Volume Adjustment Factors

The traffic input for these analyses mainly contains vehicle classification information (Card 4 FHWA format).

Vehicle Class Distribution

Tables 5.19 to 5.21 show the average AADTT and truck distributions, in the design lane in one direction, for each site within low, medium and high traffic levels, respectively. Similarly, Figures 5.12 to 5.17 present the AADTT and truck distributions within each traffic level, respectively. The TrafLoad results are in good agreement with the MDOT estimate provided by the traffic planning section. The MDOT estimate was based on more comprehensive data.

Table 5.19 Average annual daily truck traffic for low traffic levels

Vehicle Class	AADTT for Sites				% AADTT for Sites			
	308129	**064249**	**746019**	**338029**	**308129**	**064249**	**746019**	**338029**
4	6.2	4.6	3.1	10.8	1.4%	1.1%	2.1%	1.3%
5	126.8	206.4	106.7	206.5	28.6%	51.1%	72.8%	25.6%
6	23.7	20.9	6.5	34	5.3%	5.2%	4.4%	4.2%
7	3.1	2.2	1.4	3.5	0.7%	0.5%	1.0%	0.4%
8	17.9	19	4.5	59.7	4.0%	4.7%	3.1%	7.4%
9	188.8	67.4	11.4	326.6	42.6%	16.7%	7.8%	40.5%
10	28.2	32.1	6	95.7	6.4%	8.0%	4.1%	11.9%
11	19.6	1	0	6.1	4.4%	0.2%	0.0%	0.8%
12	1.3	0.1	0	0.8	0.3%	0.0%	0.0%	0.1%
13	28	50	7	62.4	6.3%	12.4%	4.8%	7.7%
TrafLoad AADTT	**444**	**404**	**147**	**806**	**100%**	**100%**	**100%**	**100%**
MDOT Estimate	**450**	**370**	**150**	**850**				

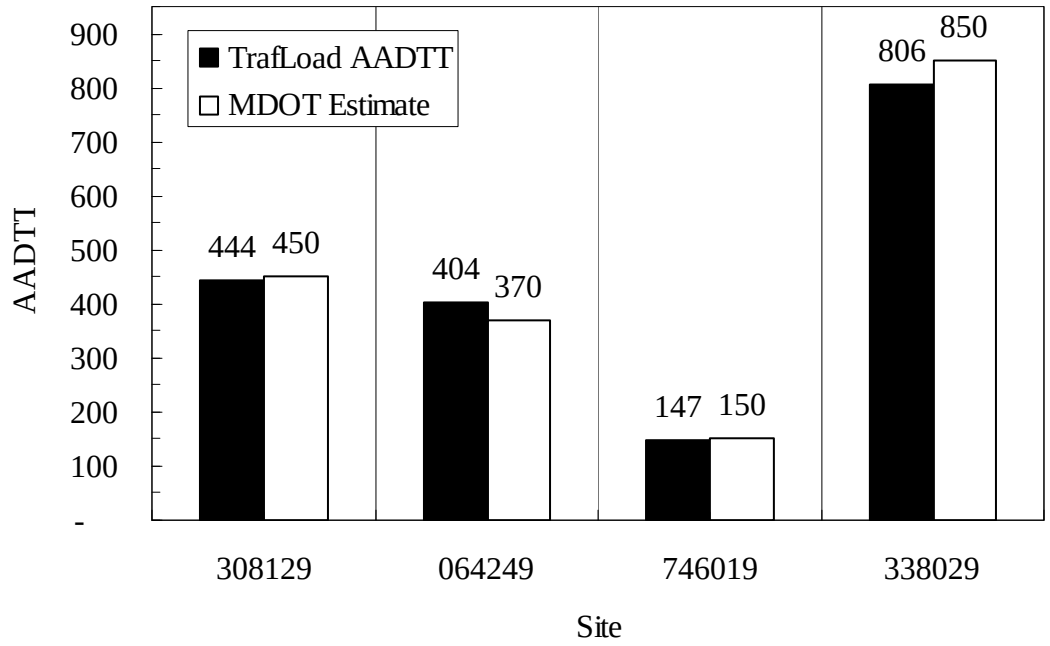

Figure 5.12 Comparison between traffic levels (TrafLoad versus MDOT)
(Low traffic levels)

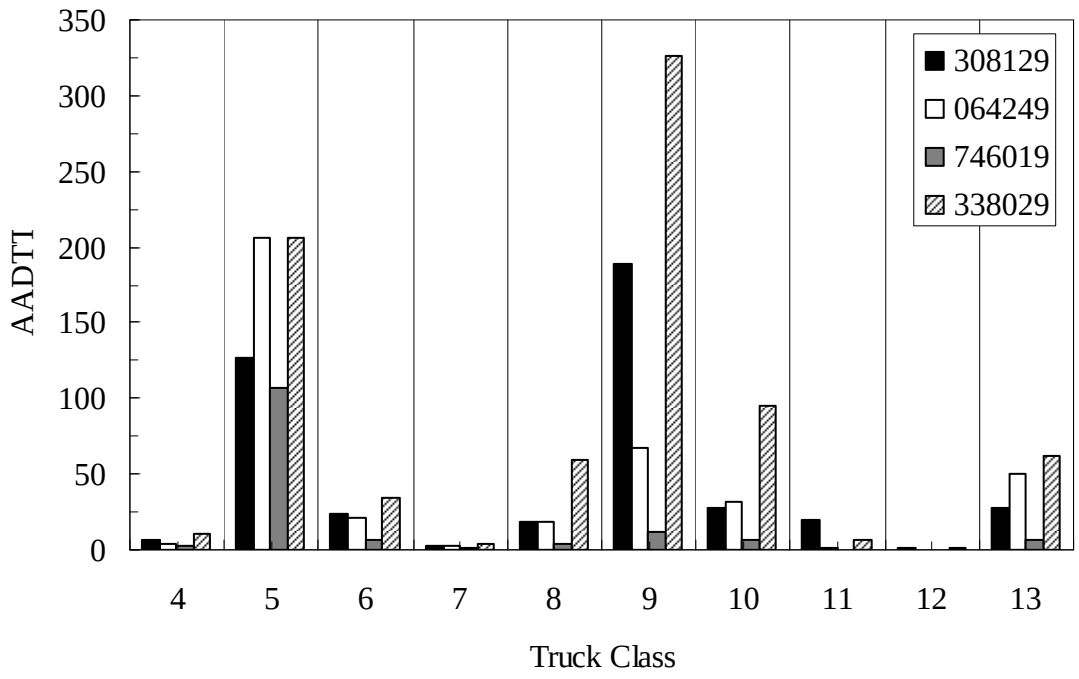

Figure 5.13 Comparison of AADTT by truck class (TrafLoad)
(Low traffic levels)

Table 5.20 Average annual daily truck traffic for medium traffic levels

Vehicle Class	AADTT for Sites				% AADTT for Sites			
	345299	**776369**	**705059**	**419759**	**345299**	**776369**	**705059**	**419759**
4	40.7	23.4	26.3	21.6	2.1%	1.3%	1.7%	1.1%
5	356.3	306.8	333.9	454.2	18.0%	17.2%	21.7%	23.1%
6	67.5	33.2	145.6	149	3.4%	1.9%	9.5%	7.6%
7	2.3	7.5	10	21.9	0.1%	0.4%	0.6%	1.1%
8	110.9	36.1	63	155.3	5.6%	2.0%	4.1%	7.9%
9	1169.6	1134.5	792.3	948.2	59.0%	63.6%	51.5%	48.3%
10	130.1	145.2	79.5	117.2	6.6%	8.1%	5.2%	6.0%
11	44.6	1.7	23.5	43.2	2.2%	0.1%	1.5%	2.2%
12	9.9	1.4	5	6.4	0.5%	0.1%	0.3%	0.3%
13	51.9	94.3	60.2	47.3	2.6%	5.3%	3.9%	2.4%
TrafLoad AADTT	**1,984**	**1,784**	**1,539**	**1,964**	**100.0%**	**100.0%**	**100.0%**	**100.0%**
MDOT Estimate	**1,850**	**1,750**	**1,500**	**2,000**				

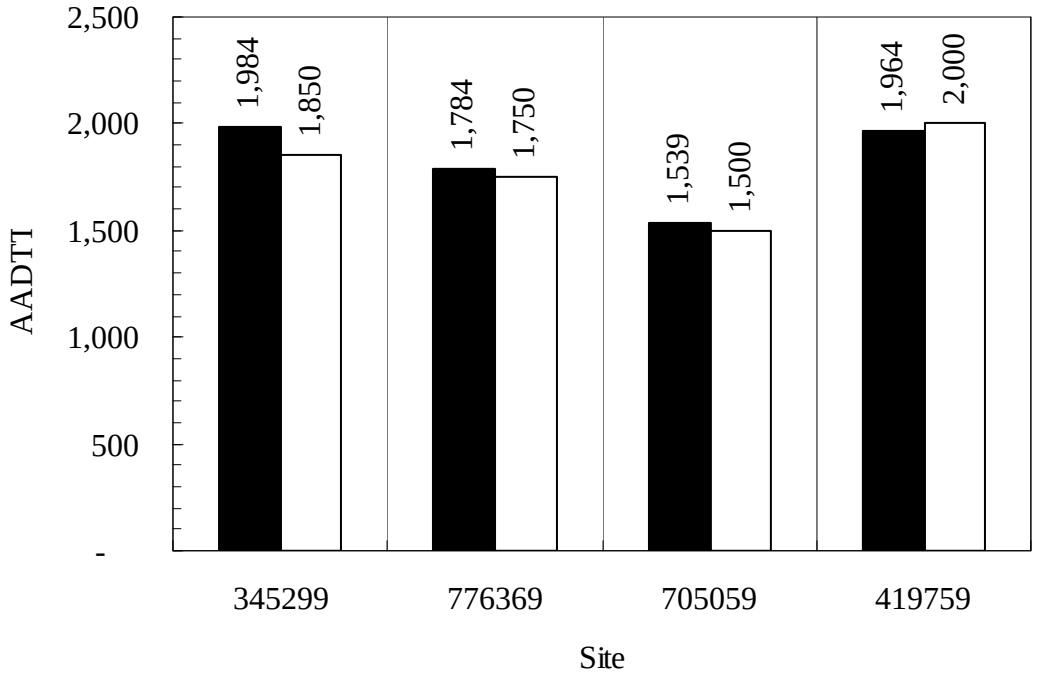

Figure 5.14 Comparison between traffic levels (TrafLoad versus MDOT)
(Medium traffic levels)

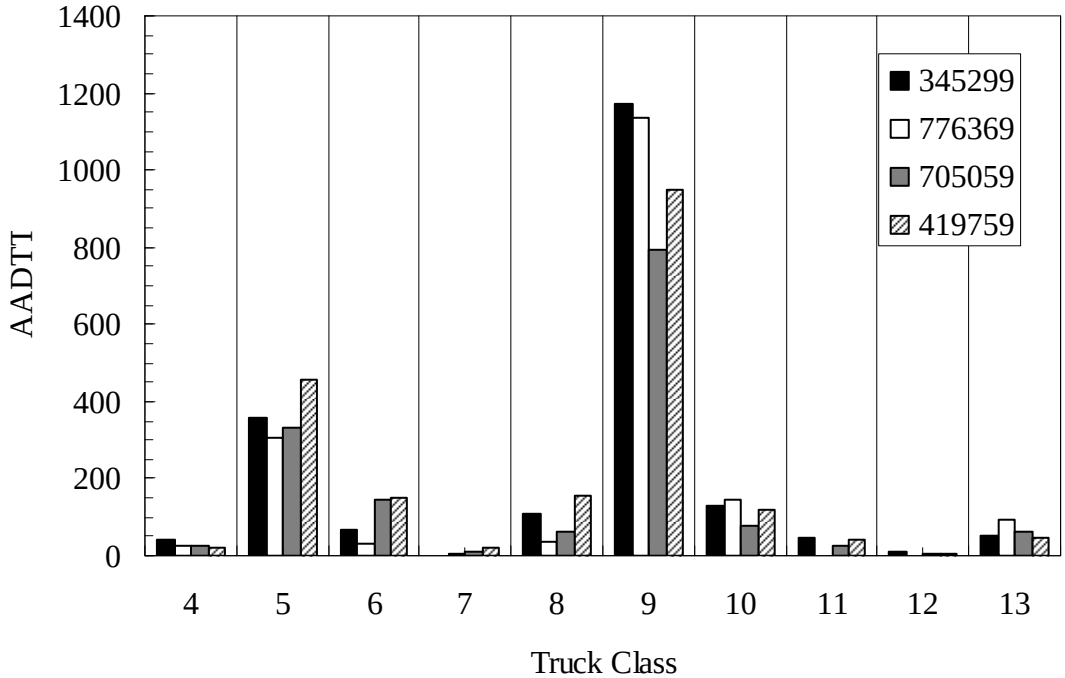

Figure 5.15 Comparison of AADTT by truck class (TrafLoad)
(Medium traffic levels)

Table 5.21 Average annual daily truck traffic for high traffic levels

Vehicle Class	AADTT for Sites				% AADTT for Sites			
	387029	**127269**	**588729**	**638209**	**387029**	**127269**	**588729**	**638209**
4	59.1	42	69.6	31	1.5%	1.3%	2.0%	1.2%
5	392.8	325.5	439.1	609.8	10.0%	10.0%	12.5%	23.2%
6	88.2	53.6	82.9	126.1	2.2%	1.7%	2.4%	4.8%
7	7.8	1.8	12.5	24.6	0.2%	0.1%	0.4%	0.9%
8	122.5	92.5	124.5	179.6	3.1%	2.9%	3.6%	6.8%
9	2904.8	2589.1	2353.2	1141.6	73.6%	79.8%	67.2%	43.4%
10	141.2	35.4	132.9	247.3	3.6%	1.1%	3.8%	9.4%
11	60	77.7	100.4	33.7	1.5%	2.4%	2.9%	1.3%
12	12	17.1	36.1	3.6	0.3%	0.5%	1.0%	0.1%
13	157	9	149.7	232	4.0%	0.3%	4.3%	8.8%
TrafLoad AADTT	**3,945**	**3,244**	**3,501**	**2,629**	**100%**	**100%**	**100%**	**100%**
MDOT Estimate	**3,940**	**3,050**	**3,300**	**2,600**				

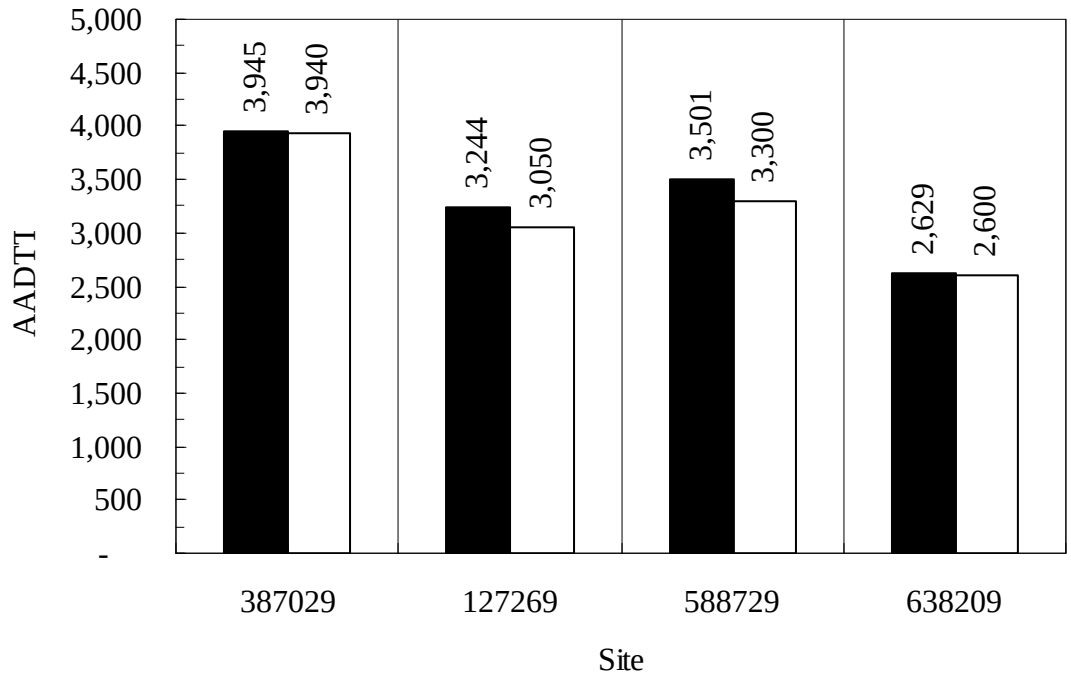

Figure 5.16 Comparison between traffic levels (TrafLoad versus MDOT)
(High traffic levels)

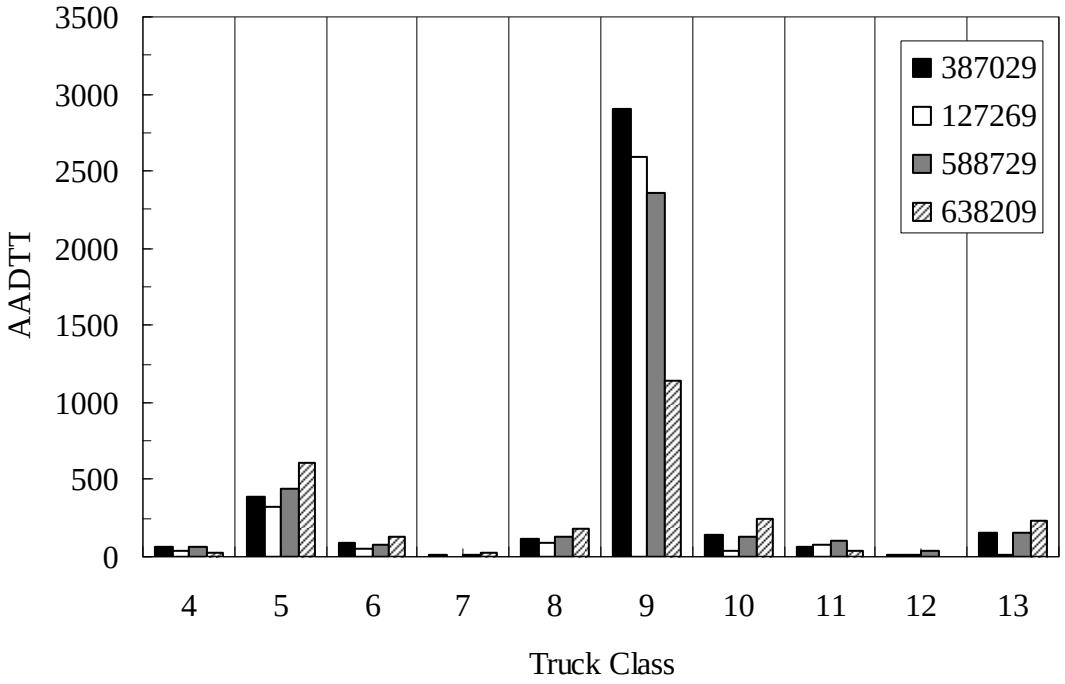

Figure 5.17 Comparison of AADTT by truck class (TrafLoad)
(High traffic levels)

Monthly Adjustment

Figures 5.18 to 5.20 show the monthly adjustment factors for each site, within low, medium, and high traffic levels, respectively. For low traffic level, only site 746019 shows an unusual trend. This result might be due to some discrepancies in the traffic volume data. The overall trends in the results show that traffic volumes are higher in the months of June to September for low traffic level sites while higher traffic volumes were observed in the months of October and November for medium traffic volume sites. Within high traffic level, site 387029 shows significant higher traffic volumes in the months of July and August.

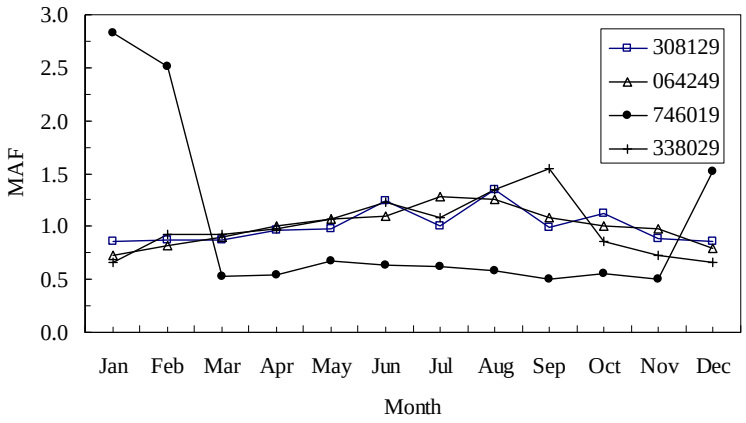

Figure 5.18 Comparison of monthly truck traffic variation (TrafLoad) (Low traffic levels)

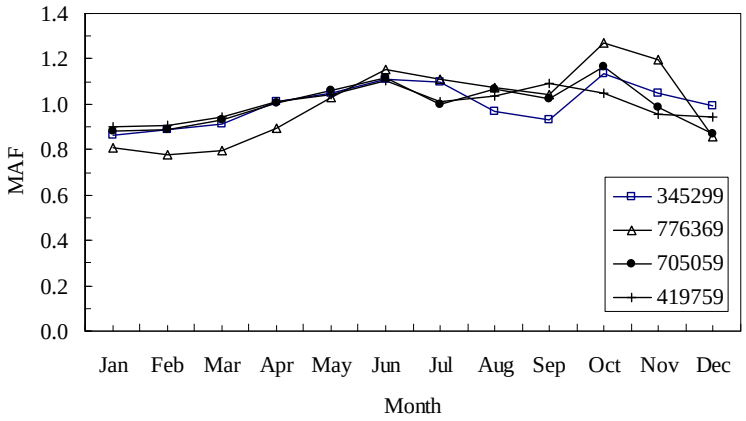

Figure 5.19 Comparison of monthly truck traffic variation (TrafLoad) (Medium traffic levels)

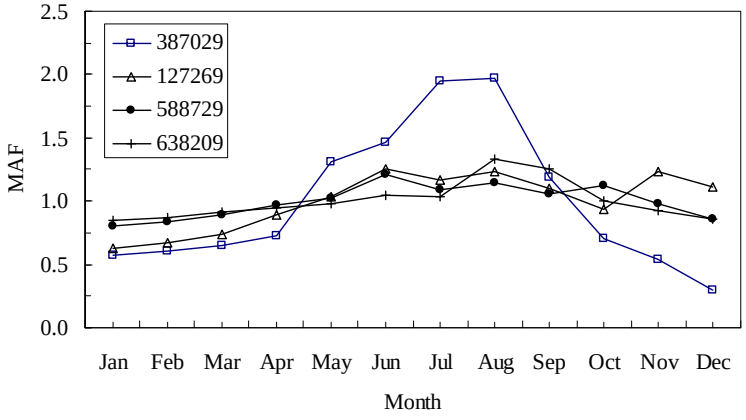

Figure 5.20 Comparison of monthly truck traffic variation (TrafLoad) (High traffic levels)

Hourly Traffic Distribution

Figures 5.21 through 5.23 show the hourly variations of traffic within all traffic levels. The results show higher traffic volumes from 7 am to 7 pm in all sites.

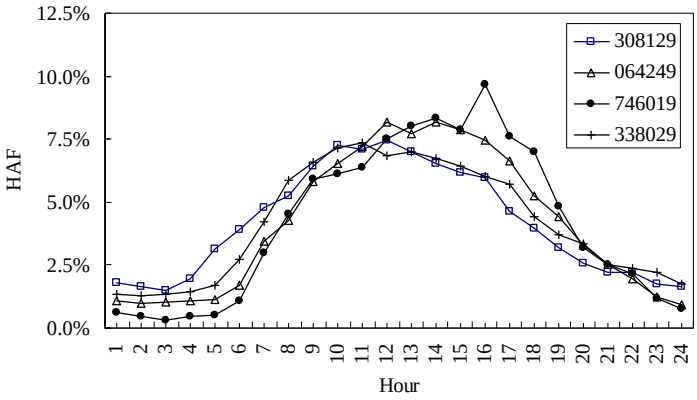

Figure 5.21 Comparison of hourly truck traffic variation (TrafLoad) -Low traffic levels

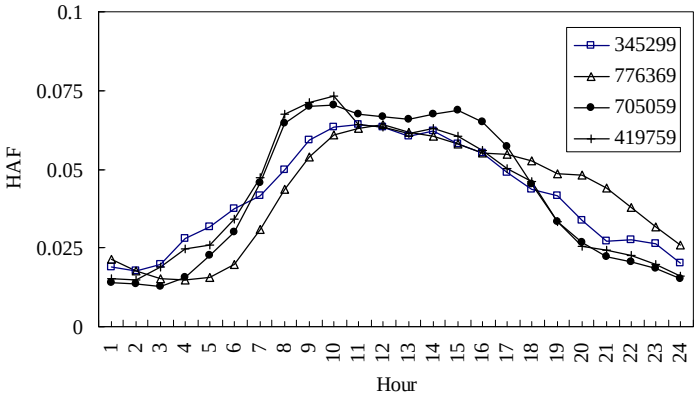

Figure 5.22 Comparison of hourly truck traffic variation (TrafLoad) - Medium traffic levels

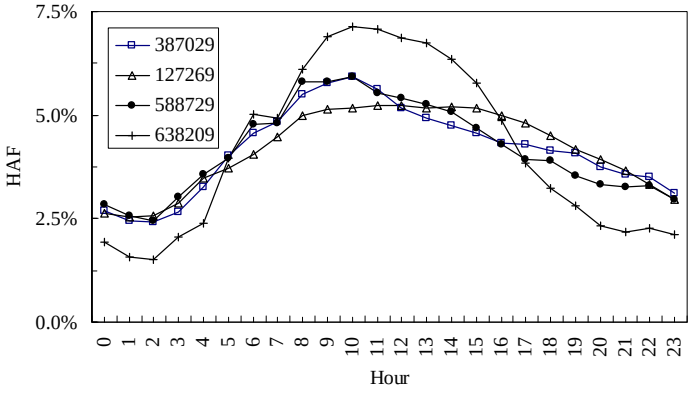

Figure 5.23 Comparison of hourly truck traffic variation (TrafLoad) - High traffic levels

5.3.1.2 Axle Distribution Factors

The axle load distributions for each axle configuration were determined within each traffic level for all sites. Figure 5.24 shows a typical single axle load spectra while Figure 5.25 presents tandem axle load spectra for site 588729. It can be seen from these results that single axle spectra has one distinct peak while tandem axle spectra is characterized by two separate peaks.

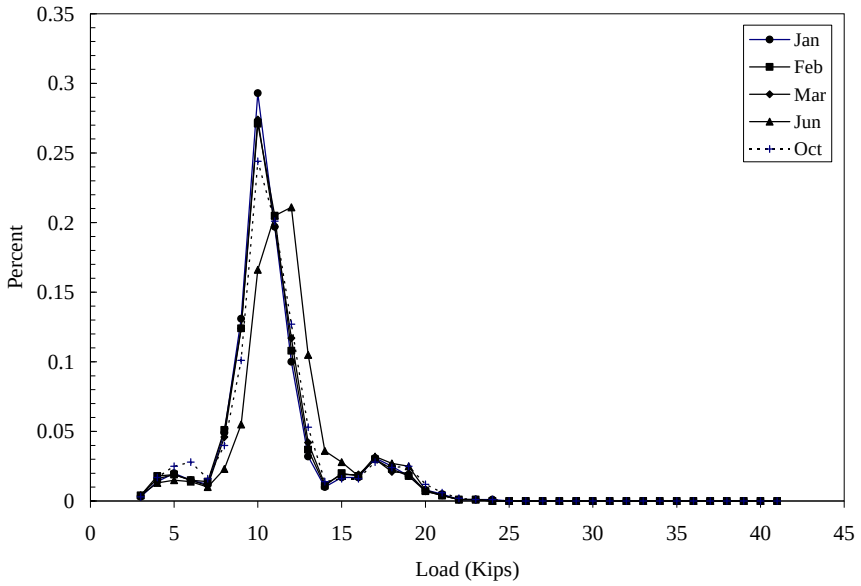

Figure 5.24 A typical axle load spectra for single axle (TrafLoad) - Site 588729

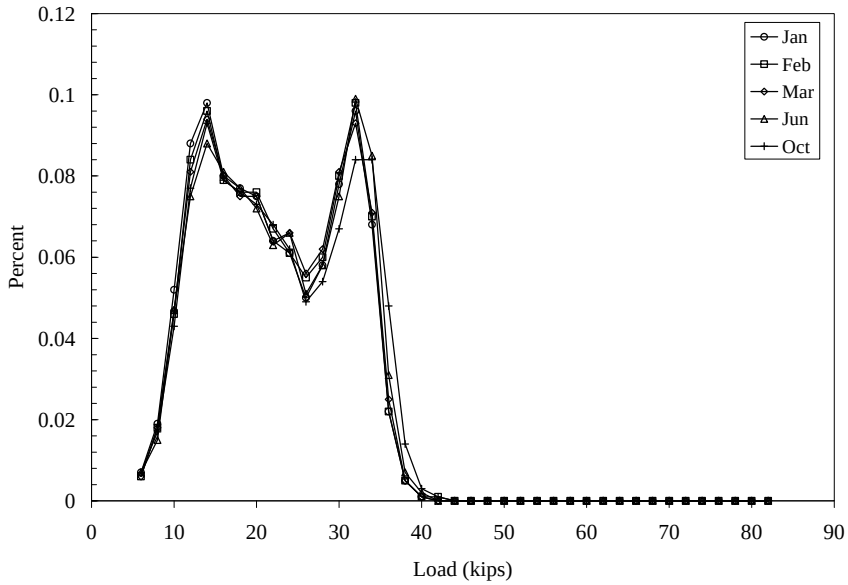

Figure 5.25 A typical axle load spectra for tandem axle (TrafLoad) - Site 588729

5.3.1.3 General Traffic Inputs

The general traffic inputs in the M-E PDG design procedure contains several inputs related to trucks and axles configurations. It should be noted that most of the input related to axle configurations such as axle spacing, dual wheel spacing, tire pressures, and axle widths are not calculated by TrafLoad. These inputs can be determined from the typical trucks within a region. However, average numbers of axles per truck are calculated by TrafLoad, which were determined for all truck classes within all sites and results are presented below.

Average Number of Axle per Vehicle Class

Figure 5.26 shows the average number of single axles within each truck class for three traffic levels while Figure 5.27 shows the same results for tandem axle configuration. Figures 5.28 and 5.29 present average number of tridem and quad axles with each site for all traffic levels, respectively.

The results show more or less a consistent pattern, however, there are some variations within all axle configurations among sites. This could be as a result of different truck configurations within different regions.

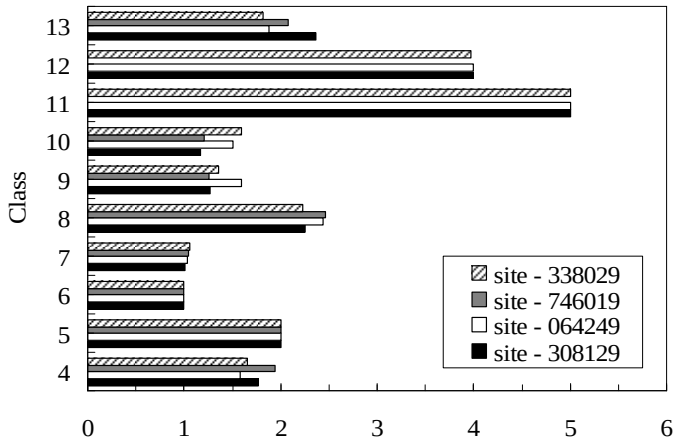

(a) Low traffic level

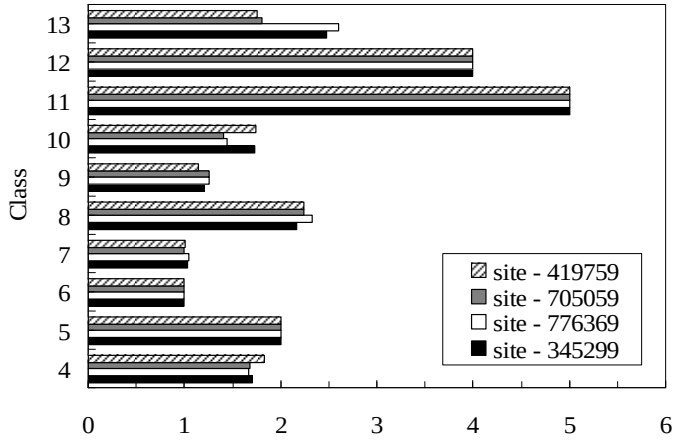

(b) Medium traffic level

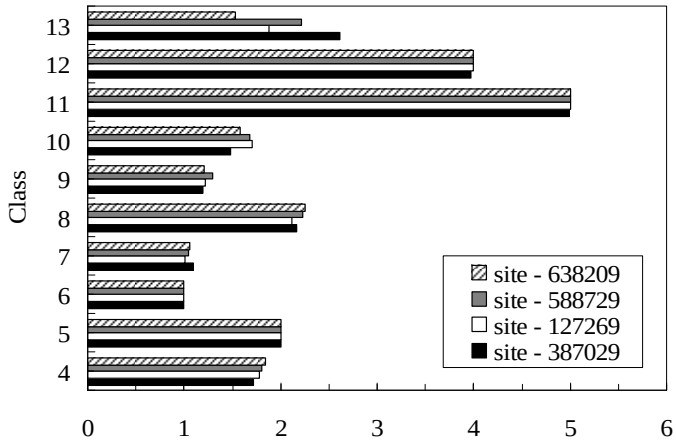

(c) High traffic level

Figure 5.26 Average number of single axle per vehicle class (TrafLoad)

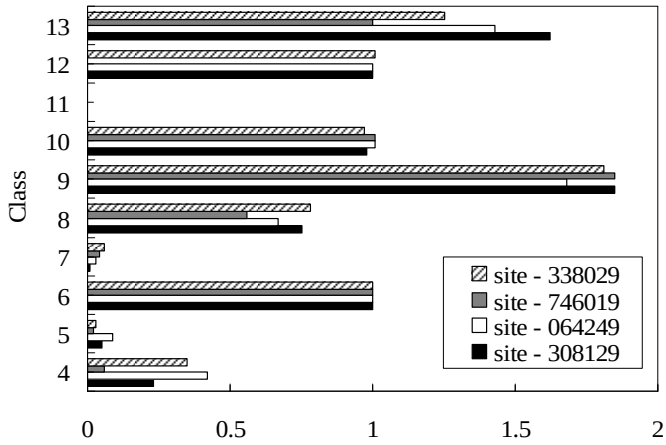

(a) Low traffic level

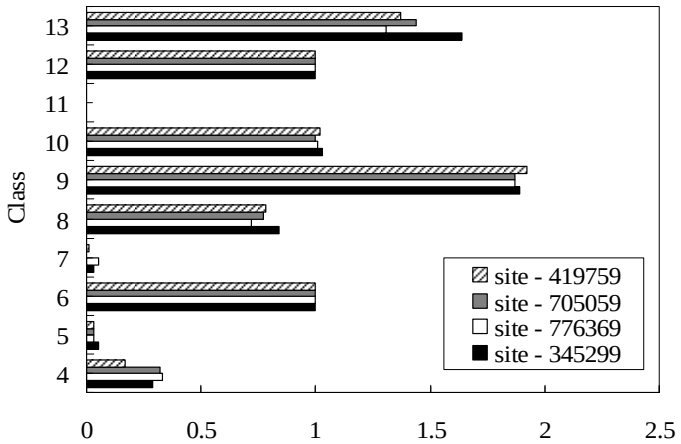

(b) Medium traffic level

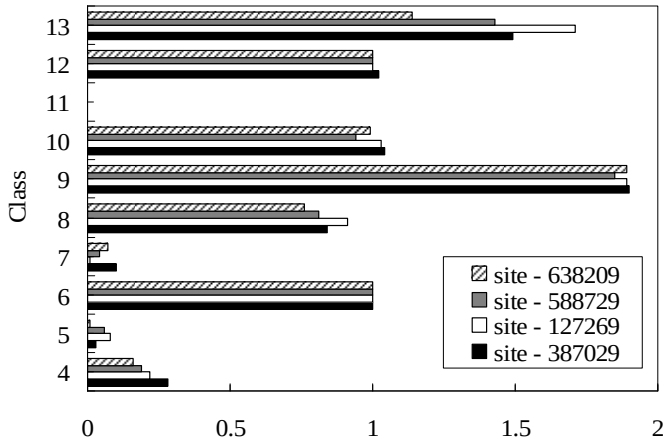

(c) High traffic level

Figure 5.27 Average number of tandem axle per vehicle class (TrafLoad)

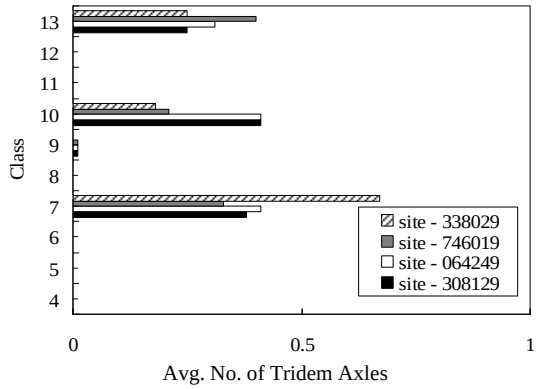

(a) Low traffic level

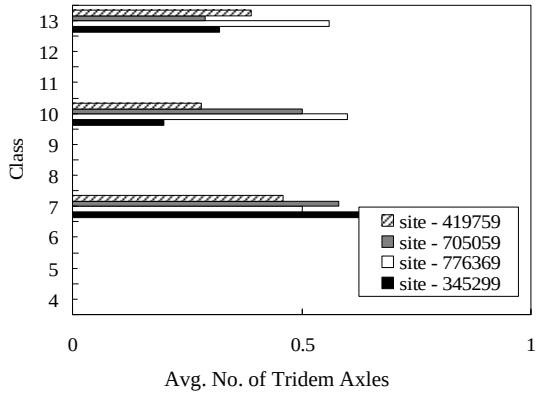

(b) Medium traffic level

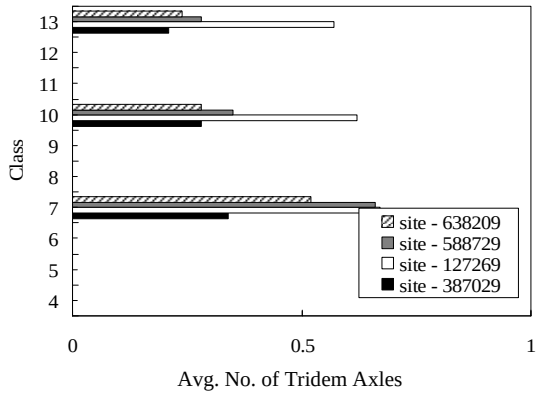

(c) High traffic level

Figure 5.28 Average number of tridem axle per vehicle class (TrafLoad)

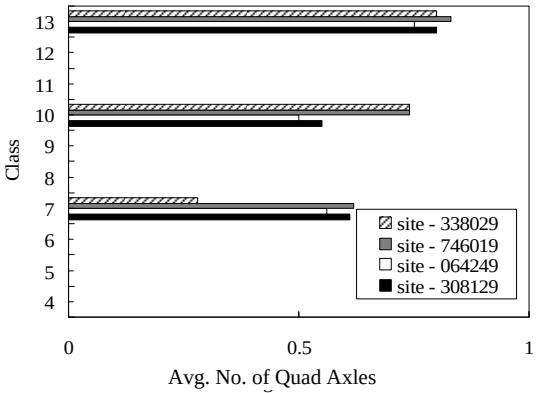

(a) Low traffic level

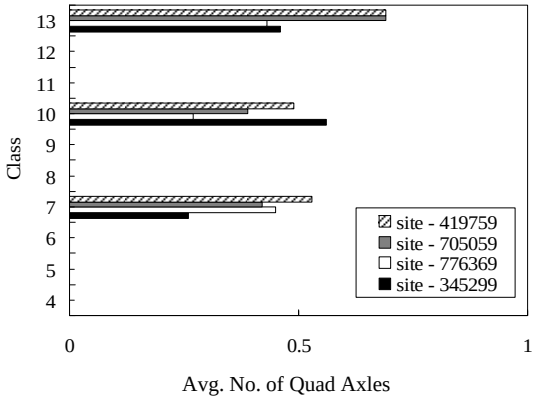

(b) Medium traffic level

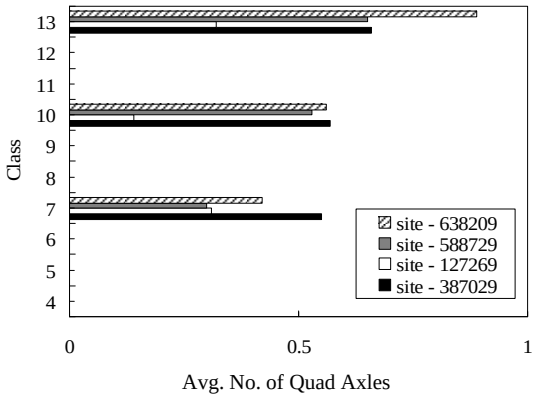

(c) High traffic level

Figure 5.29 Average number of quad axle per vehicle class (TrafLoad)

5.3.2 Effect of Traffic Levels of Rigid Pavement Performance

In order to determine the effects of traffic levels on various rigid pavement performance measures, M-E PDG software was used to analyze each site. Figure 5.21 shows the effect of traffic within low traffic level sites. Figures 5.30 (a, b and c) present predicted faulting, cracking and roughness for low traffic level, respectively. All variables were kept constant in this analysis except traffic within each site. Therefore, the effects in performance are mainly due to traffic-related inputs for each site. Similarly, Figures 5.31 and 5.32 show the performance predictions for medium and high traffic level sites.

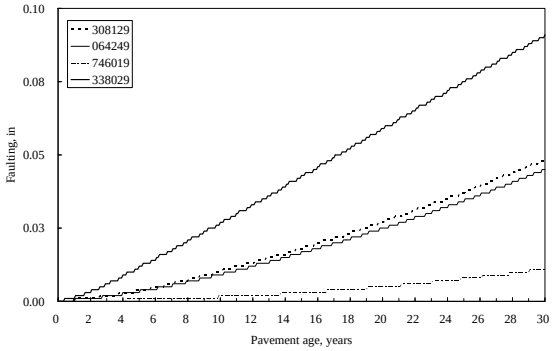

(a) faulting

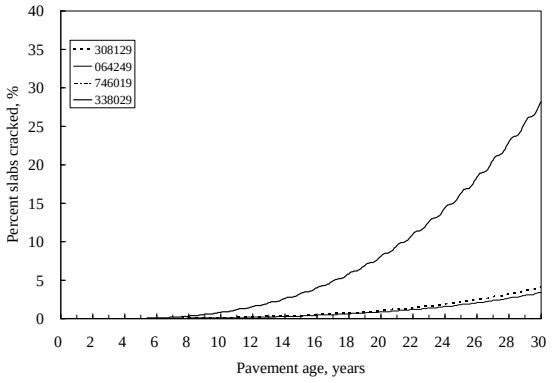

(b) % Slab cracked

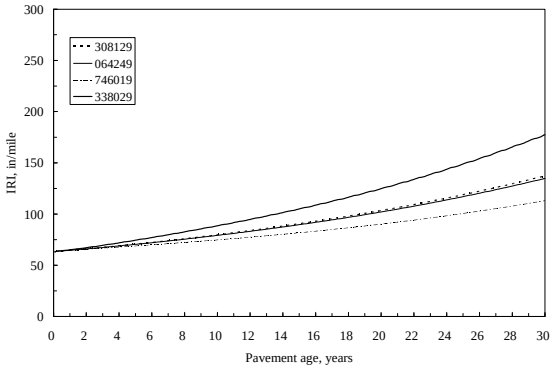

(c) IRI

Figure 5.30 Effect of low traffic levels on pavement performance

The above results show that traffic levels (low, medium and high) significantly affect the rigid pavement performance. Also within a traffic level, due to variations in truck volumes and loadings, the predicted performance can vary. However, the assessment of these effects within the same traffic level needs engineering judgment and practical considerations.

(a) faulting

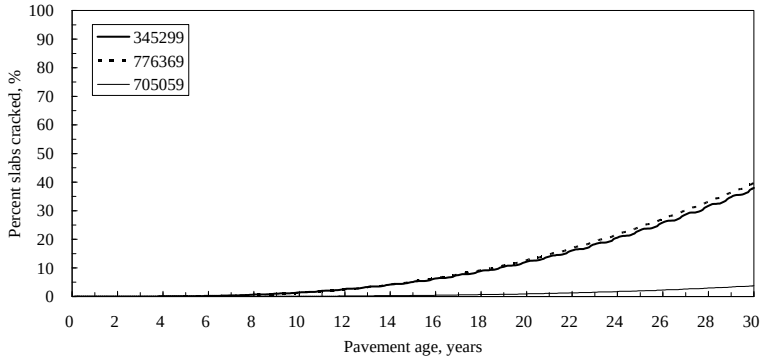

(b) % Slab cracked

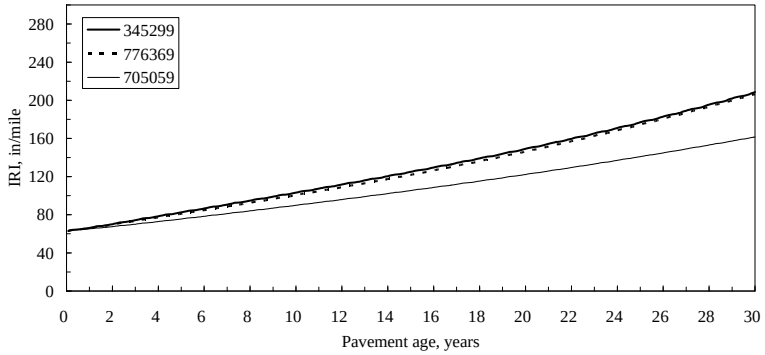

(c) IRI

Figure 5.31 Effect of medium traffic levels on pavement performance

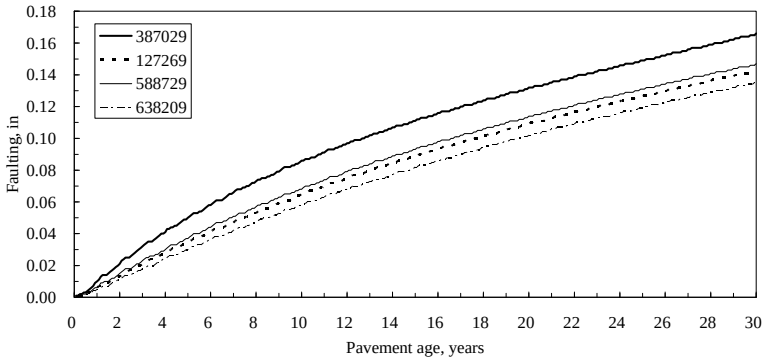

(a) faulting

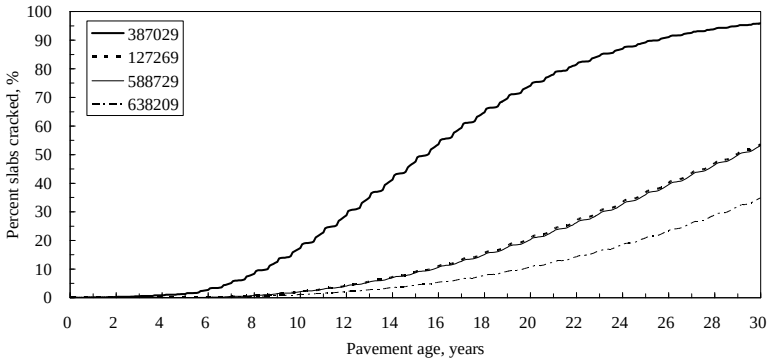

(b) % Slab cracked

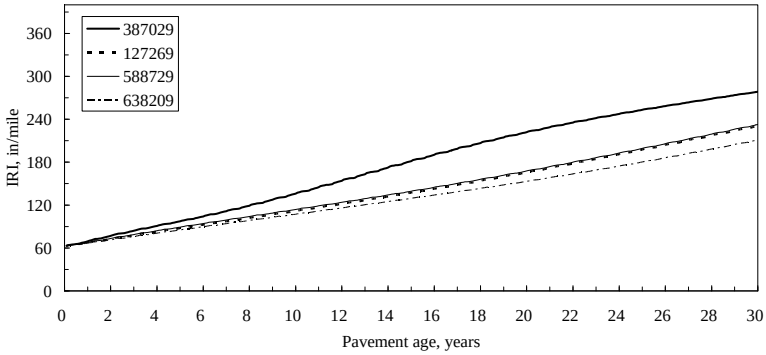

(c) IRI

Figure 5.32 Effect of high traffic levels on pavement performance

5.4 NEEDS FOR LOCAL CALIBRATION OF PERFORMANCE MODELS

The verification of current performance models, in M-E PDG, for the selected pavements in Michigan warranted a need for local calibration. The local calibration of the performance models should reflect the local materials and construction practices to encompass the particular pavement performance in Michigan.

The calibration and validation of M-E PDG performance models were achieved by utilizing the pavements sections in the LTPP database. These test sections are distributed geographically all

over the US. Thus, the coefficients in the current form are termed as “National” calibration coefficients. In addition, the current calibration of performance models may not echo the local construction materials and practices, climate and subsequent manifestation of the common distress types despite the mechanistic aspects of the guide.

Therefore, a need for local calibration was emphasized in the M-E PDG (*24*). At present, there is very limited (if any) guidance that provides agencies with assistance to perform such local calibration. Therefore, NCHRP Project 1-40B (*25*) was initiated with the objective to prepare a practical guide for highway agencies for local or regional calibration of the distress models. This study, which is still in progress, shall contain case studies illustrating a systematic procedure for calibration. Currently, some literature exists for general assistance in the calibration process. For example, the NCHRP Project 9-30 developed a detailed, statistically sound, and practical experimental plan to refine the calibration and validation of the performance models incorporated in the M-E PDG with laboratory-measured hot mix asphalt (HMA) material properties (*26*). In addition, under the same study, a statistical procedure “Jackknifing” was introduced for refining and confirming the calibration coefficients of distress prediction equations and models such as those used in the M-E PDG (*27*). It was concluded that Jackknifing provides more reliable assessments of model prediction accuracy than the alternative use of either traditional split sample validation or calibration goodness-of-fit statistics because jackknifing’s goodness-of-fit statistics are based on predictions rather than the data used for fitting the model parameters.

Several states have found that current calibrated distress prediction models don’t validate with their pavement behavior. For example, Iowa, Washington, North Dakota and Virginia are in the process of calibrating and validating the M-E PDG performance models (*28-31*). Although recently, the M-E PDG models for rigid pavements were recalibrated using additional and more recent data from the LTPP (*32*), an objective and more practical review of the prediction models in M-E PDG revealed several important aspects which will help the states to customize the distress prediction models to their local needs using local experience (*33*). For example, in Michigan, the following aspects need attention while considering the local calibration of JPCP distress models to reflect the local desires:

- The negative temperature gradients cause curling stresses to produce top-down cracking. In addition, the effect of permanent warping that occurs during concrete hardening, and moisture changes during the pavement service life also contribute to geometric deformations. These combined effects, that produce a critical tensile stress and influence of creep during the initial hardening stage, should be considered in Michigan.
- The M-E PDG recommends using a value of −10°F for the effective temperature to determine permanent curl/warp. However, this value is affected by time of placement, joint spacing, and load transfer at joints and base/slab interface conditions, some of which cannot be predicted at the design stage.
- The cracking model for JPCP assumes that shrinkage warping can be accounted for by use of an equivalent negative temperature profile that produces a concave upward curling of the slab. In Michigan, the interaction of this type of built-in curling, typical joint spacing (15-ft), and specific axle configuration seems to be critical in determining the expected cracking of JPCP.

In general, to locally calibrate M-E PDG performance models for JPCP in Michigan, the following is recommended:

- Calibration process should involve a wide spectrum of pavements within the state having different designs, materials, climate, and traffic demands. The pavement sections with outlying performance should not be included in the database for calibration. However, the determination of unusual performance should be based on sound engineering judgment coupled with local experience. If the cause of outlying performance is known, such sections may be included in the database.
- The selection of test sections should be based on sound experimental design considering several important attributes affecting pavement performance. For example, slab thickness, traffic, CTE, negative gradient to address built-in curling and concrete strength, etc. In addition, any particular construction practice should be included in the test matrix.
- The use of PMS performance data may include distress measurement variability which is another source of error in addition to model error. There is a need to quantify such errors in the calibration process to improve model predictions. An excellent discussion on this issue is provided by Schwartz (*34*).
- Another very important but mostly ignored aspect for empirical modeling is the compromise between bias and prediction variability. Bias represents a systematic error in the model prediction; therefore, it is crucial to minimize the model bias while keeping the variance within acceptable limits. Several modern statistical techniques, such as bootstrapping and jackknifing, based on random sampling from a sample can be used to validate and improve the empirical models.

CHAPTER 6 - PAVEMENT DESIGN IMPLICATIONS - RIGID

6.1 QUANTIFYING EFFECT OF SIGNIFICANT VARIABLES ON RIGID PAVEMENT PERFORMANCE

Several comprehensive sensitivity analyses including this study were performed for the M-E PDG transverse cracking, transverse joint faulting, and smoothness models (*35-39*). The results were a list of all the key input variables that had a significant impact on predicted rigid pavement performance. A summary of the design, site, and other variables that significantly influence JPCP transverse cracking, transverse joint faulting, and smoothness is presented in Table 6.1. The high rating indicates that an input has a large effect on the distress/IRI while a low/none rating indicates that an input has an insignificant effect. The information presented in this table shows that many inputs significantly affect joint faulting, transverse slab cracking, and IRI.

Table 6.1 Summary of M-E PDG Sensitivity Results for New JPCP Distress/IRI Models (*40*)

Design/Material Variable	Impact on Distress/Smoothness		
	Transverse Joint Faulting	Transverse Cracking	IRI
PCC thickness	**High**	**High**	**High**
PCC modulus of rupture and elasticity	None	**High**	Low
PCC coefficient of thermal expansion	**High**	**High**	**High**
Joint spacing	Moderate	**High**	Moderate
Joint load transfer efficiency	**High**	None	**High**
PCC slab width	Low	Moderate	Low
Shoulder type	Low	Moderate	Low
Permanent curl/warp	**High**	**High**	**High**
Base type	Moderate	Moderate	Low
Climate	Moderate	Moderate	Moderate
Subgrade type/modulus	Low	Low	Low
Truck composition (vehicle class and axle load distribution)	Moderate	Moderate	Moderate
Truck volume	**High**	**High**	**High**
Initial IRI	NA	NA	**High**

Note: Low— variable has small effect on distress/IRI
Moderate— variable has moderate effect on distress/IRI
High— variable has large effect on distress/IRI

It is important to note that while the above results were obtained for the sensitivity analysis, there could be situations where these inputs are more or less significant than shown here. Also, other inputs may become significant in different conditions such as climates. The distress models and algorithms are very complex and consider many interactions between factors. In particular, in a warmer climate, some inputs may have differing levels of effect than in other climates. The most significant inputs for JPCP design to be estimated are the following:

- PCC slab thickness
- Joint load transfer (dowels and dowel diameter)
- PCC coefficient of thermal expansion (very critical input, testing needed)
- Joint spacing
- PCC modulus of rupture and modulus of elasticity
- Base type
- Climate
- Truck volume and composition
- Subgrade type

6.1.1 Background

Recent enhancements in pavement performance prediction knowledge have revealed the strengths and weaknesses of the current models used in the Highway Economic Requirements System (HERS) and Highway Cost Allocation Study (HCAS) analytical tools. Consequently, the FHWA initiated this project—*Modification of FHWA Highway Performance Data Collection System and Pavement Performance Models*—to investigate and develop improved pavement performance prediction models for HERS and HCAS (*41, 42*). Several existing performance models for both asphalt and concrete pavements have been investigated during the course of the study to determine their suitability for HERS and HCAS. During these investigations, one set of models that emerged as a potential choice for incorporation was the set developed under the National Cooperative Highway Research Program (NCHRP) Project 1-37A—Development of the 2002 Guide for the Design of New and Rehabilitated Pavement Structures (*43-45*). It is both desirable and practical to implement the Mechanistic-Empirical Pavement Design Guide (M-E PDG) performance prediction models into the HERS and HCAS for use in policy analyses and decisions (*35, 45, 46*). In addition, adopting these models would greatly improve the accuracy and reliability of the national C&P report information as well as the allocation of damage between vehicle classes for use in highway cost allocation studies (*46*).

The NCHRP 1-37A software includes the following main performance prediction models:

- For HMA flexible pavements and flexible overlays:
  - Fatigue cracking
  - Rutting in all pavement layers
  - HMA thermal cracking
  - IRI
- For jointed plain concrete pavement (JPCP) and rigid overlays:
  - Faulting
  - Fatigue cracking
  - IRI

The above distress types and an increase in IRI are defined as "damage" to a given pavement. One of the main reasons to move to an improved performance prediction is to consider more than just smoothness (e.g., serviceability or IRI) and to include other forms of deterioration such as rutting and fatigue cracking as they can independently affect maintenance and rehabilitation costs. For the portions of the Interstate Highway System (HIS) categorized as acceptable or unacceptable, there will be the need for M&R to restore pavement condition to good or very good levels. Pavement rehabilitation is described as structural or functional enhancement of a pavement, which produces a substantial extension in service life by substantially improving pavement condition and ride quality. Pavement maintenance consists of those treatments that preserve pavement condition, safety, and ride quality, and therefore, aid a pavement in achieving its design life. The type of maintenance and rehabilitation (M&R) improvement most likely to perform well and be cost-effective for a given pavement depends on the amount of distress present. Although there are no simple rules or universally accepted distress trigger levels for identifying the type of M&R improvements that are most appropriate for a given pavement, the decision depends on several factors including the extent and severity of distresses present. Table 6.2 presents recommendations of M&R techniques best suited for concrete pavement distresses.

Table 6.2 Rehabilitation Techniques Best-Suited for Concrete Pavement Distresses (*40*)

Distress Type	Concrete Pavement Rehabilitation Techniques								
	Full-depth Patching/Slab Replacement	Partial-depth Patching/Slab Replacement	Load Transfer Restoration	Joint Resealing	Diamond Grinding	Asphalt Overlay	Asphalt Overlay of Fractured Slab	Bonded Concrete Overlay	Unbonded Concrete Overlay
Corner break	✓						✓		✓
Cracking (longitudinal and transverse)	✓						✓		✓
"D" cracking	✓					✓	✓		✓
Joint spalling	✓	✓					✓		✓
Pumping			✓						
Joint faulting			✓		✓	✓	✓	✓	✓
Polishing					✓	✓			✓

Table 6.2 shows that measuring or predicting smoothness alone is not enough to characterize the totality of pavement condition making it impossible to assess the merits of different M&R options that may be required to restore pavement condition. This is because IRI alone does not provide credible data on the causes and extent of pavement deterioration. For reasonable and credible estimates of M&R needs and estimates of costs, pavement condition must be characterized in its totality using not only overall condition indices such as IRI but also individual distress types.

Based on the performance indicators selection criteria listed, information presented in Table 2, and the distress types and IRI used by the M-E PDG to predict future pavement condition, the following performance indicators were selected (*40*):

- Transverse joint faulting
- Transverse (slab) cracking
- Transverse joint spalling
- IRI

Although the existing M-E PDG performance models have been nationally calibrated by using level 3 data, these models at the state level may require validation and local calibration. If the models show bias, they can be simply adjusted to predict the average observed distresses and IRI. This process will make it possible to identify errors and potential bias that may be introduced due to the inputs used in performance prediction. Verification and recalibration can be done after all data have been assembled by the state and defaults estimated.

While incorporation of the modified M-E PDG models in pavement analysis and design process will bridge the gap between design and pavement management process, several necessary information (data) needs to be collected for model calibrations. The necessary inputs to these models can be selected based on the relative importance in the prediction models (see Table 6.1).

6.1.2 Simplified Regression Models — M-E PDG Performance Prediction

As mentioned before, the performance prediction process in M-E PDG is very complex due to a large number of variables and their interaction between each other. The simplified M-E PDG regression models involving only a few important design variables were developed in this study. While these models are limited in scope, they can facilitate in the preliminary design process especially with regards to economic decisions for selecting appropriate materials and slab thickness. The simplified models can also help in quantifying the effects of several significant design variables. Four important design and material-related variables affecting rigid pavement performance in the M-E PDG design process were selected in the regression model development. These variables along with their levels included:

1. Slab thickness — 8, 10, 12 and 14 inches
2. Joint Spacing — 14, 16, 18 and 20 feet
3. Flexural strength — 550, 650, 750 and 900 psi
4. Coefficient of thermal expansion — 4.5, 5.5, 6.5 and 7.5 in/in per ^{o}C

All combinations involving four variables with four levels each were considered in this exercise and, a full factorial design containing, 256 (4^4) M-E PDG runs were executed. The pavement performance (cracking, faulting and IRI) predicted by the M-E PDG (Version 1.0) software at the end of 20 years was extracted and included in the database developed for regression model developments. It should be noted that site variables (climate, traffic, and soil properties) were fixed in these analyses. Therefore, these regression models can be only used for a site to relatively compare different designs. These models are presented next.

6.1.2.1 Transverse Cracking Model

Equation (1) presents the general form of cracking model considered in the M-E PDG, which represents an S-shaped curve to capture the cracking occurrence over the life of a rigid pavement. It should be noted that a linear regression model may not capture the expected cracking trend over time.

$$CRK = \frac{100}{1+\beta^{(\alpha \times TRAF + \Delta)}} \tag{1}$$

where

CRK = transverse cracking
$TRAF$ = estimate of cumulative traffic
Δ = value based on pavement design, site, materials, etc., properties
α, β = regression constants

The simplified M-E PDG cracking model was developed in an FHWA study (*40*),. Equations (2) through (4) describe the simplified transverse cracking models for rigid pavements.

$$CRACK = \left(\frac{100}{1+733085^{-0.00521 \times (ESALS \times TF)^{0.25} + \Delta}} \right) \tag{2}$$

where

$CRACK$ = percent slabs cracked
$ESALS$ = cumulative number of 18-kip equivalent single axle load

$$TF = \left(\frac{1}{1+\left[\frac{AGE}{LBAGE + 5.41} + 0.0000001 \right]^{-7.89}} \right) \tag{3}$$

where

AGE = pavement age in years
$LBAGE$ = age at which the PCC slab de-bonds from the base. $LBAGE$ depends on the underlying base material type. For ATB, $LBAGE$ = 20 years, for CTB, it is 11 years, while for granular bases, $LBAGE$ = 15 years

$$LN(\Delta) = \begin{bmatrix} 0.1424 \times Edge - 3.36 \times 10^{-7} \times E - 0.0571 \times JTSP \\ +0.000188 \times f'_c + 0.0598 \times Thick + 0.2951 \times SG \\ +0.1323 \times WF + 0.2443 \times WNF + 0.7636 \times DNF \end{bmatrix} \tag{4}$$

where

Edge = Edge support, 1 if a tied PCC shoulder or widened slab (slab width > 12 ft) is used, otherwise 0

E = 28-day PCC slab elastic modulus in psi. It is computed from the PCC compressive strength as follows: $E_{PCC} = 57000\sqrt{f_C^{'}}$, where $f_C^{'}$ = 28-day PCC compressive strength in psi

JTSP = JPCP joint spacing or slab length in feet

$f_C^{'}$ = 28-day PCC compressive strength in psi

Thick PCC slab thickness in inches

SG = SG = 1 if subgrade material is coarse grained

WF = WF = 1 if pavement is located in a wet-freeze climate (i.e., annual rainfall is > 20 in and freezing index (FI) > 150 deg F days

WNF = WNF = 1 if pavement is located in a wet-no-freeze climate (i.e., annual rainfall is > 20 in and freezing index (FI) < 150 deg F days

DNF = DNF = 1 if pavement is located in a dry-no-freeze climate (i.e., annual rainfall is < 20 in and freezing index (FI) < 150 deg F days

Model statistics:

- Number of data points, N = 6915
- Coefficient of determination, R^2 = 67 percent
- Standard error estimate, SEE = 7.9 percent slabs cracked

The above simplified cracking model was developed to facilitate the inclusion of such models in HERS. However, in this study only four input variables were considered in the regression model development. Equation (5) presents the general form of the considered model while Equation (6) shows the calibrated regression model of transverse cracking model.

$$CRK = \frac{100}{1+\beta^{\alpha(\beta_1 PCCThick+\beta_2 MOR+\beta_3 JS+\beta_4 CTE)}} \quad (5)$$

$$CRK = \frac{100}{1+10072^{-0.397(-0.412 PCCThick-0.0054 MOR+0.307 JS+0.516 CTE)}} \quad (6)$$

where

CRK = % slab cracked after 20 years

PCCThick = PCC slab thickness (inches)

MOR = Flexure strength, modulus of rupture (psi)

JS = Transverse joint spacing (ft)

CTE = Coefficient of thermal expansion of concrete (in/in per ^{o}C)

Model statistics:

- Number of data points, N = 256
- Coefficient of determination, R^2 = 93 percent
- Standard error estimate, SEE = 11.9 percent slabs cracked

The goodness-of-fit statistics of the regression model suggest that the developed model is reasonable; however, for certain combinations of variables it was observed that 100% of the slabs are cracked before 20 years. The uncertainty in predictions can be observed in Figure 6.1. It should be noted that higher R^2 value only may not indicate a very accurate regression model; the standard error of the model can be higher contributing to higher uncertainties in model predictions. However, the attention of the model is not only to predict the cracking performance but to relatively assess the performance trend due to change in values of important design variables.

The sensitivity of the developed model will further elaborate the use of such a simplified model in the preliminary design process.

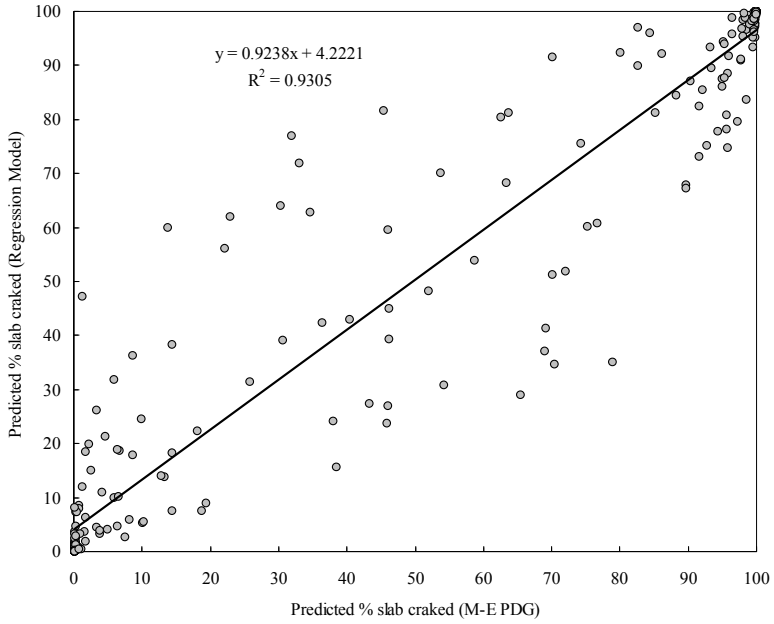

Figure 6.1 Goodness-of-fit for % slab cracking model

Cracking Model Sensitivity

Figures 6.2 and 6.3 show the sensitivity of developed cracking model for different levels of input design and material variables. These plots were developed by changing two variables at a time while keeping other variables at the average level (i.e., MDOT practice). For example, the average slab thickness, MOR, joint spacing and CTE values were fixed at 9-inch, 500 psi, 15 ft, and 6 in/in per ^{o}C, respectively. Figures 6.2 (a, b and c) illustrate the predicted % slab cracked at 20 years with varying slab thickness by three levels of MOR, joint spacing and CTE. Figures 6.2 (c, d and e) show the predicted % slab cracked at 20 years with varying joint spacing by three levels of slab thickness, MOR and CTE. Figure 6.3 shows the similar cracking trends with varying CTE and MOR by various levels of other variables. It can be seen that cracking in rigid pavements is affected by input variables at different levels. For example, slab thickness has a significant effect on future cracking; this effect is further enhanced when MOR, CTE, and joint spacing are considered at the same time. Figure 6.4 presents an example for demonstrating the use of these charts. The figure shows that for reducing expected future cracking after 20 years from 70% to 30%, at 650 psi MOR level, the slab thickness needs to be increased from 9.75- to 11- inches. Similarly, slab thickness should be increased to 12.5 inches for 30% cracking if MOR of 550 psi is selected.

Thus to reduce expected cracking from 70% to 30%, an increase of about 13% and 11% in slab thickness is required at MOR values of 650- and 550-psi, respectively. The increase in thickness can be easily converted into additional cost and a rational comparison can be made between construction and future rehabilitation/maintenance costs required for making decision at the design level. The life cycle cost analysis can be conducted to compare different design alternates at the same site.

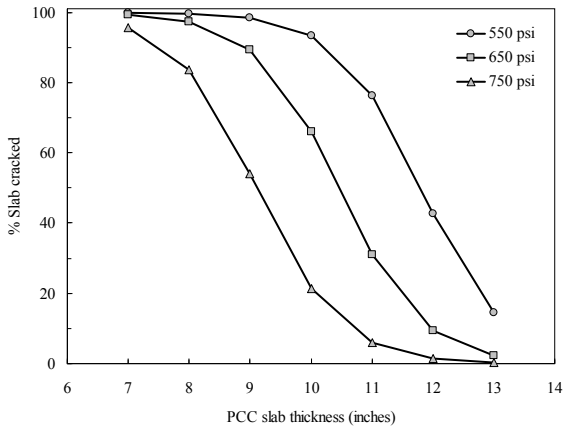

(a) Effect of slab thickness and MOR

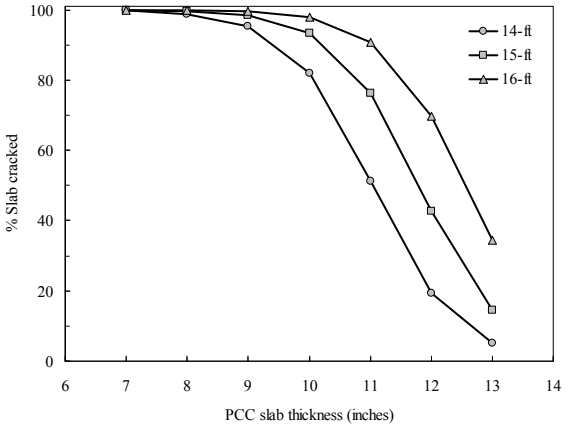

(b) Effect of slab thickness and joint spacing

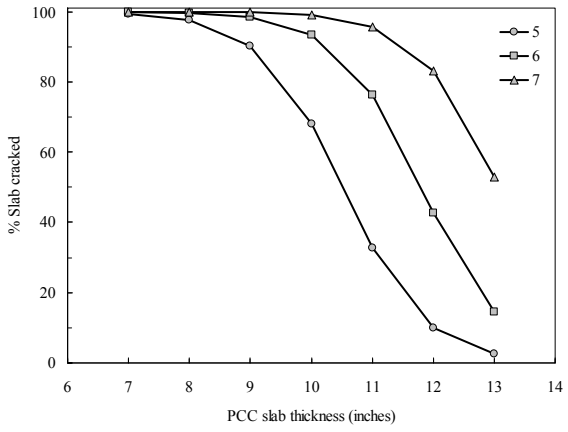

(c) Effect of slab thickness and CTE

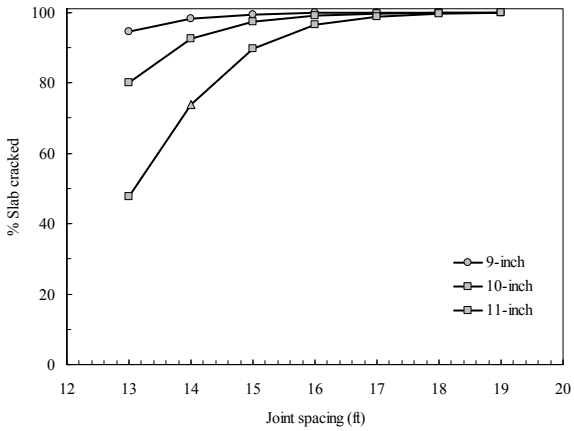

(d) Effect of joint spacing and PCC slab thickness

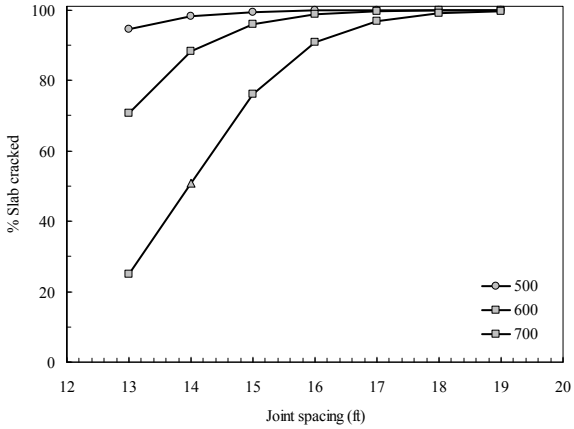

(e) Effect of joint spacing and MOR

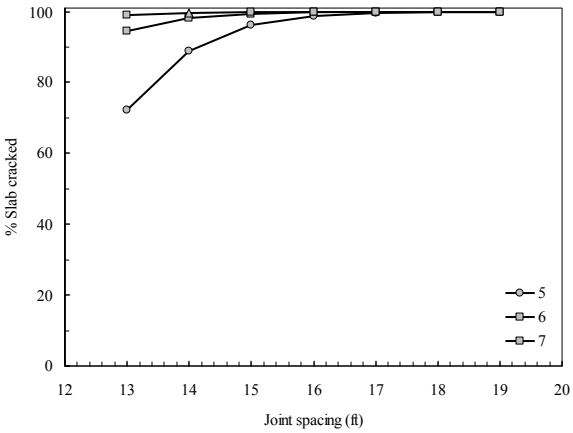

(f) Effect of joint spacing and CTE

Figure 6.2 Sensitivity of % slab cracking model — Design variables

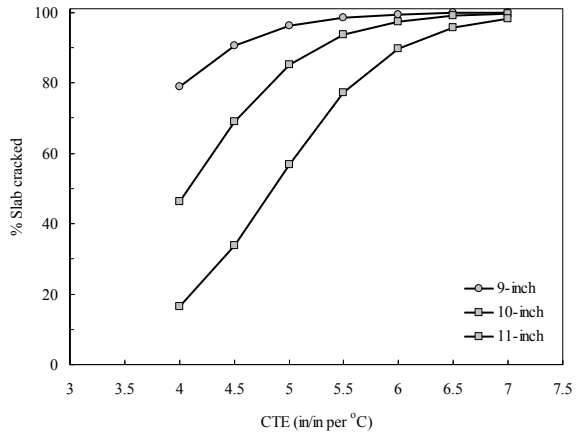

(a) Effect of CTE and slab thickness

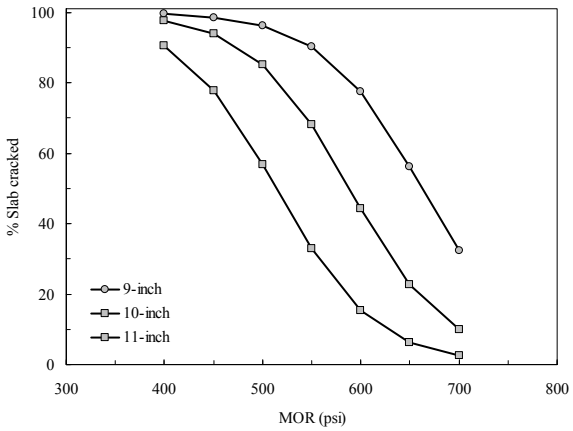

(d) Effect of MOR and slab thickness

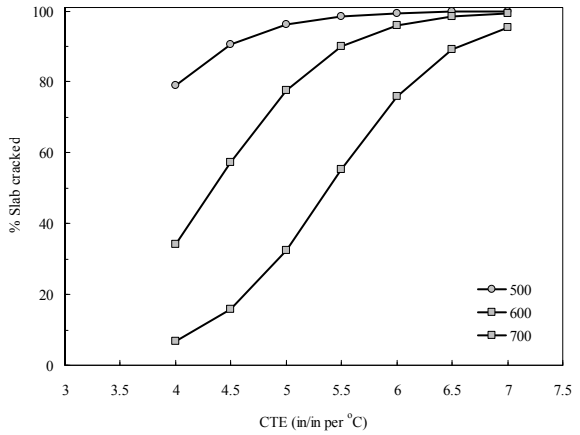

(b) Effect of CTE and MOR

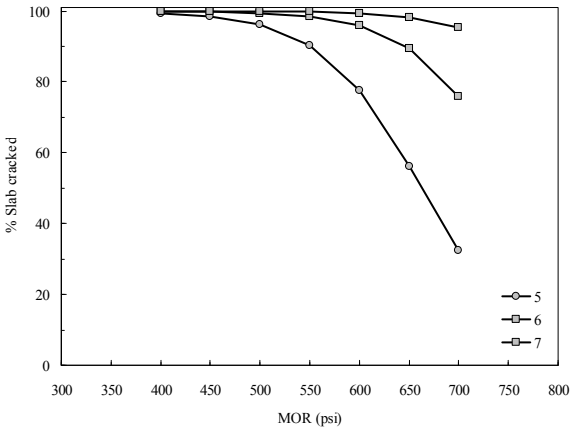

(e) Effect of MOR and CTE

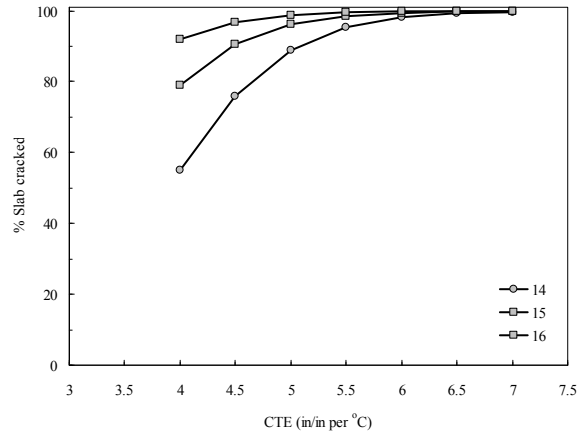

(c) Effect of CTE and joint spacing

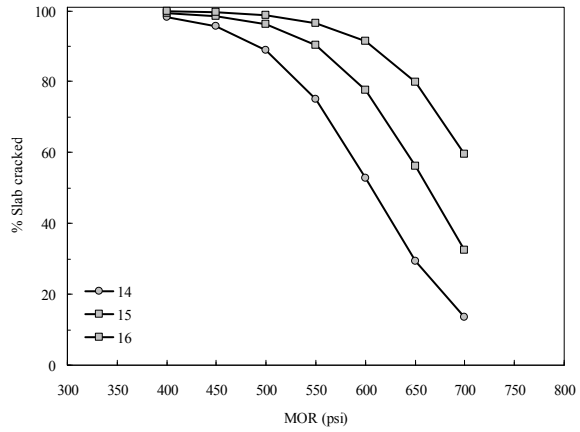

(f) Effect of MOR and joint spacing

Figure 6.3 Sensitivity of % slab cracking model — Material variables

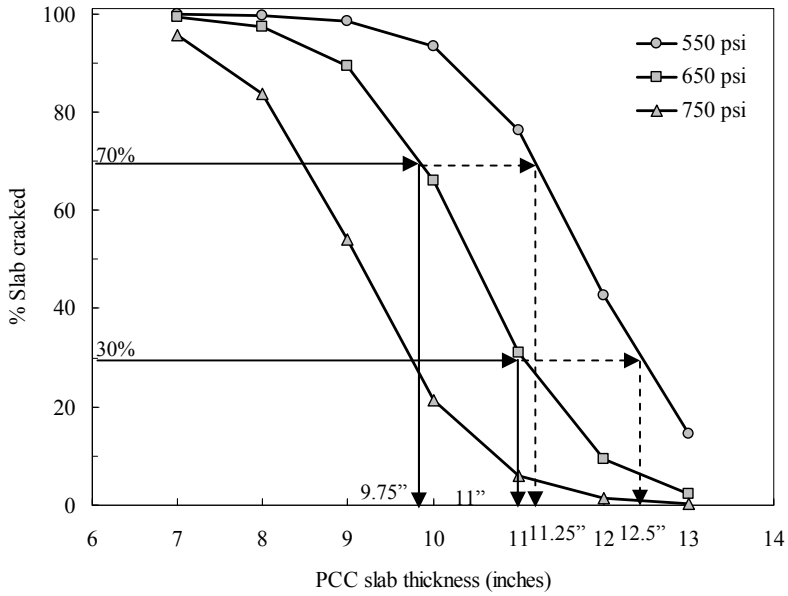

Figure 6.4 Effect of slab thickness on cracking — Example

Similar interpretation can be made from other figures presented above for making design decisions based on other design and material variables.

6.1.2.2 Transverse Joint Faulting Model

Equation (7) illustrates the general form of faulting performance in M-E PDG. This form represents a power model to capture future faulting over the life of a rigid pavement.

$$FAULT = TRAF^{\alpha}(1 - \beta \times D) \times \gamma \tag{7}$$

where

$FAULT$ = transverse joint faulting
$TRAF$ = estimate of cumulative traffic
D = Dowel diameter
γ = value based on pavement design, site, materials, etc., properties
α, β = regression constants

Equation (8) shows the transverse joint faulting model developed during an FHWA study (*40*).

$$FAULT = \left(ESALS^{0.521}\right) \times \left(1 - 0.6413 \times D\right) \times \begin{pmatrix} -9.01 \times 10^{-6} \times ATB - 9.50 \times 10^{-6} \times CTB + \\ 0.000013 \times Edge + 1.44 \times 10^{-8} \times FI + \\ 3.68 \times 10^{-6} \times JTSP + 0.000014 \times WET - \\ 4.91 \times 10^{-6} \times Thick - 9.36 \times 10^{-6} \times SG \end{pmatrix} \quad (8)$$

where

FAULT	=	mean transverse joint faulting, in
ESALS	=	cumulative number of 18-kip equivalent single axle load
D	=	dowel diameter, in
ATB	=	1 if base type is asphalt treated material, otherwise 0, for ATB = 1, base modulus = 200,000 psi
CTB	=	1 if base type is cement treated material, otherwise 0, for CTB = 1, base modulus = 1,000,000 psi
Edge	=	1 if no edge support is provided at the pavement slab edge, otherwise 0
FI	=	freezing index, deg F days
JTSP	=	JPCP joint spacing or slab length, ft
WET	=	1 if mean annual precipitation > 20 in/yr
Thick	=	PCC slab thickness in inches
SG	=	1 if subgrade material is coarse grained

The model statistics were as follows:

- Number of data points, N = 3,389
- Coefficient of determination, R^2 = 60 percent
- Standard error estimate, SEE = 0.035 in

Several faulting models were developed in this study by considering same four design variables as considering in development of cracking model. Equation (9) presents first of those faulting model. This model is based on the linear regression technique. Figure 6.5 shows the goodness-of-fit (GOF) for this model. While GOF statistics are reasonable, the GOF graphs shows that this model is not robust at higher levels of faulting.

$$\ln FAULT = \frac{1}{1.4884}\left(-5.816 - 0.051 PCCThick + 0.001 MOR + 0.094 JS + 0.386 CTE\right) \quad (9)$$

where

FAULT	=	Transverse joint faulting (inches)
PCCThick	=	PCC slab thickness (inches)
MOR	=	Flexure strength, modulus of rupture (psi)
JS	=	Transverse joint spacing (ft)
CTE	=	Coefficient of thermal expansion of concrete (in/in per ^{o}C)

Model statistics:

- Number of data points, N = 256
- Coefficient of determination, R^2 = 94 percent
- Standard error estimate, SEE = 0.017 inches

Equation (10) shows the second model developed based on power form. The GOF statistics shows that this model shows higher standard error. The uncertainty of predicted and measured faulting is exhibited by Figure 6.6.

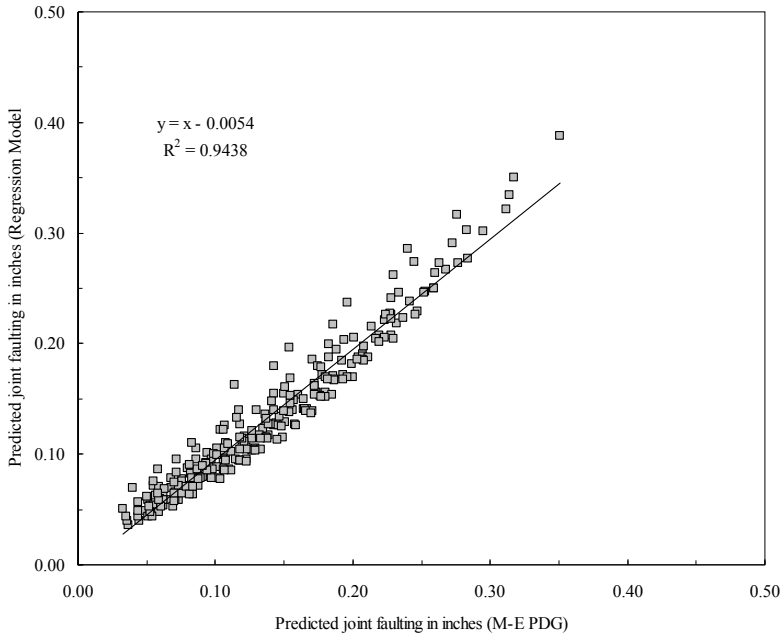

Figure 6.5 Goodness-of-fit for faulting model [Equation (9)]

$$\ln Fault = \frac{\left(-11.72 + PCCThick^{-0.42} + MOR^{0.15} + JS^{0.43} + CTE^{0.66}\right) - 0.142}{0.903} \qquad (10)$$

Model statistics:

- Number of data points, N = 256
- Coefficient of determination, R^2 = 92.8 percent
- Standard error estimate, SEE = 0.0187 inches

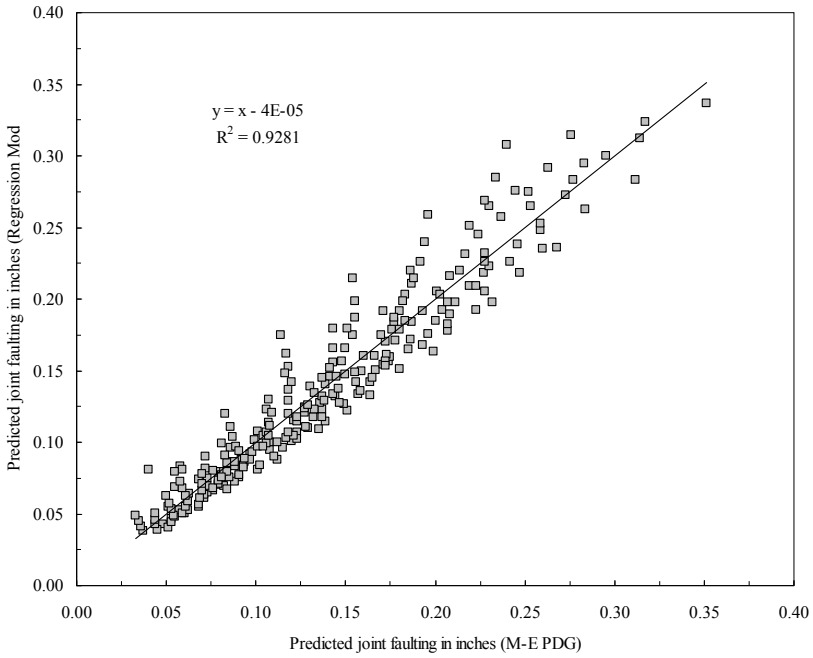

Figure 6.6 Goodness-of-fit for faulting model [Equation (10)]

Equation (11) shows the third and final model for faulting after 20 years (as predicted by M-E PDG) as a function of four design variables. This model is based on the linear regression technique but using transformed variables (*ln* transformation). The GOF statistics show that this model has the minimum standard error (as compared to other two models mentioned above). The GOF is also demonstrated by Figure 6.7. Based on the better accuracy of prediction values, this model was selected to evaluate relative importance of considered design variables.

$$\ln Fault = -11.52 - 0.54 \ln PCCThick + 0.41 \ln MOR + 1.47 \ln JS + 2.2 \ln CTE \qquad (11)$$

Model statistics:

- Number of data points, N = 256
- Coefficient of determination, R^2 = 96.6 percent
- Standard error estimate, SEE = 0.0123 inches

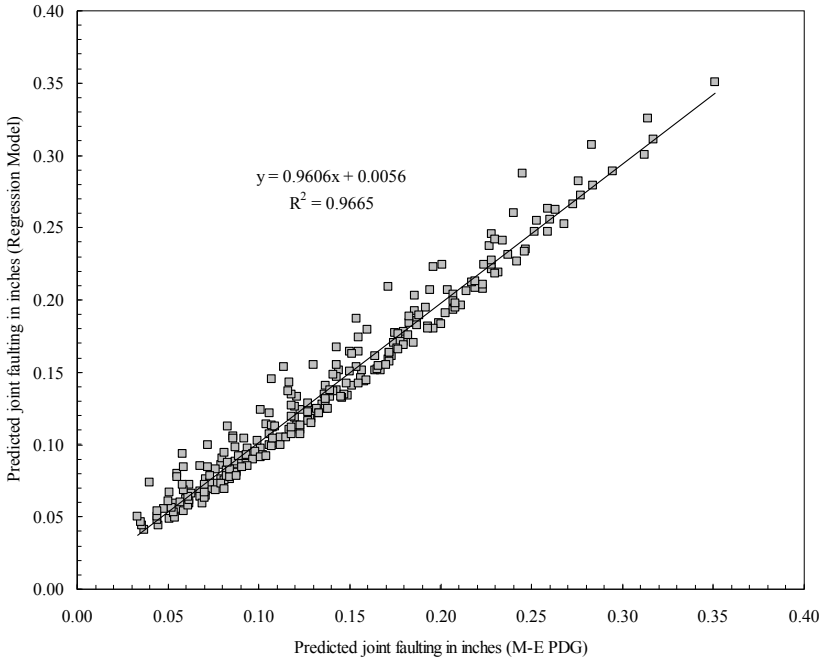

Figure 6.7 Goodness-of-fit for faulting model [Equation (11)]

Faulting model shown by Equation (11) was used to quantify the relative effect of design variables.

Faulting Model Sensitivity

Figures 6.8 and 6.9 show the sensitivity of final faulting model [Equation(11)] for all design variables considered to develop the model. It can be seen that faulting after 20 years is affected by all design variables at different levels. CTE and slab thickness seems to have the most significant effect on future faulting performance. These design charts can be used for assessing the levels of variables at preliminary design stage.

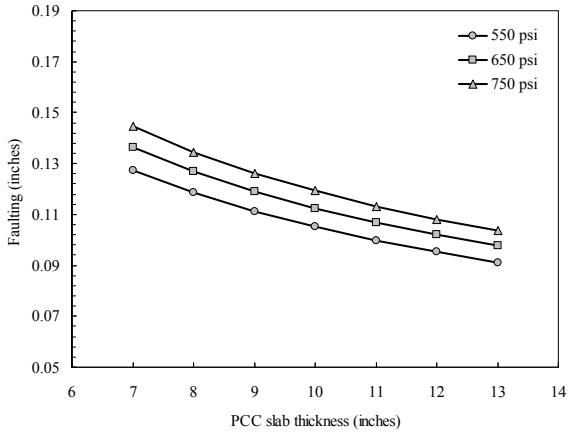

(a) Effect of slab thickness and MOR

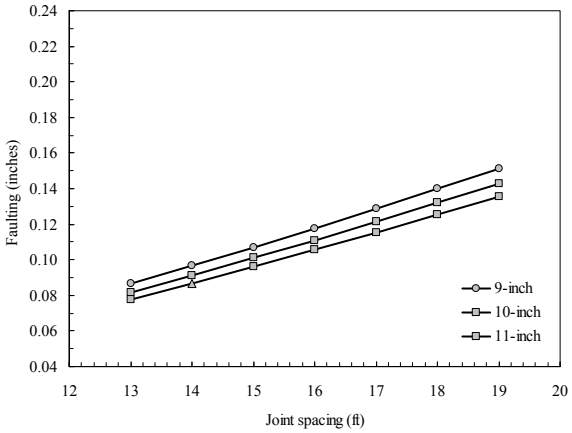

(d) Effect of joint spacing and slab thickness

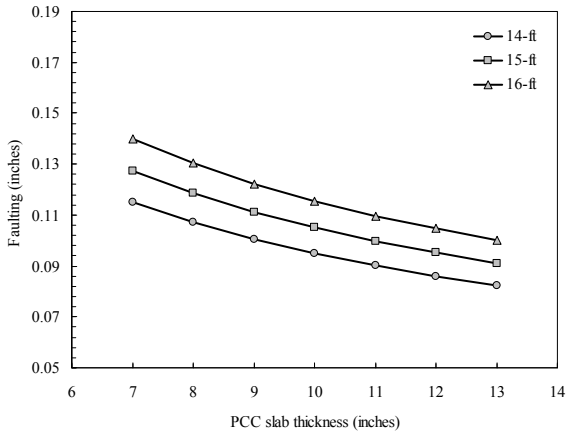

(b) Effect of slab thickness and joint spacing

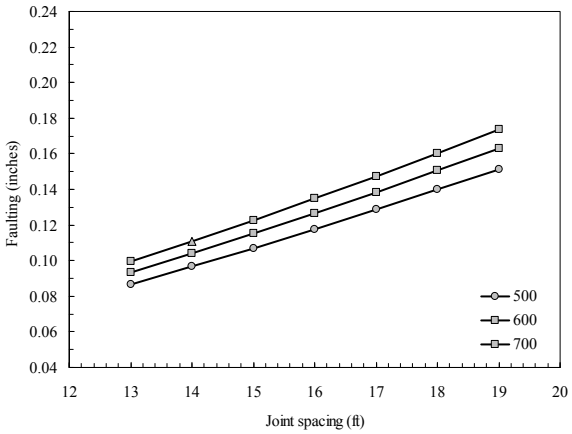

(e) Effect of joint spacing and MOR

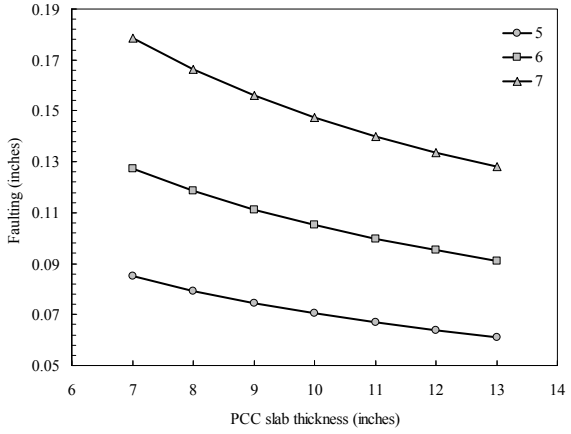

(c) Effect of slab thickness and CTE

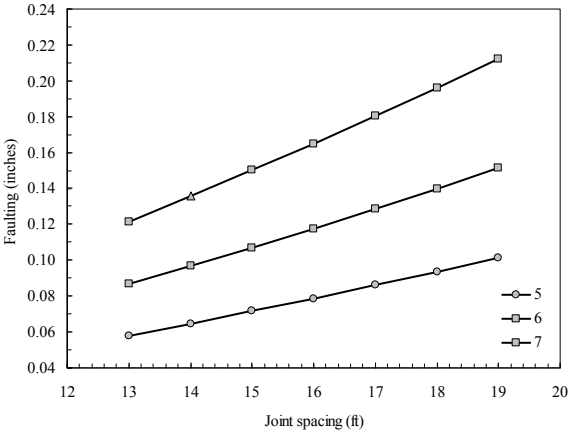

(f) Effect of joint spacing and CTE

Figure 6.8 Sensitivity of faulting model

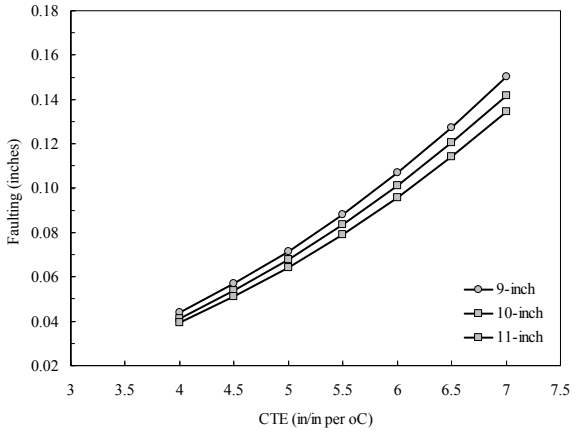

(a) Effect of CTE and slab thickness

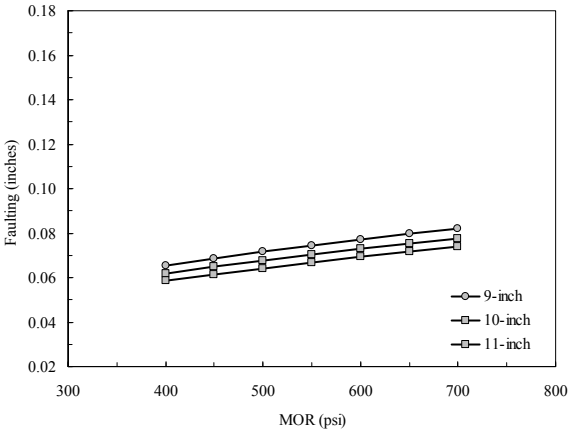

(d) Effect of MOR and slab thickness

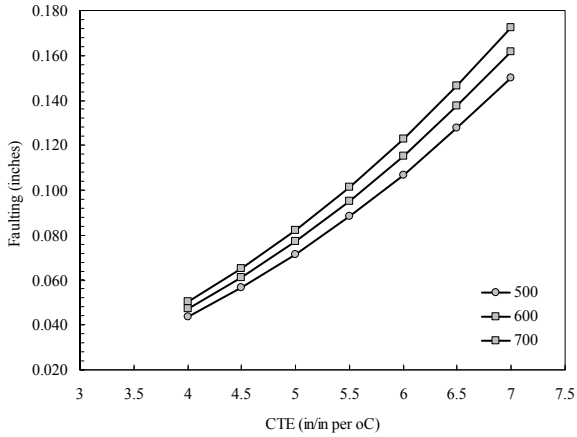

(b) Effect of CTE and MOR

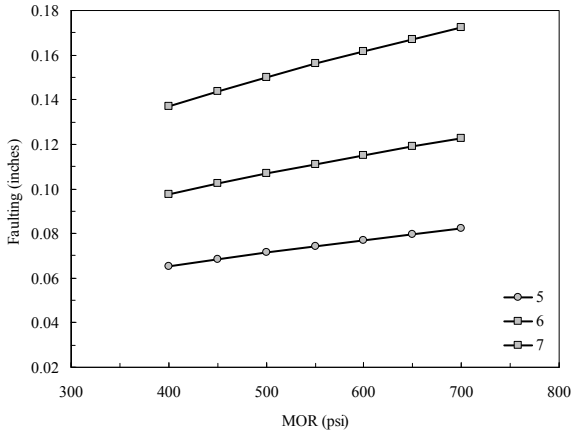

(e) Effect of MOR and CTE

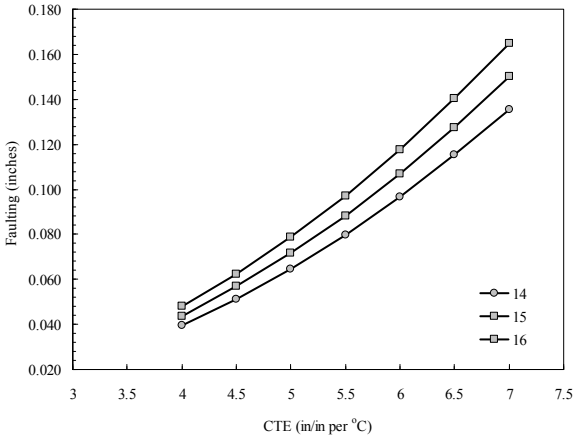

(c) Effect of CTE and joint spacing

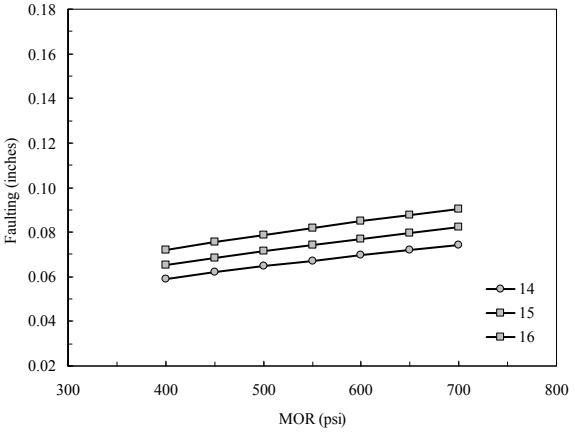

(f) Effect of MOR and joint spacing

Figure 6.9 Sensitivity of faulting model

Figure 6.10 shows an example demonstration for use of such design charts at the initial design stage. The chart shows that for a concrete CTE value of 6.5 in/in per ^{o}C, the faulting after 20 years can be reduced from 0.13- to 0.115-inch, if joint spacing is reduced from 15- to 14-ft. On the other hand to remain at the same level of expected faulting (0.13-inch), reduced joint spacing can be considered while compromising on a slightly higher CTE value. The increase in joint spacing can be transformed into added cost and a coherent comparison can be made between construction and future rehabilitation/maintenance costs. The life cycle cost analysis can be conducted to compare different design alternates at the initial stages.

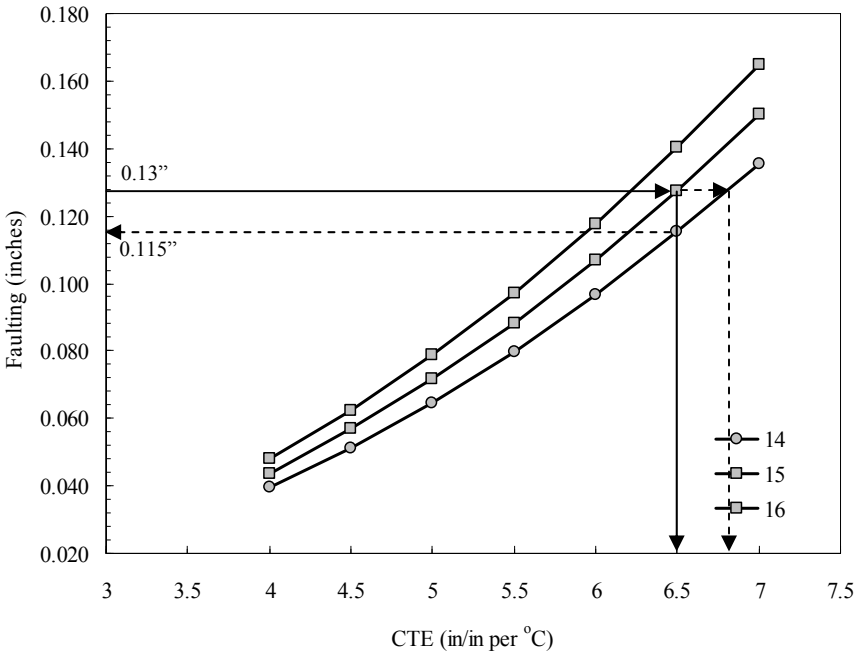

Figure 6.10 Effect of joint spacing on faulting — Example

6.1.2.3 Smoothness Model

Equations (12) and (13) present the rigid pavement roughness model developed under NCHRP 1-37A research (*36*).

$$IRI = IRI_o + C_1 \times CRK + C_2 \times SPALL + C_3 \times TFAULT + C_4 \times SF \quad (12)$$

where

IRI = predicted IRI, in/mi
IRI_o = initial smoothness measured as IRI, in/mi
CRK = percent slabs with transverse cracks (all severities)
$SPALL$ = percentage of joints with spalling (medium and high severities)
$TFAULT$ = total joint faulting cumulated per mi, in
C_1 = 0.8203, C_2 = 0.4417, C_3 = 1.4929, C_4 = 25.24

$$SF = AGE\ (1 + 0.5556 \times FI)(1 + P_{200}) \times 10^{-6} \quad (13)$$

where

AGE = pavement age, yr
FI = freezing index, °F-days
P_{200} = percent subgrade material passing No. 200 sieve

Model Statistics:

- R^2 = 60 percent
- SEE = 27.3 in/mile
- N = 183

Several smoothness models were developed in this study by considering same four design variables as considering in development of cracking and faulting models. Equation (14) presents first of those IRI model. This model is based on the linear regression technique. Figure 6.11 shows the GOF for this model. While GOF statistics are reasonable, the GOF graphs shows that this model is not robust at higher levels of IRI.

$$\ln IRI = \frac{1}{1.23}\left[\left(4.175 - 0.07 PCCThick + 0.054 JS + 0.197 CTE\right) - 30.1\right] \quad (14)$$

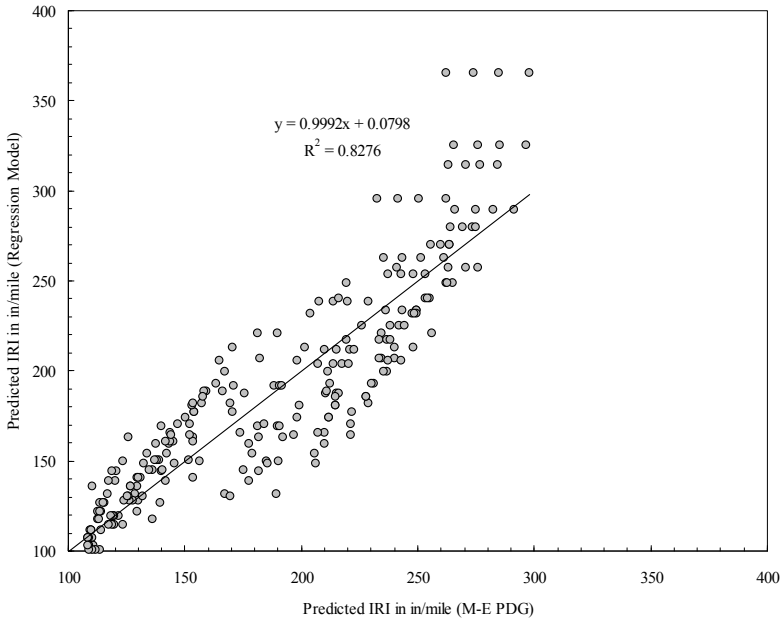

Figure 6.11 Goodness-of-fit for IRI model [Equation (14)]

Model statistics:

- Number of data points, N = 256
- Coefficient of determination, R^2 = 82.7 percent
- Standard error estimate, SEE = 26.1 in/mile

Equation (15) shows the final model for IRI after 20 years (as predicted by M-E PDG) as a function of four design variables. This model is based on the linear regression technique. The GOF statistics show that this model has the minimum standard error (as compared to other two models mentioned above). The GOF is also demonstrated by Figure 6.12. Based on the better accuracy of prediction values, this model was selected to evaluate relative importance of considered design variables. However, the GOF figure shows that the model is not robust at low levels of IRI.

$$IRI = \frac{1}{0.882}\left[\left(6.538 - 12.229PCCThick - 0.081MOR + 9.449JS + 34.989CTE\right) - 22.146\right] \quad (15)$$

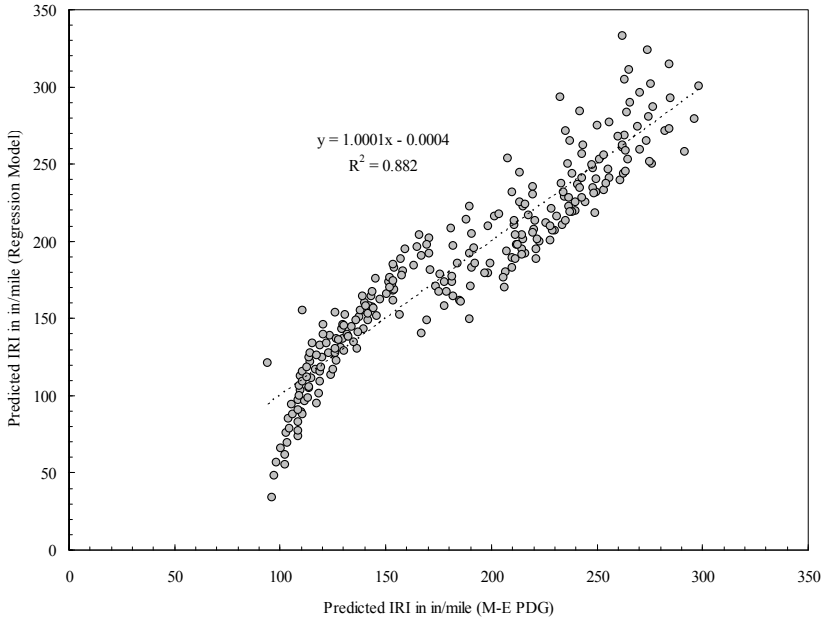

Figure 6.12 Goodness-of-fit for IRI model [Equation (15)]

Model statistics:

- Number of data points, N = 256
- Coefficient of determination, R^2 = 88.2 percent
- Standard error estimate, SEE = 20.9 in/mile

The IRI model shown by Equation (15) was used to quantify the relative effect of design variables.

IRI Model Sensitivity

Figures 6.13 and 6.14 show the sensitivity of final IRI model [Equation (15)] for all design variables considered to develop the model. It can be seen that IRI after 20 years is affected by all design variables at different levels. CTE and slab thickness seems to have the most significant effect on future ride quality in terms of IRI. Again, these design charts can be used for assessing the levels of variables at preliminary design stage.

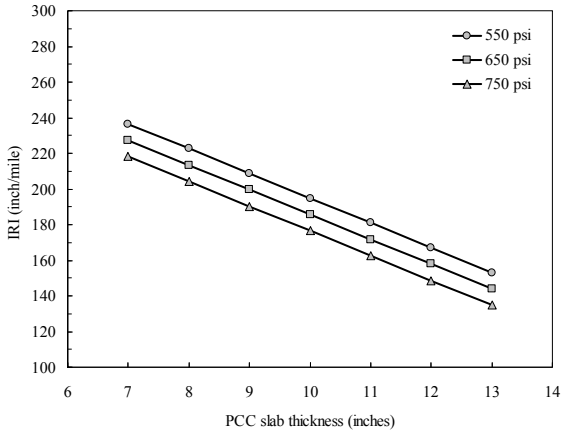

(a) Effect of slab thickness and MOR

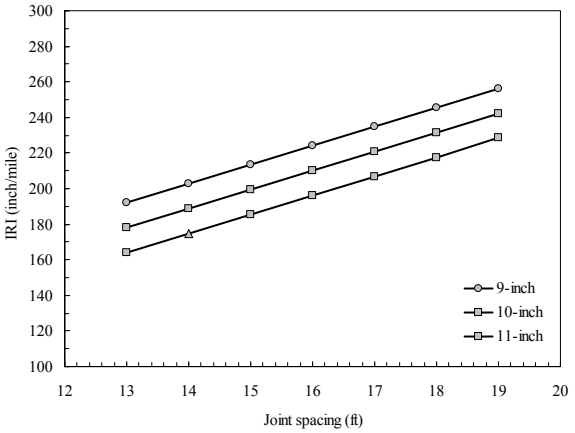

(d) Effect of joint spacing and slab thickness

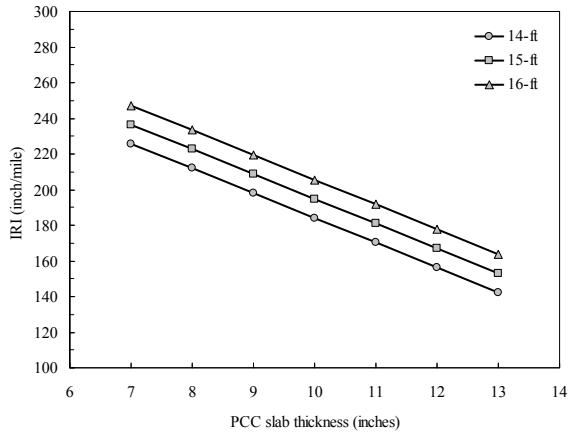

(b) Effect of slab thickness and joint spacing

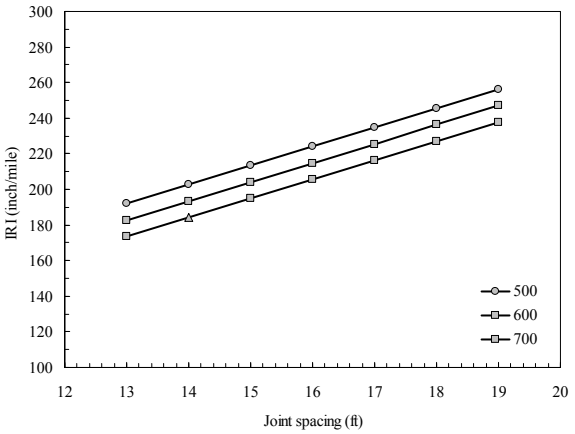

(e) Effect of joint spacing and MOR

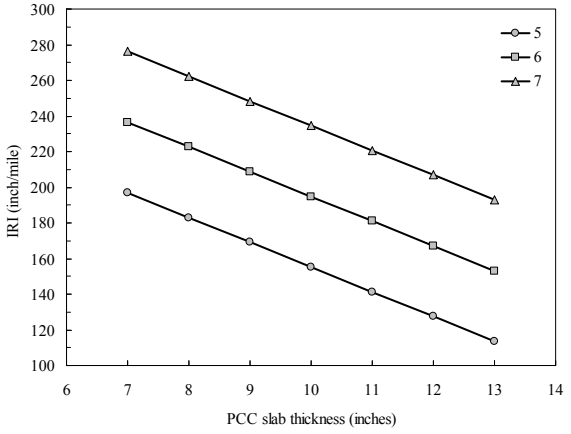

(c) Effect of slab thickness and CTE

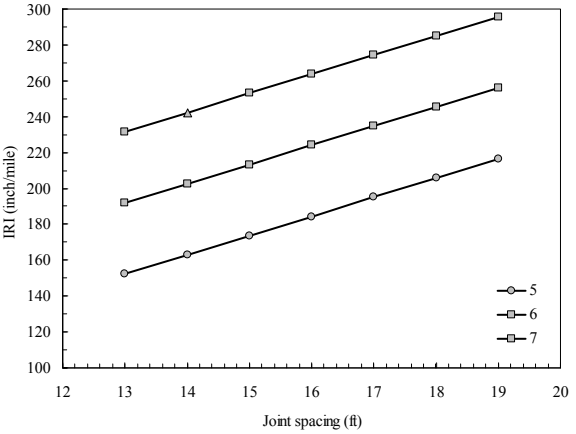

(f) Effect of joint spacing and CTE

Figure 6.13 Sensitivity of IRI model

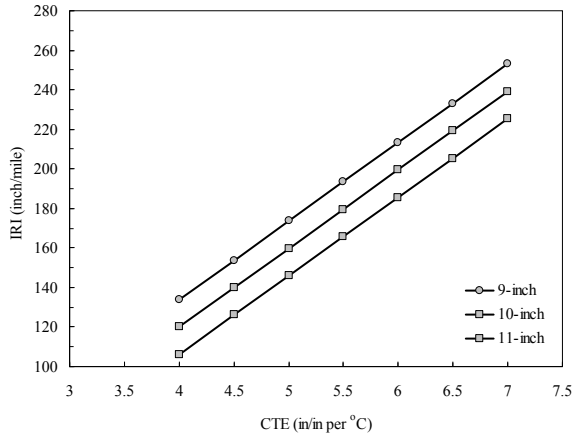

(a) Effect of CTE and slab thickness

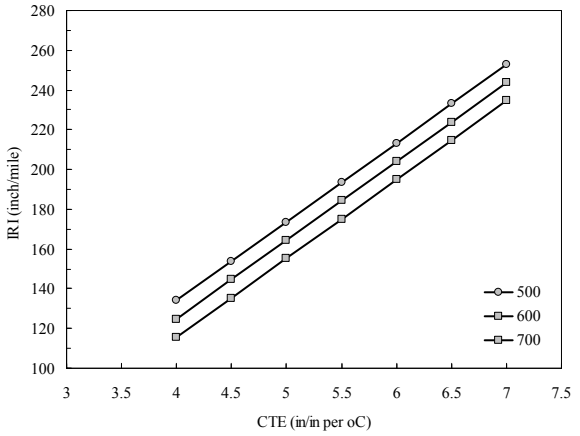

(b) Effect of CTE and MOR

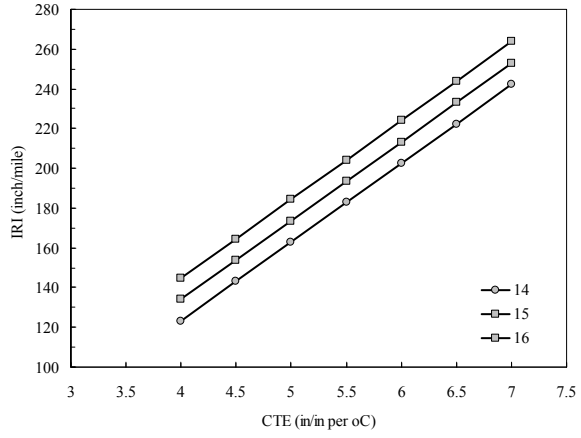

(c) Effect of CTE and joint spacing

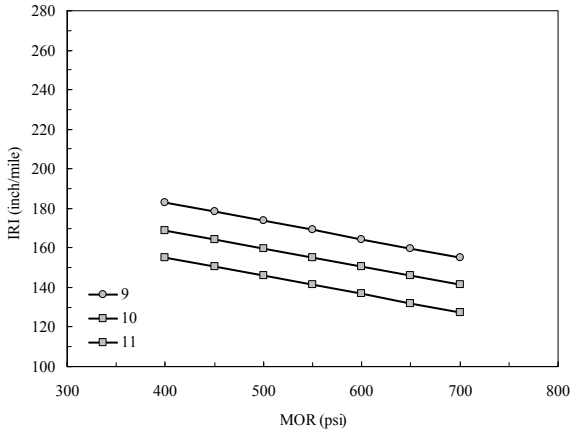

(d) Effect of MOR and slab thickness

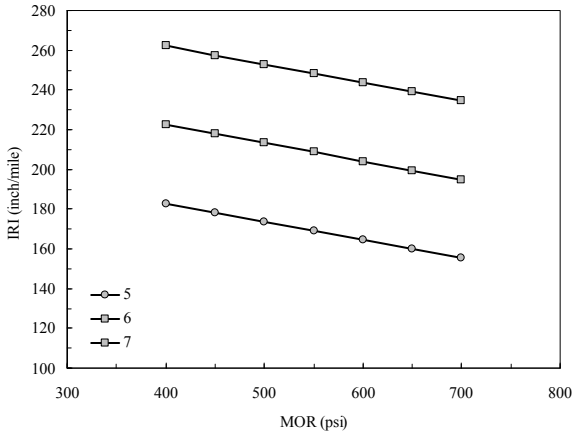

(e) Effect of MOR and CTE

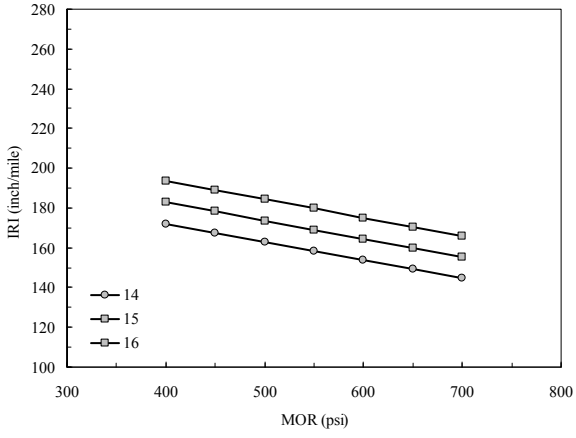

(f) Effect of MOR and joint spacing

Figure 6.14 Sensitivity of IRI model

Figure 6.15 shows an example demonstration for use of developed design charts at the initial design stage. The chart shows that for a concrete CTE value of 6 in/in per ^{o}C, the IRI after 20 years can be reduced from 195 to 160 inch/mile, if slab thickness is increased from 10- to 12.5 inches. On the other hand to remain at the same level of expected reduced IRI, reducing CTE to 5 in/in per ^{o}C can be considered at a slab thickness of about 10-inches. The increase in slab thickness can be transformed into added cost and a coherent comparison can be made between construction and future rehabilitation/maintenance costs. The life cycle cost analysis can be conducted to compare different design alternates at the initial stages.

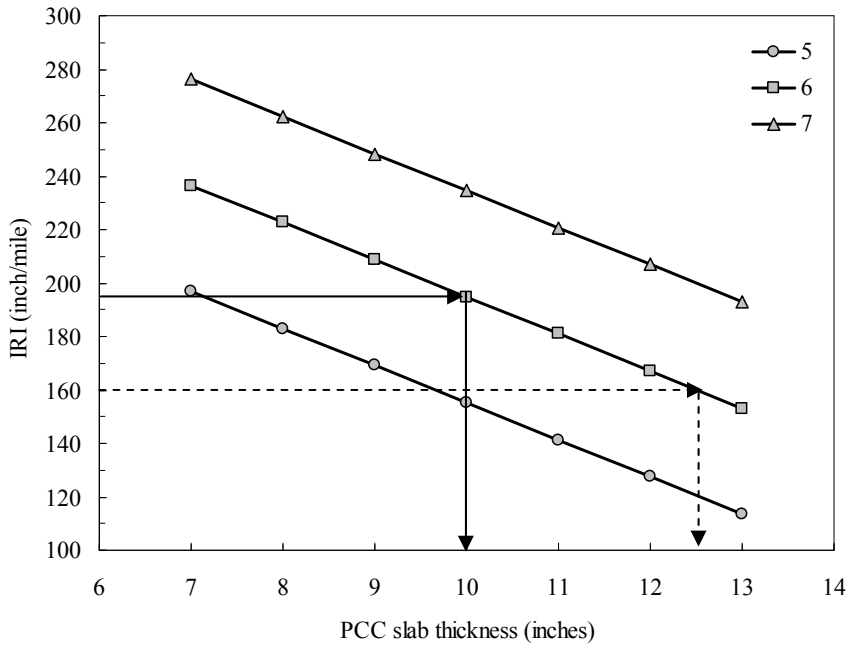

Figure 6.15 Effect of slab thickness on IRI — Example

6.1.2.4 Spalling Model

The spalling model as a function of design variables was developed under NCHRP 1-37A. Equations (16) and (17) present the rigid pavement spalling model:

$$SPALL = \left[\frac{AGE}{AGE + 0.01}\right]\left[\frac{100}{1 + 1.005^{(-12\,AGE + SCF)}}\right] \tag{16}$$

where

SPALL = percentage joints spalled (medium- and high-severities)
AGE = pavement age since construction, years
SCF = scaling factor based on site-, design-, and climate-related variables:

$$SCF = \begin{bmatrix} -1400 + 350AIR\%\left(0.5 + PREFORM\right) + \\ 3.4\, f'_c \times 0.4 - 0.2\left(FTCYC \times AGE\right) + \\ 43Thick - 536WC \end{bmatrix} \quad (17)$$

where

SCF = spalling prediction scaling factor
AIR% = PCC air content, percent
AGE = time since construction, years
PREFORM = 1 if preformed sealant is present; 0 if not
f'c = PCC compressive strength, psi
FTCYC = average annual number of freeze-thaw cycles
Thick = PCC slab thickness, in
WC = PCC water/cement ratio

Model Statistics:

- R^2 = 78 percent
- N = 179
- SEE = 6.8 percent of joints

The above spalling model can also be used for making appropriate decisions at the design stage.

6.2 EFFECT OF TRAFFIC CHARACTERIZATION (ESALS VERSUS LOAD SPECTRA) ON RIGID PAVEMENT PERFORMANCE

Traffic is the most important factor in pavement design process. Traffic characterization includes both the load magnitude and the number of load repetitions for each axle configuration. According to Huang (*47*), there are three different procedures for characterizing traffic in pavement design process: fixed traffic, fixed vehicle and variable traffic and vehicle.

In fixed traffic, pavement thickness design is based on a single-wheel load, and number of repetitions is not considered. The multiple wheels are converted to an equivalent single-wheel load (ESWL) for design. This method has been most frequently used for airport or highway pavements with heavy wheel loads but low repetitions. Typically, the heaviest wheel load expected is used for design purposes. On the other hand, in fixed vehicle/axle procedure, the thickness design is based on the number of repetitions of a standard vehicle or axle load, usually the 18-kip single axle load. If the axle load is different from 18-kip or consists of tandem or tridem axles, it must be converted to 18-kip single axle repetitions by an equivalent axle load factor (EALF). The number of repetitions under each axle single, tandem or tridem axles must be multiplied by EALF to obtain the equivalent effect based on 18-kip single axle load. The summation of the equivalent effects of all axle loads during the design period result in an equivalent single-axle load (ESAL), a single traffic parameter for design purposes. Lastly, for variable traffic and vehicles, both axles and their repetitions are considered individually. The loads are divided into number of groups, and pavement response (stresses, strains, and deflections) under each load group is determined separately and used to determine accumulative damage. The accumulative damage is subsequently related to pavement distresses (cracking, faulting and rutting etc).

In mechanistic pavement analysis and design methods, it is not necessary to apply the load equivalency concept because different loads can be considered separately in the design process. The concept of load equivalency has been used often in the empirical methods for pavement design (e.g. AASHTO). Axle load spectra have been used to develop the mechanistic-empirical pavement design guide (M-E PDG). Use of these load distributions provides a more direct and rational approach for the analysis and design of pavement structures to estimate the effects of actual traffic on pavement response and distress. In the AASHTO Guide for Design of Pavement Structures, a mixed traffic stream of different axle loads and axle configurations is converted into a design traffic number by converting each expected axle load into an equivalent number of 18-kip single-axle loads, known as equivalent single-axle loads (ESALs). Load equivalency factors (LEFs) are used to determine the number of ESALs for each axle load and axle configuration. These factors are based on the present serviceability index concept and depend on the pavement type and structure. Studies have shown that these factors also are influenced by pavement condition, distress type, failure mode, and other parameters. Regardless of the argument over empirical pavement design being based on ESALs, the concept is expected to continue to play a major role in pavement design and rehabilitation for many years to come.

For highway pavements, the use of two types of load characterizations (equivalent axle load versus axle load spectra) in mechanistic analysis and design procedures need to be evaluated.

It should be noted that traffic can be considered in terms of ESALs in mechanistic design procedure by considering a standard axle (18 kip) instead of an axle load distribution.

This assessment involves the effect of ESALs versus axle load spectra (ALS) on pavement performance. Before evaluating the effect of different load characterization on pavement performance, background for determining load characterization based on equivalency concept and load spectra is presented.

6.2.1 Background

From the flexible and rigid pavements in the AASHO Road Test (*47*), Equations (18) through (22) were used to calculate the equivalent axle load factors (EALF):

$$\log\left(\frac{W_{tx}}{W_{t18}}\right) = 4.79\log(18+1) - 4.79\log(L_x - L_2) + 4.33\log(L_2) + \frac{G_t}{\beta_x} - \frac{G_t}{\beta_{18}} \tag{18}$$

$$G_t = \log\left(\frac{4.2 - p_t}{4.2 - 1.5}\right)$$

$$\beta_x = 0.40 + \frac{0.081(L_x + L_2)^{3.23}}{(SN+1)^{5.19} L_2^{3.23}} \tag{19}$$

$$\log\left(\frac{W_{tx}}{W_{t18}}\right) = 4.62\log(18+1) - 4.62\log(L_x - L_2) + 3.28\log(L_2) + \frac{G_t}{\beta_x} - \frac{G_t}{\beta_{18}} \tag{20}$$

$$G_t = \log\left(\frac{4.5 - p_t}{4.5 - 1.5}\right)$$

$$\beta_x = 1.00 + \frac{3.63(L_x + L_2)^{5.2}}{(D+1)^{8.46} L_2^{3.52}} \tag{21}$$

where

W_{tx} = Number of *x*-axle load applications at the end of time *t*

W_{t18} = Number of *18-kip (80 kN)* single-axle load applications at the end of time *t*

L_x = Load in kips on one single, one set of tandem or one set of tridem axles

L_2 = Axle code, 1= single, 2= tandem and 3= tridem

p_t = Terminal serviceability (i.e., pavement condition at failure)

SN = Structural number, $SN = a_1D_1 + a_2D_2m_2 + a_3D_3m_3$

D = Slab thickness, inches

β_{18} = The value of β_x when L_x = 18 and L_2 =1

$$EALF = \left(\frac{W_{t18}}{W_{tx}}\right) \tag{22}$$

The load equivalency factor is defined as the number of applications of the base load of magnitude 18-kip (for single axle), which is equivalent in destructive effect to one application of load of different magnitudes (*48*). While pavements are subjected to a diverse and almost unlimited spectrum of load levels, the analysis of these complex loadings is facilitated by expressing the destructive effects of all loads in terms of equivalent numbers of applications of a standard load. Accordingly, the composite destructive effects of all loads in terms of equivalent standard axle loads (ESALs) can be determined through:

$$ESAL = \sum_{i=1}^{m} EALF_i n_i \tag{23}$$

where

m = The number of axle groups
$EALF_i$ = The equivalent axle load factor (EALF) for the i^{th}-axle load group
n_i = The numbers of passes of the i^{th}-axle load group

It should be recognized that the AASHTO load equivalency factors were empirically derived using statistical analysis of the observed data. In addition, no endeavor was made to distinguish between different modes of distress—the equivalency factors were related only to performance as measured by the present serviceability index (PSI) (*49*). Therefore, several studies have been conducted to determine and compare the load equivalency concept using mechanistic analyses where pavement responses could be utilized (*48, 50-52*). The major advantage of these approaches includes the determination of load equivalencies for other types of distresses (e.g., cracking and rutting in flexible pavements). The use of performance models, incorporating critical pavement response for a specific distress, to determine load equivalency established the power law. For example, Deacon (*48*) used a fatigue model developed in the laboratory to determine load equivalencies and compared the theoretically determined equivalent axle load factors (EALF) with the AASHTO EALF. Equation (24) presents the definition of EALF while Equation (25) shows the EALF for a standard axle in terms of the number of repetitions to failure:

$$EALF_{18} = \frac{\text{damage by X kip axle}}{\text{damage by 18 kip axle}} \tag{24}$$

$$EALF_s = \frac{1/N_{fx}}{1/N_{fs}} = N_{fs}/N_{fx} \tag{25}$$

where

$EALF_s$ = Equivalent axle load factor in terms of a standard axle
N_{fs} = The numbers of repetitions of the *standard-axle* load
N_{fx} = The numbers of repetitions of the *x-axle* load

The number of repetitions to failure can be determined from a transfer function. For example, number of repetitions to fatigue failure for a particular strain level under a load can be expressed by (*47*):

$$N_f = k\left(\frac{1}{\varepsilon}\right)^n \tag{26}$$

where

N_f = The numbers of repetitions of a load to failure
ε = The strain level due to a load
k, n = Regression constants

Combining Equations (25) and (26), the power law can be generalized as:

$$EALF = \left(\frac{\varepsilon_x}{\varepsilon_s}\right)^n \tag{27}$$

where

ε_x = The strain level due to application of a load
ε_s = The strain level due to the standard load
n = Exponent or power

It can also be assumed that for linear elastic material behavior the pavement response (in terms of stress or strain) is directly proportional to axle load (*47*). Therefore, pavement response can be replaced by axle load yielding:

$$EALF = \left(\frac{w_i}{w_s}\right)^n \tag{28}$$

where

w_i = The load in kN on an axle group
w_s = The load in kN corresponding to the *EALF*

If the pavement design is based on the equivalent 18-kip single-axle load, the equivalent single axle loads for the design lane can be calculated as:

$$ESAL = \left(\sum_{i=1}^{m} p_i \times EALF_i\right) \times ADT \times T \times A \times G \times D \times L \times 365 \times Y \tag{29}$$

where

m = Number of axle groups
p_i = Percentage of total repetition for the i^{th} axle load group
$EALF_i$ = Equivalent axle load factor (EALF) for the i^{th} axle load group
ADT = Average daily traffic
T = Percentage of trucks in ADT
A = Average number of axles per truck
G = Growth factor
L = Lane distribution factor
D = Directional distribution factor
Y = Design period in years

It was established through the AASHO Road Test that the impact of each individual axle load on flexible and rigid pavements can be approximately estimated according to the fourth power law (*47, 53*). The fourth power law implies that pavement damage by passing axles increases exponentially with the increase of their load. The damage is related to loss in pavement serviceability. Therefore, to simulate AASHTO ESALs, an exponent value of four ($n = 4$) is used in this evaluation.

In the mechanistic-empirical approach (e.g., M-E PDG) traffic is accounted in terms of axle load spectra instead of ESAL. It is required for estimating the loads that are applied to a pavement and the frequency with which those loads are applied throughout the pavement design life. For the M-E PDG, the traffic data required are the same regardless of the pavement type (i.e. flexible or rigid) or design type (new or rehabilitation)(*54*). Agencies typically collect three types of traffic data—weigh-in-motion (WIM), automatic vehicle classification (AVC), and vehicle counts. These data can be augmented by traffic estimates computed using traffic forecasting and trip generation models. WIM data are typically reported in a format similar to the FHWA W-4 Truck Weight Tables. AVC data are reported as the number of vehicles by vehicle type counted over a period of time, while vehicle counts are reported as the number of vehicles counted over a period of time. The normalized axle load distribution or spectra can only be determined from WIM data. Therefore, the level of input depends on the data source (site, regional, or national). For this design procedure, load spectra are normalized on an annual basis because no systematic or significant year-to-year or month-to-month differences were found in the analysis of the LTPP WIM data.

The axle load distribution factors simply represent the percentage of the total axle applications within each load interval for a specific axle type (single, tandem, tridem, and quad) and vehicle class (classes 4 through 13). A definition of load intervals for each axle type is provided below:

- Single axles – 3,000 lb to 40,000 lb at 1,000-lb intervals.
- Tandem axles – 6,000 lb to 80,000 lb at 2,000-lb intervals.
- Tridem and quad axles – 12,000 lb to 102,000 lb at 3,000-lb intervals.

The traffic inputs are processed in the Design Guide software/procedure for use in computing pavement responses due to applied wheel loads. The outputs are the number of axle loadings applied incrementally (hourly or monthly) at a specific location over the entire design period. The end result is to produce the following for each wheel load category and wheel location on an hourly or monthly basis (depending on the analysis type):

- Number of single axles.
- Number of tandem axles.
- Number of tridem axles.
- Number of quad axles.
- Number of truck tractors (Class 8 and above for computing JPCP top-down cracking).

Eight major steps performed by the Design Guide software for developing the "processed inputs" needed for analysis are as follows (*39*):

- Determine increments (hourly or monthly).
- Determine the AADTT value for the base year.
- Determine the normalized truck traffic class distribution for the base year.
- Determine the number of axles by axle type for each truck class.
- Determine the normalized axle load spectra for each axle type and truck class.
- Decide on the truck traffic forecast or reverse forecast function, and revise the incremental truck traffic for each successive year in the design/analysis period.
- Multiply the normalized axle load spectra and normalized truck class spectra to the incremental truck traffic to determine the total number of axle applications within each axle load group for each axle type for each hour of each month of each year in the design/analysis period.
- Specify details of the axle and tire loads.

Equations (30) through (37) present the equations required for executing above mentioned process. The equations are also mentioned in the matrix form.

$$TT_{1,j,i} = \left[AADTT_{1,j,i} \right] \left[MAF_j \right] \left[HAF_i \right] \left[DDF \right] \left[LDF \right] \left[\text{No. of Days}_j \right] \tag{30}$$

$$TT_{1,j,i} = \begin{pmatrix} T_{jan} \\ \vdots \\ T_{Dec} \end{pmatrix} = \left[AADTT_{1,j,i} \right] \begin{pmatrix} m_{11} & \cdots & m_{1n} \\ \vdots & \ddots & \vdots \\ m_{m1} & \cdots & m_{mn} \end{pmatrix}_{Class \times month} \begin{pmatrix} h_1 \\ \vdots \\ h_{24} \end{pmatrix} \left[DDF \right] \left[LDF \right] \left[\text{No. of Days}_j \right] \tag{31}$$

$TT_{1,j,i}$ = Total number of trucks in year 1 and j^{th} month during i^{th} time period

$AADTT_{1,j,i}$ = Average annual daily truck traffic in year 1 and j^{th} month during i^{th} time period

MAF_j = Monthly adjustment factor for j^{th} month

HAF_i = Hourly adjustment factor for i^{th} time period

DDF = Direction distribution factor

LDF = Lane distribution factor

No. of Days_j = Number of days in j^{th} month

$$TT_{1,j,i,k} = \left[TT_{1,j,i} \right] \left[NTP_k \right] \tag{32}$$

$$TT_{1,j,i,k} = \begin{pmatrix} t_{Jan,4} & \cdots & t_{Jan,13} \\ \vdots & \ddots & \vdots \\ t_{Dec,4} & \cdots & t_{Jan,13} \end{pmatrix} = \begin{pmatrix} T_{jan} \\ \vdots \\ T_{Dec} \end{pmatrix} \begin{pmatrix} D_4 & \cdots & D_{13} \end{pmatrix} \tag{33}$$

$TT_{1,j,i,k}$ = Number of truck in year 1 and j^{th} month during i^{th} time period for k^{th} truck class

$TT_{1,j,i}$ = Total number of trucks in year 1 and j^{th} month during i^{th} time period

NTP_k = Normalized truck class distribution

$$NA_{1,j,i,k,a} = \left[TT_{1,j,i,k} \right] \left[NAT_{k,a} \right] \tag{34}$$

$$NA_{1,j,i,k,a} = \begin{pmatrix} a_{Jan,single} & \cdots & a_{Jan,quad} \\ \vdots & \ddots & \vdots \\ a_{Dec,single} & \cdots & a_{Dec,quad} \end{pmatrix} = \begin{pmatrix} t_{Jan,4} & \cdots & t_{Jan,13} \\ \vdots & \ddots & \vdots \\ t_{Dec,4} & \cdots & t_{Jan,13} \end{pmatrix} \begin{pmatrix} a_{4,single} & \cdots & a_{4,quad} \\ \vdots & \ddots & \vdots \\ a_{13,single} & \cdots & a_{13,quad} \end{pmatrix} \tag{35}$$

$NA_{1,j,i,k,a}$ = Total number of axles by truck class within each axle configuration (single, tandem and tridem)

$TT_{1,j,i,k}$ = Number of truck in year 1 and j^{th} month during i^{th} time period for k^{th} truck class

$NAT_{k,a}$ = Average number of axles for k^{th} truck class and a^{th} axle type

$$AL_{1,j,i,k,a,w} = \left[NA_{1,j,i,k,a} \right] \left[NWP_{a,w} \right] \tag{36}$$

$$AL_{1,j,i,k,a,w} = \begin{pmatrix} a_{4,3000} & \cdots & a_{13,41000} \\ \vdots & \ddots & \vdots \\ a_{13,3000} & \cdots & a_{13,41000} \end{pmatrix} = \begin{pmatrix} a_{Jan,single} & \cdots & a_{Jan,quad} \\ \vdots & \ddots & \vdots \\ a_{Dec,single} & \cdots & a_{Dec,quad} \end{pmatrix} \begin{pmatrix} w_{4,3000} & \cdots & w_{4,4100} \\ \vdots & \ddots & \vdots \\ w_{13,3000} & \cdots & a_{13,41000} \end{pmatrix} \tag{37}$$

$AL_{1,j,i,k,a,w}$ = Number of axle repetitions within each load group

$NA_{1,j,i,k,a}$ = Total number of axles by truck class within each axle configuration (single, tandem and tridem)

$NWP_{a,w}$ = Number of weight classes

The final processed traffic data include the number of axle load repetitions within specific load groups. These repetitions are determined for each axle configuration within each truck class and month. All the axle load repetitions are used for subsequent damage analyses using Equation(38) . Allowable number of repetitions depends on calculated stress as shown by Equation(39).

$$FD = \sum \frac{n_{i,j,k,l,m,n}}{N_{i,j,k,l,m,n}} \tag{38}$$

FD = Total fatigue damage (top-down or bottom-up)

$n_{i,j,k,l,m,n}$ = Applied number of load applications at condition *i, j k, l, m, n*

$N_{i,j,k,l,m,n}$ = Allowable number of load applications at condition *i, j k, l, m, n*

i = Age

j = Month

k = Axle type (single, tandem and tridem for bottom-up cracking; short, medium and long wheelbase for top-down cracking

l = Load level (incremental load for each axle type)
m = Temperature difference
n = Traffic path

$$N_{i,j,k,l,m,n} = C_1\left(\frac{MR_i}{\sigma_{i,j,k,l,m,n}}\right)^{C_2} + 0.4371 \quad (39)$$

$N_{i,j,k,l,m,n}$ = Allowable number of load applications at condition *i, j k, l, m, n*
MR_i = PCC Modulus of rupture at age *i*, psi
$\sigma_{i,j,k,l,m,n}$ = Applied stress at condition *i, j k, l, m, n*
C_1 = Calibration constant = 2.0
C_2 = Calibration constant = 1.22

Finally, the accumulated damage with time is used for predicting pavement distresses (e.g. cracking).

Several researchers have modeled axle load spectra (*55-58*). To capture bimodal distributions observed for axle load spectra, Timm et al. (*58*) combined normal and lognormal distributions, while early work by Mohammadi and Shah (*59*) concluded that the beta and lognormal distributions were most appropriate. Recent works by Prozzi et al. (*57*) and Haider and Harichandran (*55*) considered a mixture of two log-normal and two normal distributions, respectively, to characterize axle load spectra. All these studies concluded that it would be more useful to develop a model having sound statistical interpretations both practically and theoretically.

Since the combination of truck payload and truck weight contribute to gross vehicle and axle loads, and also since these weights are the sum of the weights of several smaller components, the central limit theorem will apply, and the load distributions for loaded and unloaded truck weights should each be nearly normal. Haider and Harichandran (*55*) determined that the bimodal shape of axle spectra could be effectively captured by using a mixture of two normal distributions. Furthermore, by using LTPP axle load data they showed that a mixture of two normal distributions can reasonably fit observed single and tandem axle load distributions. This model has five parameters which need to be estimated from data (*55, 60, 61*).

6.2.2 Problem Statement

The objective of this evaluation is to assess the effects of different load characterization (ESAL versus ALS) on pavement performance. This is accomplished by characterizing axle load spectra as a bimodal mixture distribution and then using its parameters to estimate ESALs. Two specific aspects of this study are to: (a) evaluate effect of equivalent ALS— different axle load spectra which are equivalent in ESALs, on predicted pavement performance; and (b) assess effect of different axle load spectra on pavement performance by varying number of repetitions to achieve same ESALs.

6.2.3 Equivalent Axle Load Spectra

While pavement damage is inherently incorporated in the ESAL concept, it is of more practical use to relate axle load spectra and ESAL to determine the magnitude of traffic level. These traffic levels will remain in use, for the time being, to obtain a feel for pavement structural and material designs. It was established through the AASHO Road Test (*53*) and other studies (*48, 56*) that the impact of each individual axle load in terms of flexible and rigid pavements damage can approximately be estimated by using a fourth power law (*47*). The fourth power law implies that pavement damage by passing axles increases exponentially with the increase of their axle load. Equation (28) presents the fourth power law in terms of EALF, where *n* is equal to 4. Combining Equations (23) and (28), the load-pavement impact based on axle load spectra can be obtained by integrating the contributions from all the loads x_i in the axle load distribution (*57, 62*):

$$ESAL_j = \frac{N_j}{x_s^4} \int_{-\infty}^{\infty} x_i^4 f^*(x_i)\, dx \tag{40}$$

where

$ESAL_j$ = Equivalent single axle loads due to the j^{th} axle configuration

N_j = Number of repetition of the j^{th} axle configuration

x_i = Representative load (kN) within the i^{th} load bin

x_s = Standard or base axle load (kN) corresponding to the ESAL

$f^*(x_i)$ = PDF for bimodal axle load distribution

Substituting a bimodal distribution for the axle load spectra yields:

$$ESAL_j = \frac{N_j}{x_s^4} \int_{-\infty}^{\infty} x_i^4 \left(p_1 \frac{1}{\sigma_1\sqrt{2\pi}} e^{-(x_i-\mu_1)^2/2\sigma_1^2} + p_2 \frac{1}{\sigma_2\sqrt{2\pi}} e^{-(x_i-\mu_2)^2/2\sigma_2^2} \right) dx \tag{41}$$

Performing integrations analytically reduces this integral, to a closed-form solution for estimating the ESALs from a continuous axle load distribution:

$$ESAL_j = \frac{N_j}{x_s^4}\left[3p_1\sigma_1^4 + 6p_1\mu_1^2\sigma_1^2 + p_1\mu_1^4 + 3p_2\sigma_2^4 + 6p_2\mu_2^2\sigma_2^2 + p_2\mu_2^4 \right] \tag{42}$$

There are two important components in Equation(42). The first constituent is the number of repetitions of an axle type and the second constituent is the loading characteristics. While designing pavements both aspects are considered separately. Loading characteristics of an axle load spectra in terms of ESALs can be used to compare spectra at different sites. This also means that a site with a low frequency of axle loads may have more pavement damage due to higher loading characteristics or vice versa. To extract only loading contributions of an axle load distribution, Equation (42) can be reduced to a load spectra factor (ξ) if the total numbers of axle repetitions are reduced to one (*62*):

$$\xi_j = \frac{1}{x_s^4}\left[3p_1\sigma_1^4 + 6p_1\mu_1^2\sigma_1^2 + p_1\mu_1^4 + 3p_2\sigma_2^4 + 6p_2\mu_2^2\sigma_2^2 + p_2\mu_2^4\right] \quad (43)$$

where

ξ_j = Load spectra factor for the j^{th} axle configuration (i.e., equivalent average ESALs per repetition of the axle load spectra)

ξ_j represents the equivalent pavement damage in terms of ESALs by one pass of the j^{th} axle load. This simple statistic can be used to compare relative damage effects of different axle load spectra. For simplicity, only two axle configurations (single and tandem) are considered for illustration purposes. In addition, the observed share of other axle configurations (tandem and tridem) are also negligible (*61*) as compared to single and tandem axles. The total ESALs from axle load distributions can be represented by combining individual shares by axle types.

$$ESAL_{total} = ESAL_{\sin gle} + ESAL_{\tan dem} = \alpha N_T \xi_s + (1-\alpha) N_T \xi_t \quad (44)$$

where

N_T = Total axle repetitions

α = Proportion of single axle repetitions

$1-\alpha$ = Proportion of tandem axle repetitions

Equation (44) can be used to relate ESALs to axle load spectra as follows:

$$N_T = ESAL_{total} \Big/ \left[\alpha\xi_s + (1-\alpha)\xi_t\right] \quad (45)$$

$$N_s = \alpha N_T$$
$$N_t = (1-\alpha) N_T \quad (46)$$

Average daily truck traffic for a given growth rate and number of years can be determined as:

$$ADTT = \frac{N_T}{\left(\frac{(1+r)^y - 1}{r}\right) \times 365} \quad (47)$$

where

N_s = Total single axle repetitions

N_t = Total tandem axle repetitions

r = Annual growth rate

y = Number of years for traffic accumulative

The closed-form relationship between ESAL and axle load spectra was used to determine equivalent axle load spectra. These calculations are presented next.

6.2.3.1 Axle Load Spectra with Equivalent ESALs

The closed-form solution shown by Equation (42) can be used to generate equivalent axle load spectra. The equivalent axle load spectra as defined in this study are the load distributions having different characteristics but having same ESALs. Based on the assumption of bimodal normal mixture model, three such axle load spectra were generated as shown in Table 6.3. For example, Equations (48) and (49) present the calculation for the first load distribution.

$$ESAL_j = \frac{1000000}{148^4}\begin{bmatrix} 3(0.3)(20)^4 + 6(0.3)(80)^2(20)^2 + (0.3)(80)^4 + \\ 3(0.7)(47.2)^4 + 6(0.7)(140)^2(47.2)^2 + (0.7)(140)^4 \end{bmatrix} = 1\times10^6 \qquad (48)$$

$$\xi_j = \frac{1}{148^4}\begin{bmatrix} 3(0.3)(20)^4 + 6(0.3)(80)^2(20)^2 + (0.3)(80)^4 + \\ 3(0.7)(47.2)^4 + 6(0.7)(140)^2(47.2)^2 + (0.7)(140)^4 \end{bmatrix} = 1 \qquad (49)$$

It can be seen from Table 6.3 that three ALS considered have different characteristics (means and standard deviations of empty and loaded distributions) but have same number of ESAL (i.e. 1.E+06).

Table 6.3 Characteristics of axle load spectra with similar ESALs

ALS No.	Load Spectra Characteristics							ESALs
	μ_1	μ_2	σ_1	σ_2	P_1	N	Xs	
1	80	140	20	47.2	0.30	1,000,000	148	1.E+06
2	90	150	20	32.1	0.30	1,000,000	148	1.E+06
3	100	158	20	7.7	0.30	1,000,000	148	1.E+06

Figure 6.16 shows the plot of the generated equivalent axle load spectra. It should be noted that these load spectra were generated for a tandem axle configuration.

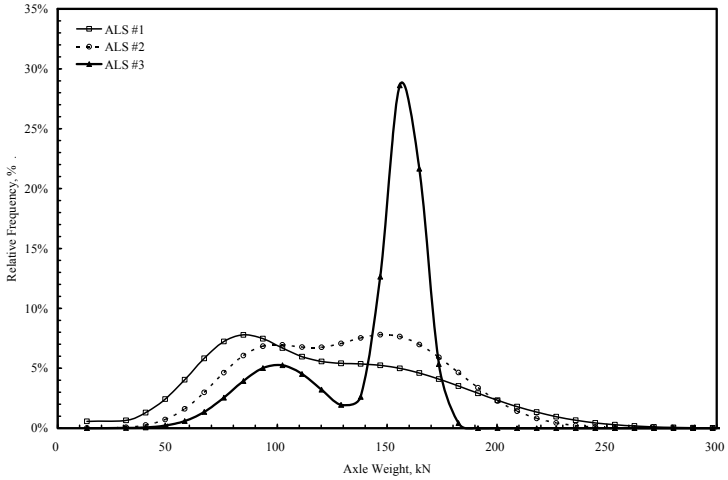

Figure 6.16 Axle load spectra having similar ESALs

Equation (42) also implies that there is another way of generating axle load spectra which have similar ESALs. One can achieve different ESALs by changing the repetitions (*N*).

6.2.3.2 Equivalent ESALs for Different Axle Load Spectra

For different axle load distributions same ESALs can be matched by changing *N*. For example, the number of repetitions can be calculated to match 1 million ESAL for a given loading characteristics. Equation (50) presents a sample calculation.

$$1000000 = \frac{N}{148^4}\left[\begin{array}{l} 3(0.3)(14)^4 + 6(0.3)(60)^2(14)^2 + (0.3)(60)^4 + \\ 3(0.7)(20)^4 + 6(0.7)(120)^2(20)^2 + (0.7)(20)^4 \end{array}\right] \qquad (50)$$

$$N = 2,743,626$$

Table 6.4 shows the loading characteristics and required number of repetitions for three tandem axle load spectra considered in this study. In terms of ADTT, the heavier loading will need less repletion to reach a given ESALs. Thus, ALS #1 will have the highest ADTT and ALS #3 will have the least. Figure 6.17 shows the loading characteristics of these three distributions.

Table 6.4 Characteristics of axle load spectra and number of repetitions to cause similar ESALs

ALS No.	Load Spectra Characteristics							ESALs	Normalized ADTT	ADTT
	μ_1	μ_2	σ_1	σ_2	P_1	N	Xs			
1	60	120	14	20.0	0.30	2,743,626	148	1.E+06	1.0	15,000
2	70	160	15	25.0	0.50	1,225,022	148	1.E+06	2.2	6,818
3	80	170	20	25.0	0.30	707,262	148	1.E+06	3.9	3,846

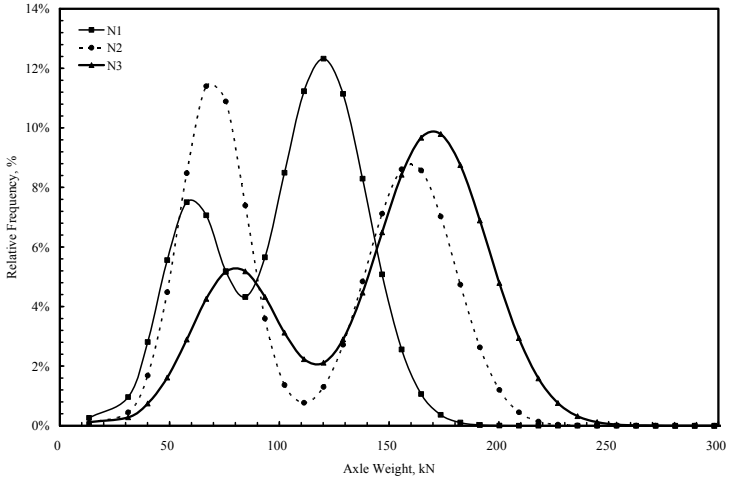

Figure 6.17 Axle load spectra having dissimilar ESALs

Once the load spectra have been defined, the next step is execute M-E PDG by incorporating these specific load spectra to assess their effects on predicted pavement performance.

6.2.4 Performance Prediction using M-E PDG

Traffic is one of the key factors influencing the performance of Jointed Plain Concrete Pavements (JPCP). The new M-E PDG uses each axle load distribution to describe traffic loads while classification and count data are also required to represent load repetitions. The latter data are used to calculate hourly and monthly traffic volumes, vehicle class distributions, and growth factors.

In this study, the effects of loading characteristics and traffic levels in terms of repetition on pavement performance were evaluated using Version 1.0 of the M-E PDG software. Two JPCP pavement cross-sections were assumed in these analyses with 9-inch (thin) and 11-inch (thick) slab thickness over an 8-inch thick crushed gravel base on A-6 subgrade. A fixed joint spacing of 15-ft with doweled joints was assumed. It should be noted that all structural, environmental and materials related inputs were fixed in this analysis and only the effects of traffic loadings (axle load spectra) and traffic levels (repetitions) on JPCP performance were studied. The six tandem axle load distributions were used to investigate pavement performance after 30 years of service life for thin and thick cross-sections. Three performance measures, cracking, faulting, and roughness (IRI), as predicted by M-E PDG were evaluated to investigate their correlations with load distribution properties.

6.2.4.1 Axle Load Spectra with Equivalent ESALs

Three axle load spectra (see Table 6.3) having similar ESALs were used in M-E PDG, Figures 6.18 and 6.19 show the performance predictions for thin and thick pavements, respectively. It can be seen from these figures that all distress types are some what similar with no practical difference between all load distributions except cracking.

The cracking model in M-E PDG includes both top-down and bottom-up cracking; however, either one of them is assumed to happen at one time. In other words, only one type of cracking (top-down or bottom-up) is assumed to happen at one time. Also, the load combination for top-down cracking assumes a steering axle and a tandem axle. The steering axle is assumed to have a fixed load of 12-kip while the tandem axle has a load spectra distribution. Therefore, to further investigate, the accumulated damage only bottom-up cracking information was extracted from M-E PDG output and % slab cracked were calculated separately. Figures 6.20 and 6.21 present the plots of damage and cracking for thin and thick cross-sections, respectively. It can be observed that bottom-up cracking is different for three equivalent load distributions considered. These results suggest that load spectra may have unique effect on cracking performance although they have similar ESALs. However, the difference in cracking between equivalent load spectra is reduced over longer time period.

On the other hand, for all practical purposes, faulting and IRI predictions are similar between different load spectra.

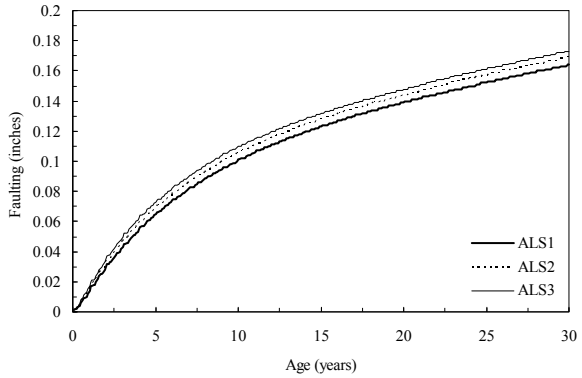

(a) Predicted faulting

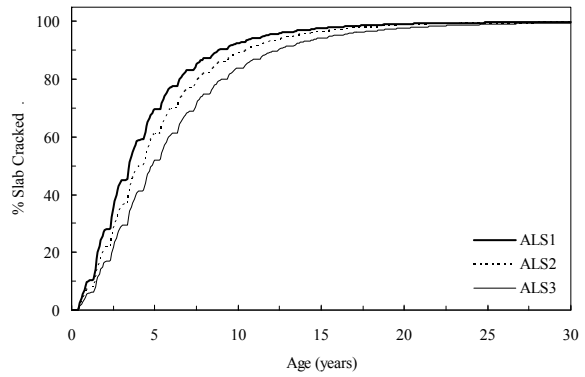

(b) Predicted cracking (top-down + bottom-up)

(c) Predicted IRI

Figure 6.18 Pavement performance —Thin Section

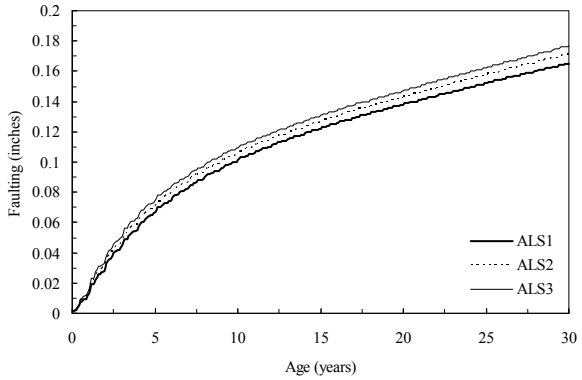

(a) Predicted faulting

(b) Predicted cracking(top-down + bottom-up)

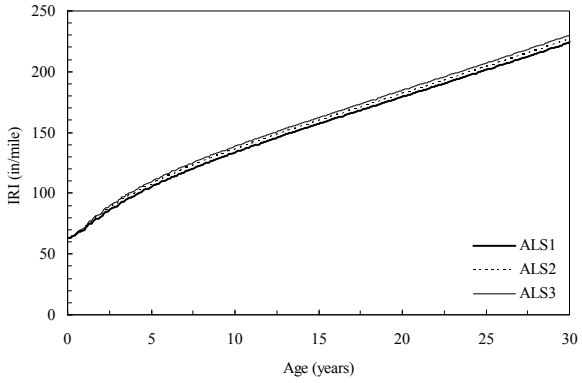

(c) Predicted IRI

Figure 6.19 Pavement performance —Thick Section

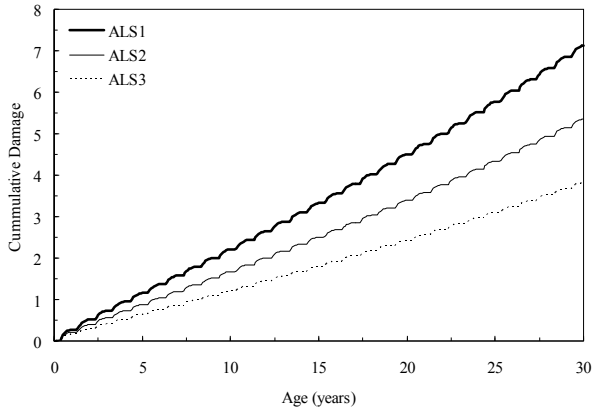

(a) Predicted damage (bottom-up)

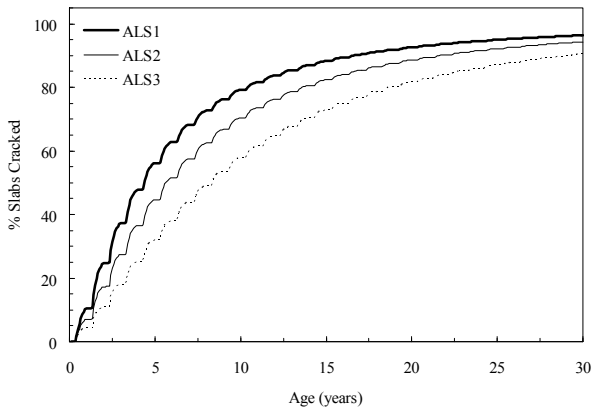

(b) Predicted cracking (bottom-up)

Figure 6.20 Cracking performance —Thin Section

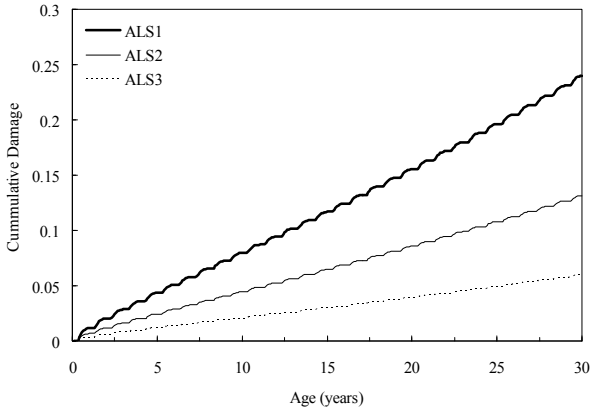

(a) Predicted damage (bottom-up)

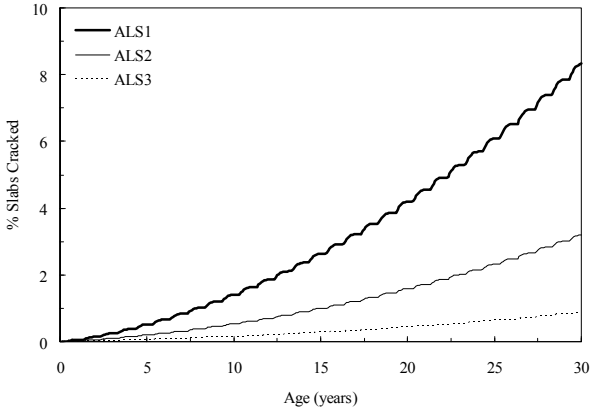

(b) Predicted cracking (bottom-up)

Figure 6.21 Cracking performance —Thick Section

6.2.4.2 Different Axle Load Spectra

The second hypothesis tested in this study was to match ESAL from different axle load spectra by changing number of repetitions. Three load spectra are shown in Table 6.4 with their respective ADTT to achieve the required ESALs. In this analysis, the uniqueness of each load spectra was not considered and ESALs were matched by changing the repetitions. Figures 6.22 and 6.23 show the predicted pavement performance for thin and thick cross-sections, respectively. It can be seen that in this case all the distresses (cracking, faulting, and IRI) are different for each load spectra. Again, the accumulated damage due to bottom-up cracking was used to determine only bottom-up cracking as shown in Figures 6.24 and 6.25. The results show that predicted cracking performance is significantly different between three load spectra.

Load spectra with higher number of repetitions showed higher faulting and IRI development over time for both thin and thick pavements [see Figures 6.22 (a and c) and 6.23 (a and c)].

The trends for cracking reveal that the heaviest load spectra with least number of repetitions caused maximum cracking for thin pavement while the lightest load spectra with the highest number of repetitions caused more cracking in thick pavement [see Figures 6.22 (b) and 6.23 (b)]. In case of bottom-up, more cracking is caused by the heaviest loadings for both thin and thick pavements (see Figures 6.24 and 6.25).

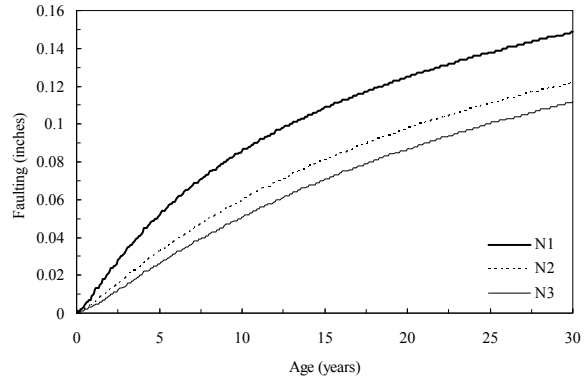

(a) Predicted faulting

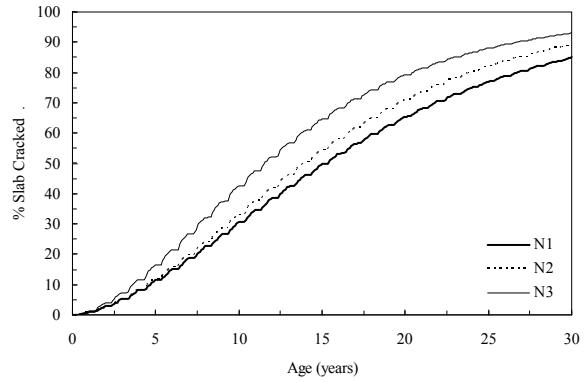

(b) Predicted cracking (top-down + bottom-up)

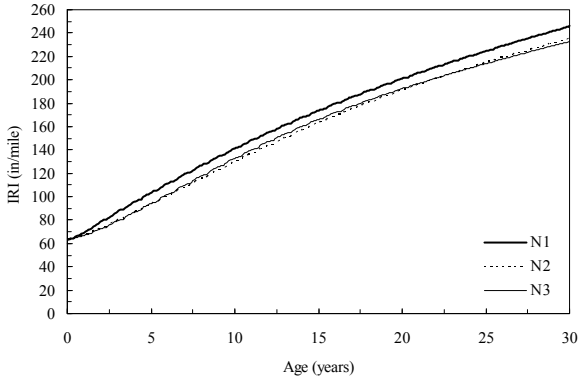

(c) Predicted IRI

Figure 6.22 Pavement performance —Thin Section

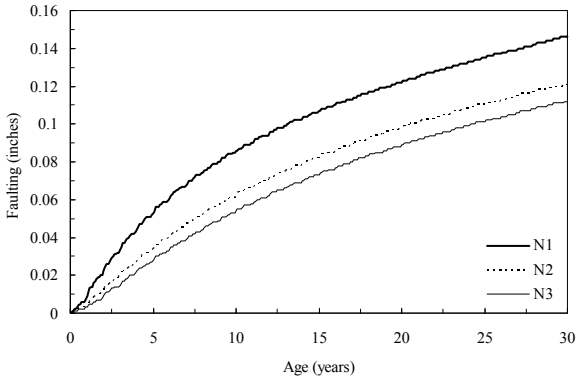

(a) Predicted faulting

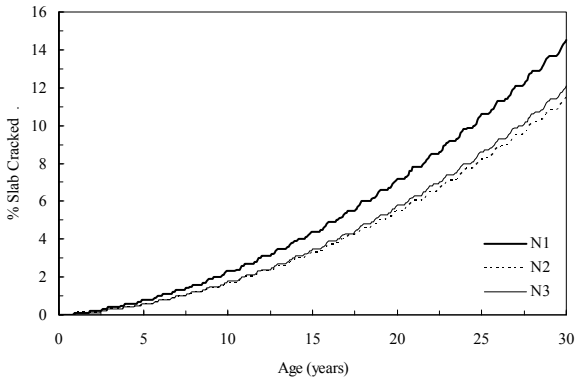

(b) Predicted cracking (top-down + bottom-up)

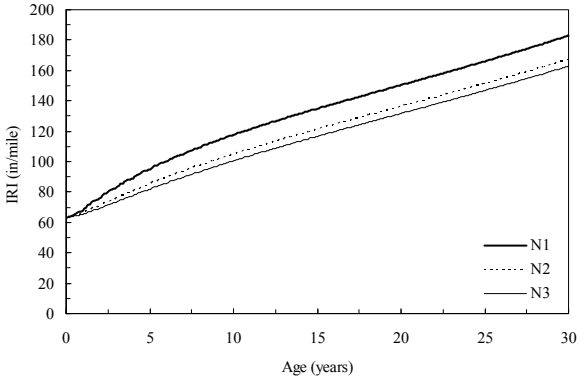

(c) Predicted IRI

Figure 6.23 Pavement performance —Thick Section

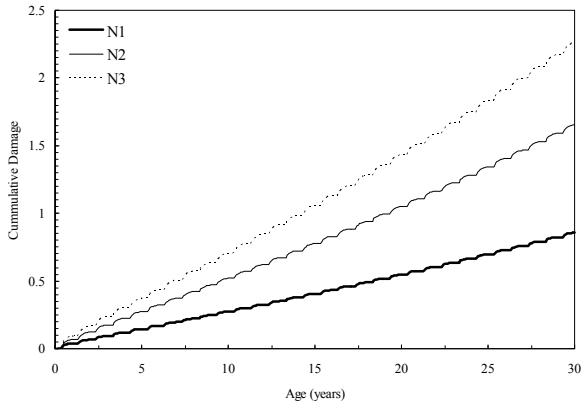

(a) Predicted damage (bottom-up)

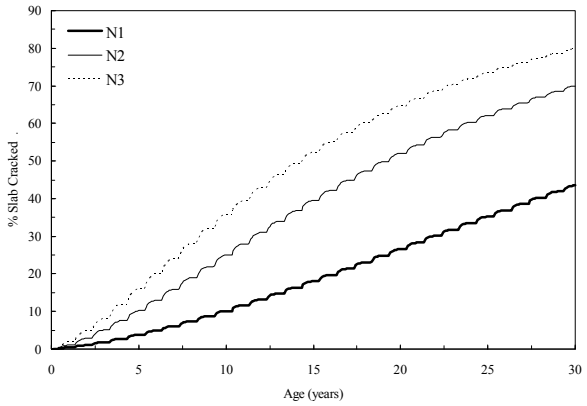

(b) Predicted cracking (bottom-up)

Figure 6.24 Cracking performance —Thin Section

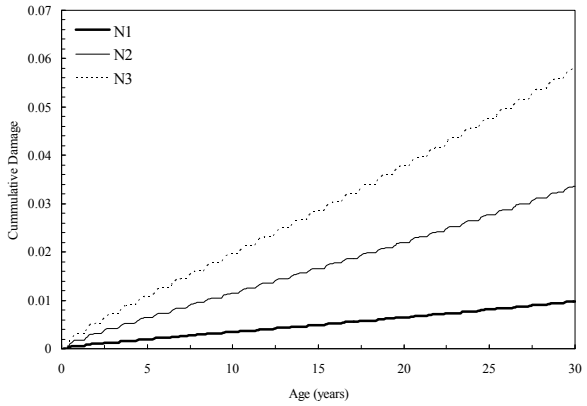

(a) Predicted damage (bottom-up)

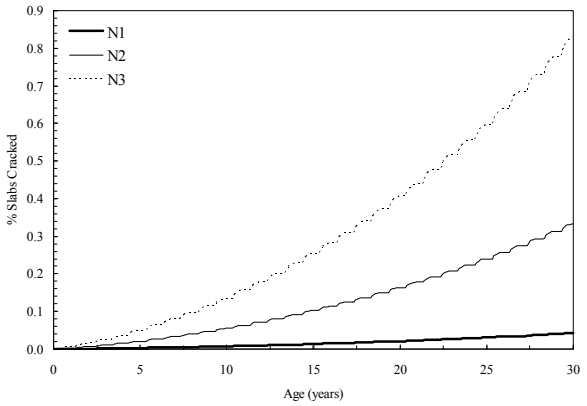

(b) Predicted cracking (bottom-up)

Figure 6.25 Cracking performance —Thick Section

6.2.5 Conclusions

Based on the above preliminary analyses following conclusions can be made:

For pavement analysis and design, influence of traffic loads and repetitions can be characterized by: (a) ESALs, and (b) axle load spectra. The M-E PDG uses the latter; however, the analysis in this new design process can be simplified by using equivalent single axle loads (ESALs) for each axle type. Similarly, a concept of equivalent axle load spectra can be used in mechanistic procedures to achieve similar performance prediction as achieved by using an axle load spectra. The equivalent axle load spectra for each axle configuration can be developed by using site-specific loadings. The number of repetitions (ADTT) can be adjusted to achieve desired level of ESALs during the design life. However, it is important to determine the design ESALs from a site-specific axle load spectra.

On the other hand, assuming axle load spectra which are not site-specific and achieving desired level of ESALs by changing number of repetitions may not give reliable estimates of expected pavement performance as compared to site-specific axle load spectra.

CHAPTER 7 - CONCLUSIONS - RIGID

Based on the analyses performed, several conclusions were made and are summarized in the subsequent sections of this chapter. For reader convenience, the conclusions are summarized in chronological order according to the various tasks in this study.

7.1 SENSITIVITY ANALYSES

The M-E PDG requires detailed information on several input variables. In order to identify the most important variables which significantly affect the performance prediction, sensitivity analyses were performed. The approach used to conduct the sensitivity analysis in this research contains: (1) one variable at a time to investigate the effect of individual input variables on performance (preliminary sensitivity analyses), and (2) full factorial design matrix to investigate the interaction effects of input variables on performance (detailed sensitivity analyses). The first task involves a preliminary analysis for each input variable to eliminate the less significant variables while the second task deals with detailed analyses including interaction between sensitive variables identified by the first task. The results from the above two tasks are presented below.

7.1.1 Preliminary Sensitivity

- Based on the preliminary sensitivity results, a list of 23 sensitive (practically significant) input variables (characterizing environment, traffic, and pavement materials, etc) was established. It should be noted that these variables were identified by the preliminary sensitivity by considering three levels for each variable entirely based on the theoretical results (predicted performance by M-E PDG) and this list does not reflect the state-of-the-practice in Michigan.

- The list contains the following variables:
  - Traffic—AADTT, axle load spectra, monthly adjustment and hourly adjustment factors
  - Design—Slab thickness, joint spacing, edge support, dowel diameter and spacing
  - Material—CTE, MOR, f_c', E, base type, base thickness, passing #200, plasticity index, soil type
  - Environment—Temperature, precipitation and freezing index

- Certain variables can not be determined at the design stage; for example, it is not clear for the design engineer to identify permanent curl/wrap effective temperature difference and surface shortwave absorptivity for a particular site. However, these input variables significantly affect the predicted pavement performance. Consequently, these variables were not considered and their default values in M-E PDG were adopted in further analysis. Perhaps there is a need to quantify these variables by adopting some testing protocols in the future.

7.1.2 Detail Sensitivity

A reduced list of variables, based on engineering judgment MDOT practice, and RAP feedback to decrease the number of runs within an achievable practical limit was prepared. The factorial consists of six variables at two levels and the environment has three levels. The main objectives of the statistical analyses are to: (a) obtain the real main effects with some level of confidence, (b) explore the interactive effects between various input variables, and (c) provide guidance with respect to input selection. It should be noted that in the following sections, the main effects are described first, followed by the interactive effects. Following conclusions can be made based on the results of these analyses:

7.1.2.1 Slab Cracking

Slab thickness: The effect of slab thickness, as expected, is very significant on cracking. Rigid pavements with thin slab thickness showed more cracking than those with thick slabs. Also, this effect is more pronounced over a longer life of a pavement.

Edge support: In general, rigid pavements with asphalt shoulders (untied) showed more cracking than those with tied shoulders. The effect of edge support is not as significant as slab thickness.

Base type: The results of the predicted cracking show that at early age, rigid pavements with permeable asphalt treated base (PATB) performed marginally better than those with dense graded aggregate base (DGAB). However, over the long-term the effect of base type diminishes for cracking.

Coefficient of Thermal Expansion (CTE): The pavements constructed with higher coefficient of thermal expansion (CTE) concrete mixture showed much more cracking than those constructed with a lower CTE value concrete mixture. This effect is very significant and is consistent throughout the life span.
Modulus of Rupture (MOR): Similarly, the effect of modulus of rupture (MOR) on cracking seems to be the most significant. Pavements slabs having a higher MOR exhibited little or no cracking as compared to those with lower MOR, which showed a very high level of cracking.

Subgrade type: The effect of subgrade type on cracking is fairly insignificant.

Climate: Three locations were selected to investigate the effect of climate on pavement performance in Michigan. On average, the local climate variations seem to have only a slight effect on cracking. Rigid pavements located in Pellston exhibited higher amount of cracking than those located in Detroit and Lansing areas. The effect of location seems to be consistent throughout the pavement life. It was observed that higher cracking potential is associated with locations having higher freeze index and number of freeze/thaw cycles.

CTE by slab thickness: For a lower level of CTE, slab thickness has a significant effect on cracking. This effect is of both practical and statistical significant. On the other hand, for higher level of CTE, the slab thickness did not show a very significant difference in cracking. From the

design perspective, the results of this interactive effect imply that if the CTE of concrete is high, then, increasing slab thickness will not help in achieving improved cracking performance.

MOR by slab thickness: The effect of slab thickness on cracking is more prominent for lower MOR than for higher MOR concrete. This means that for cracking, change in thickness is more important for lower MOR values in designing rigid pavements. These effects are of both statistical and practical significance.

CTE by MOR: The interaction between CTE and MOR was found to be the most important for rigid pavements. These effects are of both statistical and practical significance. The combination of higher CTE with lower MOR is significant for cracking. This also means that higher flexural strength of concrete can compensate for a higher CTE value.

7.1.2.2 Joint Faulting

Slab thickness: The effect of slab thickness is very significant on faulting. Rigid pavement with thin slab thickness showed higher faulting than those with thick slabs. Also, the results show that this effect is more pronounced at latter life of a pavement.

Edge support: In general, rigid pavements with asphalt shoulders (untied) showed higher faulting than those with tied shoulders. However, the effect of edge support is not as significant as slab thicknesses.

Base type: Two types of bases were used in this analysis; a dense graded aggregate base (DGAB) and a permeable asphalt treated base (PATB). The base thickness was fixed at 6-inches and 10-inch thick sand subbase (see Chapter 2) was considered in all the runs. The results of the predicted faulting show that at early age, rigid pavements with PATB base performed slightly better than those with DGAB base. However, in long-term (after 30 years) the effect of base type increases for faulting.
CTE: A significant effect of CTE was observed on faulting performance. The pavement slabs with higher CTE showed much higher faulting than those with a lower CTE value. This effect is consistent and increases throughout the life span of a rigid pavement.

MOR: MOR effect on faulting performance of rigid pavement seems to be the least significant. Pavement slabs having a higher MOR exhibited less faulting as compared to those with lower MOR, which showed slightly higher level of faulting. This effect increases over life span of rigid pavements.

Subgrade type: A significant effect was noticed for subgrade type. The pavements constructed on fine subgrade exhibited higher amount of faulting than those constructed on coarse subgrade. The effect of subgrade type is more pronounced in long-term.

Climate: In order to investigate the effects of climate on joint faulting for rigid pavements within Michigan, three locations were selected in this analysis. On average, the climate seems to have a very low effect on faulting. Rigid pavements located in Detroit exhibited higher amount of

faulting than those located in Pellston and Lansing area. The effect of location seems to be consistent with time.

CTE by Slab Thickness: For a higher level of CTE, slab thickness has a significant effect on the faulting. This effect is of both practical and statistical significance. On the other hand, for lower level of CTE, the slab thickness did not show a very significant difference in faulting performance. From the design perspective, the results of this interactive effect imply that if the CTE for a concrete is higher, increasing slab thickness will help in achieving better faulting performance.

MOR by Slab Thickness: The effect of slab thickness on faulting is more prominent for higher MOR than for lower MOR concrete. This means that for faulting, change in thickness is more important for higher MOR values in designing rigid pavements. These effects are of both statistical and practical significance.

Soil Type by CTE: The interaction between soil type and CTE was found to be the most important for rigid pavements. The combination of higher CTE with fine subgrade soil is drastic for faulting. This also means that a lower CTE value of concrete can compensate for pavements constructed on fine grained subgrade soils. These effects are of both statistical and practical significance.

Climate by CTE: The interaction between climate and CTE was both statistically and practically significant. Therefore, it is very important to consider CTE values while designing a pavement in a particular climate even within the state of Michigan. Results show that rigid pavements in Detroit region are more prone to faulting while Lansing and Pellston showed slightly lower levels of predicted faulting. Therefore, for pavement design, a lower CTE value will help in better joint faulting performance. However, It should be noted that pavements with doweled joints and short joint spacing (as is the practice in MI) are less prone to faulting over there design life

7.1.2.3 Roughness (IRI)

Slab thickness: The effect of slab thickness is very significant on pavement roughness. Rigid pavement with thin slabs developed higher roughness than those with thick slabs. Also, the results show that this effect is more pronounced over a longer life of a pavement.

Edge support: In general, rigid pavements with asphalt shoulders (untied) developed higher roughness than those with tied shoulders. However, the effect of edge support is not significant.

Base type: The pavements with PATB base developed slightly less roughness than those with DGAB base. However, the effect of base type is consistent on roughness development.

CTE: A significant effect of CTE was observed for roughness development. The pavements with higher CTE showed much higher roughness than those with a lower CTE value. This effect is consistent and increases throughout the life span of a rigid pavement.

MOR: Similarly, MOR effect on roughness development of rigid pavement seems to be the most significant. Pavements slab having a higher MOR exhibited much less roughness as compared to those with lower MOR, which showed a very high level of roughness. This effect is also consistent over life span of rigid pavements. This effect can be explained from the cracking magnitude as well i.e., the roughness prediction model is a function of slab cracking.

Subgrade type: A significant effect was noticed for subgrade type. The pavements constructed on fine subgrade showed higher roughness than those constructed on coarse subgrade, especially in long-term.

Climate: On average, the climate seems to have a marginal effect on roughness development within Michigan. Rigid pavements located in Pellston exhibited higher amount of roughness than those located in Detroit and Lansing area. The effect of location seems to be consistent with time.

CTE by Slab Thickness: For a lower level of CTE, slab thickness has a significant effect on the roughness. The practical significance of this effect is marginal. On the other hand, for higher level of CTE, the slab thickness did not show a very significant difference in roughness development. This higher value of CTE is masking the effect of slab thickness because pavement with thin and thick slabs exhibited a high roughness. From the design perspective, the results of this interactive effect imply that if the CTE for a concrete is higher, increasing slab thickness will not help in achieving better roughness performance.

Soil Type by CTE: The effect of soil types (site conditions) on roughness is more prominent for lower CTE value than for higher CTE value. This means that for roughness, change in CTE is more important for pavement to be constructed on fine soil types. These effects are of both statistical and of marginal practical significance.

Climate and Soil Types: The interaction between climate (location) and subgrade type (site conditions) was found to be important for rigid pavements. The combination of fine subgrade soils with location like Pellston is drastic for roughness development. This also means that higher slab thicknesses and lower CTE values can compensate for such critical site conditions and weather. These effects are of both statistical and of marginal practical significance.

7.2 SATELLITE SENSITIVITY ANALYSES

Several separate analyses were conducted as satellite studies; these evaluations included (a) studying the effect of CTE, slab thickness and joint spacing on pavement performance, (b) verifying (at very preliminary level) M-E PDG performance prediction for Michigan pavements, and (c) determining the impact of traffic inputs on pavement performance. The results of analyses from these evaluations are presented briefly in the following sections.

7.2.1 Effects of Joint Spacing, CTE and Slab Thickness on Pavement Performance

The results are presented by each performance measure separately.

7.2.1.1 Slab Cracking

Joint spacing: The joint spacing of rigid pavement slab has a significant effect on the cracking performance. Concrete pavements having a higher joint spacing have exhibited more cracking as compared to those having lower joint spacing. This effect is also of practical significance.

Slab thickness: Rigid pavements with thicker PCC slabs out perform those with thinner PCC slab thickness. The effect of slab thickness on cracking is of practical significance.

CTE: Concrete pavements having a higher CTE value has shown higher amount of cracking than those which have a lower CTE value. This effect is also of practical significance.

Joint spacing by slab thickness: For a lower level of slab thickness, joint spacing has a significant effect on the cracking. This effect is of both practical and statistical significance. On the other hand, for higher level of slab thickness, the joint spacing did not show a very significant difference in cracking performance, especially for thick slabs (12- and 14-inch). This is because thinner slabs are prone to cracking irrespective of joint spacing at the later ages. Joint spacing has a very significant effect for thinner slabs at early ages. From the design perspective, the results of this interactive effect imply that if the joint spacing for a concrete slab is larger, increasing slab thickness will only help in achieving improved cracking performance to a certain extent.

7.2.1.2 Joint Faulting

Joint spacing: Rigid pavements with higher joint spacing show significant higher faulting at joints than those with lower joint spacing. This effect is consistent over the life span of the pavements. However, the effects seems is of practical significance between 20 to 30 years of service life.

Slab thickness: Rigid pavements with thicker PCC slabs out performed those with thinner PCC slab thickness. The effect of slab thickness on faulting is more or less practical significant if higher dowel diameter is used for thicker slabs.

CTE: Concrete pavements having a higher CTE value has shown higher amount of faulting than those which have a lower CTE value. This effect is also of practical significance.

Joint Spacing by Slab Thickness: The effect of slab thickness on faulting is more prominent for higher joint spacing. This means that for faulting, change in thickness is more important for longer joint spacing in designing rigid pavements. These effects are of both statistical and practical significance at older age.

CTE by Slab Thickness: For a higher level of CTE, slab thickness has a significant effect on the faulting. This effect is of both practical and statistical significance. On the other hand, for lower level of CTE, the slab thickness did not show a very significant difference in faulting performance. From the design perspective, the results of this interactive effect imply that if the

CTE for a concrete is higher, increasing slab thickness will help in achieving better faulting performance.

7.2.1.3 Roughness (IRI)

CTE: Concrete pavements having a higher CTE value has shown higher amount of roughness than those which have a lower CTE value. This effect is marginal with regards to practical significance.

No statistical significant interaction was found between the input variables for roughness development.

7.2.2 Preliminary Verification of M-E PDG Performance Prediction for Michigan

The main objectives of this task were to (a) verify the M-E PDG performance predictions in Michigan, and (b) identify the suitability needs for calibration of M-E PDG performance models in Michigan. To accomplish these objectives, the rigid pavement sections in Michigan (SPS-2 and MDOT) were analyzed using M-E PDG software (version 1.0).

- For the SPS-2 sections located in Michigan, most of the observed distresses in several sections match reasonably with the M-E PDG predictions. One of the reasons for these better matches is that the performance models in the M-E PDG were calibrated using the LTPP data. However, the predicted performance is different from observed distresses for some of these sections. The plausible causes of such discrepancies could be construction-related issues or the lack of traffic data history which may not be explained by the mechanistic-empirical design procedures.
- For MDOT sites, the observed distresses in several sections do not match reasonably with the M-E PDG predictions. The probable reasons for these poor matches include the; (a) error in national calibrated M-E PDG performance models, (b) error in distress measurement, and (c) construction-related issues.

7.2.3 Effect of Traffic on Pavement Performance

In order to determine the effects of traffic levels on various rigid pavement performance measures, the M-E PDG software was used to analyze selected Michigan sites (observed traffic characteristics). All other variables were kept constant in this analysis except traffic. Therefore, the effects on performance are mainly due to traffic-related inputs. The results showed:

- Traffic levels (low, medium and high) significantly affect the rigid pavement performance.
- Also within a traffic level, due to variations in truck volumes and loadings, the predicted performance can vary considerably. This implies that the default traffic values (respective truck traffic classification, TTC) in M-E PDG may not be representative of the actual traffic of a particular site. Therefore, traffic data plays a key role in the new design process using M-E PDG.

7.3 PAVEMENT DESIGN IMPLICATIONS

7.3.1 Quantification of Significant Variables Effects on Pavement Performance

Since performance prediction process in M-E PDG is very complex due to a large number of variables. The simplified M-E PDG regression models involving only a few critical design variables were developed. Four important design and material-related variables (slab thickness, joint spacing, flexural strength, and coefficient of thermal expansion) affecting rigid pavement performance in the M-E PDG design process were selected in the regression model development. While these models are limited in scope, they can facilitate in the preliminary design process especially with regards to economic decisions for selecting appropriate materials and slab thickness. The simplified models can also help in quantifying the effects of several significant design variables on pavement performance.

7.3.2 Effects of Traffic Characterization on Pavement Performance

The use of two types of load characterizations (equivalent axle load versus axle load spectra) in mechanistic analysis and design procedures were evaluated. The results showed that:

- The concept of equivalent axle load spectra can be used in mechanistic procedures to achieve similar performance prediction as achieved by using an axle load spectra. The equivalent axle load spectra for each axle configuration can be developed by using site-specific loadings. The number of repetitions (ADTT) can be adjusted to achieve expected level of ESALs during the design life. However, it is important to determine the design ESALs from a site-specific axle load spectra.
- On the other hand, assuming axle load spectra which are not site-specific and achieving expected level of ESALs by changing number of repetitions may not give reliable estimates of expected pavement performance as compared to site-specific axle load spectra.

CHAPTER 8 - PRELIMINARY SENSITIVITY ANALYSIS-FLEXIBLE

8.1 INTRODUCTION

Unlike the AASHTO 1993 Design Guide, which requires very limited data information for design of flexible pavements, to analyze and design a pavement using the new M-E PDG, a large number of design inputs related to layer materials, environment, traffic, etc. need to be considered. It is important that a designer has sufficient knowledge of how a particular input parameter will affect the output or pavement distress. Also, the extent to which different input variables would affect performance would differ. The user therefore, should also know the relative sensitivity of predicted pavement performance to different input variables.

Ideally all the input variables should be studied together to determine their effects on predicted pavement performance as well interaction of effects of different variables. Such sensitivity would require either a full factorial set of experiments using experiment design methods or at least a partial factorial analysis. However, since the number of input variables is so large, especially in the case of flexible pavements such exhaustive analysis would be practically impossible. Therefore, as the first step, one-to-one sensitivity analysis was performed. In this analysis the value of one variable was varied at a time to determine if that input variable has significant impact on predicted performance. As a result, a smaller number of input variables were chosen from the full set of input variables for carrying out detailed sensitivity analysis. This chapter presents the details and results from the preliminary one-to-one sensitivity analysis.

In the beginning of this project the research team was working with the then available version of the M-E PDG software (version 0.90). In October 2006, an updated version 0.91 of M-E PDG was released. This version was used to complete the following tasks with respect to flexible pavement analysis.

(a) Preparation of Initial Sensitivity Test Matrix
(b) Input Variable Ranges for Robustness
(c) Identification of Variables Significant for Pavement Performance

8.2 PREPARATION OF INITIAL SENSITIVITY MATRIX

To conduct the robustness and sensitivity analyses of the input variables, it is essential to determine practical variations of these variables. The primary sources for the magnitudes of input parameters are the following Long Term Pavement Performance (LTPP) experiments: GPS-1, GPS-2, GPS-6, GPS-7, SPS-1 and SPS-9. These experiments are located throughout the US.

Data were collected from the above-mentioned sources and plotted to determine the nature of distribution and statistical characteristics. All the projects from above-mentioned experiments which had relevant data were used. The number of projects for different input variables ranged from 50 to a few thousands. If fewer than 50 data points were available default values for the M-

E PDG software were used. Appendix B-2 shows some sample plots showing distribution of data collected. The general procedure for selection of parameter values for the sensitivity analysis was outlined in chapter 3 of this report. In principle the same procedure was to be used for analysis of rigid as well as flexible pavements. However because of differences in the nature of input variables between rigid pavements and flexible pavements, the procedures used for the two pavement types are slightly different in terms of the details. The following approaches were used to choose the range for analysis.

(1) For rigid pavement analysis, in those cases where data did not follow normal distribution, 25^{th} and 75^{th} percentiles were used. In the case of flexible pavements it was found that the majority of input variables did not follow a normal distribution. It was also observed that in the case of non-normally distributed data 5^{th} and 95^{th} percentile values provided a better range for analysis. Therefore, these values were chosen for the analysis. Mean values for input variable distributions were used as an input for the base case.
(2) If the data was normally distributed the plan was to use mean and ($\mu \pm 2\sigma$) values as mid and extreme values for the analysis. However, to be consistent with the approach mentioned above, 5^{th} and 95^{th} percentile values were selected in these cases also.
(3) In some cases, like air voids, it was found that the data available in LTPP database was in error. In those cases data used for calibration of MEPDG models were used. The criteria applied were similar to those outlined in (1) and (2) above.
(4) In those cases where very little data was available engineering judgment was used to select either the extreme values available or data close to the extreme values.
(5) In the remaining cases extreme values for the software range were selected. However, engineering judgment was used in these cases to avoid improbable values. It was observed that in some cases the software does allow improbable values to be input.

Table 8.1 shows the ranges for each input variables for flexible pavements used in the preliminary sensitivity analysis.

Some parameters required a special procedure for selection. Some of these cases follow:

(1) Dynamic modulus of asphalt concrete is expected to be a very important input for design and analysis purposes. However, dynamic modulus is measured at five different temperatures and at four different frequencies for each temperature. Therefore, the simple approach of finding 5^{th} and 95^{th} percentile would not be possible. The following procedure was followed instead:
    a. Pick E* values for lowest temperature and lowest frequency
    b. Identify mixtures corresponding to 5th and 95th percentile
    c. Check if they have similar position for the same temperature and highest frequency
    d. Repeat a. to c. for the highest temperature and check the selected mixtures
    e. Iterate as required to find a more representative mixture
(2) Creep Compliance is also a very important input for the thermal cracking model in the MEPDG software. However, creep compliance is generally measured at three different temperatures (-20, -10 and 0 ^{o}C) and values corresponding to seven different instances in time (1, 2, 5, 10, 20, 50 and 100 sec) during each test are required by the thermal

cracking model. However it was observed that LTPP database does not provide data for all the three temperatures. Only the mid temperature of -10 ^{o}C matched between what is required and what is available. Therefore, it was decided that for creep compliance, Level 2 analysis would be performed. To choose those mixes which would represent 5th, 50th and 95th percentiles creep compliance at 100 sec was considered. This is a reasonable assumption because for each temperature creep compliance verses time gives a smooth curve. Therefore, it is expected that the curve corresponding to different mixtures would largely follow the ranking as their corresponding values at 100 sec.

(3) In the case of aggregate gradation for asphalt mix, base/subbase and subgrade, the amount of material retained on each sieve is a separate input in the software. However, it was deemed practical that three different gradations are identified for the three levels rather than three levels for each sieve size. It is understood that this would lead to some amount of subjectivity because even slight change in some gradation proportions, like percent fines, can lead to appreciable difference in the overall performance of that mix, soil or aggregate. However such issues are addressed through satellite studies.

(4) The standard definition of "effective binder content (V_{be})" is based on weight. LTPP data base also documents effective binder content based on weight. However, MEPDG uses the definition by volume. Effective binder content by volume can be calculated if the following values are known for the mixes

a. Binder content by wt. (P_b)
b. Specific gravity of the binder (G_b)
c. Bulk specific gravity of the mix (G_{mb})
d. Maximum theoretical specific gravity of the mix (G_{mm})
e. Combined bulk specific gravity of the aggregate (G_{sc})

LTPP database has data corresponding to all these parameters in different modules. However, for the calculation all five parameter values are required for each mix. The intersection set amongst the five models in LTPP database based on mix turned out to be extremely small. Therefore the following empirical relationship was used to estimate the effective binder content.

$$V_{be} = 2 * P_b$$

This relationship has been reported in Appendix EE-1 of the MEPDG documentation.

Table 8.1. M-E Pavement Design Guide Input Variables— Structure Data for Flexible Pavements

Inputs		Data	25th Percentile	75th Percentile	Low 5th Percentile	Mid 50th Percentile	High 95th Percentile
Surface Properties		Surface Shortwave absortivity	-	-	0.8	0.85	0.98
Layers - Asphalt Material Properties	General	Asphalt material type	-	-	AC	AC	AC
		Layer thickness (in.)	4	7.9	2	6	12
	Asphalt Mix	Modulus of asphalt material at different temperatures and different frequencies - Level 1 (site)	Freq. = 0.1 Hz	Temp. = 0 F	663500	2460000	3255000
			1	0	984000	2810000	3605000
			10	0	1375000	3295000	3700000
			25	0	1670000	3375000	3615000
			0.1	40	392500	1016000	1163500
			1	40	683500	1515000	1940000
			10	40	1050000	2140000	2435000
			25	40	1250000	2595000	2540000
			0.1	70	82050	196500	387500
			1	70	149000	386000	734500
			10	70	296500	745500	1255000
			25	70	394500	926500	1450000
			0.1	100	48800	100150	82000
			1	100	61900	158500	156500
			10	100	99850	315000	368500
			25	100	128000	414000	499000
			0.1	130	24400	34200	44400
			1	130	28350	48350	78300
			10	130	40300	82200	180000
			25	130	41550	108500	247500
		Cumulative percent retained 3/4-in. sieve - Level 2 (regional) and Level 3 (default)	-	-	0	11.62	30
		Cumulative percent retained 3/8-in. sieve - Level 2 (regional) and Level 3 (default)	-	-	1.16	35.3	47
		Cumulative percent retained #4 sieve - Level 2 (regional) and Level 3 (default)	-	-	27.65	52.64	52.8
		Percent passing #200 sieve - Level 2 (regional) and Level 3 (default)	-	-	11.12	7.28	8.38

Table 8.1. M-E Pavement Design Guide Input Variables— Structure Data for Flexible Pavements

Inputs	Data		25th Percentile	75th Percentile	Low 5th Percentile	Mid 50th Percentile	High 95th Percentile
Layers - Asphalt Material Properties	Asphalt Binder	Superpave PG Grade	-	-	PG 46-34	PG 58-22	PG 76-16
		Superpave Dynamic Shear Modulus (G*) (Pa)	-	Temp = 58C	3800	7700	15500
			-	Temp = 64C	2100	3400	6900
			-	Temp = 70C	1500	1600	3200
		Superpave Dynamic Shear Delta (Degrees)	-	Temp = 58C	77.8	81.2	85.1
				Temp = 64C	78.3	83.4	86.3
				Temp = 70C	77.9	85.9	88.2
		Softening Point (F)	113.75	118.25	110	115	122
		Absolute Viscosity (Poise)	2226	4777	1120	3991	7897
		Kinematic Viscosity (Centistokes)	327.4	592	230.04	430	889.6
		Specific Gravity	1.01	1.03	0.99875	1.022	1.037
		Viscosity Grade	-	-	AC-2.5	AC - 20	AC-40
	Asphalt General	Reference temperature	N/A	N/A	N/A	N/A	N/A
		Effective binder content (%)	9	10.4	7.4	10	13.2
		Air voids (%)	7.0	10.0	4.7	8.3	11.4
		Total unit weight (pcf)	141.8	148.9	135.1	145.4	155.4
		Poisson's ratio	0.29	45	0.20	0.35	0.50
		Thermal conductivity (BTU/hr-ft-oF) ***[Software Range: 0.5 to 1]***	-	-	0.5	0.75	1.0
		Heat capacity (BTU/lb-F) ***[Software Range: 0.1 to 0.5]***	-	-	0.1	0.3	0.5
Layers - Unbound Layer Base/Subbase	General	Unbound Material			A-2-6	A-1-b	Crushed Stone
		Thickness (in.)	-	-	4	10	16
	Strength Properties	Poisson's Ratio	-	-	0.25	0.35	0.40
		Coefficient of lateral pressure, Ko ***[Software Range: 0.2 to 3]***	-	-	0.2	0.5	1.0
		Level 2 (Seasonal or Representative Input) - Modulus (psi) ***[Software Range:18000 to 40000]***			18000	29000	40000
		Level 3 (Representative Input only) - Modulus (psi) ***[Software Range:18000 to 40000]***			18000	29000	40000

Table 8.1. M-E Pavement Design Guide Input Variables— Structure Data for Flexible Pavements

Inputs	Data		25th Percentile	75th Percentile	Low 5th Percentile	Mid 50th Percentile	High 95th Percentile
Layers - Unbound Layer Base/Subbase		Plasticity Index			1	6	15
		Liquid Limit			1	14	32
		Compacted (Yes/No)			No	Yes	
		Passing #200 sieve (%)			27.4	13.4	8.7
Layers - Unbound Layer Base/Subbase	ICM	Passing #80 sieve (%)			32	20.8	12.9
		Passing #40 sieve (%)			37.1	37.6	20
		Passing #10 sieve (%)			47.6	64	33.8
		Passing #4 sieve (%)			55.4	74.2	44.7
		Passing 3/8" sieve (%)			72.4	82.3	57.2
		Passing 1/2" sieve (%)			78.1	85.8	63.1
		Passing 3/4" sieve (%)			85.3	90.8	72.7
		Passing 1 1/2" sieve (%)			94.6	96.7	85.8
		Passing 2" sieve (%)			97	98.4	91.6
		Passing 3 1/2" sieve (%)			100	99.4	97.6
		Maximum Dry Unit Wt. (pcf)				120	
		Specific Gravity, Gs				2.7	
		Sat. Hydraulic Conductivity (ft/hr0				0.0023	
		Optimum Gravimetric Water Content (%)				9.1	
		af				5.821	
		bf				0.4621	
		cf				3.85	
		hr				126.8	
Layers - Unbound Layer Subgrade	General	Unbound Material			A-7-6 MR = 8000	A-5 MR = 15500	A-1-a MR = 40000
	Strength Properties	Poisson's Ratio ***[Software Range: 0.1 to 0.4]***	-	-	0.25	0.35	0.40
		Coefficient of lateral pressure, Ko ***[Software Range: 0.2 to 3]***			0.2	0.5	1.0
		Level 2 (Seasonal or Representative Input) - Modulus (psi)			3500	15500	29000
		Level 3 (Representative Input only) - Modulus (psi)			3500	15500	29000

Table 8.1. M-E Pavement Design Guide Input Variables— Structure Data for Flexible Pavements

Inputs	Data		25th Percentile	75th Percentile	Low 5th Percentile	Mid 50th Percentile	High 95th Percentile
Layers - Unbound Layer Subgrade	ICM	Plasticity Index			1	5	29
		Liquid Limit			6	28	51
		Compacted (Yes/No)			yes	No	
		Passing #200 sieve (%)			79.2	60.6	8.7
		Passing #80 sieve (%)			84.9	73.9	12.9
		Passing #40 sieve (%)			88.8	82.7	20
		Passing #10 sieve (%)			93.0	89.9	33.8
		Passing #4 sieve (%)			94.9	93.0	44.7
		Passing 3/8" sieve (%)			96.9	95.6	57.2
		Passing 1/2" sieve (%)			97.5	96.7	63.1
		Passing 3/4" sieve (%)			98.3	98.0	72.7
		Passing 1 1/2" sieve (%)			99.3	99.4	85.8
		Passing 2" sieve (%)			99.6	99.6	91.6
		Passing 3 1/2" sieve (%)			99.9	99.8	97.6
		Maximum Dry Unit Wt. (pcf)				91.3	
		Specific Gravity, Gs				2.77	
		Sat. Hydraulic Conductivity (ft/hr0				4.9e-8	
		Optimum Gravimetric Water Content (%)				28.8	
		af				750	
		bf				0.911	
		cf				0.772	
		hr				4.75	

Table 8.1. M-E Pavement Design Guide Input Variables— Structure Data for Flexible Pavements

Inputs	Data		25th Percentile	75th Percentile	Low 5th Percentile	Mid 50th Percentile	High 95th Percentile
Thermal Cracking	Average tensile strength at 14 oF (psi)				200	413.44	1000
	Creep test duration (sec)				100	100	100
	Creep Compliance (1/GPa) at 14 oF (Level 2)	Time= 1 s			2.34E-07	3.72E-07	6.14E-07
		2 s			2.55E-07	4.14E-07	7.17E-07
		5 s			2.83E-07	4.76E-07	8.83E-07
		10 s			3.17E-07	5.31E-07	1.03E-06
		20 s			3.45E-07	5.93E-07	1.24E-06
		50 s			4.07E-07	7.31E-07	1.62E-06
		100 s			4.83E-07	8.76E-07	2.08E-06
	VMA (%)				N/A	N/A	N/A
	Aggregate coefficient of thermal contraction				1e-7	5e-6	1e-4
	Mix coefficient of thermal contraction				2.2	2.8	3.4

8.3 INPUT VARIABLE RANGES FOR ROBUSTNESS

In this subtask, the MEPDG software was run to develop the performance curves for the different distress measures. Three cases were designed for each variable mentioned in Table 8.1. The base case corresponds to the case where mid values for all the input variables were used. For different levels of analysis, as provided for in the software, different base cases were defined. Appendix B-1 gives the summary of all the inputs for the base case using level 3. Performance curves were obtained for three cases corresponding to low, medium (base case) and high value. For each case, only one variable was varied at a time. First, the lower value for that variable was used while keeping all the other variables constant. Then the upper value for that same variable was used while still keeping all the other variables constant at mid values. This was repeated for each variable. The expected advantage of this strategy is that since only one variable is being changed at a time three cases corresponding to lower, mid and higher values can be compared to determine significance of that variable while avoiding the effect of other variables. However, it should be noted that this benefit may not be realized fully because several inputs are closely interdependent. This is discussed in detail in later sections.

The results corresponding to the three values (low, medium, high) for each variable were plotted on the same graph to determine their effects on various performance measures. Fatigue cracking, transverse cracking, rutting and IRI were selected as the performance measures. Figure 8.1 through Figure 8.8 show examples of plots comparing effect of input variables on the selected four pavement performance measures.

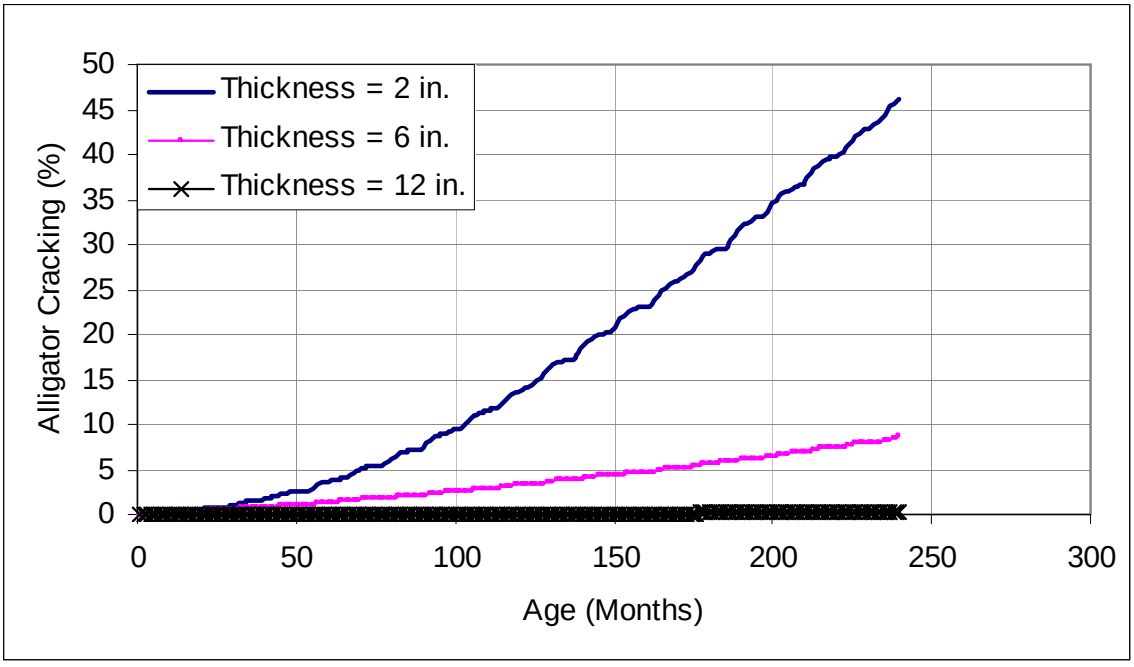

Figure 8.1. Effect of AC thickness on alligator cracking

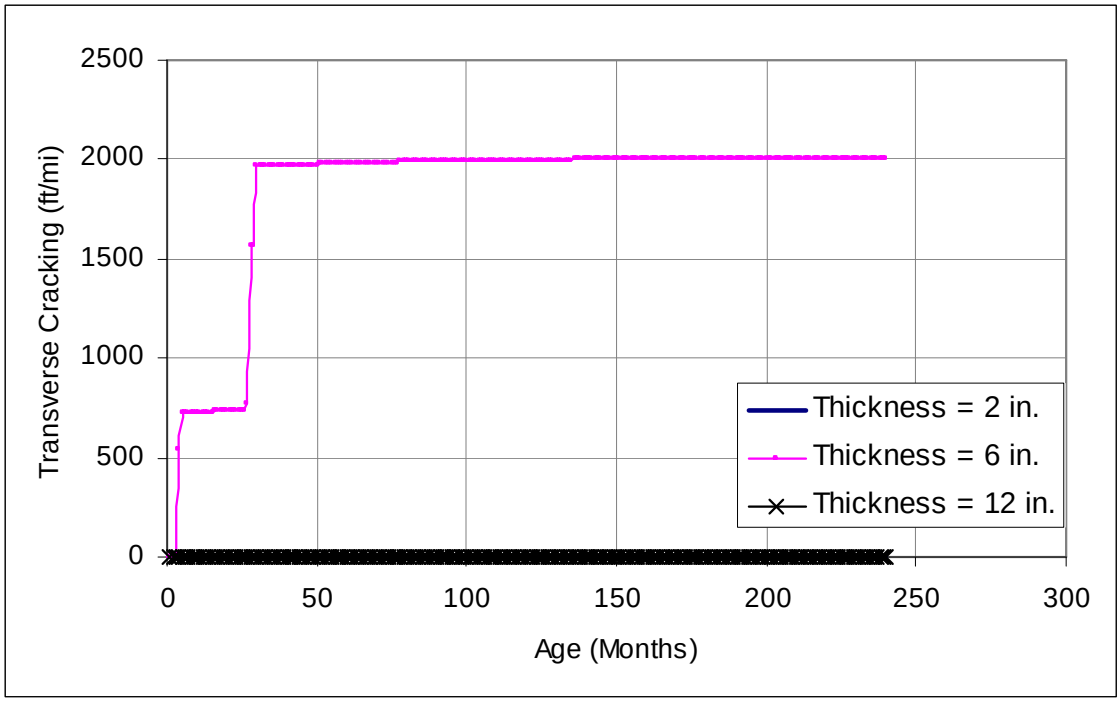

Figure 8.2. Effect of AC thickness on transverse cracking

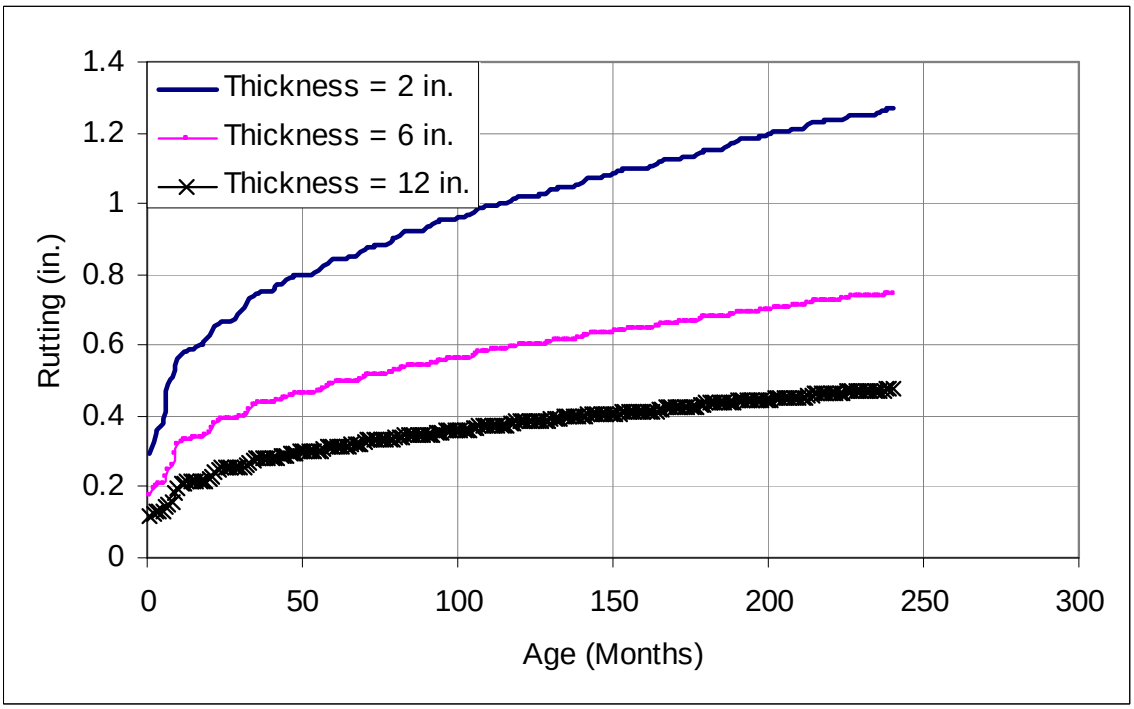

Figure 8.3. Effect of AC thickness on rutting

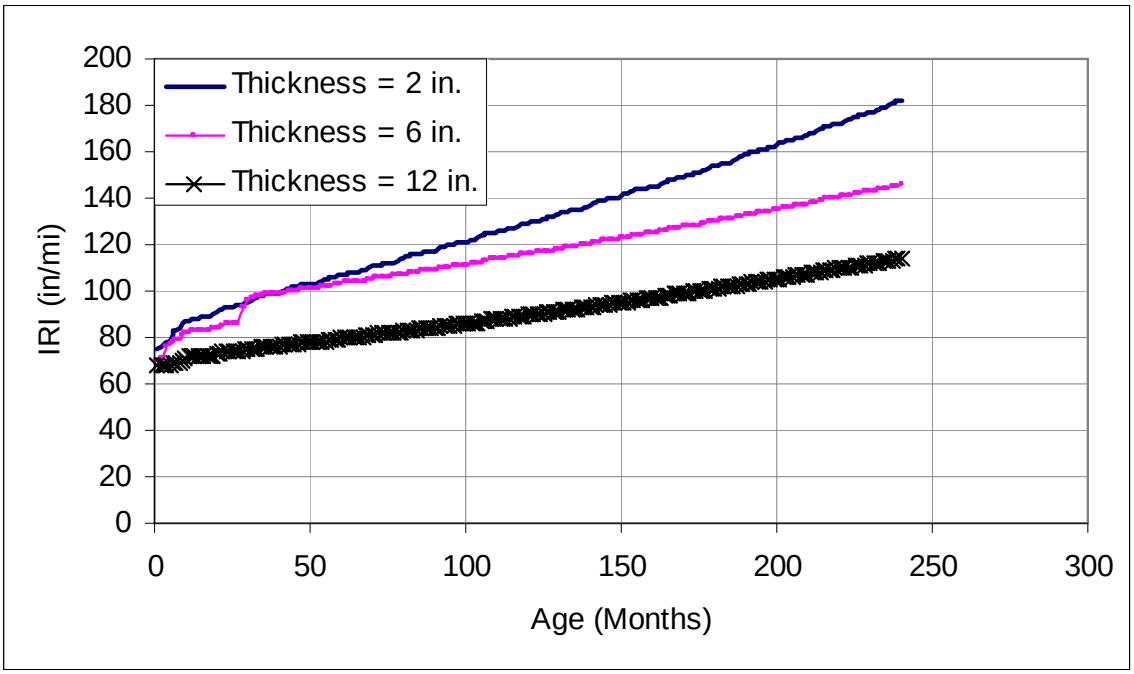

Figure 8.4. Effect of AC thickness on IRI

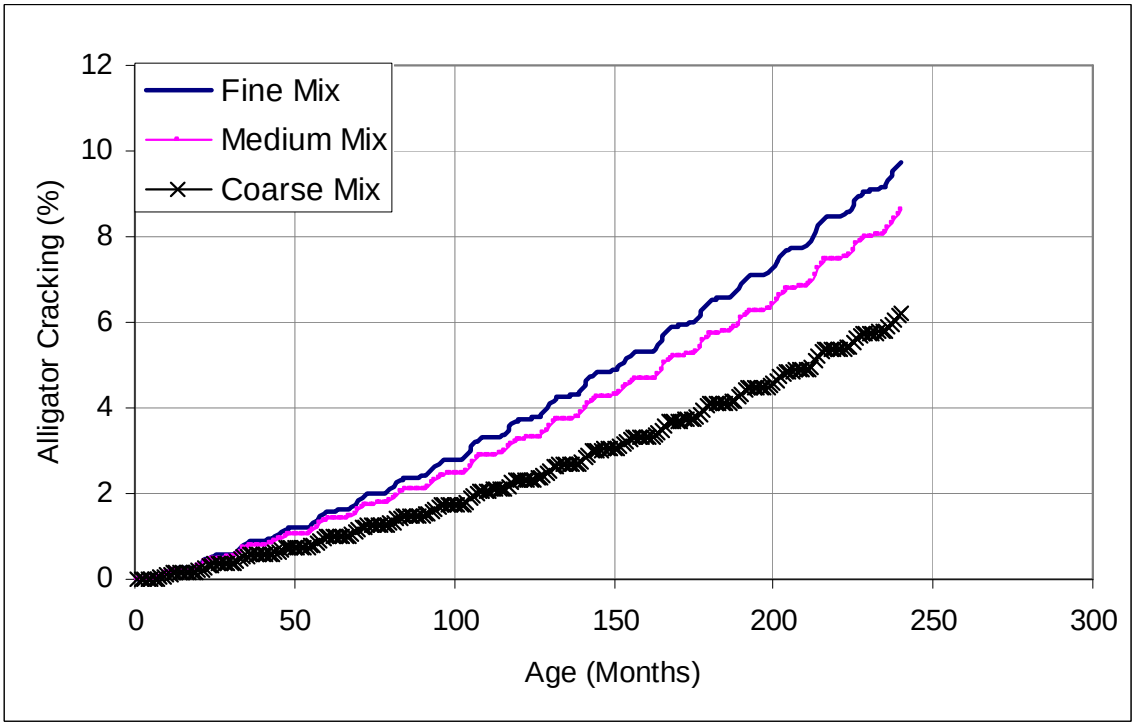

Figure 8.5. Effect of mix gradation on alligator cracking

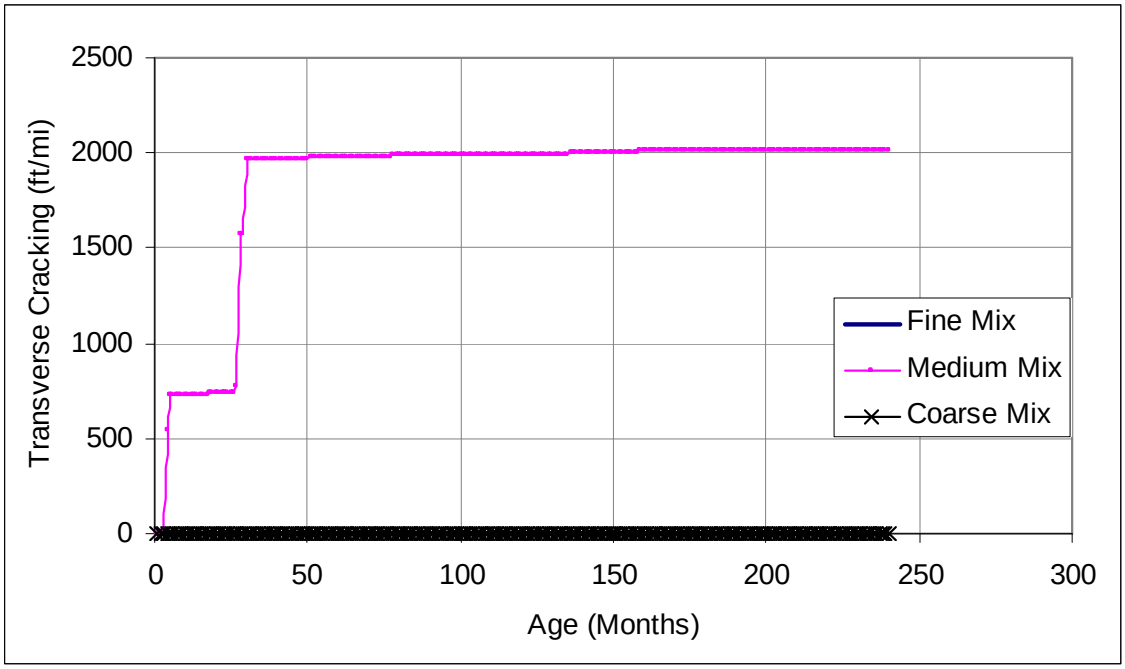

Figure 8.6. Effect of mix gradation on transverse cracking

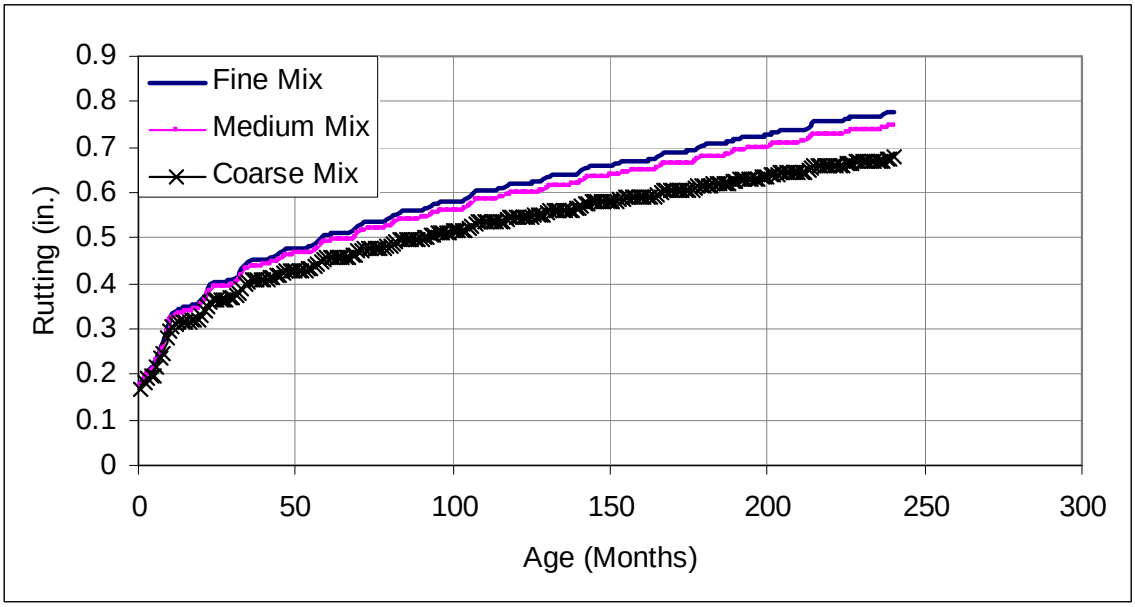

Figure 8.7. Effect of mix gradation on rutting

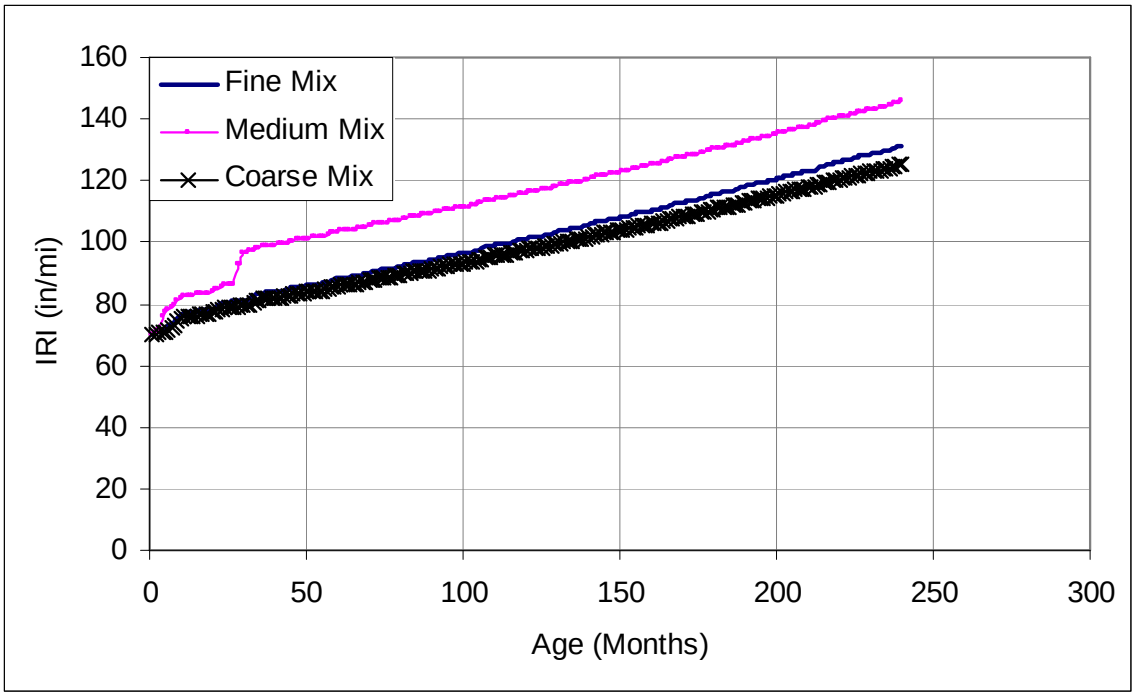

Figure 8.8. Effect of mix gradation on IRI

8.4 IDENTIFICATION OF VARIABLES SIGNIFICANT FOR PAVEMENT PERFORMANCE

The results from the robustness analysis were used to identify the variables significant for pavement performance. Visual inspection combined with FHWA criteria and engineering judgment was employed to identify the sensitive variables. Figure 8.9 through Figure 8.11 show the FHWA criteria (Reference: Common Characteristics of Good and Poorly Performing AC Pavements—FHWA-RD-99-193). Table 8.2 shows the summary of results of this preliminary sensitivity analysis.

Input variables which had significant effect on pavement performance were selected. These variables are listed in Table 8.3. It should also be noted that, as evident from Figure 8.2 and Figure 8.6, transverse cracking is appreciably high when using the medium (base) values while it is zero for low and high values. This seems to be an anomaly rather than an expected result. This apparent discrepancy was reported to the MEPDG development team. Since IRI is directly related to transverse cracking IRI also shows a sudden jump in the base case. In this report this behavior has been overlooked in identifying significant variables.

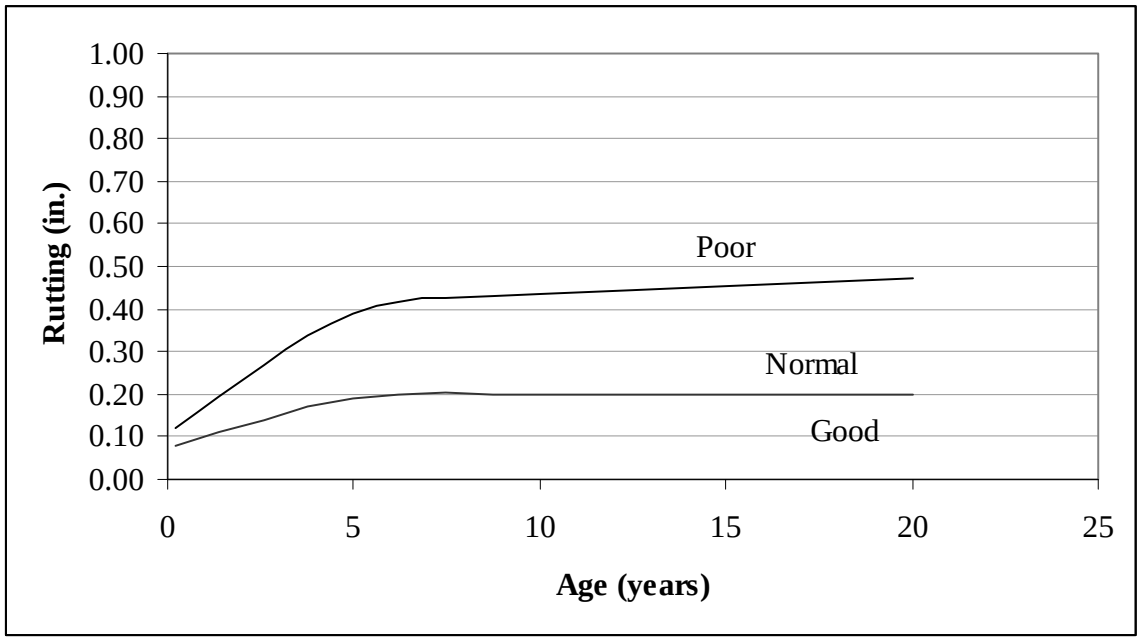

Figure 8.9. Performance criteria for Rutting

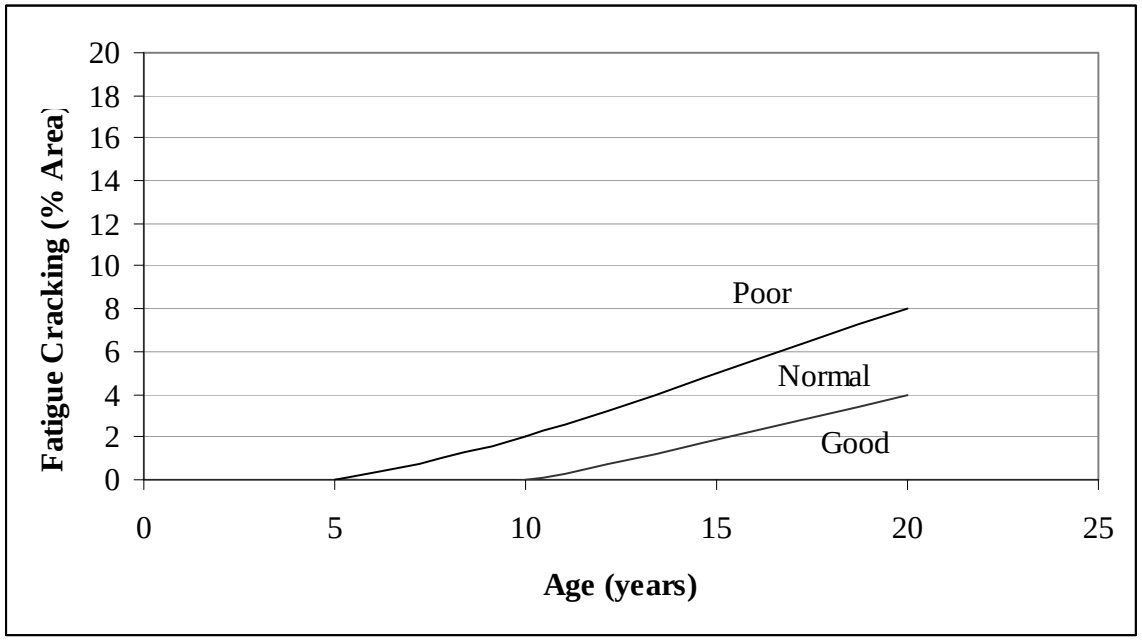

Figure 8.10. Performance criteria for Fatigue Cracking

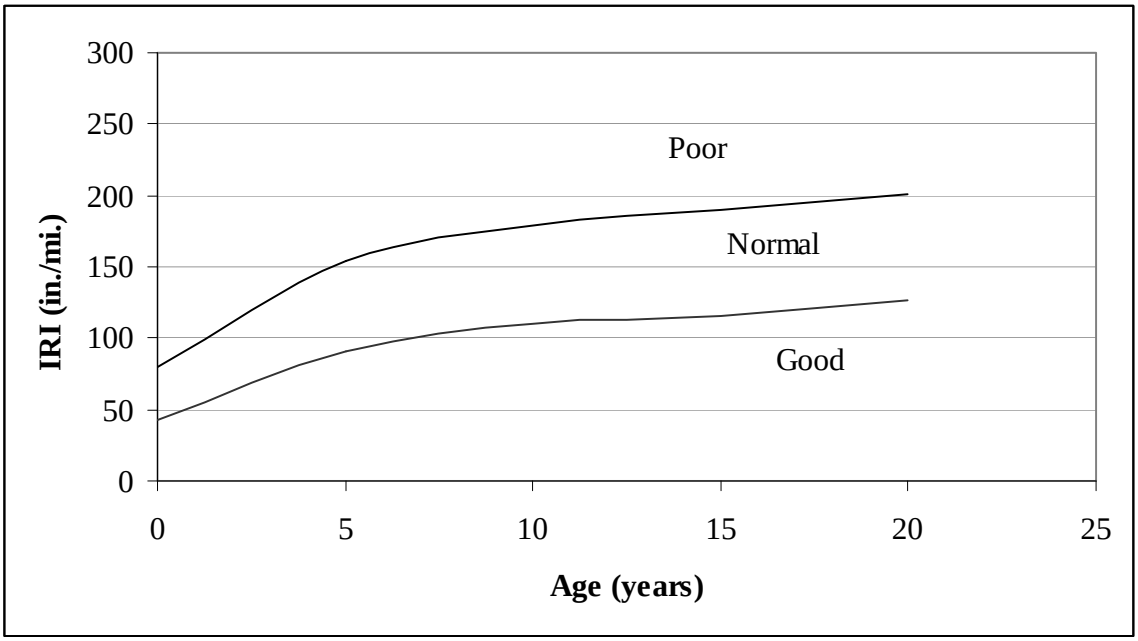

Figure 8.11. Performance criteria for IRI

Table 8.2. Results of Preliminary Sensitivity Analysis — Structure Data for Flexible Pavements

Inputs		Data	Alligator Cracking	Transverse Cracking	Rutting	IRI
Surface Properties		Surface Shortwave absortivity (0.8 to 0.98)	III	III	III	III
Layers - Asphalt Material Properties	General	Asphalt material type (AC)	N/A	N/A	N/A	N/A
		Layer thickness (2 in to 12 in.)	I	III	I	I
	Asphalt Mix	Modulus of asphalt material at different temperatures and different frequencies - (Lean mix to stiff mix)	I	III	I	II
		Aggregate Gradation Characteristics (Fine to coarse)	I	III	II	II
	Asphalt Binder	Superpave Performance Grade	I	III	I	II
		Superpave Dynamic Shear Modulus (Low to High)	II	III	I	III
		Superpave Dynamic Shear Delta (Low to High)	III	III	III	III
		Softening Point (110 F to 122 F)	III	III	III	III
		Absolute Viscosity (1120 to 7897 Poise)	III	III	III	III
		Kinematic Viscosity (230 to 889 Centistokes)	III	III	III	III
		Specific Gravity (0.999 to 1.037)	III	III	III	III
		Viscosity Grade (AC 2.5 to AC 40)	I	III	I	III
	Asphalt General	Reference temperature (70 F)	N/A	N/A	N/A	N/A
		Effective binder content (7.4% to 13.2%)	I	III	II	III
		Air voids (4.7% to 11.4%)	I	III	I	II
		Total unit weight (135.1 to 155.4 pcf)	III	III	III	III
		Poisson's ratio (0.2 to 0.45)	II	III	II	II
		Thermal conductivity (0.5 to 1.0 BTU/hr-ft-F)	III	III	III	III
		Heat capacity (0.1 to 0.5BTU/lb-F)	II	III	II	II

Note: I: Very Sensitive, II: Sensitive, III: Insensitive, N/A: Not applicable, N/R: No run

Table 8.2. Results of Preliminary Sensitivity Analysis — Structure Data for Flexible Pavements

Inputs	Data		Alligator Cracking	Transverse Cracking	Rutting	IRI
Layers - **Unbound Layer Base/Subbase**	General	Unbound Material (A-2-7 through Crushed Stone)	I	III	II	II
		Thickness (4 to 16 in.)	I	III	II	II
	Strength Properties	Poisson's Ratio (0.25 to 0.4)	III	III	III	III
		Coefficient of lateral pressure, Ko (0.2 to 1.0)	III	III	III	III
		Level 2 (Seasonal or Representative Input) - Modulus (18,000 to 40,000 psi)	I	III	II	III
		Level 3 (Representative Input only) - Modulus ((18,000 to 40,000 psi)	I	III	II	III
	ICM	Plasticity Index	I	III	II	III
		Liquid Limit	I	III	II	III
		Compacted (Yes/No)	III	III	III	III
		Gradation (Fine to Coarse)	I	III	II	II
		Maximum Dry Unit Wt. (pcf)	N/R	N/R	N/R	N/R
		Specific Gravity, Gs	N/R	N/R	N/R	N/R
		Sat. Hydraulic Conductivity (ft/hr0	N/R	N/R	N/R	N/R
		Optimum Gravimetric Water Content (%)	N/R	N/R	N/R	N/R
		af	N/R	N/R	N/R	N/R
		bf	N/R	N/R	N/R	N/R
		cf	N/R	N/R	N/R	N/R
		hr	N/R	N/R	N/R	N/R

Note: I: Very Sensitive, II: Sensitive, III: Insensitive, N/A: Not applicable, N/R: No run

Table 8.2. Results of Preliminary Sensitivity Analysis — Structure Data for Flexible Pavements

Inputs	Data		Alligator Cracking	Transverse Cracking	Rutting	IRI
Layers - **Unbound Layer Subgrade**	General	Unbound Material (A-7-6 to A-1-a)	II	III	II	III
	Strength Properties	Poisson's Ratio (0.25 to 0.4)	III	III	III	III
		Coefficient of lateral pressure, Ko (0.2 to 1.0)	III	III	III	III
		Level 2 (Seasonal or Representative Input) - Modulus (3,500 to 29,000 psi)	I	III	I	III
		Level 3 (Representative Input only) - Modulus (3,500 to 29,000 psi)	I	III	I	III
	ICM	Plasticity Index (0.1 to 10)	III	III	II	III
		Liquid Limit (6 to 51)	III	III	II	III
		Compacted (Yes/No)	III	III	III	III
		Gradation (Fine to Coarse)	II	III	II	III
		Maximum Dry Unit Wt. (pcf)	N/R	N/R	N/R	N/R
		Specific Gravity, Gs	N/R	N/R	N/R	N/R
		Sat. Hydraulic Conductivity (ft/hr)	N/R	N/R	N/R	N/R
		Optimum Gravimetric Water Content (%)	N/R	N/R	N/R	N/R
		af	N/R	N/R	N/R	N/R
		bf	N/R	N/R	N/R	N/R
		cf	N/R	N/R	N/R	N/R
		hr	N/R	N/R	N/R	N/R

Note: I: Very Sensitive, II: Sensitive, III: Insensitive, N/A: Not applicable, N/R: No run

Table 8.2. Results of Preliminary Sensitivity Analysis — Structure Data for Flexible Pavements

Inputs	Data	Alligator Cracking	Transverse Cracking	Rutting	IRI
Thermal Cracking	Average tensile strength at 14 oF (psi)				
	Creep test duration (100 sec)	N/A	N/A	N/A	N/A
	Creep Compliance (1/GPa) at 14 oF (Level 2)	II	I	II	II
	VMA (%)	N/A	N/A	N/A	N/A
	Aggregate coefficient of thermal contraction	N/R	N/R	N/R	N/R
	Mix coefficient of thermal contraction	N/R	N/R	N/R	N/R

Note: I: Very Sensitive, II: Sensitive, III: Insensitive, N/A: Not applicable, N/R: No run

Table 8.3. List of significant input variables

Inputs	Data	
Layers - Asphalt Material Properties	General	Layer thickness (2 to 12 in.)
	Asphalt Mix	Aggregate Gradation Characteristics (Fine to coarse)
	Asphalt Binder	Superpave Dynamic Shear Modulus (Low to High)
	Asphalt General	Effective binder content (7.4% to 13.2%)
		Air voids (4.7% to 11.4%)
		Poisson's ratio (0.2 to 0.45)
		Heat capacity (0.1 to 0.5BTU/lb-F)
Layers - Unbound Layer Base/Subbase	General	Unbound Material (A-2-7 through Crushed Stone)
		Thickness (4 to 16 in.)
	Strength Properties	Level 3 (Representative Input only) - Modulus (18,000 to 40,000 psi)
	ICM	Plasticity Index (1 to 15)
		Liquid Limit (1 to 32)
		Gradation (Fine to Coarse)
Layers - Unbound Layer Subgrade	General	Unbound Material (A-7-6 to A-1-a)
	Strength Properties	Level 3 (Representative Input only) - Modulus (3,500 to 29,000 psi)
	ICM	Plasticity Index (1 to 29)
		Liquid Limit (6 to 51)
		Gradation (Fine to Coarse)
Thermal Cracking	Average tensile strength at 14 ^{o}F (psi)	
	Creep Compliance (Level 2) (Low Creep to High creep)	

As mentioned earlier in this report various input variables for flexible pavement analysis, as used in MEPDG software, present different types of complexity. It is important to identify them in order to determine their significance. It is also important to develop a strategy to deal with each of these cases.

(1) In the MEPDG software, level 3 analysis does not require inputting specific values for certain asphalt mix related variables, such as the dynamic modulus, the creep compliance and (G*, δ) of the binder. Instead, since these values are dependent on the aggregate gradation, binder type, air voids and other asphalt mix variables, a built-in model estimates these values based on other inputs and uses them in the performance models. However, if level 2 (for creep compliance only) or level 1 is to be used then individual values for these variables need to be entered by the user. In the results presented here for all the variables, except those

required only in level 1 and level 2 analysis (for creep compliance only), level 3 analyses were run. Therefore, in those cases, the dynamic modulus and creep compliance were estimated by the software and hence can not be considered as being held constant. In the case of determining the sensitivity of these asphalt mix related variables themselves, level 1 or 2 (for creep compliance) runs were used and other input variables were held constant.

(2) It was observed that when values of plasticity index and liquid limit for the base material were changed from 29 and 50 respectively to 15 and 32 while keeping all other parameters constant there was no difference in performance. However when these values are reduced further the effect becomes prominent, as shown in Figure 8.12 and Figure 8.13. The reason two plots have been presented rather than one is that two curves corresponding to (29 and 50) and (12 and 32) fall exactly onto each other and therefore would not be visible in one plot.

This is probably due to the fact that fine-grained soils are categorized across zones defined by LL and PI limits. Within the same zone, the individual LL and PI values may be different, but the general behavior of the soil is similar, until the values cross a boundary. Therefore, PI and LL for the base material should be considered as a significant variable. However, PI and LL are directly dependent on the type of base material. Therefore, base material type, gradation, PI and LL can be clustered together and considered as one significant variable for further sensitivity analyses.

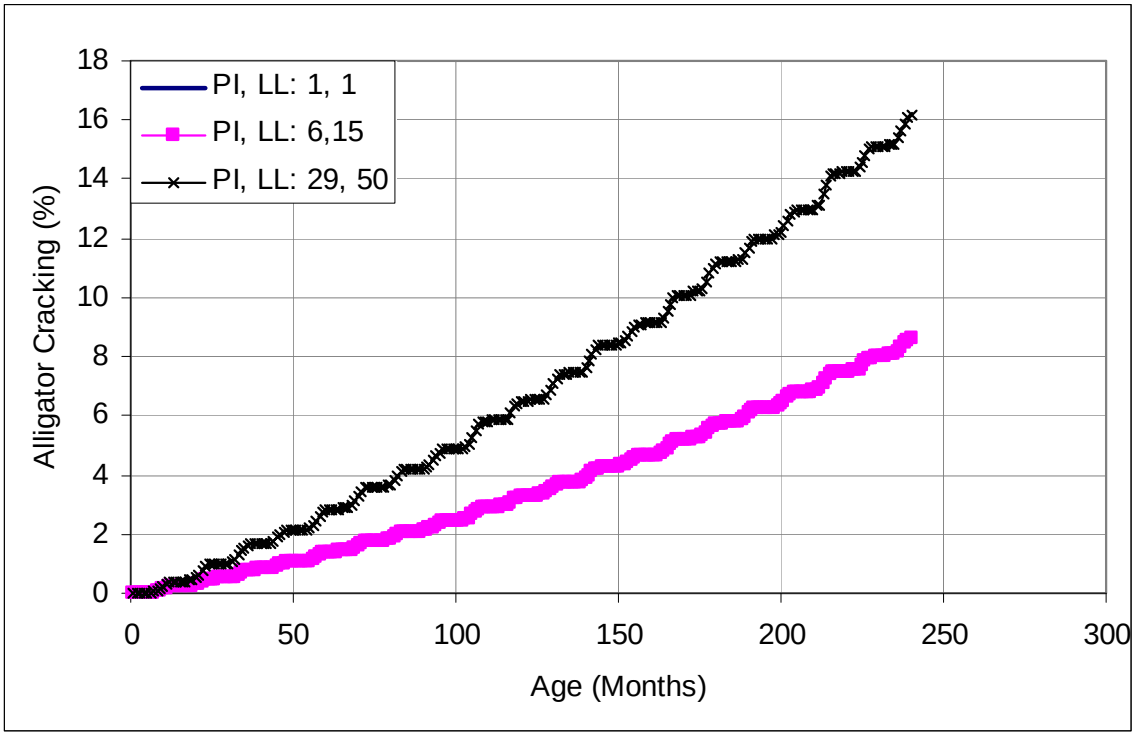

Figure 8.12. Effect of PI and LL (base material) on alligator cracking

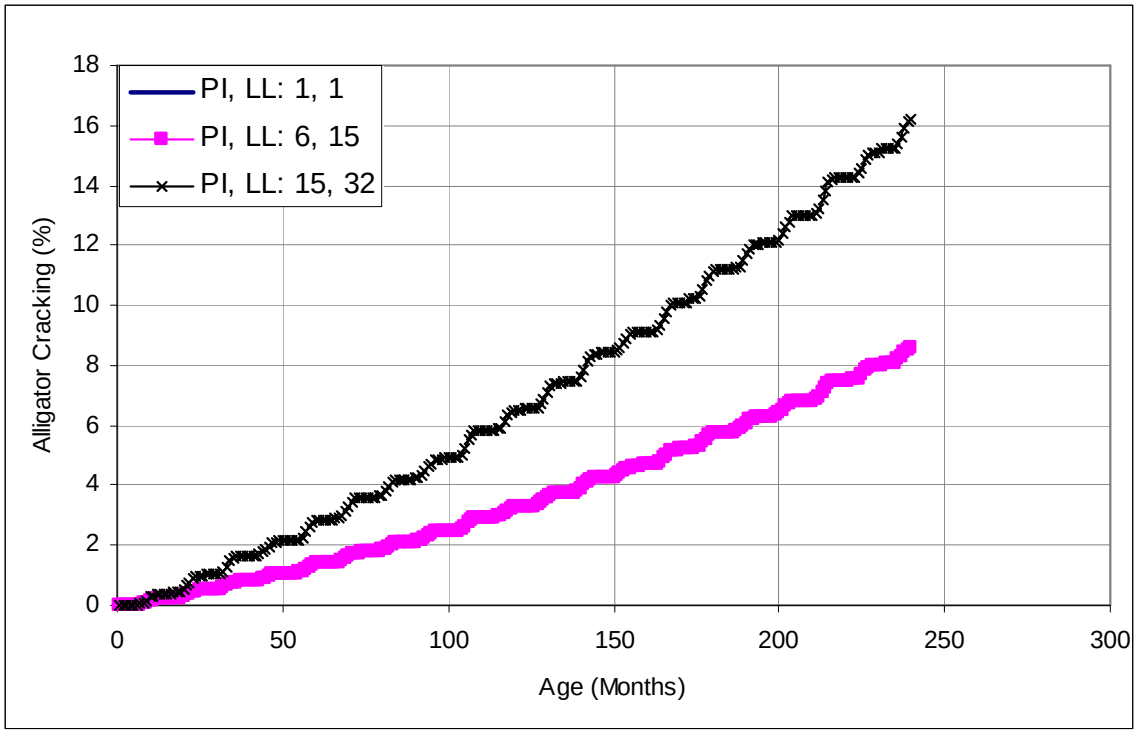

Figure 8.13. Effect of PI and LL (base material) on alligator cracking

(3) It is also expected that the modulus of base material, as used in MEPDG software, would be closely related to its gradation, plasticity index and liquid limit. Therefore the base modulus can also be clustered together with the base material for sensitivity analysis.

(4) The logic presented in the points above with respect to base material would hold for the subgrade material as well. Therefore, subgrade material can also be considered as one variable with its gradation, plasticity index, liquid limit, and modulus clustered with it.

(5) Some of the cells in Table 8.2 are marked as N/R if no sensitivity analysis was performed for the corresponding input variables. The decision to have no run in these case was made either because the values were specific to material chosen and therefore automatically change with material choice or if separate satellite sensitivity analysis was to be carried out later on.

Considering all these factors the following list of input variables was deemed appropriate for detailed sensitivity analysis, as shown in Table 8.4. There are 11 variables listed in this table. Even with two levels for each variable it would have required 2048 runs for a full factorial sensitivity analysis. However, creep compliance and average tensile strength could be studied separately. This is because these two inputs are used in thermal cracking model which works separately from the other models. The analysis would be repeated for each of the three climates, namely corresponding to Pellston, Lansing and Detroit.

Table 8.4. Final List of selected significant input variables

Cluster	Category	Variable
Asphalt Material Properties	General	Layer thickness
		Aggregate Gradation Characteristics
	Asphalt Binder	Superpave PG Grade
	Asphalt General	Effective binder content
		Air voids
Base/Subbase	General	Unbound Material
		Thickness
Subgrade	General	Unbound Material
Thermal Cracking	Average tensile strength at 14 F	
	Creep Compliance (Level 2)	
Climate	Climatic Regions	

8.5 CONCLUSION

All the input variables for analysis of flexible pavements using MEPDG software were identified. An exhaustive one-to-one sensitivity analysis was performed to identify the variables which have significant effect on pavement performance. Based on engineering judgment and practicality a final list of significant variables was identified for detailed analysis.

CHAPTER 9 - DETAILED SENSITIVITY ANALYSES - FLEXIBLE

9.1 INTRODUCTION

The previous chapter presented findings from the preliminary sensitivity analysis. Sensitivity analysis had been separately carried out for each of the inputs for flexible pavements in the MEPDG software. This helped identify the variables which seem to affect performance appreciably. It was also decided that certain variables, although distinct inputs for the software, could be grouped together and treated as one variable for the purpose of detailed sensitivity analysis. The rationale behind this decision was that those properties affect each other. For example, material type for base course is closely linked with the gradation and modulus of that material. Twelve variables or groups of variables were identified for the detailed sensitivity analysis.

9.2 DEVELOPMENT OF SENSITIVITY MATRIX

As stated earlier in the report two levels were to be determined for each of the identified variables for the detailed sensitivity analysis. This was to be followed by developing a full factorial matrix of runs for all the variables. A discussion was held with MDOT RAP members to determine these levels for each of the variables. This was followed by further e-mail communication between the RAP and the MSU research team. Based on the feed back provided by the RAP levels for all the variables were identified and are shown in Table 9.1.

The extreme right column in Table 9.1 assigns a variable number to all the inputs. It should be noted that in some cases multiple inputs have been assigned the same variable number. This means that those variables are clustered together for the purpose of analysis. In other words they would be changed together in the sensitivity analysis.

In the case of climate, which is one of the variables identified as sensitive for performance, three different climatic regions, namely Pellston, Lansing and Detroit were identified rather than two. If the rest of the 11 variables had 2 levels each a full factorial test matrix would mean that the total number of runs required would be $3*2^{11} = 6144$. This is truly a large number of runs. Considering the fact that one run takes about 50 minutes 6144 runs would translate into 5120 hours or about 213 days of nonstop computation on one computer processor. Therefore, it was further decided that the effect of creep compliance and average tensile strength would be studied separately as a satellite study. This would bring the computational time down by fifty percent.

Table 9.2 shows the first 32 of the 3072 cases of the runs for the detailed sensitivity analysis. Each row shows the combination of levels used for all the variables corresponding to that run number. All of the 32 cases shown correspond to Lansing climate. The variable numbers in this table correspond to those assigned in Table 9.1.

Table 9.1: Variables identified for detailed sensitivity analysis (upper and lower levels)

Cluster		Surrogate Variable		Lower Level	Upper Level	Var no.
Materials	Asphalt Mix	Layer thickness (in.)		4	12	1
		Aggregate Gradation	Cum. % Retained on 3/4 in.	12	0	2
			Cum. % Retained on 3/8 in.	25	10	
			Cum. % Retained on #4 Sieve	35	30	
			% Passing #200 Sieve	7	3	
		Effective Binder Content (%)		7.4 (Pbe = 3.7)	13.2 (Pbe = 6.6)	3
		Superpave Binder Grade		PG 64-34	PG 58-22	4
		Air Voids (%)		4.7	11.4	5
	Base	Thickness (in)		4	6	6
		Material Type		4 G	21 AA	7
		Gradation*	% Passing 37.5 mm Sieve	100	100	
			% Passing 25 mm Sieve		92.5	
			% Passing 19 mm Sieve	70		
			% Passing 12.5 mm Sieve	50	62.5	
			% Passing 2.36 mm Sieve	17.5	32.5	
			% Passing 0.6 mm Sieve	11.5		
			% Passing #200 Sieve	6	6	
		Modulus (psi)		10000	35000	
	Subbase	Thickness (in)		8	30	8
		Material Type		Class II	Class II	9
		Gradation*	% Passing 37.5 mm Sieve	100	100	
			% Passing 25 mm Sieve	60	100	
			% Passing 12.5 mm Sieve			
			% Passing 2.36 mm Sieve			
			% Passing 0.6 mm Sieve			
			% Passing 0.15 mm Sieve	10	30	
			% Passing #200 Sieve	2	10	
		Modulus (psi)		5000	15000	
	Subgrade	MaterialType		A-7-6	A-2-6	10
		Gradation*	% Passing 37.5 mm Sieve	99	100	
			% Passing 25 mm Sieve	98	100	
			% Passing 12.5 mm Sieve	95	80	
			% Passing 2.36 mm Sieve	85	50	
			% Passing 0.6 mm Sieve	83	15	
			% Passing #200 Sieve	79	7	
		Modulus (psi)		3000	12500	
		PI		5	30	
		LL		6	40	
Thermal Cracking	Average tensile strength at 14 F			200	1000	Satellite Study
	Creep Compliance at 14 F (1/GPa)		t = 1 sec	0.034	0.089	
			t = 2 sec	0.037	0.104	
			t = 5 sec	0.041	0.128	
			t = 10 sec	0.046	0.15	
			t = 20 sec	0.05	0.18	
			t = 50 sec	0.059	0.235	
			t = 100 sec	0.07	0.301	
Climate	Climatic Regions			Pellston, Lansing, Detroit		11

Table 9.2. Sample of full factorial sensitivity analysis matrix

	Variable Number									
Run no.	1	2	3	4	5	6	7	8	9	10
1	Low	Low	Low	Low	Low	Low	Low	Low	Low	Low
2	Low	Low	Low	Low	Low	Low	Low	Low	Low	High
3	Low	Low	Low	Low	Low	Low	Low	Low	High	Low
4	Low	Low	Low	Low	Low	Low	Low	Low	High	High
5	Low	Low	Low	Low	Low	Low	Low	High	Low	Low
6	Low	Low	Low	Low	Low	Low	Low	High	Low	High
7	Low	Low	Low	Low	Low	Low	Low	High	High	Low
8	Low	Low	Low	Low	Low	Low	Low	High	High	High
9	Low	Low	Low	Low	Low	Low	High	Low	Low	Low
10	Low	Low	Low	Low	Low	Low	High	Low	Low	High
11	Low	Low	Low	Low	Low	Low	High	Low	High	Low
12	Low	Low	Low	Low	Low	Low	High	Low	High	High
13	Low	Low	Low	Low	Low	Low	High	High	Low	Low
14	Low	Low	Low	Low	Low	Low	High	High	Low	High
15	Low	Low	Low	Low	Low	Low	High	High	High	Low
16	Low	Low	Low	Low	Low	Low	High	High	High	High
17	Low	Low	Low	Low	Low	High	Low	Low	Low	Low
18	Low	Low	Low	Low	Low	High	Low	Low	Low	High
19	Low	Low	Low	Low	Low	High	Low	Low	High	Low
20	Low	Low	Low	Low	Low	High	Low	Low	High	High
21	Low	Low	Low	Low	Low	High	Low	High	Low	Low
22	Low	Low	Low	Low	Low	High	Low	High	Low	High
23	Low	Low	Low	Low	Low	High	Low	High	High	Low
24	Low	Low	Low	Low	Low	High	Low	High	High	High
25	Low	Low	Low	Low	Low	High	High	Low	Low	Low
26	Low	Low	Low	Low	Low	High	High	Low	Low	High
27	Low	Low	Low	Low	Low	High	High	Low	High	Low
28	Low	Low	Low	Low	Low	High	High	Low	High	High
29	Low	Low	Low	Low	Low	High	High	High	Low	Low
30	Low	Low	Low	Low	Low	High	High	High	Low	High
31	Low	Low	Low	Low	Low	High	High	High	High	Low
32	Low	Low	Low	Low	Low	High	High	High	High	High

9.3 EFFECT OF INPUT VARIABLES ON FATIGUE CRACKING

The detailed analyses were performed in two steps. Initially, the descriptive statistics such as mean performance for each input variable were summarized. Differences in mean effects give main effects for each of the variables. However, since interaction of effects from different variables can lead to misleading conclusions if only main effects are considered interaction effects were also studied. This was done though analysis of variance, ANOVA.

9.3.1 Main Effects

Figure 9.2 shows the main effects of the ten variables on flexible pavement fatigue cracking performance in the form of time series for two levels for each variable. Figure 9.1 shows the trends for all the main effects and Table 9.3 lists the magnitude of main effects at different times

during the life of the pavement. A positive slope in Figure 9.1 means that going from level 1 to level 2 leads to higher fatigue cracking. If the slope of the line in the plot for any input variable is almost zero it signifies that fatigue cracking is not sensitive to that particular variable. The following is a discussion of these effects.

AC Thickness: As expected, AC thickness has a significant effect on fatigue cracking. It is also notable in this case that fatigue damage is very significant from early stages in the case of thin pavements. This is primarily because such a thin structure cannot withstand heavy traffic applied in this case.

AC Aggregate Gradation: The effect of asphalt concrete aggregate gradation may not be so significant. However it should be noted that in this analysis the two levels of aggregates used did not have markedly different gradations.

AC Effective Binder Content: Effective binder content of the top AC layer has a significant impact on fatigue performance of the pavement. As would be expected pavement with higher effective binder content has less fatigue cracking. However the rate of fatigue cracking is somewhat similar after about 6 years of age.

AC Binder Grade: The two binder grades chosen for this analysis were the ones that are most commonly used in Michigan. The results show that there may be very little difference in fatigue performance of these two binder grades.

AC Air Avoids: Air voids in the top layer asphalt concrete has a significant impact on fatigue performance. Lower air voids translate into a densely packed pavement layer leading to a greater fatigue resistance.

Base Thickness: The vast majority of pavements in Michigan have either 4 inch or 6 inch bases. The difference in thickness is not significant and therefore, the time history plot also shows that the difference in fatigue performance is not significant.

Base Material Type: The two types selected for the sensitivity study were the materials that are most commonly used in the state of Michigan. The time history plots show significant impact of the material type on fatigue performance of the pavement.

Subbase Thickness: Subbase thicknesses chosen for the sensitivity analysis represent the extreme cases which would be used on Michigan pavements. There is marginal difference in the fatigue performance of pavements with an 8 inch subbase as compared to those with a 30 inch subbase.

Subbase Material: The two materials chosen in this study do show some difference in fatigue performance.

Subgrade Material: Subgrade layer is the farthest layer from the surface course which is directly subjected to traffic loads. The plot shows that the difference in fatigue performance is minimal.

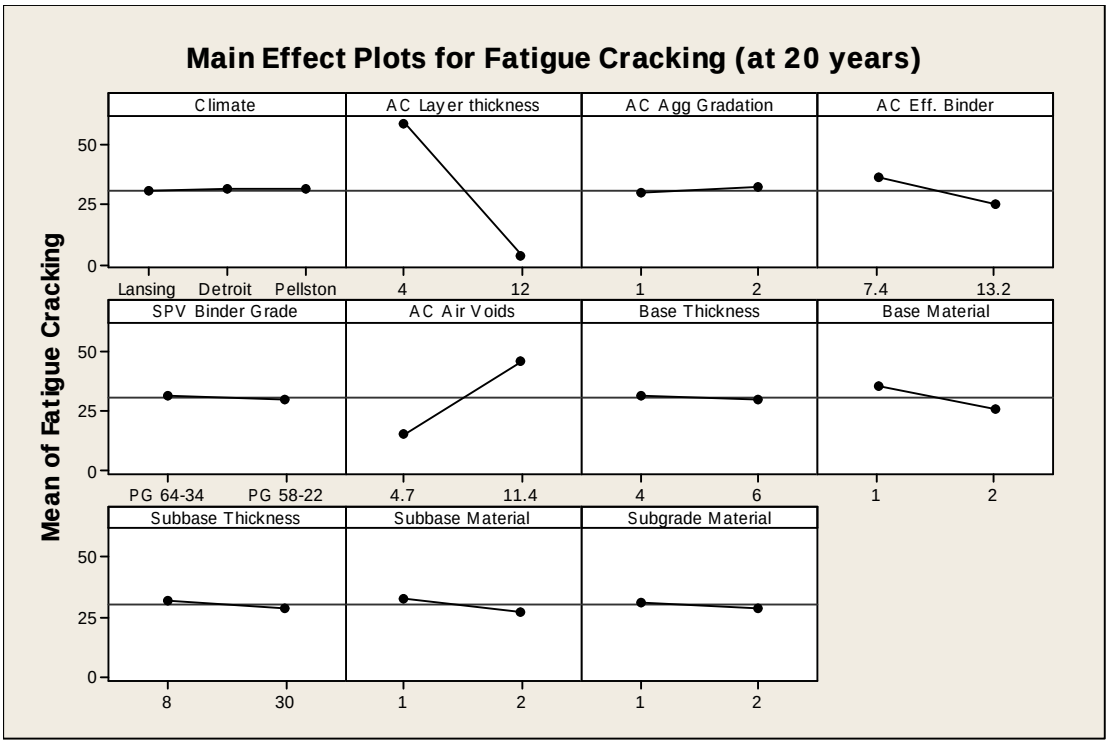

Figure 9.1. Main effects of input variables on fatigue cracking

Table 9.3: Main effects of input variables on fatigue cracking

Input Variable	Levels	Fatigue Cracking					Mean Differences				
		1 month	5 years	10 years	15 years	20 years	$\Delta_{1/12}$	Δ_5	Δ_{10}	Δ_{15}	Δ_{20}
AC Thickness (inches)	4	1.12	35.56	46.15	53.27	58.47					
	12	0.01	0.61	1.22	1.88	2.54	1.11	34.95	44.94	51.39	55.93
AC Agg Gradation	Coarse	0.45	16.91	22.41	26.30	29.20					
	Fine	0.67	19.12	24.72	28.53	31.43	-0.22	-2.22	-2.30	-2.23	-2.23
AC Effective Binder Content	7.4	0.92	23.16	28.97	33.03	36.10					
	13.2	0.21	12.98	18.34	22.02	24.77	0.71	10.18	10.63	11.01	11.33
AC SPV Grade	PG 58-22	0.45	17.48	23.04	26.88	29.77					
	PG 64-34	0.68	18.59	24.15	28.01	30.91	-0.23	-1.11	-1.11	-1.12	-1.14
AC Air Voids	4.7	0.03	4.23	8.19	11.94	15.19					
	11.4	1.07	31.37	38.57	42.58	45.18	-1.04	-27.14	-30.38	-30.64	-30.00
Base Thickness	4	0.60	18.75	24.43	28.35	31.31					
	6	0.53	17.33	22.78	26.56	29.40	0.07	1.43	1.64	1.79	1.91
Base Material	4 G	0.87	22.75	28.40	32.30	35.19					
	21 AA	0.26	13.37	18.88	22.70	25.62	0.61	9.38	9.52	9.59	9.58
Subbase thickness	8	0.63	19.22	25.04	29.07	32.10					
	30	0.50	16.88	22.19	25.87	28.65	0.13	2.34	2.85	3.20	3.45
Subbase Material	Class II	0.69	20.32	26.20	30.27	33.31					
	Class II'	0.44	15.79	21.05	24.70	27.47	0.25	4.53	5.15	5.57	5.84
Subgrade Material	A-7-6	0.64	18.82	24.58	28.62	31.67					
	A-2-6	0.48	17.29	22.67	26.34	29.09	0.16	1.53	1.91	2.28	2.58

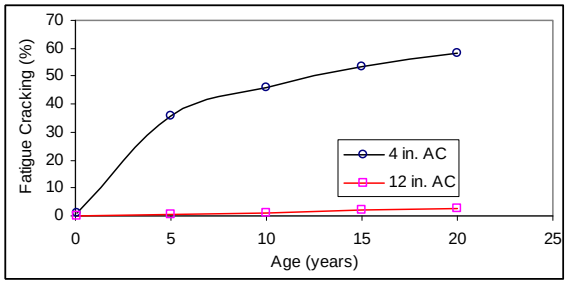

(a) Effect of Thickness on fatigue cracking

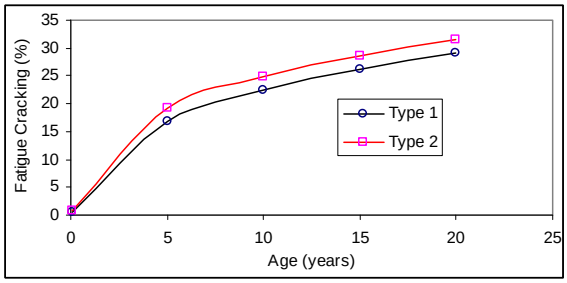

(b) Effect of AC agg. Gradation on fatigue cracking

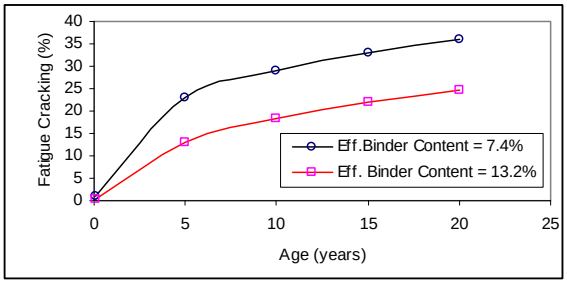

(c) Effect of AC binder content on fatigue cracking

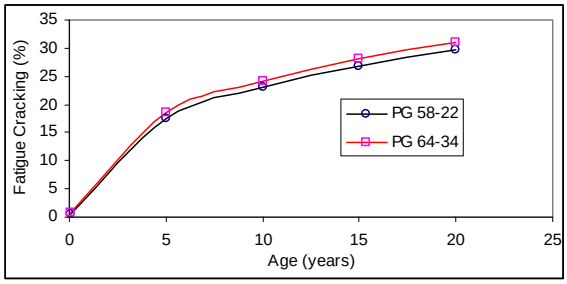

(d) Effect of AC binder grade on fatigue cracking

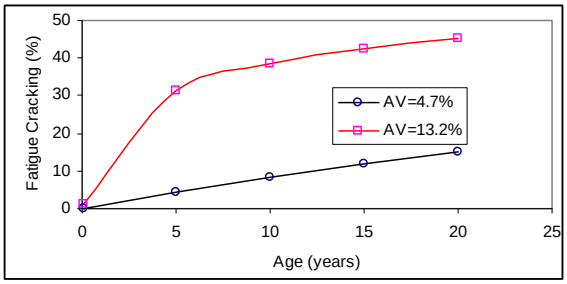

(e) Effect of AC air voids on fatigue cracking

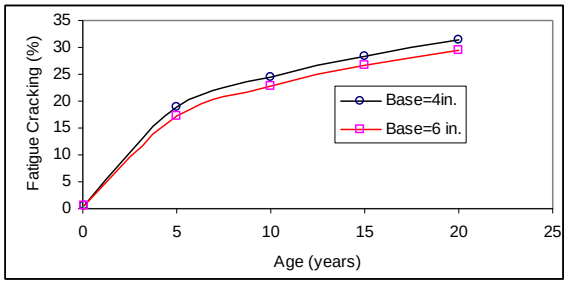

(f) Effect of base thickness on fatigue cracking

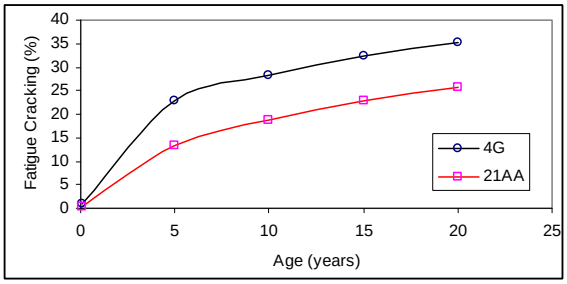

(g) Effect of base material on fatigue cracking

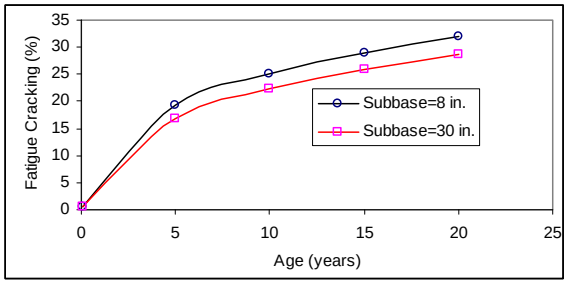

(h) Effect of subbase thickness on fatigue cracking

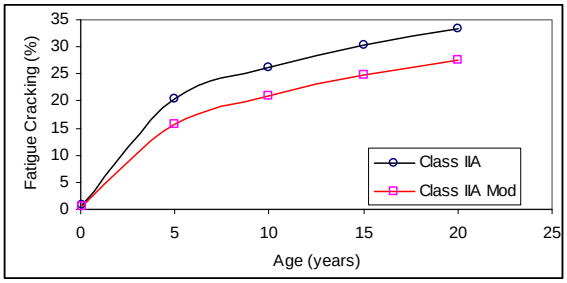

(i) Effect of subbase material on fatigue cracking

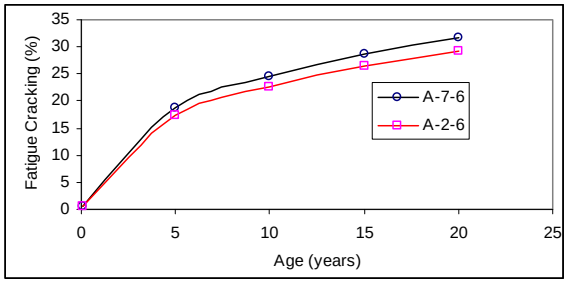

(j) Effect of subgrade material on fatigue cracking

Figure 9.2. Average effects of parameters on fatigue cracking

9.3.2 Interaction Effects

Interaction effects are extremely important in such analysis since the main effect of one variable can be dependent on the value of one or more other variables. In the case of fatigue cracking the interaction between AC layer thickness and AC air voids is highly pronounced. It is also notable that effects of AC layer thickness interact with effects of AC effective binder content, base material and subbase material. P-values for other interactions are also nearly equal to zero. Although statistically any interaction effect leading to p-value less than 0.05 should be considered as significant, practically many of them would not have any significant influence on performance. Lower p-value is a result of lower error/variability in the M-E PDG replicate run results. This in turn is so because M-E PDG uses models to predict performance, which would give identical or very close results in every run for the same values of inputs. Therefore, adjusted sums of squares (Ajd SS) or adjusted mean squares (Adj MS) should be considered in this analysis which allows direct comparison of magnitude of effects also. This also helps compare otherwise too many variables for HMA which was not so for PCC pavements.
Table 9.4 shows ANOVA calculations for main and interaction effects of all input variables on fatigue cracking.

Table 9.4: Analysis of Variance for Fatigue at 20 years, using Adjusted SS for Tests

Source	DF	Seq SS	Adj SS	Adj MS	F	p-value
Climate	2	248	248	124	4.11	0.017
AC Layer Thickness	1	2402135	2402135	2402135	79498.96	0
AC Agg Gradation	1	5223	5223	5223	172.86	0
AC Eff. Binder	1	96300	96300	96300	3187.06	0
SPV Binder Grade	1	1623	1623	1623	53.72	0
AC Air Voids	1	720603	720603	720603	23848.45	0
Base Thickness	1	2005	2005	2005	66.34	0
Base Material	1	67662	67662	67662	2239.27	0
Subbase Thickness	1	7874	7874	7874	260.58	0
Subbase Material	1	24234	24234	24234	802.03	0
Subgrade Material	1	4212	4212	4212	139.41	0
Climate*AC Layer thickness	2	4	4	2	0.06	0.94
Climate*AC Agg Gradation	2	75	75	37	1.24	0.289
Climate*AC Eff. Binder	2	89	89	45	1.48	0.228
Climate*SPV Binder Grade	2	41	41	20	0.67	0.511
Climate*AC Air Voids	2	166	166	83	2.75	0.064
Climate*Base Thickness	2	3	3	1	0.05	0.955
Climate*Base Material	2	32	32	16	0.53	0.591
Climate*Subbase Thickness	2	1	1	0	0.01	0.985
Climate*Subbase Material	2	17	17	8	0.28	0.759
Climate*Subgrade Material	2	2	2	1	0.04	0.961
AC Layer thickness*AC Agg Gradation	1	5811	5811	5811	192.31	0
AC Layer thickness*AC Eff. Binder	1	49403	49403	49403	1634.99	0
AC Layer thickness*SPV Binder Grade	1	127	127	127	4.19	0.041
AC Layer thickness*AC Air Voids	1	577484	577484	577484	19111.9	0
AC Layer thickness*Base Thickness	1	1120	1120	1120	37.07	0

Table 9.4(contd.): Analysis of Variance for Fatigue at 20 years, using Adjusted SS for Tests

Source	DF	Seq SS	Adj SS	Adj MS	F	p-value
AC Layer thickness*Base Material	1	49154	49154	49154	1626.77	0
AC Layer thickness*Subbase Thickness	1	3189	3189	3189	105.55	0
AC Layer thickness*Subbase Material	1	12900	12900	12900	426.93	0
AC Layer thickness*Subgrade Material	1	282	282	282	9.33	0.002
AC Agg Gradation*AC Eff. Binder	1	121	121	121	3.99	0.046
AC Agg Gradation*SPV Binder Grade	1	29	29	29	0.96	0.326
AC Agg Gradation*AC Air Voids	1	57	57	57	1.89	0.169
AC Agg Gradation*Base Thickness	1	9	9	9	0.3	0.582
AC Agg Gradation*Base Material	1	36	36	36	1.21	0.272
AC Agg Gradation*Subbase Thickness	1	4	4	4	0.14	0.703
AC Agg Gradation*Subbase Material	1	79	79	79	2.62	0.106
AC Agg Gradation*Subgrade Material	1	140	140	140	4.62	0.032
AC Eff. Binder*SPV Binder Grade	1	54	54	54	1.8	0.18
AC Eff. Binder*AC Air Voids	1	1935	1935	1935	64.03	0
AC Eff. Binder*Base Thickness	1	14	14	14	0.46	0.498
AC Eff. Binder*Base Material	1	42	42	42	1.39	0.238
AC Eff. Binder*Subbase Thickness	1	57	57	57	1.89	0.169
AC Eff. Binder*Subbase Material	1	289	289	289	9.56	0.002
AC Eff. Binder*Subgrade Material	1	692	692	692	22.92	0
SPV Binder Grade*AC Air Voids	1	198	198	198	6.55	0.011
SPV Binder Grade*Base Thickness	1	1	1	1	0.04	0.834
SPV Binder Grade*Base Material	1	3	3	3	0.08	0.771
SPV Binder Grade*Subbase Thickness	1	20	20	20	0.67	0.415
SPV Binder Grade*Subbase Material	1	0	0	0	0	0.948
SPV Binder Grade*Subgrade Material	1	1	1	1	0.03	0.857
AC Air Voids*Base Thickness	1	19	19	19	0.62	0.432
AC Air Voids*Base Material	1	1166	1166	1166	38.58	0
AC Air Voids*Subbase Thickness	1	120	120	120	3.98	0.046
AC Air Voids*Subbase Material	1	867	867	867	28.71	0
AC Air Voids*Subgrade Material	1	169	169	169	5.59	0.018
Base Thickness*Base Material	1	1400	1400	1400	46.34	0
Base Thickness*Subbase Thickness	1	25	25	25	0.83	0.363
Base Thickness*Subbase Material	1	344	344	344	11.39	0.001
Base Thickness*Subgrade Material	1	146	146	146	4.83	0.028
Base Material*Subbase Thickness	1	6	6	6	0.21	0.644
Base Material*Subbase Material	1	38	38	38	1.27	0.26
Base Material*Subgrade Material	1	532	532	532	17.62	0
Subbase Thickness*Subbase Material	1	540	540	540	17.87	0
Subbase Thickness*Subgrade Material	1	2894	2894	2894	95.76	0
Subbase Material*Subgrade Material	1	859	859	859	28.42	0
Error		2994	90467	90467	30	
Total		3071	4135393			

Figure 9.3 shows interaction plots for fatigue cracking. The name of the input variable is shown in the diagonal cells. To find the interaction plot for any two variables one should locate the two variable cells from among all the cells on the main diagonal and look at the plot which is in the same row as the first variable and the same column as the second variable. Each plot has two lines. Those two lines represent the average fatigue cracking for the two levels chosen for the first input variable. Each line has two points. Those two points represent the average fatigue for the two levels of the second variable. The distance between the two lines, therefore, shows the average effect of the first variable on fatigue cracking. The slope of the line shows the effect of the second variable. The difference in the slopes of the two lines shows that there is an interaction effect. The plot marked with "* "in Figure 9.3 shows an example. AC thickness (row) and AC Air Voids (column) are the two variables plotted here. The top line corresponds to AC thickness of 4 inches (low level) and the bottom to 12 inches (upper level) thickness. The distance between the two lines therefore represent effect of AC thickness on fatigue cracking. The slopes of these lines show the effect of AC air voids at two AC thickness levels. Difference in slopes of the two lines shows that there is interaction of effects from the two factors namely AC thickness and AC air voids. In other words when AC thickness is 4 inches AC air voids effects fatigue cracking more (steeper slope of the upper line) than when AC thickness is 12 inches (flatter slope of the lower line).

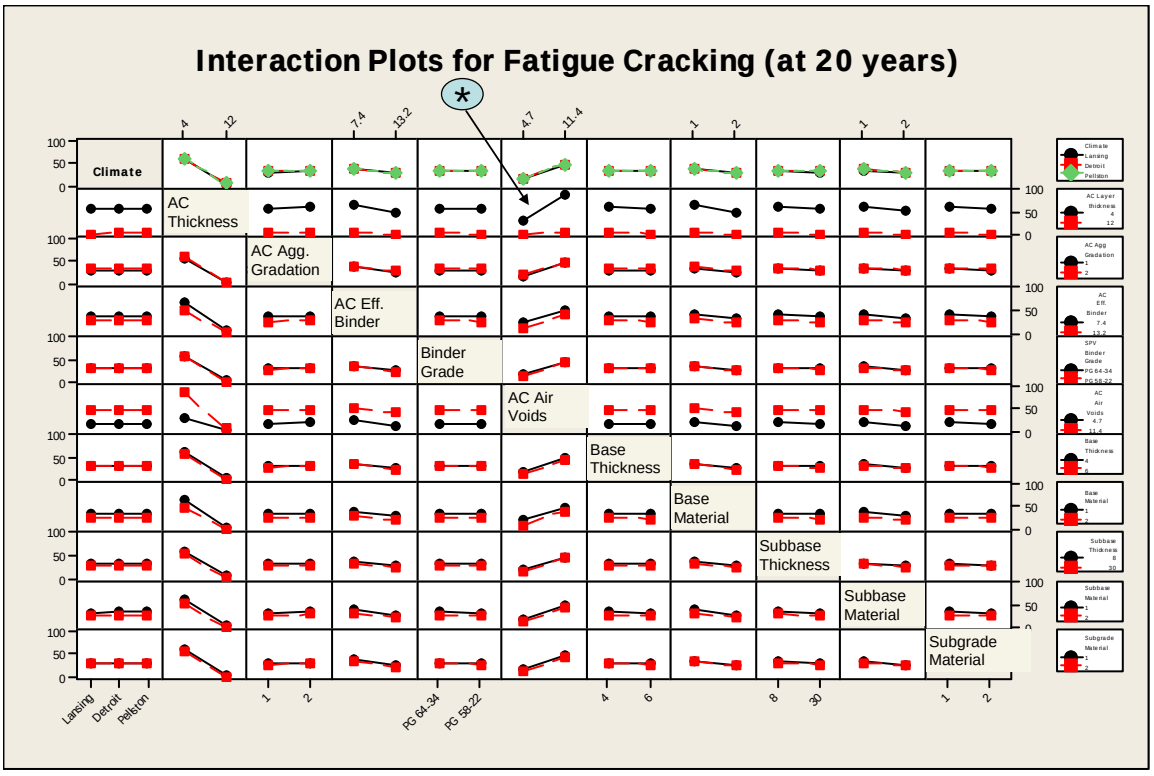

Figure 9.3. Interaction plots for fatigue cracking at the end of 20 years

9.4 EFFECT OF INPUT VARIABLES ON LONGITUDINAL CRACKING

9.4.1 Main Effects

The plots in Figure 9.4 show the average effect of different input variables on longitudinal cracking. Figure 9.5 shows the trends for all the main effects and Table 9.5 lists the magnitude of main effects at different times during the life of the pavement. It is clear that the pavements did not show extensive longitudinal cracking in almost any case. Relatively speaking AC thickness and AC air voids have maximum impact on longitudinal cracking performance of the pavements. AC binder content, base, subbase and subgrade material also seem to have appreciable impact on longitudinal cracking performance. The differences in performance for the chosen values of AC aggregate gradation, asphalt grade, base and subbase thickness is not significant at all. However it should be noted that the two levels chosen for some of these variables were quite close to each other. These levels were chosen based on MDOT practice as far as possible. Therefore although wider ranges for these variables could have been chosen they would not have led to results of any relevance to MDOT. On the other hand Subbase thickness, notably, varies significantly from 8 inches to 30 inches and yet there is almost no difference in longitudinal cracking performance.

Table 9.5: Main effects of input variables on longitudinal cracking

		Long. Cracking					Mean Differences				
Input Variable	Levels	1 month	5 years	10 years	15 years	20 years	$\Delta_{1/12}$	Δ_5	Δ_{10}	Δ_{15}	Δ_{20}
AC Thickness (inches)	4	24.78	1854.23	2657.45	3239.20	3693.76					
	12	0.01	2.63	6.24	10.59	14.77	24.78	1851.60	2651.21	3228.61	3678.99
AC Agg Gradation	Level 1	9.53	837.43	1218.11	1500.34	1720.46					
	Level 2	15.24	1015.11	1436.22	1735.04	1969.25	-5.71	-177.68	-218.11	-234.70	-248.79
AC Effective Binder	7.4	21.70	1305.31	1754.21	2071.83	2316.02					
	13.2	3.09	551.01	908.08	1175.43	1388.66	18.60	754.29	846.13	896.39	927.36
AC SPV Grade	PG 58-22	9.28	894.95	1293.73	1582.72	1808.58					
	PG 64-34	15.51	959.40	1364.10	1657.46	1886.83	-6.23	-64.45	-70.37	-74.74	-78.25
AC Air Voids	4.7	0.23	93.79	222.18	370.48	517.47					
	11.4	23.70	1721.32	2390.87	2823.72	3132.34	-23.48	-1627.54	-2168.69	-2453.24	-2614.88
Base Thickness	4	14.16	1031.01	1458.02	1763.58	2001.15					
	6	10.63	823.88	1201.01	1478.41	1696.48	3.53	207.12	257.01	285.16	304.67
Base Material	Level 1	21.33	1347.44	1838.75	2183.38	2446.38					
	Level 2	3.46	508.75	823.26	1063.42	1257.69	17.86	838.70	1015.50	1119.96	1188.69
Subbase thickness	8	11.77	908.01	1296.72	1578.05	1792.84					
	30	13.02	946.57	1361.61	1662.89	1903.48	-1.25	-38.55	-64.89	-84.84	-110.64
Subbase Material	Level 1	19.83	1357.58	1846.05	2181.00	2431.03					
	Level 2	4.95	498.69	816.20	1066.20	1273.60	14.88	858.89	1029.85	1114.81	1157.44
Subgrade Material	Level 1	4.52	545.14	835.58	1060.46	1242.33					
	Level 2	20.27	1308.48	1820.57	2176.96	2449.33	-15.75	-763.34	-984.99	-1116.50	-1207.00

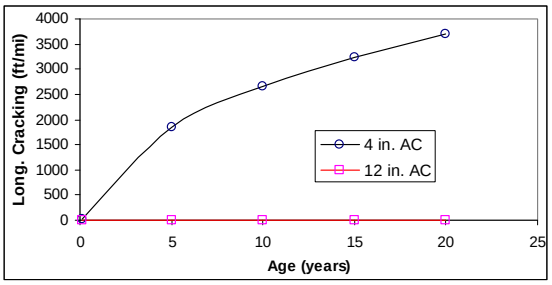

(a) Effect of Thickness on long. cracking

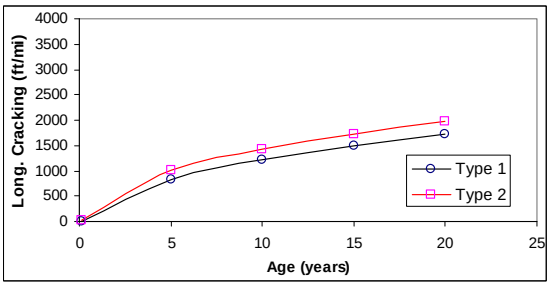

(b) Effect of AC agg. Gradation on long. cracking

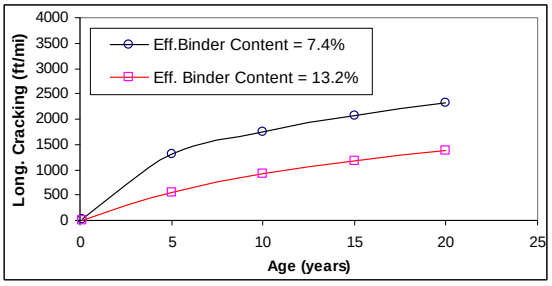

(c) Effect of AC binder content on long. cracking

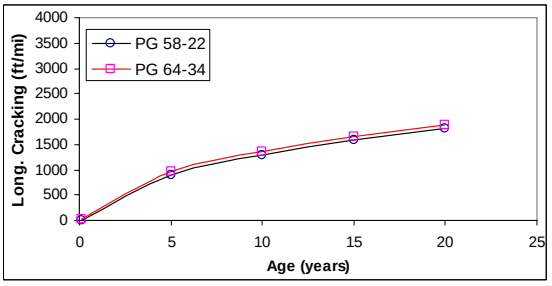

(d) Effect of AC binder grade on long. cracking

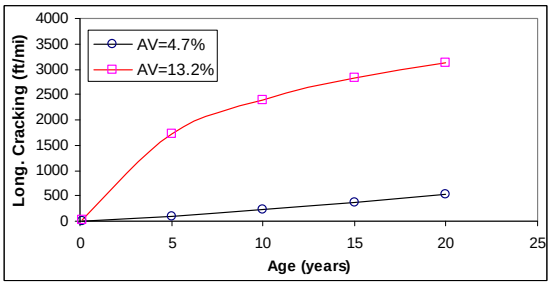

(e) Effect of AC air voids on long. cracking

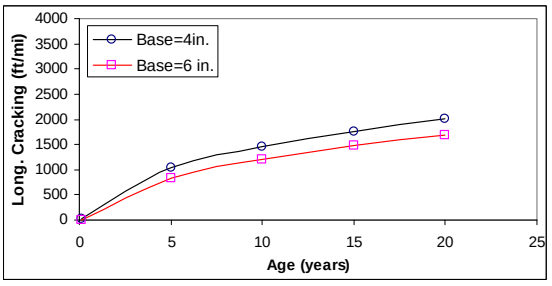

(f) Effect of base thickness on long. cracking

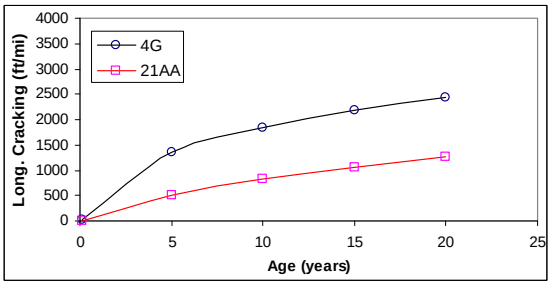

(g) Effect of base material on long. cracking

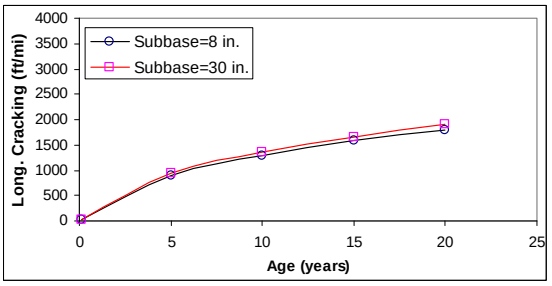

(h) Effect of subbase thickness on long. cracking

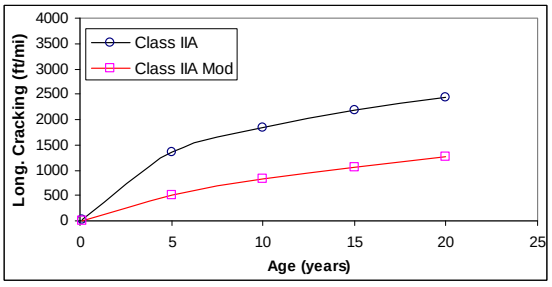

(i) Effect of subbase material on long. cracking

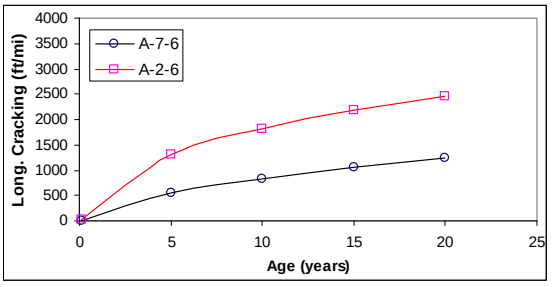

(h) Effect of subgrade material on long. cracking

Figure 9.4. Main effects of parameters on longitudinal cracking

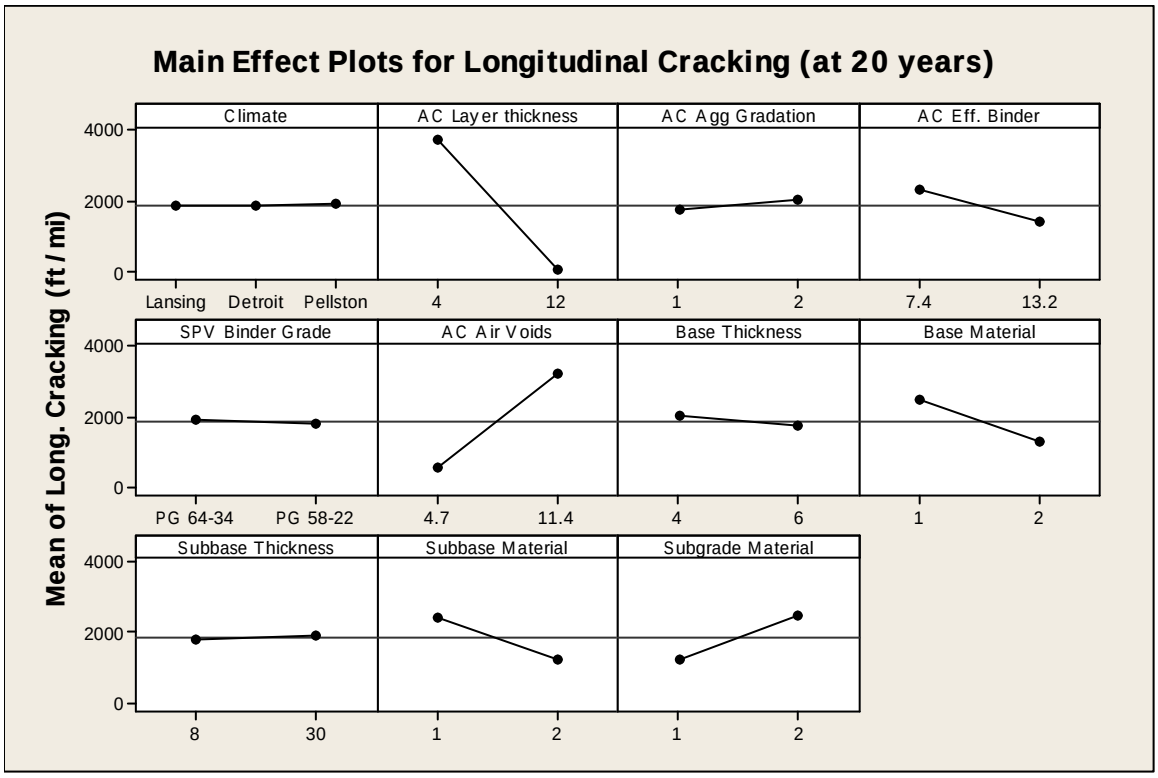

Figure 9.5. Main effects of input variables on longitudinal cracking

9.4.2 Interaction Effects

The effect of AC layer thickness has appreciable interaction with effects of AC air voids, subgrade material, base material and subbase material in that order. Other interactions are relatively not so significant from practical point of view. Figure 9.6 shows all the two-way interaction plots. Table 9.6 shows the ANOVA calculations for main as well as interaction effects on longitudinal cracking.

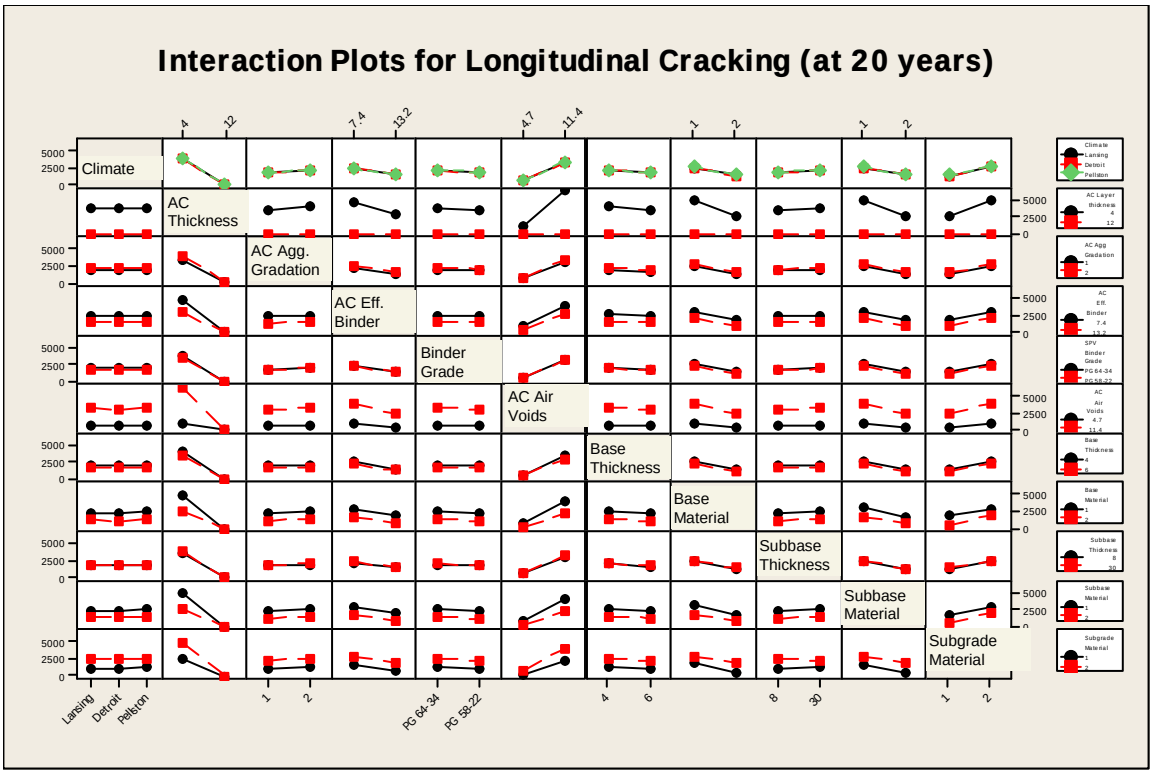

Figure 9.6. Interaction plots for longitudinal cracking at the end of 20 years

Table 9.6: Analysis of Variance for Longitudinal Cracking at 20 years, using Adjusted SS for Tests

Source	DF	Seq SS	Adj SS	Adj MS	F
Climate	2	596546	596546	298273	0.3
AC Layer thickness	1	1.04E+10	1.04E+10	1.04E+10	10407.45
AC Agg Gradation	1	54994511	54994511	54994511	55.06
AC Eff. Binder	1	6.55E+08	6.55E+08	6.55E+08	655.8
SPV Binder Grade	1	6410644	6410644	6410644	6.42
AC Air Voids	1	5.49E+09	5.49E+09	5.49E+09	5496.38
Base Thickness	1	66284468	66284468	66284468	66.36
Base Material	1	1.08E+09	1.08E+09	1.08E+09	1078.37
Subbase Thickness	1	11590886	11590886	11590886	11.6
Subbase Material	1	1.02E+09	1.02E+09	1.02E+09	1023.18
Subgrade Material	1	1.15E+09	1.15E+09	1.15E+09	1151.75
Climate*AC Layer thickness	2	460313	460313	230157	0.23
Climate*AC Agg Gradation	2	55922	55922	27961	0.03
Climate*AC Eff. Binder	2	222147	222147	111074	0.11
Climate*SPV Binder Grade	2	296896	296896	148448	0.15
Climate*AC Air Voids	2	456032	456032	228016	0.23

Table 9.6. (continued) Analysis of Variance for Longitudinal Cracking at 20 years, using Adjusted SS for Tests

Source	DF	Seq SS	Adj SS	Adj MS	F
Climate*Base Thickness	2	33763	33763	16881	0.02
Climate*Base Material	2	156591	156591	78296	0.08
Climate*Subbase Thickness	2	21674	21674	10837	0.01
Climate*Subbase Material	2	433472	433472	216736	0.22
Climate*Subgrade Material	2	41511	41511	20755	0.02
AC Layer thickness*AC Agg Gradation	1	66822996	66822996	66822996	66.9
AC Layer thickness*AC Eff. Binder	1	6.15E+08	6.15E+08	6.15E+08	615.77
AC Layer thickness*SPV Binder Grade	1	3046105	3046105	3046105	3.05
AC Layer thickness*AC Air Voids	1	5.6E+09	5.6E+09	5.6E+09	5607.26
AC Layer thickness*Base Thickness	1	66881449	66881449	66881449	66.96
AC Layer thickness*Base Material	1	1.05E+09	1.05E+09	1.05E+09	1053.81
AC Layer thickness*Subbase Thickness	1	11836403	11836403	11836403	11.85
AC Layer thickness*Subbase Material	1	9.78E+08	9.78E+08	9.78E+08	979.53
AC Layer thickness*Subgrade Material	1	1.12E+09	1.12E+09	1.12E+09	1125.79
AC Agg Gradation*AC Eff. Binder	1	634560	634560	634560	0.64
AC Agg Gradation*SPV Binder Grade	1	271712	271712	271712	0.27
AC Agg Gradation*AC Air Voids	1	6957137	6957137	6957137	6.97
AC Agg Gradation*Base Thickness	1	70274	70274	70274	0.07
AC Agg Gradation*Base Material	1	78533	78533	78533	0.08
AC Agg Gradation*Subbase Thickness	1	57889	57889	57889	0.06
AC Agg Gradation*Subbase Material	1	181782	181782	181782	0.18
AC Agg Gradation*Subgrade Material	1	1261646	1261646	1261646	1.26
AC Eff. Binder*SPV Binder Grade	1	3621	3621	3621	0
AC Eff. Binder*AC Air Voids	1	92815802	92815802	92815802	92.93
AC Eff. Binder*Base Thickness	1	1103167	1103167	1103167	1.1
AC Eff. Binder*Base Material	1	13107983	13107983	13107983	13.12
AC Eff. Binder*Subbase Thickness	1	6300865	6300865	6300865	6.31
AC Eff. Binder*Subbase Material	1	1484400	1484400	1484400	1.49
AC Eff. Binder*Subgrade Material	1	14960300	14960300	14960300	14.98
SPV Binder Grade*AC Air Voids	1	299	299	299	0
SPV Binder Grade*Base Thickness	1	1228	1228	1228	0
SPV Binder Grade*Base Material	1	52691	52691	52691	0.05
SPV Binder Grade*Subbase Thickness	1	362828	362828	362828	0.36
SPV Binder Grade*Subbase Material	1	28113	28113	28113	0.03
SPV Binder Grade*Subgrade Material	1	1136201	1136201	1136201	1.14
AC Air Voids*Base Thickness	1	15584596	15584596	15584596	15.6
AC Air Voids*Base Material	1	2.4E+08	2.4E+08	2.4E+08	240.11
AC Air Voids*Subbase Thickness	1	6849577	6849577	6849577	6.86
AC Air Voids*Subbase Material	1	1.99E+08	1.99E+08	1.99E+08	198.84
AC Air Voids*Subgrade Material	1	2.62E+08	2.62E+08	2.62E+08	261.84
Base Thickness*Base Material	1	43584033	43584033	43584033	43.64
Base Thickness*Subbase Thickness	1	4976050	4976050	4976050	4.98
Base Thickness*Subbase Material	1	46801978	46801978	46801978	46.86

Table 9.6 (continued). Analysis of Variance for Longitudinal Cracking at 20 years, using Adjusted SS for Tests

Source	DF	Seq SS	Adj SS	Adj MS	F
Base Thickness*Subgrade Material	1	299891	299891	299891	0.3
Base Material*Subbase Thickness	1	1370952	1370952	1370952	1.37
Base Material*Subbase Material	1	14961383	14961383	14961383	14.98
Base Material*Subgrade Material	1	9685169	9685169	9685169	9.7
Subbase Thickness*Subbase Material	1	4413519	4413519	4413519	4.42
Subbase Thickness*Subgrade Material	1	40243342	40243342	40243342	40.29
Subbase Material*Subgrade Material	1	191657	191657	191657	0.19
Error 2	994	2.99E+09	2.99E+09	998792	
Total 3	71	3.35E+10			

9.5 EFFECT OF INPUT VARIABLES ON TRANSVERSE CRACKING

9.5.1 Main Effects

ME-PDG predicted appreciable transverse cracking in almost all the cases, as shown in Figure9.7. The maximum transverse cracking was over 1900 ft/mi, which would translate into approximate crack spacing of 38ft. Figure 9.8 shows the trends for all the main effects and Table 9.7 lists the magnitude of main effects at different times during the life of the pavement. As would be expected binder grade has significant impact on transverse cracking performance of the pavements analyzed. Superpave recommends very specific grades of asphalt for each climatic zone. Within the range of present analysis it can be said that the Superpave asphalt grading system is very important for the good performance of Superpave mixes in terms of transverse cracking.

AC thickness, AC binder content and AC air voids also significantly affect transverse cracking performance, although to a lesser degree than asphalt grade. Aggregate gradation of asphalt layer also has some significance in this regard but to a much lesser degree. As expected base and subbase thickness and material for these layers do not seem to affect transverse cracking performance to any significant degree. Subgrade material also does not have any affect. This is explained by the fact that transverse cracking occurs because of contraction of asphalt layer and stiffening of the binder in severe winters. The lower layers, namely base, subbase and subgrade have very little to do with this phenomena except for providing friction resistance to the top asphalt layer.

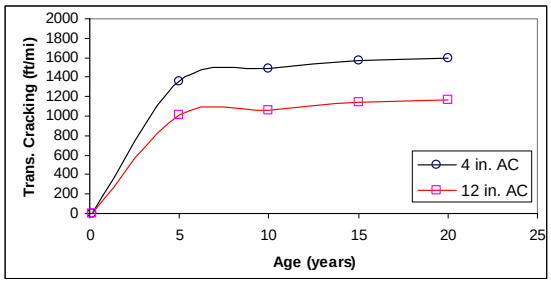

(a) Effect of Thickness on transv. cracking

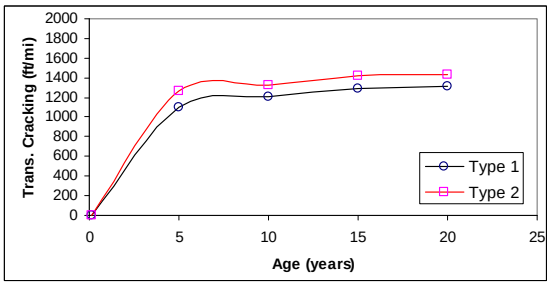

(b) Effect of AC agg. Gradation on transv. cracking

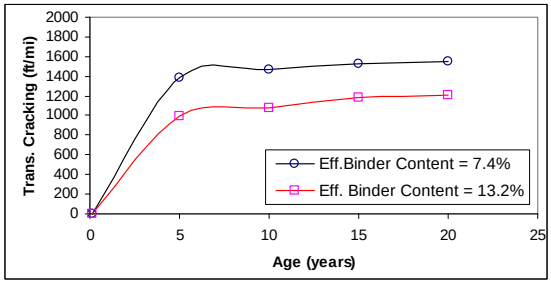

(c) Effect of AC binder content on transv. cracking

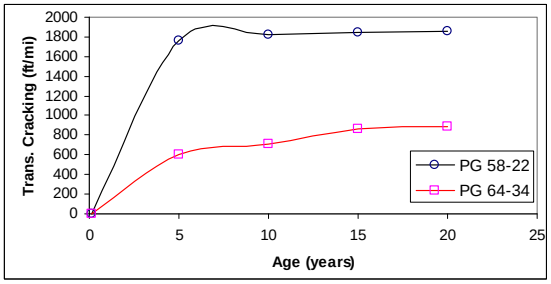

(d) Effect of AC binder grade on transv. cracking

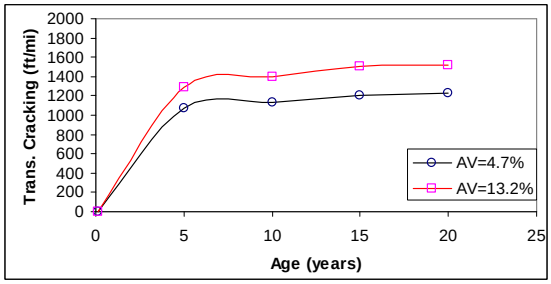

(e) Effect of AC air voids on transv. cracking

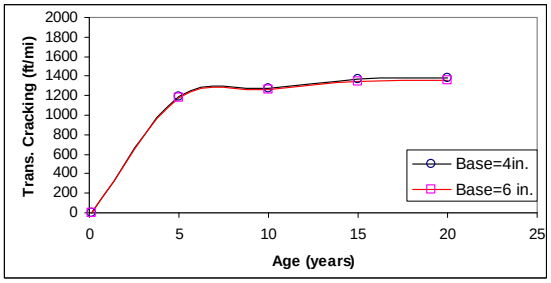

(f) Effect of base thickness on transv. cracking

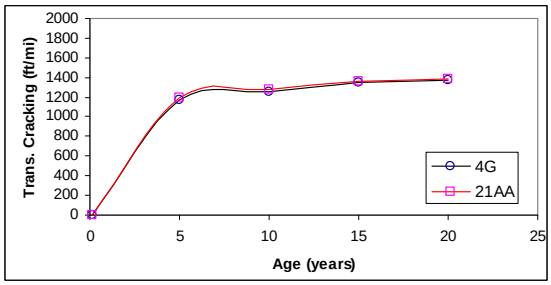

(g) Effect of base material on transv. cracking

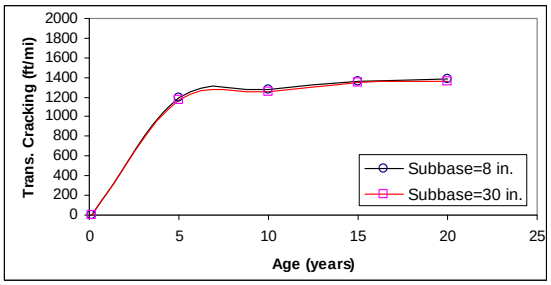

(h) Effect of subbase thickness on transv. cracking

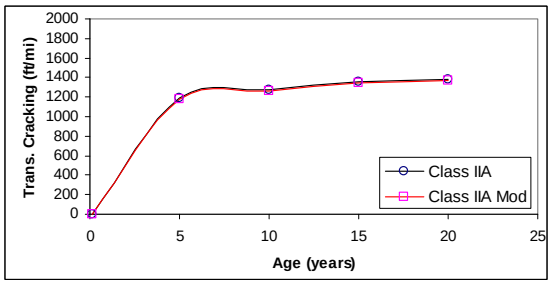

(i) Effect of subbase material on transv. cracking

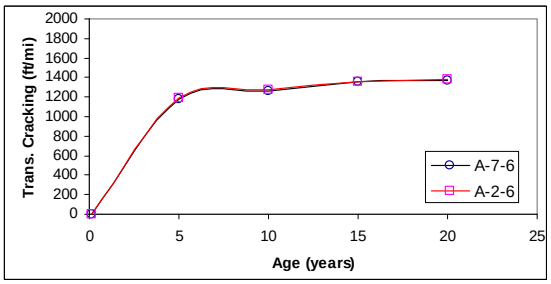

(j) Effect of subgrade material on transv. cracking

Figure9.7. Main effects of parameters on transverse cracking

Table 9.7. Main effects of input variables on transverse cracking

Input Variable	Levels	Transv. Cracking					Mean Differences				
		1 month	5 years	10 years	15 years	20 years	$\Delta_{1/12}$	Δ_5	Δ_{10}	Δ_{15}	Δ_{20}
AC Thickness (inches)	4	0	1358	1484	1572	1594					
	12	0	1015	1060	1148	1163	0	343	425	424	431
AC Agg Gradation	Level 1	0	1104	1208	1295	1315					
	Level 2	0	1261	1327	1415	1432	0	-157	-119	-120	-117
AC Effective Binder	7.4	0	1382	1467	1530	1549					
	13.2	0	990	1075	1187	1205	0	392	392	343	344
AC SPV Grade	PG 58-22	0	1762	1821	1843	1854					
	PG 64-34	0	604	714	867	893	0	1158	1106	975	961
AC Air Voids	4.7	0	1067	1130	1201	1223					
	11.4	0	1293	1401	1506	1521	0	-226	-272	-306	-298
Base Thickness	4	0	1192	1279	1366	1386					
	6	0	1173	1256	1344	1361	0	19	22	22	25
Base Material	Level 1	0	1169	1257	1348	1367					
	Level 2	0	1196	1278	1362	1380	0	-28	-22	-15	-13
Subbase thickness	8	0	1191	1279	1365	1385					
	30	0	1174	1256	1345	1362	0	18	23	20	23
Subbase Material	Level 1	0	1192	1273	1359	1378					
	Level 2	0	1174	1263	1351	1368	0	17	10	8	10
Subgrade Material	Level 1	0	1179	1263	1352	1371					
	Level 2	0	1186	1272	1358	1376	0	-7	-9	-6	-6

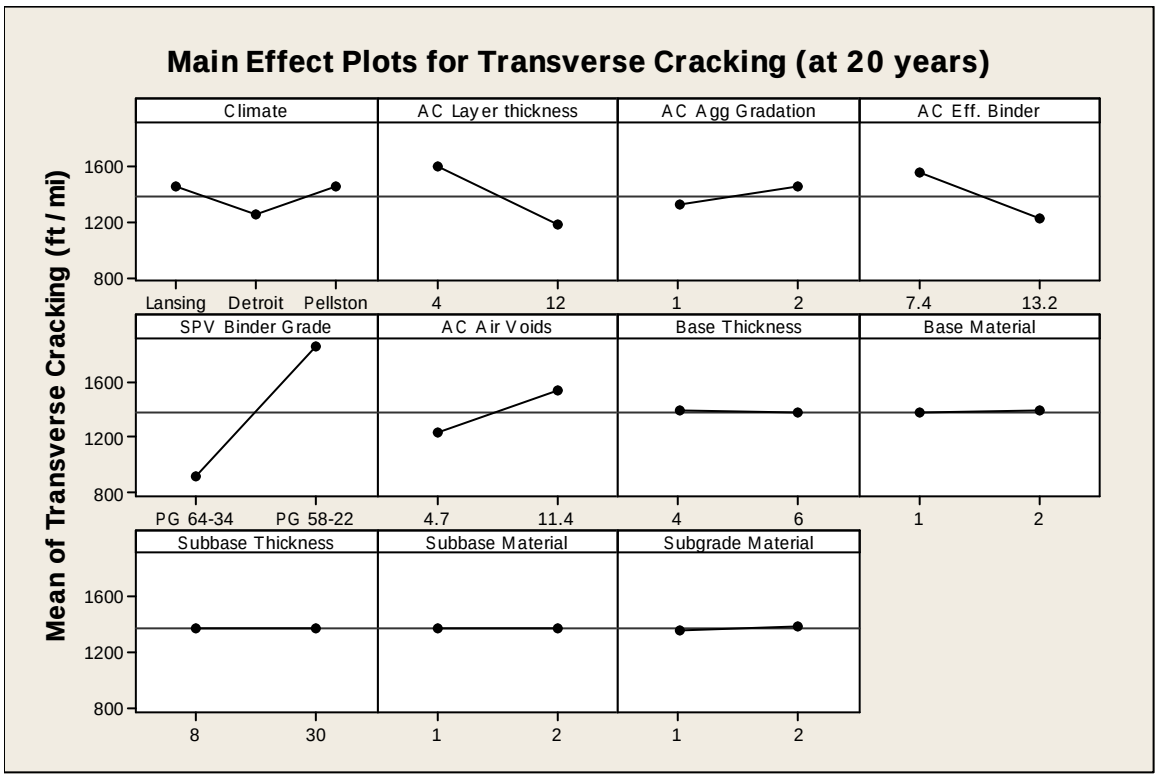

Figure 9.8. Main effects of input variables on transverse cracking

9.5.2 Interaction Effects

Figure 9.9 shows all the two-way interaction plots. Table 9.8 shows the ANOVA calculations for main as well as interaction effects on transverse cracking. ANOVA shows that the effect of binder grade interacts most significantly with those of AC air voids and AC aggregate gradations. The effect of binder grade also has interaction with that of the effective binder content. All other interactions are practically negligible.

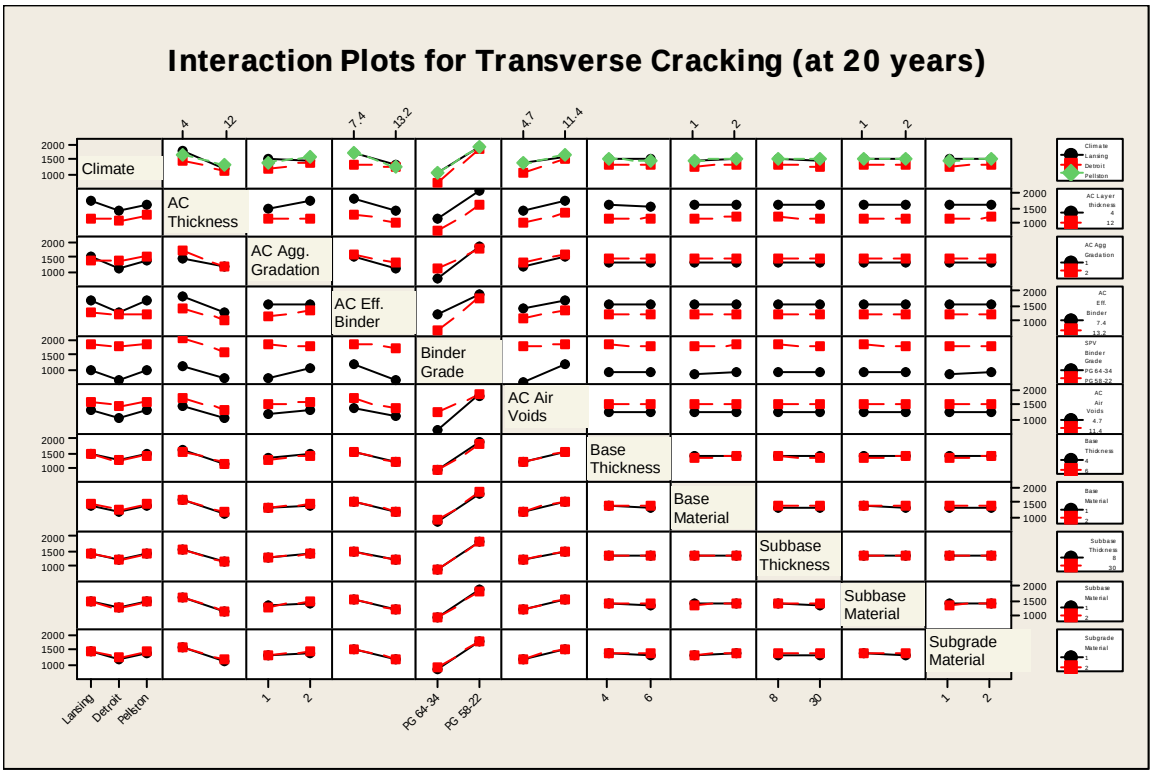

Figure 9.9. Interaction plots for transverse cracking at the end of 20 years

Table 9.8. Analysis of Variance for Transverse Cracking at 20 years, using Adjusted SS for Tests

Source	DF	Seq SS	Adj SS	Adj MS	F
Climate	2	30055916	30055916	15027958	123.26
AC Layer thickness	1	1.42E+08	1.42E+08	1.42E+08	1165.74
AC Agg Gradation	1	12623328	12623328	12623328	103.54
AC Eff. Binder	1	88921650	88921650	88921650	729.36
SPV Binder Grade	1	6.92E+08	6.92E+08	6.92E+08	5675.71
AC Air Voids	1	74511891	74511891	74511891	611.17
Base Thickness	1	147280	147280	147280	1.21

Table 9.8. (contd.) Analysis of Variance for Transverse Cracking at 20 years, using Adjusted SS for Tests

Source	DF	Seq SS	Adj SS	Adj MS	F
Base Material	1	441205	441205	441205	3.62
Subbase Thickness	1	100454	100454	100454	0.82
Subbase Material	1	1124	1124	1124	0.01
Subgrade Material	1	225613	225613	225613	1.85
Climate*AC Layer thickness	2	8116077	8116077	4058038	33.29
Climate*AC Agg Gradation	2	17886380	17886380	8943190	73.35
Climate*AC Eff. Binder	2	23456668	23456668	11728334	96.2
Climate*SPV Binder Grade	2	10174880	10174880	5087440	41.73
Climate*AC Air Voids	2	5429964	5429964	2714982	22.27
Climate*Base Thickness	2	414384	414384	207192	1.7
Climate*Base Material	2	14094	14094	7047	0.06
Climate*Subbase Thickness	2	99121	99121	49560	0.41
Climate*Subbase Material	2	10589	10589	5295	0.04
Climate*Subgrade Material	2	33730	33730	16865	0.14
AC Layer thickness*AC Agg Gradation	1	12527051	12527051	12527051	102.75
AC Layer thickness*AC Eff. Binder	1	2692233	2692233	2692233	22.08
AC Layer thickness*SPV Binder Grade	1	224511	224511	224511	1.84
AC Layer thickness*AC Air Voids	1	435557	435557	435557	3.57
AC Layer thickness*Base Thickness	1	414620	414620	414620	3.4
AC Layer thickness*Base Material	1	7699	7699	7699	0.06
AC Layer thickness*	1	267	267	267	0
Subbase Thickness					
AC Layer thickness*Subbase Material	1	6820	6820	6820	0.06
AC Layer thickness*Subgrade Material	1	1749	1749	1749	0.01
AC Agg Gradation*AC Eff. Binder	1	3559717	3559717	3559717	29.2
AC Agg Gradation*SPV Binder Grade	1	32395750	32395750	32395750	265.72
AC Agg Gradation*AC Air Voids	1	1579817	1579817	1579817	12.96
AC Agg Gradation*Base Thickness	1	79631	79631	79631	0.65
AC Agg Gradation*Base Material	1	105229	105229	105229	0.86
AC Agg Gradation*Subbase Thickness	1	243613	243613	243613	2
AC Agg Gradation*Subbase Material	1	347389	347389	347389	2.85
AC Agg Gradation*Subgrade Material	1	76103	76103	76103	0.62
AC Eff. Binder*SPV Binder Grade	1	30966513	30966513	30966513	254
AC Eff. Binder*AC Air Voids	1	94618	94618	94618	0.78
AC Eff. Binder*Base Thickness	1	277227	277227	277227	2.27
AC Eff. Binder*Base Material	1	81423	81423	81423	0.67
AC Eff. Binder*Subbase Thickness	1	65598	65598	65598	0.54
AC Eff. Binder*Subbase Material	1	379668	379668	379668	3.11
AC Eff. Binder*Subgrade Material	1	106810	106810	106810	0.88
SPV Binder Grade*AC Air Voids	1	64443737	64443737	64443737	528.59
SPV Binder Grade*Base Thickness	1	2468	2468	2468	0.02
SPV Binder Grade*Base Material	1	202467	202467	202467	1.66
SPV Binder Grade*Subbase Thickness	1	48269	48269	48269	0.4

Table 9.8. (contd.) Analysis of Variance for Transverse Cracking at 20 years, using Adjusted SS for Tests

Source	DF	Seq SS	Adj SS	Adj MS	F
SPV Binder Grade*Subgrade Material	1	334219	334219	334219	2.74
AC Air Voids*Base Thickness	1	100125	100125	100125	0.82
AC Air Voids*Base Material	1	284	284	284	0
AC Air Voids*Subbase Thickness	1	61882	61882	61882	0.51
AC Air Voids*Subbase Material	1	1168	1168	1168	0.01
AC Air Voids*Subgrade Material	1	74146	74146	74146	0.61
Base Thickness*Base Material	1	265967	265967	265967	2.18
Base Thickness*Subbase Thickness	1	19	19	19	0
Base Thickness*Subbase Material	1	120294	120294	120294	0.99
Base Thickness*Subgrade Material	1	4839	4839	4839	0.04
Base Material*Subbase Thickness	1	61659	61659	61659	0.51
Base Material*Subbase Material	1	375163	375163	375163	3.08
Base Material*Subgrade Material	1	51914	51914	51914	0.43
Subbase Thickness*Subbase Material	1	20390	20390	20390	0.17
Subbase Thickness*Subgrade Material	1	76667	76667	76667	0.63
Subbase Material*Subgrade Material	1	114420	114420	114420	0.94
Error	2994	3.65E+08	3.65E+08	121917	
Total	3071	1.62E+09			

9.6 EFFECT OF INPUT VARIABLES ON RUTTING

9.6.1 Main Effects

As Figure 9.10 shows rutting predictions from M-E PDG program are very high in all the cases. It has been observed in other M-E PDG runs also that the rutting model used in M-E PDG over-predicts rutting. However, the results do show expected trends in relative terms for various input parameters analyzed in this study. Figure 9.11 shows the trends for all the main effects and Table 9.9 lists the magnitude of main effects at different times during the life of the pavement. Thickness of the asphalt layer and subgrade material combined with subgrade modulus have a significant influence on rutting performance of the pavements studied in this case. AC binder content, AC air voids, base and subabse material and their thicknesses also have appreciable influence on the amount of expected rutting in asphalt pavements. From Figure 9.10 it appears that asphalt layer aggregate gradation, binder grade and base thickness do not have much influence. But it should be noted, once again, that these inputs were varied to a much smaller degree in this sensitivity analysis than other inputs (to reflect Michigan conditions).

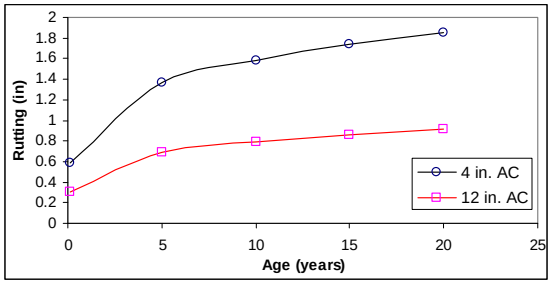

(a) Effect of Thickness on rutting

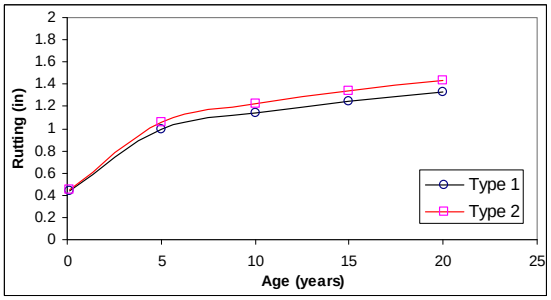

(b) Effect of AC agg. Gradation on rutting

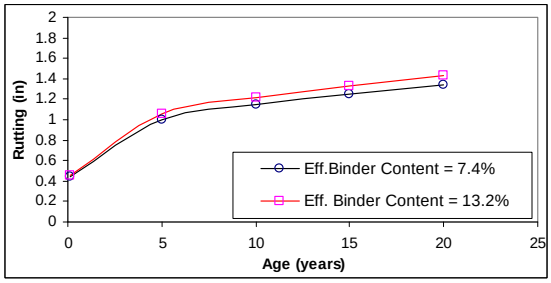

(c) Effect of AC binder content on rutting

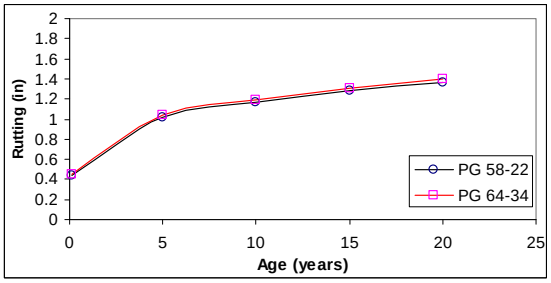

(d) Effect of AC binder grade on rutting

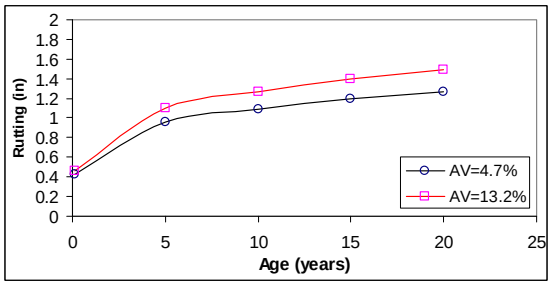

(e) Effect of AC air voids on rutting

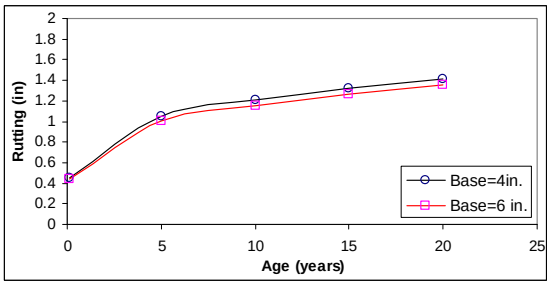

(f) Effect of base thickness on rutting

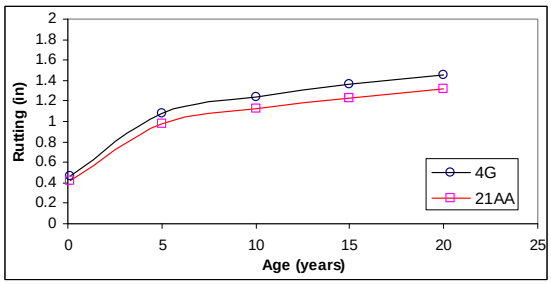

(g) Effect of base material on rutting

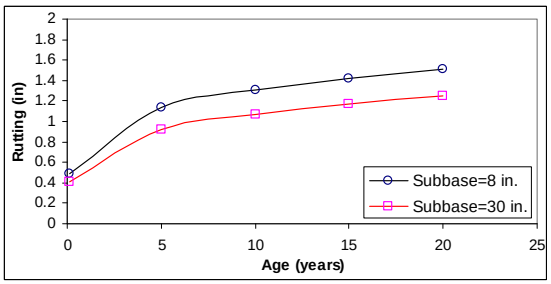

(h) Effect of subbase thickness on rutting

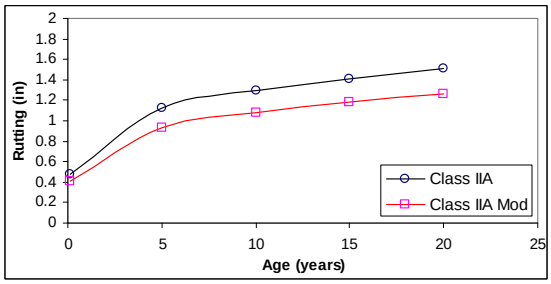

(i) Effect of subbase material on rutting

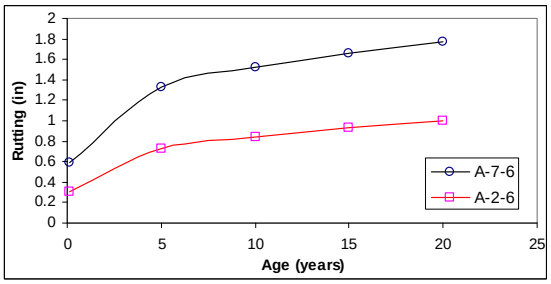

(j) Effect of subgrade material on rutting

Figure 9.10. Main effects of parameters on rutting

Table 9.9. Main effects of input variables on rutting

Input Variable	Levels	Rutting					Mean Differences				
		1 month	5 years	10 years	15 years	20 years	$\Delta_{1/12}$	Δ_5	Δ_{10}	Δ_{15}	Δ_{20}
AC Thickness (inches)	4	0.59	1.37	1.58	1.74	1.85					
	12	0.30	0.69	0.79	0.86	0.92	0.29	0.68	0.79	0.87	0.94
AC Agg Gradation	Level 1	0.44	0.99	1.14	1.25	1.33					
	Level 2	0.45	1.06	1.23	1.34	1.44	-0.02	-0.07	-0.09	-0.10	-0.11
AC Effective Binder Content	7.4	0.44	1.00	1.15	1.26	1.34					
	13.2	0.45	1.05	1.22	1.33	1.43	-0.01	-0.05	-0.07	-0.08	-0.09
AC SPV Grade	PG 58-22	0.43	1.02	1.17	1.28	1.37					
	PG 64-34	0.46	1.04	1.19	1.31	1.40	-0.02	-0.02	-0.02	-0.03	-0.03
AC Air Voids	4.7	0.43	0.96	1.09	1.19	1.27					
	11.4	0.46	1.10	1.27	1.40	1.49	-0.04	-0.14	-0.18	-0.20	-0.23
Base Thickness	4	0.45	1.05	1.21	1.32	1.41					
	6	0.44	1.01	1.16	1.27	1.35	0.02	0.05	0.05	0.06	0.06
Base Material	Level 1	0.47	1.08	1.24	1.36	1.45					
	Level 2	0.42	0.98	1.12	1.23	1.31	0.04	0.10	0.12	0.13	0.14
Subbase thickness	8	0.48	1.13	1.30	1.42	1.51					
	30	0.41	0.92	1.07	1.17	1.25	0.08	0.21	0.24	0.25	0.26
Subbase Material	Level 1	0.48	1.12	1.29	1.41	1.51					
	Level 2	0.41	0.93	1.08	1.18	1.26	0.07	0.19	0.22	0.23	0.25
Subgrade Material	Level 1	0.59	1.33	1.53	1.66	1.77					
	Level 2	0.30	0.73	0.84	0.93	1.00	0.29	0.61	0.68	0.73	0.77

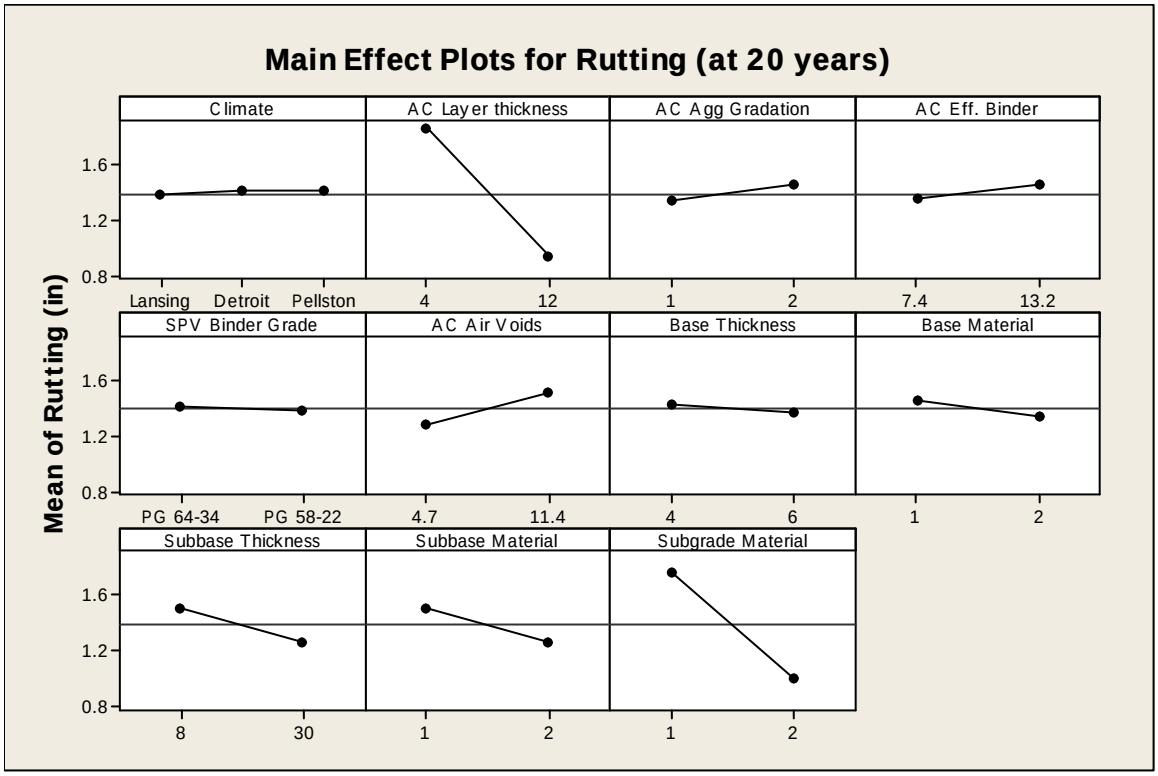

Figure 9.11. Main effects of input variables on rutting

9.6.2 Interaction Effects

Figure 9.12 shows all the two-way interaction plots. Table 9.10 shows the ANOVA calculations for main as well as interaction effects on rutting. The effect of subgrade material has significant interaction with those of subbase thickness and asphalt layer thickness. The effect of AC layer thickness also has appreciable interaction with the effects of subbase material, base material and subbase thickness in that order.

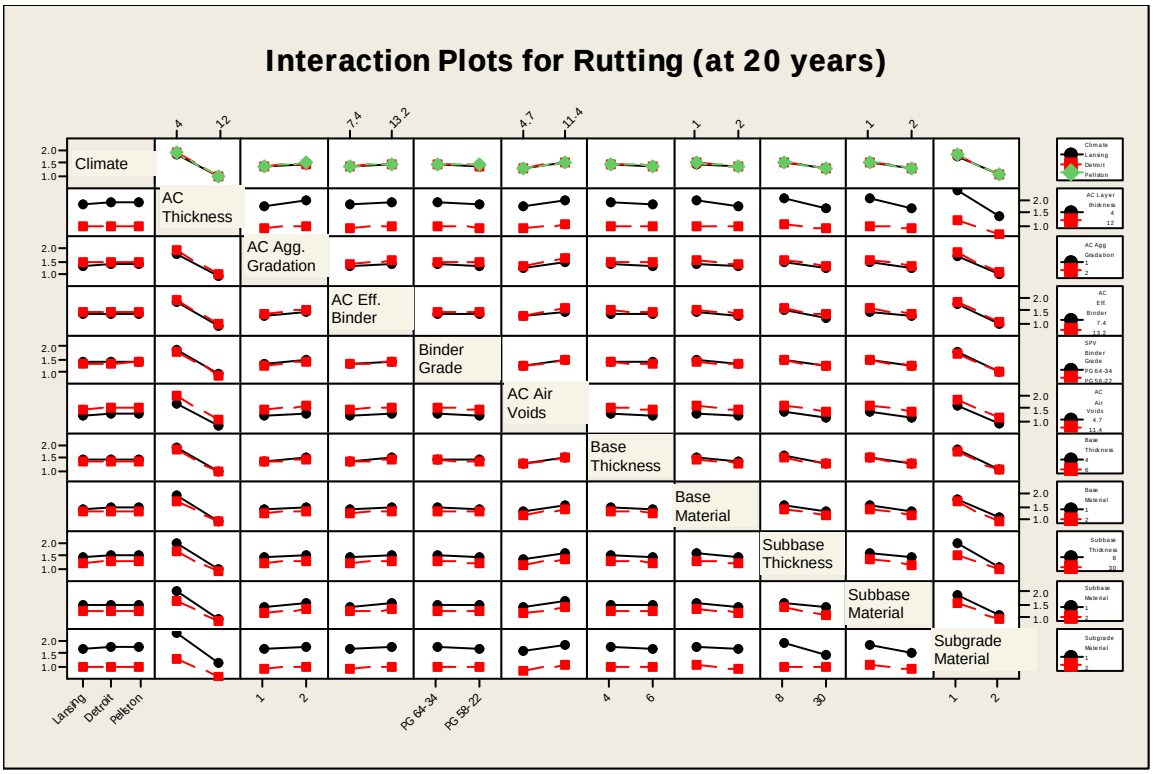

Figure 9.12. Interaction plots for rutting at the end of 20 years

Table 9.10. Analysis of Variance for Rutting 240, using Adjusted SS for Tests

Source	DF	Seq SS	Adj SS	Adj MS	F
Climate	2	0.687	0.687	0.344	38.22
AC Layer thickness	1	667.926	667.926	667.926	74284.51
AC Agg Gradation	1	10.861	10.861	10.861	1207.95
AC Eff. Binder	1	7.935	7.935	7.935	882.52
SPV Binder Grade	1	1.274	1.274	1.274	141.72
AC Air Voids	1	43.669	43.669	43.669	4856.73
Base Thickness	1	1.914	1.914	1.914	212.92

Table 9.10. (contd.) Analysis of Variance for Rutting 240, using Adjusted SS for Tests

Source	DF	Seq SS	Adj SS	Adj MS	F
Subbase Thickness	1	49.217	49.217	49.217	5473.73
Subbase Material	1	43.063	43.063	43.063	4789.34
Subgrade Material	1	442.71	442.71	442.71	49236.74
Climate*AC Layer thickness	2	0.281	0.281	0.14	15.62
Climate*AC Agg Gradation	2	0.052	0.052	0.026	2.92
Climate*AC Eff. Binder	2	0.066	0.066	0.033	3.65
Climate*SPV Binder Grade	2	0	0	0	0.02
Climate*AC Air Voids	2	0.001	0.001	0	0.04
Climate*Base Thickness	2	0.003	0.003	0.002	0.17
Climate*Base Material	2	0.002	0.002	0.001	0.09
Climate*Subbase Thickness	2	0.03	0.03	0.015	1.69
Climate*Subbase Material	2	0.011	0.011	0.006	0.63
Climate*Subgrade Material	2	0.022	0.022	0.011	1.2
AC Layer thickness*AC Agg Gradation	1	2.123	2.123	2.123	236.15
AC Layer thickness*AC Eff. Binder	1	1.034	1.034	1.034	115.03
AC Layer thickness*SPV Binder Grade	1	0.003	0.003	0.003	0.33
AC Layer thickness*AC Air Voids	1	3.092	3.092	3.092	343.85
AC Layer thickness*Base Thickness	1	0.724	0.724	0.724	80.53
AC Layer thickness*Base Material	1	7.635	7.635	7.635	849.16
AC Layer thickness*	1	6.78	6.78	6.78	754.08
Subbase Thickness					
AC Layer thickness*Subbase Material	1	11.122	11.122	11.122	1236.9
AC Layer thickness*Subgrade Material	1	37.263	37.263	37.263	4144.21
AC Agg Gradation*AC Eff. Binder	1	0.228	0.228	0.228	25.34
AC Agg Gradation*SPV Binder Grade	1	0.196	0.196	0.196	21.76
AC Agg Gradation*AC Air Voids	1	0.963	0.963	0.963	107.08
AC Agg Gradation*Base Thickness	1	0.012	0.012	0.012	1.38
AC Agg Gradation*Base Material	1	0.061	0.061	0.061	6.78
AC Agg Gradation*Subbase Thickness	1	0.017	0.017	0.017	1.93
AC Agg Gradation*Subbase Material	1	0.096	0.096	0.096	10.67
AC Agg Gradation*Subgrade Material	1	0.096	0.096	0.096	10.69
AC Eff. Binder*SPV Binder Grade	1	0.088	0.088	0.088	9.74
AC Eff. Binder*AC Air Voids	1	1.321	1.321	1.321	146.89
AC Eff. Binder*Base Thickness	1	0.011	0.011	0.011	1.28
AC Eff. Binder*Base Material	1	0.041	0.041	0.041	4.59
AC Eff. Binder*Subbase Thickness	1	0	0	0	0.03
AC Eff. Binder*Subbase Material	1	0.044	0.044	0.044	4.93
AC Eff. Binder*Subgrade Material	1	0.051	0.051	0.051	5.67
SPV Binder Grade*AC Air Voids	1	0.001	0.001	0.001	0.1
SPV Binder Grade*Base Thickness	1	0.038	0.038	0.038	4.22
SPV Binder Grade*Base Material	1	0.028	0.028	0.028	3.07
SPV Binder Grade*Subbase Thickness	1	0	0	0	0.01
SPV Binder Grade*Subbase Material	1	0.083	0.083	0.083	9.25
SPV Binder Grade*Subgrade Material	1	0.171	0.171	0.171	19.05

Table 9.10. (contd.) Analysis of Variance for Rutting 240, using Adjusted SS for Tests

Source	DF	Seq SS	Adj SS	Adj MS	F
AC Air Voids*Base Material	1	0.319	0.319	0.319	35.53
AC Air Voids*Subbase Thickness	1	0.048	0.048	0.048	5.36
AC Air Voids*Subbase Material	1	0.093	0.093	0.093	10.32
AC Air Voids*Subgrade Material	1	0.4	0.4	0.4	44.49
Base Thickness*Base Material	1	0.623	0.623	0.623	69.25
Base Thickness*Subbase Thickness	1	0.098	0.098	0.098	10.87
Base Thickness*Subbase Material	1	0.034	0.034	0.034	3.81
Base Thickness*Subgrade Material	1	0.531	0.531	0.531	59.02
Base Material*Subbase Thickness	1	0.095	0.095	0.095	10.54
Base Material*Subbase Material	1	0.245	0.245	0.245	27.24
Base Material*Subgrade Material	1	0.207	0.207	0.207	23.04
Subbase Thickness*Subbase Material	1	3.116	3.116	3.116	346.58
Subbase Thickness*Subgrade Material	1	38.643	38.643	38.643	4297.74
Subbase Material*Subgrade Material	1	4.059	4.059	4.059	451.45
Error	2994	26.92	26.92	0.009	
Total	3071	1430.986			

9.7 EFFECT OF INPUT VARIABLES ON IRI

9.7.1 Main Effects

IRI of any pavement changes as a result of many distresses that appear on the pavements because of traffic loading, environmental influences and pavement material behavior in different situations. Therefore, individual differences in other forms of distresses discussed above would have their influence on IRI as well.

The plots in Figure 9.13 show the average effect of different input variables on IRI. Figure 9.14 shows the trends for all the main effects and Table 9.11 lists the magnitude of main effects at different times during the life of the pavement. Almost all the ten input variables being studied here except asphalt grade and base thickness (within the limited range studied) have significant influence on IRI. The two levels used for asphalt grade were PG 58-22 and PG 64-34. Therefore, there was only one grade difference in the high temperature of these two grades. Base thickness was only varied from 4 to 6 inches; hence the small difference in performance.

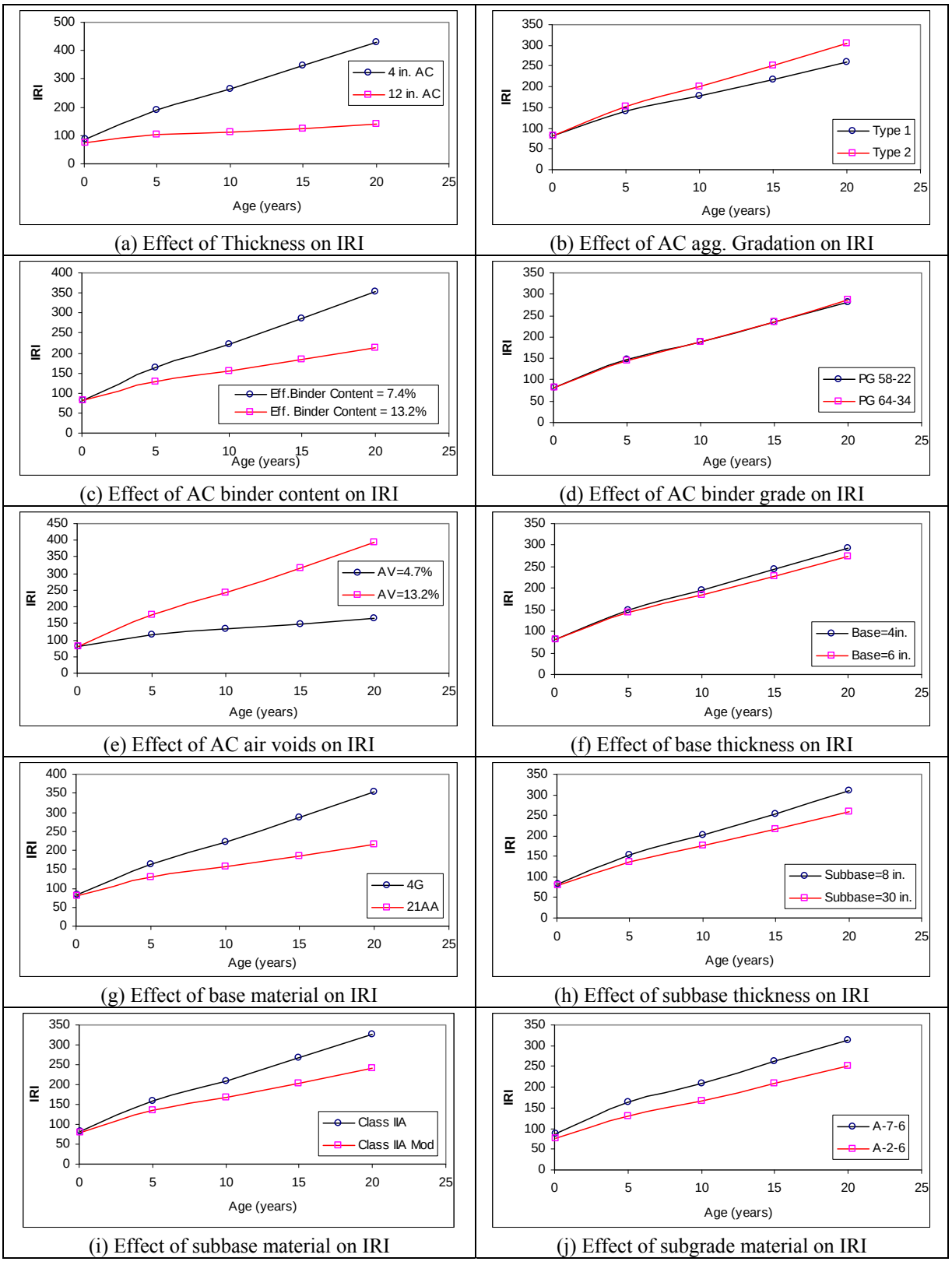

(a) Effect of Thickness on IRI

(b) Effect of AC agg. Gradation on IRI

(c) Effect of AC binder content on IRI

(d) Effect of AC binder grade on IRI

(e) Effect of AC air voids on IRI

(f) Effect of base thickness on IRI

(g) Effect of base material on IRI

(h) Effect of subbase thickness on IRI

(i) Effect of subbase material on IRI

(j) Effect of subgrade material on IRI

Figure 9.13. Main effects of parameters on IRI

Table 9.11. Main effects of input variables on IRI

Input Variable	Levels	IRI					Mean Differences				
		1 month	5 years	10 years	15 years	20 years	$\Delta_{1/12}$	Δ_5	Δ_{10}	Δ_{15}	Δ_{20}
AC Thickness (inches)	4	87.6	190.9	264.5	345.1	429.0					
	12	74.6	102.1	113.4	125.8	138.6	13.0	88.7	151.1	219.3	290.5
AC Agg Gradation	Level 1	80.9	139.9	177.4	218.6	261.0					
	Level 2	81.3	152.7	200.0	251.7	305.9	-0.4	-12.8	-22.6	-33.0	-44.9
AC Effective Binder Content	7.4	81.2	163.5	221.7	286.0	353.2					
	13.2	80.9	129.3	155.9	184.6	214.0	0.3	34.3	65.7	101.3	139.1
AC SPV Grade	PG 58-22	80.7	149.0	189.9	234.4	281.2					
	PG 64-34	81.4	143.7	187.6	236.1	285.8	-0.6	5.3	2.3	-1.7	-4.7
AC Air Voids	4.7	80.1	116.5	132.2	148.9	166.0					
	11.4	82.0	174.8	242.6	317.4	395.3	-1.9	-58.3	-110.4	-168.6	-229.3
Base Thickness	4	81.7	149.5	194.1	243.0	293.8					
	6	80.4	143.2	183.3	227.4	273.2	1.2	6.4	10.8	15.6	20.6
Base Material	Level 1	82.3	164.1	222.0	286.0	352.3					
	Level 2	79.8	128.6	155.5	184.6	214.8	2.5	35.5	66.5	101.4	137.5
Subbase thickness	8	82.9	155.0	202.5	254.6	308.8					
	30	79.3	137.8	175.0	215.9	258.3	3.6	17.2	27.5	38.7	50.5
Subbase Material	Level 1	82.8	158.7	210.2	266.9	325.6					
	Level 2	79.3	134.1	167.3	203.7	241.5	3.4	24.6	42.9	63.1	84.1
Subgrade Material	Level 1	87.1	162.3	209.7	261.3	314.6					
	Level 2	75.0	130.5	167.9	209.4	252.6	12.1	31.8	41.7	51.9	62.0

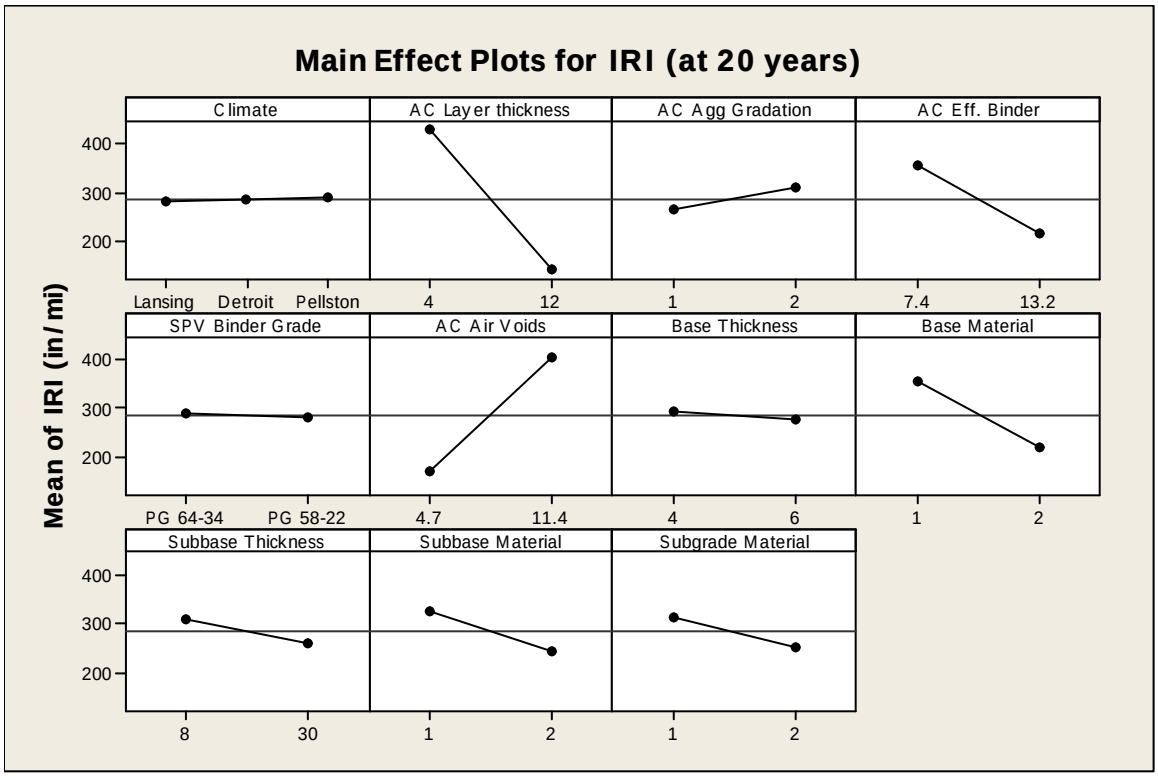

Figure 9.14. Main effects of input variables on IRI

9.7.2 Interaction Effects

Figure 9.15 shows all the two-way interaction plots. Table 9.12 shows the ANOVA calculations for main as well as interaction effects on IRI. ANOVA calculations in Table 9.12 show that interaction of effects of AC layer thickness and AC air voids is much more significant than all other interactions in the case of IRI. Effects of AC layer thickness also have interaction with effects of AC effective binder content, base material and subbase material although to a lesser degree. Effects of AC effective binder content and base material also interact to an appreciable degree.

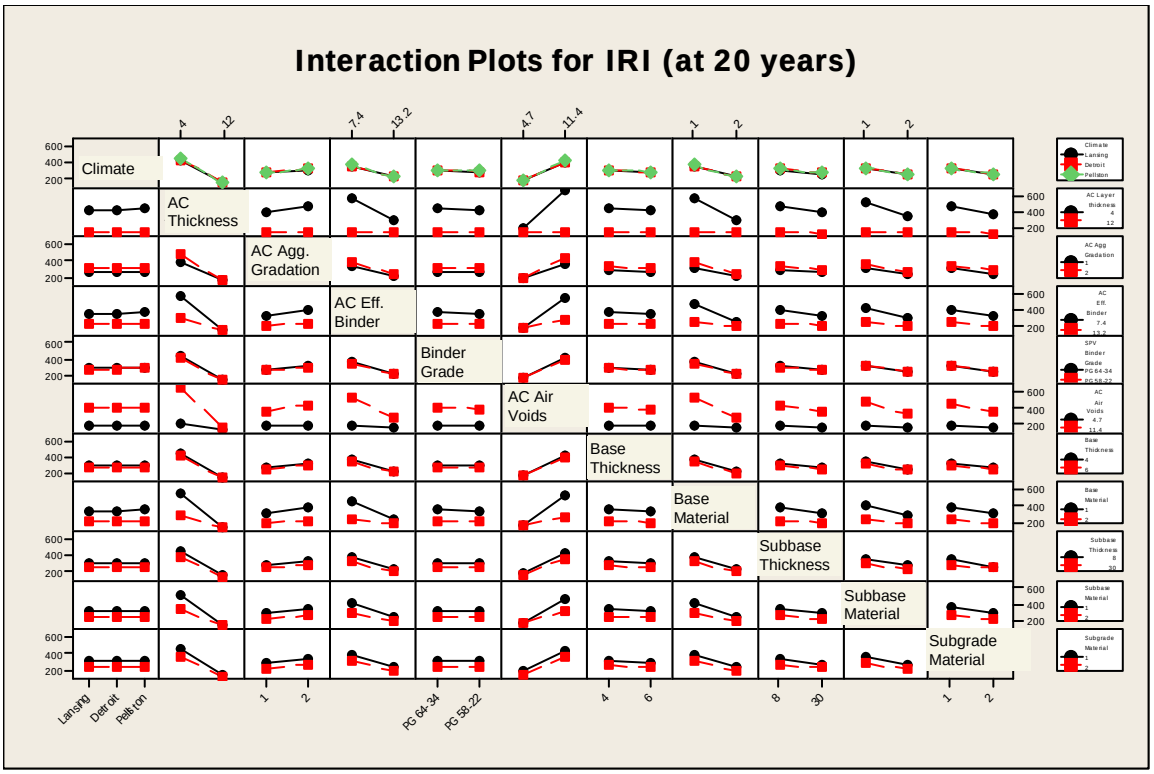

Figure 9.15. Interaction plots for IRI at the end of 20 years

Table 9.12. Analysis of Variance for IRI at 20 years, using Adjusted SS for Tests

Source	DF	Seq SS	Adj SS	Adj MS	F
Climate	2	32811	32811	16406	0.79
AC Layer thickness	1	64430412	64430412	64430412	3103.42
AC Agg Gradation	1	1656180	1656180	1656180	79.77
AC Eff. Binder	1	14604589	14604589	14604589	703.46
SPV Binder Grade	1	28615	28615	28615	1.38
AC Air Voids	1	42923124	42923124	42923124	2067.48
Base Thickness	1	285203	285203	285203	13.74

Table 9.12.(contd.) Analysis of Variance for IRI at 20 years, using Adjusted SS for Tests

Source	DF	Seq SS	Adj SS	Adj MS	F
Base Material	1	14255361	14255361	14255361	686.64
Subbase Thickness	1	1860119	1860119	1860119	89.6
Subbase Material	1	5267165	5267165	5267165	253.7
Subgrade Material	1	2842614	2842614	2842614	136.92
Climate*AC Layer thickness	2	21125	21125	10562	0.51
Climate*AC Agg Gradation	2	3834	3834	1917	0.09
Climate*AC Eff. Binder	2	14915	14915	7457	0.36
Climate*SPV Binder Grade	2	380	380	190	0.01
Climate*AC Air Voids	2	18170	18170	9085	0.44
Climate*Base Thickness	2	464	464	232	0.01
Climate*Base Material	2	16933	16933	8467	0.41
Climate*Subbase Thickness	2	605	605	303	0.01
Climate*Subbase Material	2	3402	3402	1701	0.08
Climate*Subgrade Material	2	787	787	394	0.02
AC Layer thickness*AC Agg Gradation	1	1511630	1511630	1511630	72.81
AC Layer thickness*AC Eff. Binder	1	14231773	14231773	14231773	685.5
AC Layer thickness*SPV Binder Grade	1	93456	93456	93456	4.5
AC Layer thickness*AC Air Voids	1	39166117	39166117	39166117	1886.51
AC Layer thickness*Base Thickness	1	258073	258073	258073	12.43
AC Layer thickness*Base Material	1	13882648	13882648	13882648	668.68
AC Layer thickness*	1	1002118	1002118	1002118	48.27
Subbase Thickness					
AC Layer thickness*Subbase Material	1	4742041	4742041	4742041	228.41
AC Layer thickness*Subgrade Material	1	1087863	1087863	1087863	52.4
AC Agg Gradation*AC Eff. Binder	1	304066	304066	304066	14.65
AC Agg Gradation*SPV Binder Grade	1	3803	3803	3803	0.18
AC Agg Gradation*AC Air Voids	1	1123238	1123238	1123238	54.1
AC Agg Gradation*Base Thickness	1	2556	2556	2556	0.12
AC Agg Gradation*Base Material	1	520081	520081	520081	25.05
AC Agg Gradation*Subbase Thickness	1	21849	21849	21849	1.05
AC Agg Gradation*Subbase Material	1	103924	103924	103924	5.01
AC Agg Gradation*Subgrade Material	1	2645	2645	2645	0.13
AC Eff. Binder*SPV Binder Grade	1	41677	41677	41677	2.01
AC Eff. Binder*AC Air Voids	1	11993213	11993213	11993213	577.68
AC Eff. Binder*Base Thickness	1	83191	83191	83191	4.01
AC Eff. Binder*Base Material	1	4007007	4007007	4007007	193.01
AC Eff. Binder*Subbase Thickness	1	308808	308808	308808	14.87
AC Eff. Binder*Subbase Material	1	1448975	1448975	1448975	69.79
AC Eff. Binder*Subgrade Material	1	288814	288814	288814	13.91
SPV Binder Grade*AC Air Voids	1	117304	117304	117304	5.65
SPV Binder Grade*Base Thickness	1	2245	2245	2245	0.11
SPV Binder Grade*Base Material	1	33091	33091	33091	1.59
SPV Binder Grade*Subbase Thickness	1	4541	4541	4541	0.22

Table 9.12.(contd.) Analysis of Variance for IRI at 20 years, using Adjusted SS for Tests

Source	DF	Seq SS	Adj SS	Adj MS	F
SPV Binder Grade*Subbase Material	1	5899	5899	5899	0.28
SPV Binder Grade*Subgrade Material	1	2939	2939	2939	0.14
AC Air Voids*Base Thickness	1	181946	181946	181946	8.76
AC Air Voids*Base Material	1	11297821	11297821	11297821	544.18
AC Air Voids*Subbase Thickness	1	807678	807678	807678	38.9
AC Air Voids*Subbase Material	1	3479390	3479390	3479390	167.59
AC Air Voids*Subgrade Material	1	553338	553338	553338	26.65
Base Thickness*Base Material	1	14404	14404	14404	0.69
Base Thickness*Subbase Thickness	1	41003	41003	41003	1.98
Base Thickness*Subbase Material	1	171158	171158	171158	8.24
Base Thickness*Subgrade Material	1	38419	38419	38419	1.85
Base Material*Subbase Thickness	1	260679	260679	260679	12.56
Base Material*Subbase Material	1	1229564	1229564	1229564	59.22
Base Material*Subgrade Material	1	324293	324293	324293	15.62
Subbase Thickness*Subbase Material	1	34	34	34	0
Subbase Thickness*Subgrade Material	1	929379	929379	929379	44.77
Subbase Material*Subgrade Material	1	300234	300234	300234	14.46
Error 2	994	62158818	62158818	20761	
Total 3	71	3.26E+08			

9.8 CONCLUSION

Preliminary sensitivity analysis identified eleven variables which have significant influence on flexible pavement performance. A full factorial matrix was constructed for all these variables with three levels for climate and two levels each for all the other ten variables. The matrix therefore had 3072 sets of inputs leading to 3072 M-E PDG runs. The performance predicted by M-E PDG for all these runs were analyzed using statistical methods for each of the five performance measures, namely fatigue cracking, longitudinal cracking, transverse cracking, rutting and IRI. The absolute and relative effects of each of the variables were determined. The results from detailed sensitivity analysis – flexible pavements confirmed the conclusions derived from the preliminary sensitivity analysis. The table of these significant variables has been presented in the beginning of the chapter (Table 9.1). In addition to this confirmation, this analysis also gave further insight into the magnitude of effects. ANOVA for the runs gave insight into the interaction of effects of different variables for each of the performance measures. Apart from the main effects only two-way interactions were found to be significant. In other words interactions between sets of three or more variables were found to be not significant.

CHAPTER 10 - SATELLITE STUDIES - FLEXIBLE

10.1 INTRODUCTION

One of the objectives in this project involved evaluating the reasonableness of M-E Design Guide damage and performance equations. The steps to achieving that objective involved

(a) Preparation of initial sensitivity test matrix
(b) Input variable ranges for robustness
(c) Determination of significance for input variables on pavement performance

As the first step, the practical ranges (levels) of input variables for the preliminary sensitivity analysis were identified. This was followed by the preparation of a test matrix followed by a preliminary sensitivity study. This sensitivity analysis had been separately carried out for each of the inputs for flexible pavements in the MEPDG software. This helped identify the variables which seemed to affect performance appreciably. It was also decided that certain variables, although distinct inputs for the software, could be grouped together and treated as one variable for the purpose of the detailed sensitivity analysis. Finally 12 variables or groups of variables were identified for the detailed sensitivity analysis as shown in Table 10.1.

As stated earlier in this report two levels were to be determined for each of the identified variables for the detailed sensitivity analysis except for the climatic region which was to have three. It was further decided that the effect of creep compliance and average tensile strength would be studied separately as a satellite study. Creep compliance and tensile strength are used in the thermal cracking model of ME-PDG. The results of the satellite study on thermal cracking are presented in this chapter.

All the runs in the detailed sensitivity analysis were carried out using level 3 analysis of M-E PDG software. In that case the user does not need to input the values of complex modulus of the asphalt layers. Material and mixture properties are used instead to estimate complex modulus of asphalt concrete. Complex modulus is a crucial input for the distress models used by the software. Therefore, it was decided that a satellite study be done to better understand the sensitivity of predicted distresses to complex modulus. The details and results from this study are also presented in this chapter.

Table 10.1. Variables identified for detailed sensitivity analysis (upper and lower levels)

Cluster		Surrogate Variable		Lower Level	Upper Level	Var no.
Materials	Asphalt Mix	Layer thickness (in.)		4	12	1
		Aggregate Gradation	Cum. % Retained on 3/4 in.	12	0	2
			Cum. % Retained on 3/8 in.	25	10	
			Cum. % Retained on #4 Sieve	35	30	
			% Passing #200 Sieve	7	3	
		Effective Binder Content (%)		7.4 (Pbe = 3.7)	13.2 (Pbe = 6.6)	3
		Superpave Binder Grade		PG 64-34	PG 58-22	4
		Air Voids (%)		4.7	11.4	5
	Base	Thickness (in)		4	6	6
		Material Type		4 G	21 AA	7
		Gradation*	% Passing 37.5 mm Sieve	100	100	
			% Passing 25 mm Sieve		92.5	
			% Passing 19 mm Sieve	70		
			% Passing 12.5 mm Sieve	50	62.5	
			% Passing 2.36 mm Sieve	17.5	32.5	
			% Passing 0.6 mm Sieve	11.5		
			% Passing #200 Sieve	6	6	
		Modulus (psi)		10000	35000	
	Subbase	Thickness (in)		8	30	8
		Material Type		Class II	Class II	9
		Gradation*	% Passing 37.5 mm Sieve	100	100	
			% Passing 25 mm Sieve	60	100	
			% Passing 12.5 mm Sieve			
			% Passing 2.36 mm Sieve			
			% Passing 0.6 mm Sieve			
			% Passing 0.15 mm Sieve	10	30	
			% Passing #200 Sieve	2	10	
		Modulus (psi)		5000	15000	
	Subgrade	MaterialType		A-7-6	A-2-6	10
		Gradation*	% Passing 37.5 mm Sieve	99	100	
			% Passing 25 mm Sieve	98	100	
			% Passing 12.5 mm Sieve	95	80	
			% Passing 2.36 mm Sieve	85	50	
			% Passing 0.6 mm Sieve	83	15	
			% Passing #200 Sieve	79	7	
		Modulus (psi)		3000	12500	
		PI		5	30	
		LL		6	40	
Thermal Cracking	Average tensile strength at 14 F			200	1000	Satellite Study
	Creep Compliance at 14 F (1/GPa)		t = 1 sec	0.034	0.089	
			t = 2 sec	0.037	0.104	
			t = 5 sec	0.041	0.128	
			t = 10 sec	0.046	0.15	
			t = 20 sec	0.05	0.18	
			t = 50 sec	0.059	0.235	
			t = 100 sec	0.07	0.301	
Climate	Climatic Regions			Pellston, Lansing, Detroit		11

10.2 THE THERMAL CRACKING MODEL

Like other modules of ME-PDG, the thermal cracking model can be run at three hierarchical levels. Level 1 requires the following lab measured data for the mixes being analyzed:

(1) Creep compliance values measured at three different temperatures (-20^o C, -10^o C and 0^o C) and at six (or seven) instances from the start of the test (1, 2, 5, 10, 50 and 100, (1000) seconds).
(2) Tensile strength at -10^o C
(3) Aggregate coefficient of thermal contraction.

At Level 2 creep compliance tests results are required only for -10^o C at the same six instances in time as for Level 1. Tensile strength at -10^o C and aggregate coefficient of thermal contraction are also required.

At Level 3 the most important inputs, namely creep compliance and tensile strength, are calculated from other mixture inputs. Therefore, the user does not have to measure creep compliance or tensile strength in the laboratory. The accuracy of the thermal cracking model, therefore, is directly dependent on the accuracy of the models used for estimating creep compliance and tensile strength.

As stated earlier creep compliance tests are conducted at three different temperatures and the results are reported for six or seven different instances of time during the testing. However, for it to be used in the thermal cracking model a master curve is prepared using the time-temperature superposition principle. The master curve is then modeled using a power law as shown in equation 1.

$$D(t) = D_1 t^m \quad (1)$$

where:
D = Creep compliance
t = reduced time
D_1 and m are fracture coefficients

Equations 2 and 3 show the relationship between mixture characteristics and fracture coefficients D_1 and m.

$$\log(D_1) = -8.5421 + 0.01306T + 0.7957\log(V_a) + 2.0103\log(VFA) - 1.923(A_{RTFO}) \quad (2)$$

where:
T = Test temperature (^{o}C)
V_a = Air voids (%)
VFA = Voids filled with asphalt (%)
A_{RTFO} = Intercept of binder viscosity-temperature relationship for the RTFO condition

$$m = 1.1628 - 0.00185T - 0.0459V_a - 0.01126VFA + 0.00247Pen_{77} + 0.001683Pen_{77}^{0.4605}t \quad (3)$$

where:
T = Test temperature (^{o}C)
V_a = Air voids (%)

VFA = Voids filled with asphalt (%)

Pen_{77} = Penetration at 77 F = $10^{290.5013-\sqrt{81177.288+257.0694*10^{(A+2.72973*VTS)}}}$

A = Intercept of binder viscosity-temperature relationship

Tensile strength at -10 ^{o}C is also correlated with mixture properties. The same variables which appear in equations 2 and 3 also affect tensile strength as shown in equation 4.

$$S_t = 7416.712 - 114.016V_a - 0.304V_a^2 - 122.592VFA + 0.704VFA^2 + 405.71\log(Pen_{77}) - 2039.296\log(A_{RTFO}) \quad (4)$$

where:

S_t= Tensile strength in psi

VFA = Voids filled with asphalt (%)

Pen_{77} = Penetration at 77 F = $10^{290.5013-\sqrt{81177.288+257.0694*10^{(A+2.72973*VTS)}}}$

10.3 THERMAL CRACKING ANALYSIS

In the detailed sensitivity analysis for the other eleven variables low and high levels were chosen for each of them. The low and high levels corresponded to 5th and 95th percentile of similar data from the Long Term Pavement Performance (LTPP) database. The LTPP database was used for this purpose because it would be representative of US pavements. Also, extreme levels for each variable were considered to check for the reasonableness of the ME-PDG software. Then all possible combinations of all the 11 variables were used to define cases for the sensitivity analysis.

In the case of thermal cracking analysis also, certain variables affecting thermal cracking performance, i.e. creep compliance and tensile strength, were varied. However, the additional feature of this analysis was that inputs were derived from real mixes. During construction certain quality characteristics have variability along the same project and with the same mixture in use because of mixture variability or variability inherent in the construction process itself. Air voids and asphalt content are two such variables which were varied in this analysis.

10.3.1 Asphalt Mixtures Selected for Thermal Cracking Analysis

The Michigan Department of Transportation has provided us with 140 files of different mix designs used in Michigan during 2007. In many cases different mix design files corresponded to different asphalt concrete layers in the pavement. These 140 files were related to 82 distinct projects. Also, 31 of these projects did not have mix designs corresponding to the top asphalt concrete layer. Therefore, the remaining 51 projects were used in this analysis. Table 10.2 gives some of the details of the top asphalt layer mix designs for all of these projects.

Table 10.2. Mix design details for top asphalt layer for selected projects

Job Number	Mix Type	Mix Design Number	Project Location	VMA	VFA	P200/Pbe	Gmm	Gmb	RAP	AC	Asphalt Grade
38182A	5E1	07MD048	US131	15.99	75	1.18	2.458	2.359	18	6.09	58-28
46086A	5E3	07MD142	M17 FROM US12BR EASTERLY TO US 12	15.8	74.7	1.02	2.468	2.369	15	5.47	70-28
48762A	5E10	07MD280	M59	16.12	75.2	1.16	2.49	2.391	13	6.84	70-28
51506A	5E30	07MD235	I69	15.64	74.4	1.3	2.563	2.461	15	6.1	70-22
53367A	5E3	07MD304	M60	15.44	74.1	1.21	2.489	2.389	15	5.83	64-28
55420A	5E30	07MD114	I94	15.96	74.9	1.14	2.567	2.465	10	5.64	70-22
55659A	5E10	07MD086	M1	16.22	75.3	0.93	2.503	2.403	12	5.69	70-22
55662A	5E3	07MD152	M136	17.04	76.5	1.08	2.514	2.414	22	6.07	64-22
59135A	5E03	07MD341	US2	15.8	74.7	1.23	2.476	2.377	10	6.01	58-28
59468A	5E10	07MD303	I75	16.43	75.7	1.3	2.474	2.375	18	5.99	64-28
59970A	5E10	07MD176	US131	15.83	74.7	1.29	2.452	2.354	16	6.29	64-28
60136A	5E3	07MD084	CLINTON COUNTY	16.32	75.5	0.91	2.46	2.358	21	6.14	64-28
60281A	5E3	07MD323	M69	16.18	75.3	1.28	2.464	2.366	10	6.22	58-34
60299A	5E10	07MD360	US12	16.23	75.4	1.06	2.498	2.398	15	6.32	64-28
60388A	5E10HS	07MD095	US12	15.68	74.5	1.04	2.471	2.372	15	5.54	70-28
60481A	5E30	07MD134	I75	15.41	74	1.28	2.492	2.393	12	6.02	70-28
74483A	5E3	07MD226	M134	15.52	74.2	1.24	2.473	2.374	0	5.85	58-34
74885A	5E10	07MD348	DIVISION AVE.	16.65	76	1.09	2.467	2.369	18	6.26	70-28
75127A	5E30	07MD100	US23	15.47	74.1	1.35	2.503	2.403	16	6.79	70-28
75286A	5E3	07MD207	M28	15.79	74.7	0.96	2.494	2.394	21	5.54	58-34
75492A	5E3	07MD326	HARPER AVE.	15.93	75.5	0.91	2.501	2.403	0	6.58	70-22
79022A	5E30	07MD050	S02US23	16.77	76.1	1.1	2.491	2.391	15	5.6	70-28
79794A	5E3	07MD049	M100	16.4	75.6	0.98	2.502	2.402	12	5.93	64-28
80141A	5E3	07MD396	M35	15.62	74.4	1.12	2.494	2.394	17	5.94	58-34
80159A	5E3	07MD149	US41	16	75	1.21	2.472	2.373	14	5.81	58-34
80199A	5E1	07MD351	M28	15.84	74.8	1.07	2.478	2.379	25	5.89	52-34
80221A	5E03	07MD232	M94	16.59	75.9	0.96	2.49	2.39	27	5.81	52-34
83821A	5E3	07MD335	HAGADORN RD	16.33	75.5	1.01	2.463	2.365	15	6.14	64-28
83974A	5E1	07MD82	BARRY COUNTY	15.84	74.7	1.13	2.455	2.357	26	5.95	58-28
84359A	5E3	07MD310	HENRY ST	16.15	75.2	1.12	2.468	2.37	10	6.09	58-28
84364A	5E10	07MD101	GETTY ST.	16.1	75.1	1.01	2.513	2.412	12	5.91	64-28
84420A	5E1	07MD385	FOUTH ST.	15.04	73.4	1.15	2.507	2.407	17	5.21	58-34
85423A	5E10	07MD195	US223	16.38	75.6	1	2.465	2.366	15	6.3	64-28
85906A	5E30	07MD307	I96	15.91	74.9	1.21	2.485	2.386	13	6.5	70-28
86055A	5E10	07MD292	I94	16.04	75.1	1.17	2.489	2.389	15	6.08	64-28
87023A	5E10	07MD215	M11	16.12	75.2	1.18	2.487	2.388	10	6.2	70-22
87028A	5E3	07MD131	M46	16.15	75.2	1	2.51	2.51	12	5.94	64-22
87030A	5E3	07MD091	KENT COUNTY	16.02	75	0.95	2.471	2.372	17	5.98	70-22
87118A	5E10	07MD090	KENT & MONTCALM COUNTY	15.77	74.6	1.19	2.482	2.383	21	5.94	64-22
87245A	5E10	07MD234	M89	16.09	75.1	1.26	2.505	2.405	17	6.18	64-22
87293A	5E10	07MD137	WARREN AV. FROM SCHAEFER RD. TO LONYO RD.	16.48	75.7	1.12	2.512	2.411	13	5.99	70-22
87299A	5E10	07MD197	M130	15.66	74.5	1.06	2.477	2.378	15	5.59	70-28
87357A	5E10	07MD170	US12	16.49	75.7	0.89	2.455	2.357	10	6.27	64-22
87374A	5E10	07MD180	M59	15.83	74.7	1.16	2.485	2.385	18	6.7	70-22
87383A	5E30	07MD059		16.27	75.4	1.15	2.516	2.416	13	5.79	70-22
87452A	5E10	07MD161	US127	16.28	75.4	1.12	2.468	2.369	15	6.29	64-22
87511A	5E30	07MD332	I94	15.93	74.8	1.25	2.485	2.386	10	6.97	70-28
87665A	5E3	07MD230	M35	15.98	75	1.04	2.477	2.378	16	5.87	58-28
88408A	5E3	07MD140	WIENEKE RD. FROM STATE ST. TO WEISS ST.	16.03	75.1	0.92	2.432	2.335	10	6.12	64-28
89318A	5E3	07MD200	ROMEAO PLANK FROM 30 MILE RD. TO 31 MILE RD.	17.13	76.6	1.13	2.463	2.365	0	6.82	64-22
90106A	5E10	07MD274	FAIRVIEW RD	15.9	74.8	1.2	2.505	2.405	14	5.96	70-28

The 51 selected projects had mix designs for pavements with different volumes of expected traffic. Figure 10.1 pictorially shows the fractions of all the projects with 1, 3, 10 and 30 million ESALs expected traffic during their design life of 20 years. Figure 10.2 shows the distribution of

the projects based on the asphalt grade used in the top layer. All the mixes were Superpave mixes. As would be expected, many of the projects had asphalt content around 6%. There was almost a normal distribution of the projects around this 6% as shown in Figure 10.3.

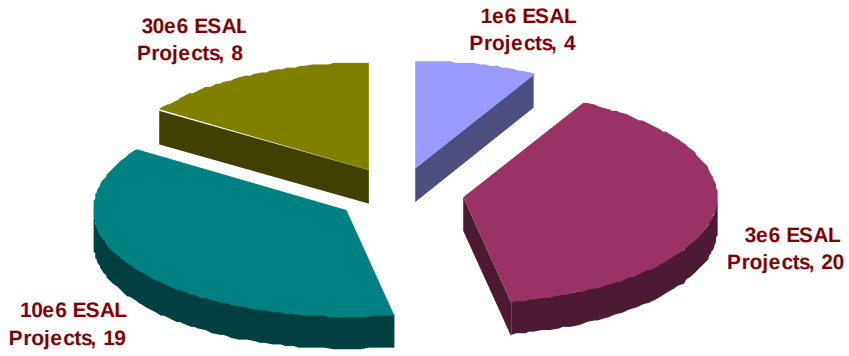

Figure 10.1. Distribution of the selected projects based on expected volume of traffic

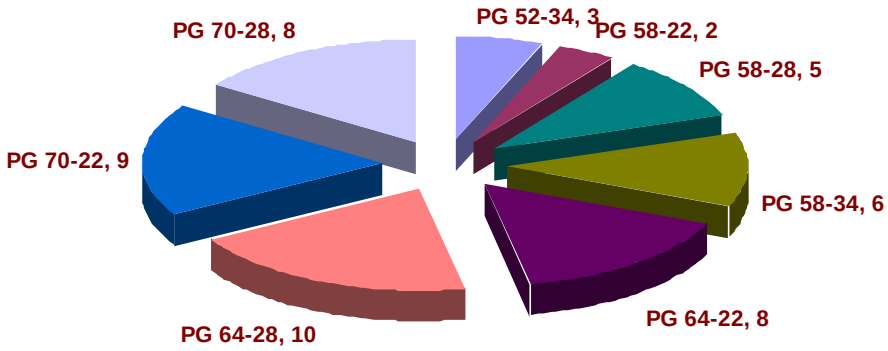

Figure 10.2. Distribution of projects based on asphalt grade used in the top layer

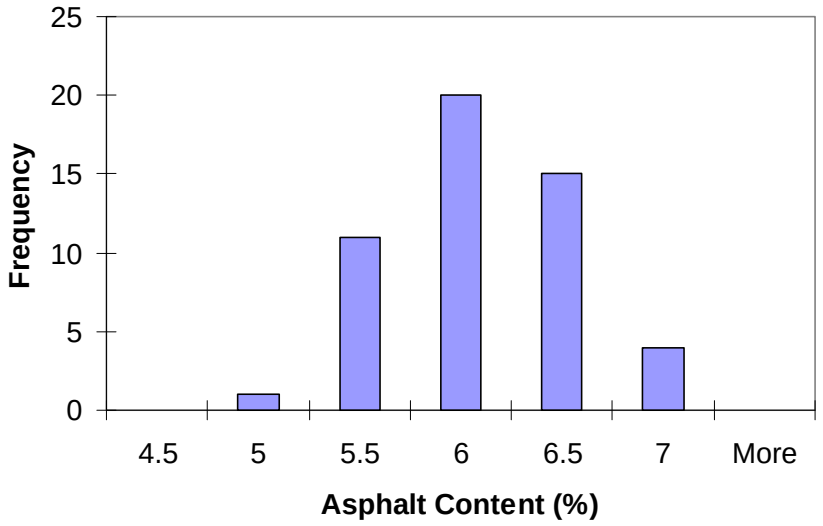

Figure 10.3. Distribution of selected projects based on asphalt content

10.3.2 Inputs for Analysis Runs

The mix designs provided by MDOT had job mix formula details for different asphalt concrete layers. In total there were 51 projects with these details. These projects had at least the top layer mix design. In cases where only top layer details were provided it was assumed that the there was only one asphalt concrete layer. Also to be able to compare the results, the total thickness of the asphalt layer was fixed for each level of expected traffic as shown in Table 10.3.

Mix design is carried with a target traffic loading, which is close to the expected loading that the pavement may experience during its design life. Design life was assumed to be 20 years in all the cases considered here. The expected traffic loading was given in terms of equivalent single axle load (ESAL). However, the ME-PDG software does not use the concept of ESAL. Detailed axle spectra are used instead to account for the different damage mechanisms separately according to mechanistic principles.

The national average Traffic loading spectra for US were used in this analysis. AADTT was varied using trial runs to get the required number of ESALs at 20 years. Table 10.3 shows the AADTT obtained from this analysis.

Table 10.3. Asphalt concrete layer thicknesses and AADTT for different traffic levels

Expected Traffic Load (ESALs)	Asphalt Concrete Thickness	AADTT
1 million	3	201
3 millions	4	603
10 millions	8	2009
30 millions	12	6028

Some assumptions were made for the pavement structure because the design files do not have details of other non-asphalt concrete layers. It was assumed that all the pavements had a 6 inch thick base layer of A-1-a material with a modulus of 30,000 psi. All the pavements were also assumed to have a subbase layer with a modulus of 15,000 psi. Pavements with expected traffic loading of 30 million ESALs were assumed to have 30 inches thick subbase layer whereas all other pavements had 8 inches thick subbase layer. Subgrade modulus was assumed to be 10,000 psi in all the cases.

Air voids designated in the mix design files correspond to the target air voids of 4%. However, ME-PDG requires in-situ air voids immediately after compaction. In-situ air voids depend on compaction pattern, roller passes, mix variability, paver characteristics etc. Therefore, for the same mix design the actual in-situ air voids could be quite varied in the same project. Consequently, it was decided that all the 51 projects would be run for two levels of air voids being 6% and 9%. This translated to 102 runs required for the analysis. In addition, some extra runs were also performed to address specific issues which would be described in the following section. It is important to note that all these runs assume that the project is newly constructed and that no repair or rehabilitation steps are taken during the period that they are analyzed for.

10.3.3 Thermal Cracking Analysis Results

As described in the last section the projects analyzed in this satellite study had quite varied characteristics. The goal of this mini-study was to see how Michigan mixes are expected to perform from a thermal cracking point of view. Figure 10.4 and Figure 10.5 show the amount of predicted thermal cracking at the end of a design life of 20 years for all the selected projects. A sequential project number was assigned to the projects for the sake of convenience. The projects were divided into four categories based on the expected traffic of 1, 3, 10 or 30 million ESALs. All the projects with the same expected traffic were plotted together for easy comparison with projects in other categories. Figure 10.4 and Figure 10.5 show the predicted thermal cracking for 6% and 9% in-situ air voids, respectively.

It is quite noticeable that almost all of the mixtures were predicted to perform very well in thermal cracking. There are only few projects which show some amount of thermal cracking. These projects are listed in Table 10.4, which shows the predicted thermal cracking corresponding to air voids of 6% and 9%. It is significant to note that a change of air voids from 6 to 9% leads to nearly four times higher thermal cracking in most of the cases. Therefore, based on this limited study it seems that thermal cracking is very sensitive to air voids.

In those cases where there was no thermal cracking with 6% air voids this trend is not visible because the mix may have much higher compliance than the threshold. Therefore, even with higher air voids of 9% they have no thermal cracking.

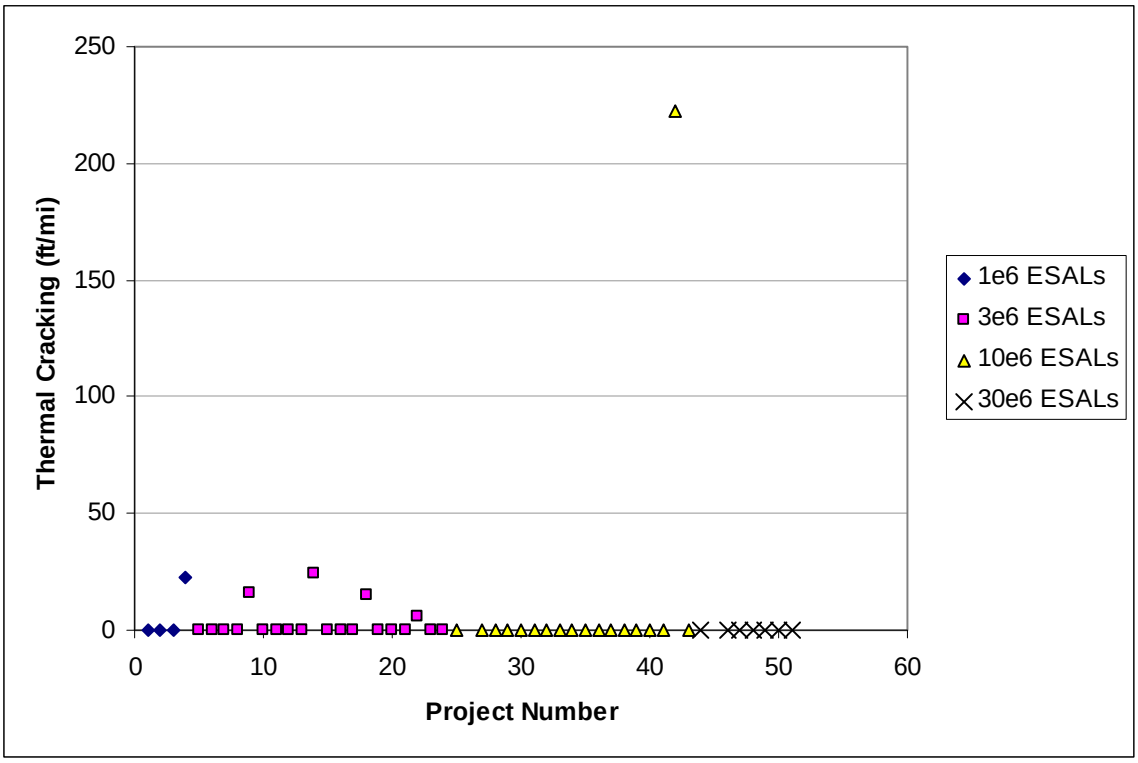

Figure 10.4. Predicted thermal cracking at the end of 20 years (in-situ air voids = 6%)

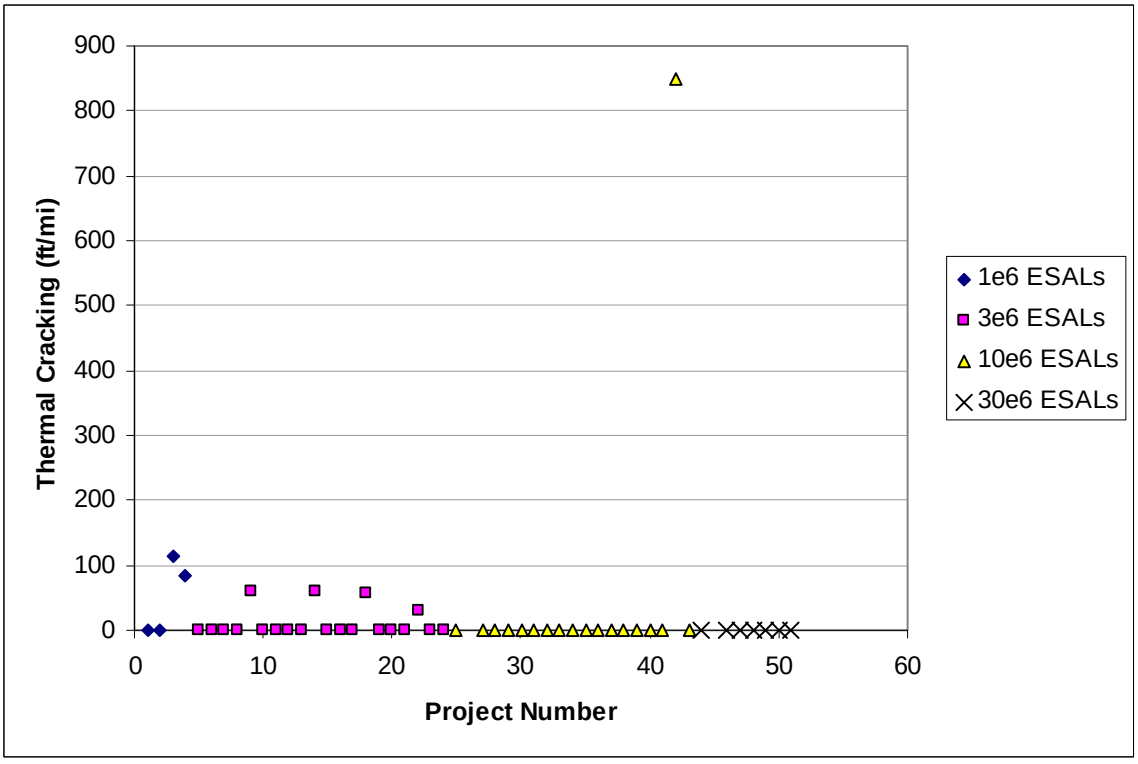

Figure 10.5. Predicted thermal cracking at the end of 20 years (in-situ air voids = 9%)

Table 10.4. Projects with highest predicted thermal cracking

Job Number	ESALs	Asphalt Content (%)	Asphalt Grade	Thermal Cracking (ft/mi) AV=6%	Thermal Cracking (ft/mi) AV=9%
60136	3	6.14	64-28	15.5	59.3
79794	3	5.58	64-28	23.9	61.1
83821	3	5.07	58-22	15.1	57.6
84420	1	5.21	58-34	22.3	82.6
87452	10	6.29	64-22	222	850

It was also decided that further analysis should be done to study the effect of asphalt content, which is another input in the creep compliance prediction model. For the projects mentioned in Table 10.4 asphalt content was reduced, first by 0.5% and then by 1.0%. Figure 10.6 shows the change in thermal cracking performance as a result of these changes in the mix characteristics.

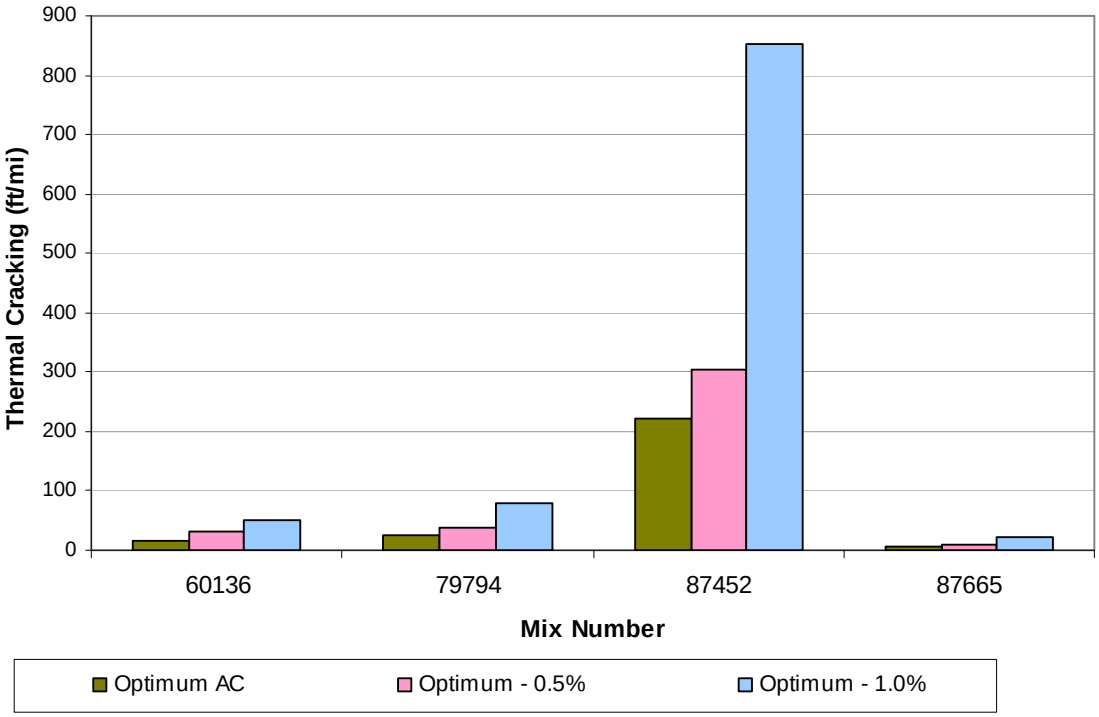

Figure 10.6. Change in thermal cracking when asphalt content is reduced by 0.5 and 1.0%

It would have been very interesting to study the effect of asphalt grade on thermal cracking performance. However, since the vast majority of the projects have zero thermal cracking this comparison study was not done.

10.4 COMPLEX MODULUS SATELLITE STUDY

In the detailed sensitivity analysis a full factorial matrix was prepared for the eleven variables being studied and the corresponding ME-PDG runs were performed. In a full factorial matrix like this all possible combinations of the high and low levels of all the variables are considered. In many cases these combinations may not represent realistic mixes at all. At level 3, the complex modulus is calculated using several of these variables. The complex modulus in turn is used for predicting pavement performance. Therefore it was decided to further augment the study by running ME-PDG with real mixes to study the effect of complex modulus, especially comparing level 1 versus level 3 predictions.

Ideally the best way to compare the level 1 versus level 3 predictions would be to use input mixture characteristics, as required for level 3 by ME-PDG software, and generate the predictions followed by predictions using actual laboratory measured complex modulus values for the same mixture. However, we could not obtain measured complex modulus data for these mixes.

10.4.1 The Projects and Their Performance

The projects selected for the thermal cracking satellite study could also be used for the complex modulus mini-study because they represent real Michigan mixes. Therefore, the same 51 projects were used in this mini-study also. Rutting and fatigue cracking performance were used to compare the effect of complex modulus for the various mixtures and different values of quality characteristics. Longitudinal cracking performance was not included in this analysis because of the erratic trends it had shown in the earlier sensitivity analyses. Figure 10.7 and Figure 10.8 show predicted rutting performance for all the projects, with 6% and 9% in-situ air voids, respectively. The projects have been categorized based on expected traffic. Projects belonging to the same category were plotted together in these plots.

Half of an inch of rutting is considered to be the limit for interstate asphalt pavements. Almost all of the projects show more rutting than that at the end 20 years of design life. However, it has already been observed in our previous analyses that ME-PDG with its current models over-predicts rutting.

Figure 10.9 and Figure 10.10 show predicted fatigue performance for 6% and 9% air voids respectively. The figures show reasonable fatigue performance for mixes with 1, 10 and 30 million ESALs, and poor performance for the 3 million ESALs mixes. The reasons for the latter performance cannot be fully explained at this point, although it probably is related to the structural design selected for these mixes.

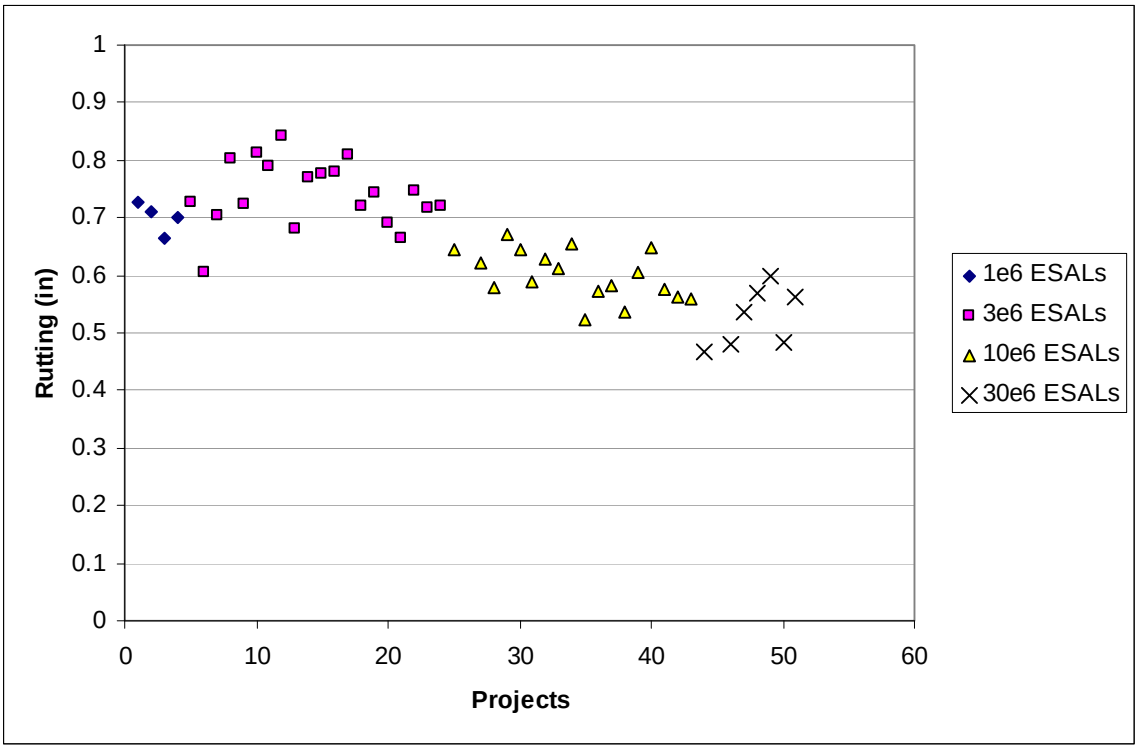

Figure 10.7. Rutting performance for selected projects (in-situ air voids = 6%)

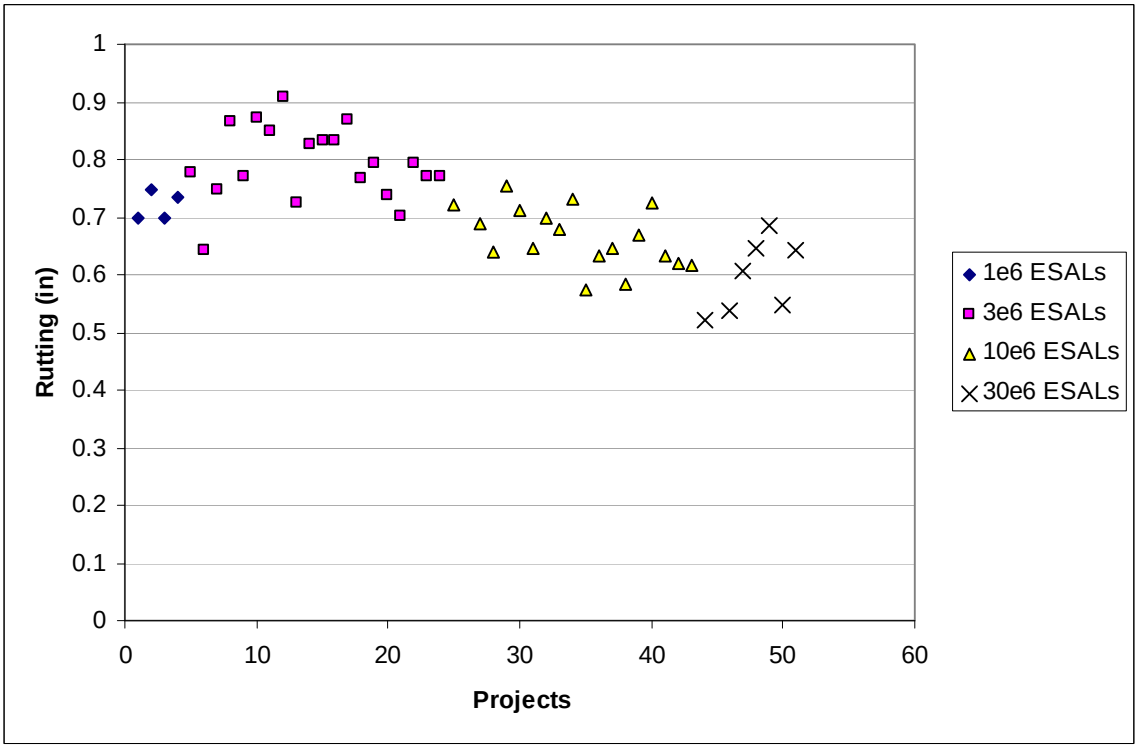

Figure 10.8. Rutting performance for selected projects (in-situ air voids = 9%)

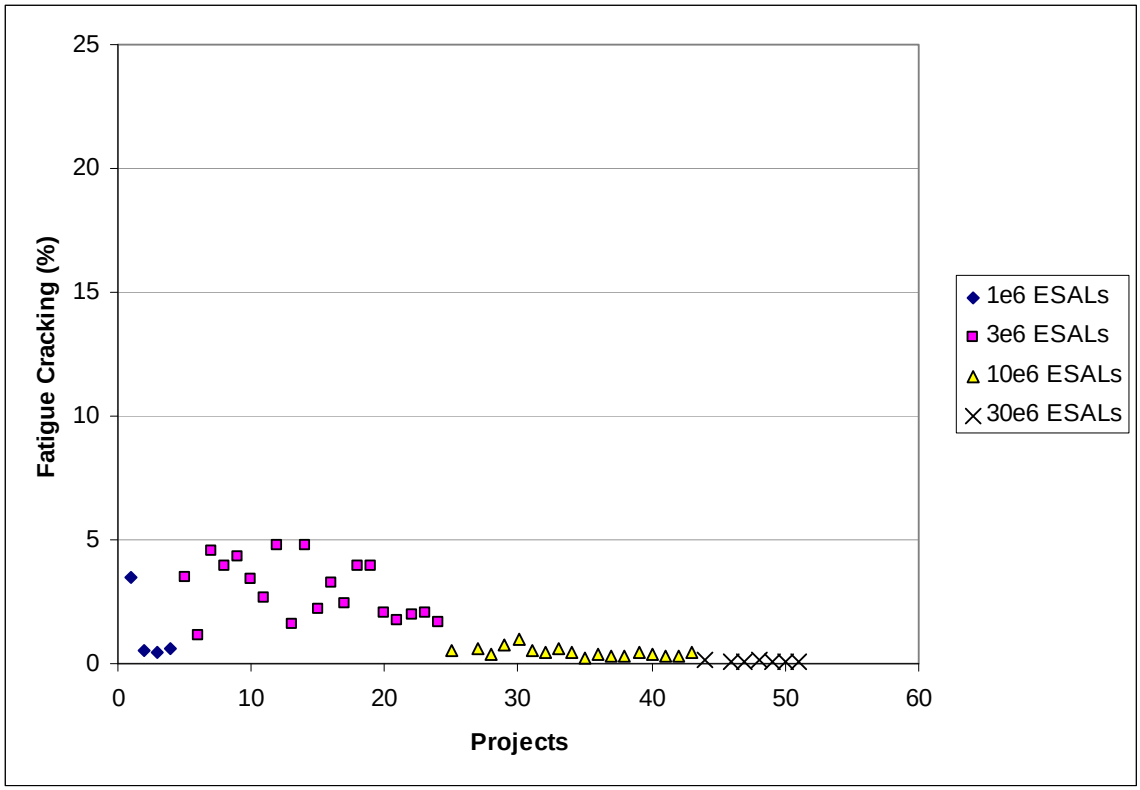

Figure 10.9. Fatigue cracking performance for selected projects (in-situ air voids = 6%)

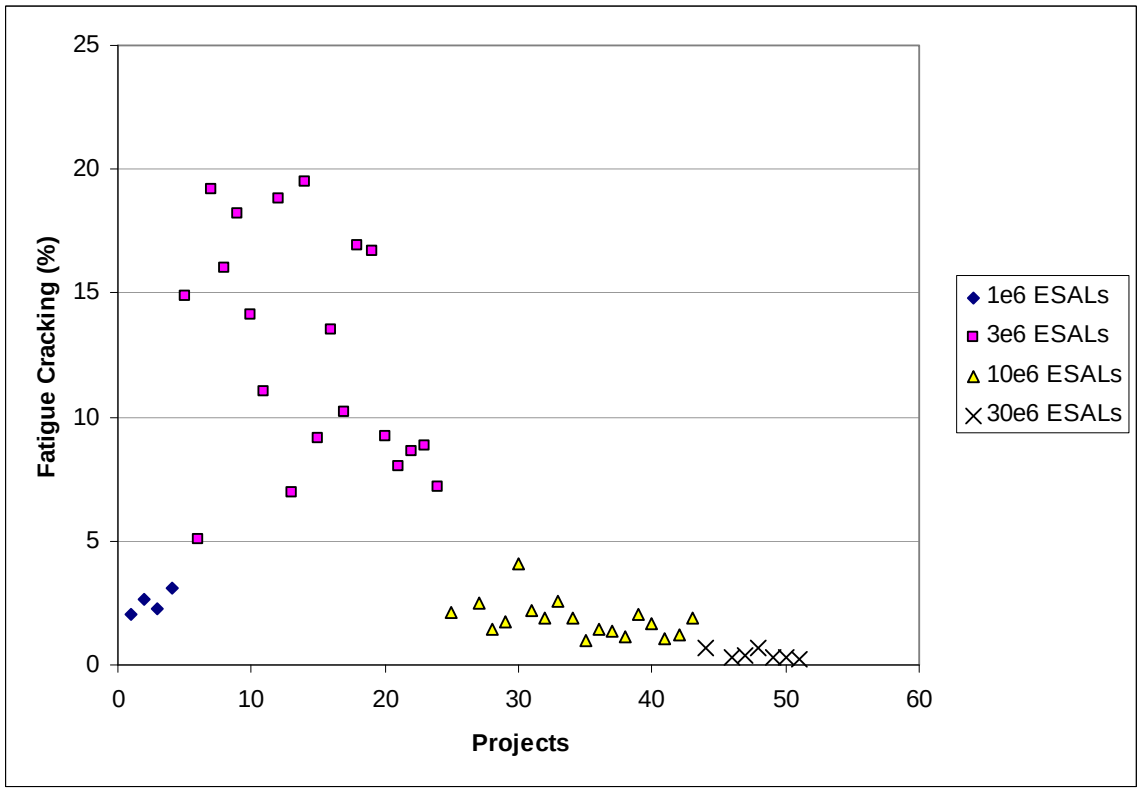

Figure 10.10. Fatigue cracking performance for selected projects (in-situ air voids = 9%)

Table 10.5 shows rutting at the end of 20 years for all the projects with expected traffic of 3 million ESALs. Comparing the rutting levels for pavements with 9% versus 6%in-situ air voids, the ratio is quite constant and close to 1.07 in all the cases. This ratio was found to be close to 1.10 for the 10 million ESAL projects. Increase in total rutting, therefore, is only slight as a result of increase in air voids from 6% to 9%. This can be explained by the fact that most of the rutting was due to the unbound layers. Only 17% to 22% of total rutting occurs in the asphalt layer, roughly 20% in base and subbase layers and 60% in the subgrade.

Table 10.5. Predicted rutting at 20 years for 3 million ESAL projects

Job No.	Rutting (in) (AV=6%)	Rutting (in) (AV=9%)	Ratio
46086	0.728	0.778	1.07
53367	0.605	0.642	1.06
55662	0.703	0.747	1.06
59135	0.804	0.865	1.08
60136	0.723	0.771	1.07
60281	0.811	0.872	1.08
74483	0.79	0.849	1.07
75286	0.842	0.908	1.08
75492	0.682	0.726	1.06
79794	0.771	0.827	1.07
80141	0.777	0.832	1.07
80159	0.78	0.834	1.07
80221	0.808	0.869	1.08
83821	0.72	0.768	1.07
84359	0.742	0.795	1.07
87028	0.692	0.738	1.07
87030	0.663	0.703	1.06
87665	0.746	0.795	1.07
88408	0.718	0.769	1.07
89318	0.721	0.772	1.07

Table 10.6 shows fatigue performance at the end of 20 years for all the projects with expected traffic of 3 million ESALs. The ratio of fatigue cracking for 9% air voids to that for 6% air voids is about 4 in almost all the cases. The same ratio was observed in the case of 10 million ESALs projects as well.

10.4.2 Effect of Asphalt Concrete Layer Modulus

We then selected some of these projects to study the difference in equivalent asphalt modulus estimated from mix properties. The projects with maximum and minimum fatigue cracking were

selected for the cases of 3 and 10 million ESALs, respectively. Figure 10.11 show these asphalt moduli.

Table 10.7 gives maximum asphalt concrete moduli for in-situ air voids of 6% and 9%. The first two projects in the table belong to the 3 million ESALs category and the last two to 10 million ESALs category. The ratio of the AC moduli, i.e. for 9% versus 6%, is close to 0.8 (i.e., 20% reduction) in all the four cases. This shows that the complex modulus is very sensitive to in-situ air voids. Earlier it was noted that fatigue cracking was several times higher for mixes with 9% air voids as compared to those with 6% air voids. This can be explained by the 20% reduction in asphalt modulus. Recall from the discussion above that the same decrease in AC moduli leads to only 7 to 11 percent increase in rutting over 20 years for the same pavements. So rutting does not seem to be very sensitive to asphalt layer modulus.

Table 10.6. Predicted fatigue cracking at 20 years for 3 million ESAL projects

Job Number	Fatigue Cracking (%) (AV = 6%)	Fatigue Cracking (%) (AV = 9%)	Ratio
46086	3.49	14.9	4.3
53367	1.1	5.08	4.6
55662	4.51	19.2	4.3
59135	3.92	16	4.1
60136	4.3	18.2	4.2
60281	3.44	14.1	4.1
74483	2.63	11	4.2
75286	4.77	18.8	3.9
75492	1.57	6.92	4.4
79794	4.79	19.5	4.1
80141	2.16	9.14	4.2
80159	3.23	13.5	4.2
80221	2.45	10.2	4.2
83821	3.95	16.9	4.3
84359	3.97	16.7	4.2
87028	2.08	9.2	4.4
87030	1.76	8.01	4.6
87665	1.99	8.63	4.3
88408	2.03	8.8	4.3
89318	1.68	7.15	4.3

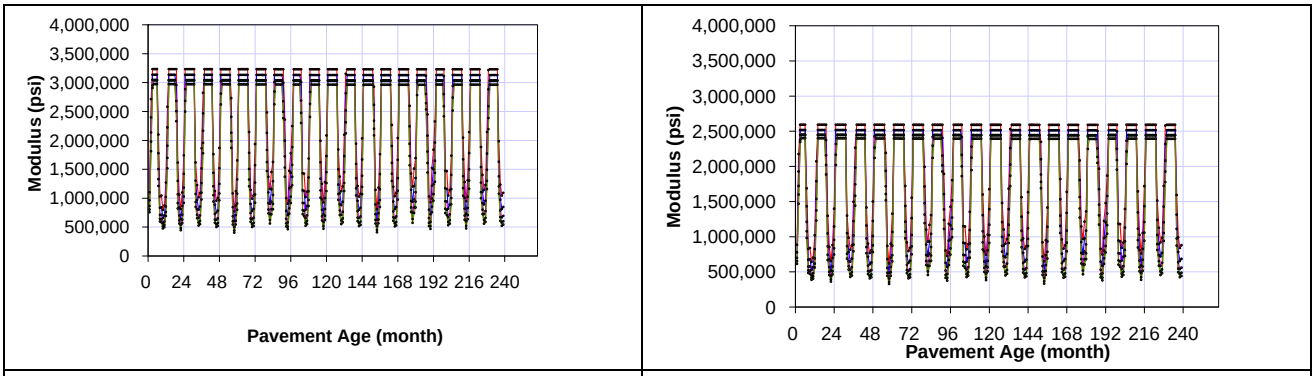

(a) Project Number: 75286, AV = 6%

(b) Project Number: 75286, AV = 9%

(c) Project Number: 89318, AV = 6%

(d) Project Number: 89318, AV = 9%

(e) Project Number: 60388, AV = 6%

(f) Project Number: 60388, AV = 9%

(g) Project Number: 87374, AV = 6%

(h) Project Number: 87374, AV = 9%

Figure 10.11. Equivalent modulus for asphalt layers

Table 10.7. Comparing maximum asphalt layer moduli

Job Number	AC Modulus (ksi) (AV=6%)	AC Modulus (ksi) (AV=9%)	Ratio
75286	3234	2593	0.80
89318	2907	2310	0.79
60388	3541	2839	0.80
87374	3269	2600	0.80

10.5 VERIFICATION OF M-E PDG PERFORMANCE PREDICTION IN MICHIGAN

For any state highway agency to use M-E PDG at any level it is important to evaluate M-E PDG software performance prediction and compare them with in-service pavement sections in that state. Therefore, this validation study was done for Michigan under this project. In order to accomplish the objectives of research in this task, the availability of following data was deemed critical.

- Pavement material-related data inputs
- Pavement layers cross-sectional information
- Traffic in terms of truck volumes and axle load spectrum
- Pavement performance (time series with age) data (cracking, rutting, IRI etc,)

The state of Wisconsin is working on the regional calibration of the M-E PDG performance models. For this purpose, MDOT had provided them with the above mentioned pavement data for five flexible pavement sections. The particular requirements for this data were:

- Pavement sections should be old enough to exhibit some level of distresses;
- Pavement sections should include a mix of good and poor performing pavements; and
- Only AADTT and estimated growth rates were desired by Wisconsin study as this study is using national average for truck loadings and classifications

The research team used the same data for conducting performance prediction validation. However, there are some issues pertaining to the detailed traffic requirements, especially WIM data for those exact five locations (for flexible pavement sections). MDOT provided an estimated percentage of vehicle classification by considering the WIM stations in vicinity of those locations. This data included the mix of traffic for all these specific sites based on the available truck volume and loading data from the nearby WIM stations. However, it was also pointed out that three or more years old MDOT WIM data have certain accuracy issues:

- Data older than 3 years were collected based on the piezo-sensor technology, which had serious calibration issues;
- Temperature dependency of piezo-sensors;
- Because of the above reasons, this data contains an error of about ± 20 – 25% in GVWs.

Nonetheless, in the past 3 years the WIM data collected by MDOT is more accurate with an error of ± 3 – 5% in GVWs. The accuracy of the newer MDOT WIM data was improved because of following reasons:

- Use of quartz-sensors and bending plate technology
- Adoption of improved calibration procedures

In order to increase the number of sections in this exercise, it was also decided that the research team will also look at the flexible pavement sections in SPS-1 experiments. The SPS-1 site in Michigan on Old Route 27 in Clinton County. The required data for these sections were extracted from the LTPP database. Next, the results from the SPS-1 (in Michigan) and the MDOT pavement sections are presented.

10.5.1 LTPP SPS-1 Pavement Sections in Michigan

The main advantages and motivations for using the SPS-1 flexible pavement sections in this research include:

- Availability of traffic, materials and pavement cross-sectional data in the LTPP database
- Accessibility of at least 5 to 10 years of performance data (rutting, fatigue, longitudinal and transverse cracking and IRI)
- Pavement performance under local traffic and environment in Michigan.

One of the limitations in using the SPS-1 pavements is that the pavement design does not reflect the typical MDOT practice. The same pavement design for these test sections was repeated in several sites to populate the SPS-1 experiment design. Nevertheless, these pavement sections have undergone more than 10 years of unique truck traffic and Michigan climate. A brief introduction to the SPS-1 experiment is given below.

The SPS -1 experiment consisted of 192 factor level combinations, which consist of 8 site-related (subgrade soil and climate) and 24 pavement structure combinations. The experiment design required that 48 test sections representing all structural factors and subgrade type combinations in the experiment were to be constructed in each of the climatic zones, with 24 test sections to be constructed on fine-grained soil and 24 test sections to be constructed on coarse-grained soil.

The SPS-1 experiment examines the effects of both site and structural factors. The site factors include: climatic region, subgrade soil (fine- and coarse-grained), and traffic level (as a covariate) on pavement sections incorporating different levels of structural factors. The structural factors include:

• Drainage (presence or lack of it),

• Asphalt concrete (AC) surface thickness – 102 mm (4-inch) and 178 mm (7-inch),

- Base type – dense-graded untreated aggregate base (DGAB), dense-graded asphalt-treated base (ATB) and open graded permeable asphalt treated base (PATB) and a combination of the three,
- Base thickness – 203 mm (8-inch) and 305 mm (12-inch) for un-drained sections; and 203 mm (8-inch), 305 mm (12-inch) and 406 mm (16-inch) for drained sections.

The study design stipulates a traffic load level in excess of 100,000 Equivalent Single Axle Loads (ESALs) per year for the study lane.

10.5.1.1 Traffic Inputs

All the Michigan SPS-1 pavement sections are located sequentially on US-127 (formerly US-27) near St. Johns. Therefore, essentially the design lane of these sections has experienced the same amount of traffic in terms of loading and repetitions. The axle load spectra and AADTT along with the truck classification data were extracted from the LTPP database (Release 21). The axle load spectra for different axle configurations were also imported in the M-E PDG software; however, due to limited space, these are not presented in this report.

10.5.1.2 Material Inputs

Several material related inputs required for various pavement layers, including; (a) layer thicknesses, (b) layer material types, (c) material properties and (d) other structural details, were extracted from the LTPP database whenever available. In cases, where material-related input was not available in the LTPP database, level 3 inputs were assumed.

The performance predicted by M-E PDG would be only as accurate as the assumptions and the prediction models themselves. It was observed that data corresponding to different states in the experiment differed in their completeness. Data for sections in the state of Michigan had fewer details of material properties than most of the other states. For example there was no information provided regarding asphalt content used in permeable asphalt treated base. However, it could be a critical input because depending on the pavement structure PATB could form the bottom-most layer of all the asphalt bound layers. The bottom most layer is critical for bottom-up cracking (fatigue cracking), especially if the overlying layers are not very thick. An effort was made to study the missing details from other states and make reasonable assumptions. Appendix B gives details of all the input values used in the study. The following list gives the most important assumptions that were made in the study.

1. Aggregate gradation for all the asphalt bound surface and binder courses were not available. So, gradation was assumed to be the same for both the layers, and values provided for either of the layers were used for both, where ever required. Also there was more than one test conducted. So, the average of the tests was used.
2. Aggregate gradation for open graded permeable asphalt treated base, used in some sections, was not available for Michigan sites. Therefore, gradation for this layer used in other states under SPS-1 experiment was used.

3. Required inputs for the climate were interpolated from those for Lansing, Grand Rapids and Saginaw, MI. These three locations of weather stations form a triangle around the SPS-1 site in Michigan.
4. The grade of asphalt used was not also available from the LTPP database. The computer program LTPPBind (Version 3.1) was used to determine the performance graded binder suitable for this climate and traffic. PG binder PG 58-22 was used as input.
5. Asphalt content (or effective binder content) values were not available for some of the layers for the Michigan sections. Wherever necessary asphalt content from other SPS-1 sites for the same type of layer (in similar pavement structure) in other locations of SPS-1 experiment had to be used. Mostly, asphalt content for the top layer was assumed to be 5.7% and that for the binder layer to be 4.5%.
6. As required, assumptions similar to item 5 were used for in-situ air voids also.
7. Plasticity index and liquid limit for the subgrade were assumed to be 5% and 21% respectively.
8. It was observed that there was a lot of variation in number of trucks through different years. Therefore the most reasonable AADTT was used.

10.5.1.3 Results and Discussion from SPS-1 Site Study

Figure 10.12 and Figure 10.15 through Figure 10.18 show performance predicted by M-E PDG software versus actual performance. SPS-1 sites were labeled as section 115, 116, 117, 118, 120, 121, 123 and 124.

Figure 10.12 shows longitudinal cracking predictions for all the sections. In reality all the sections had none or very, very little longitudinal cracking. Performance predicted by the M-E PDG software is also similar except for sections 120 and 121. Later on it was found that sections 120 and 121 had to be overlaid in 1997 which may possibly explain the reason behind the difference between observed and predicted performance. It is noticeable that these two sections had much larger predicted longitudinal cracking than all other sections.

Figure 10.13 shows the pavement structure with other layer details for sections 120 and 121. In both of these pavement structures the asphalt concrete surface and binder layers together are only 3.6 inches and 3.9 inches respectively. These two layers were constructed directly on open graded permeable asphalt treated base (PATB) layer. PATB is expected to have lower asphalt content and relatively higher air voids content. These conditions make it especially vulnerable to bottom up alligator cracking as well as longitudinal cracking. In essence even slight differences in asphalt content and air voids, therefore, would lead to vastly different performance prediction.

Figure 10.16 shows transverse crack spacing for all the sections. The plots do not seem to show the actual crack spacing. This is because there was zero crack reported on these sections. Therefore, observed (actual) crack spacing would be theoretically infinite and would not appear within the range of y-axis used in the plots.

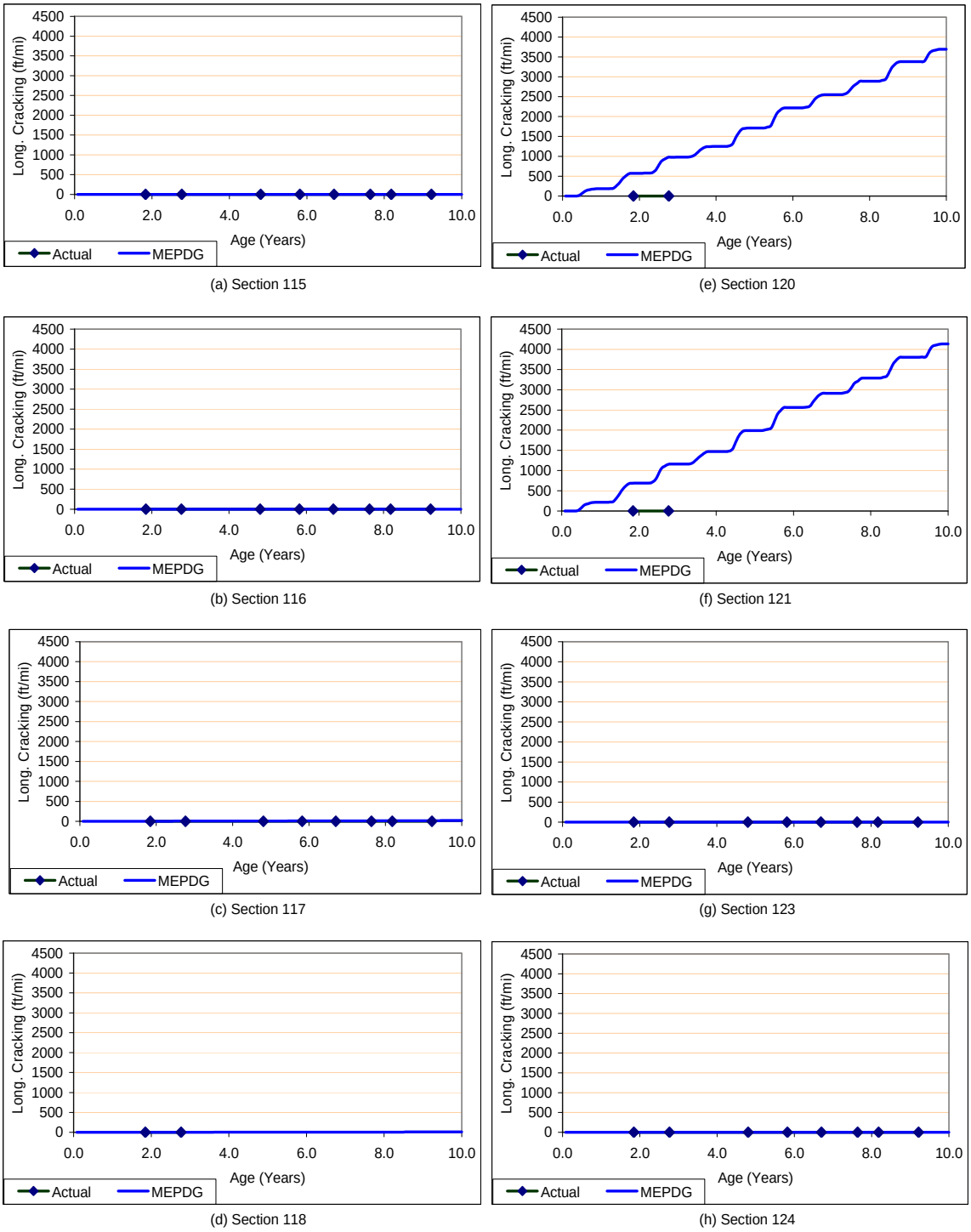

(a) Section 115

(e) Section 120

(b) Section 116

(f) Section 121

(c) Section 117

(g) Section 123

(d) Section 118

(h) Section 124

Figure 10.12. Observed longitudinal cracking versus that predicted by M-E PDG for SPS-1 sections

Layer No.	Layer Description
5	Original Surface Layer (Layer Type:AC)1.8 Inch
4	AC Layer Below Surface (Binder Course) (Layer Type:AC)1.8 Inch
3	Base Layer (Layer Type:PATB)4 Inch
2	Base Layer (Layer Type:GB)8 Inch
1	Subgrade (Layer Type:SS) Inch

Section 120

Layer No.	Layer Description
5	Original Surface Layer (Layer Type:AC)1.9 Inch
4	AC Layer Below Surface (Binder Course) (Layer Type:AC)2 Inch
3	Base Layer (Layer Type:PATB)4 Inch
2	Base Layer (Layer Type:GB)8 Inch
1	Subgrade (Layer Type:SS) Inch

Section 121

Figure 10.13. Pavement structure for sections 120 and 121

The LTPP database did not have values for asphalt content and air voids, or bulk specific gravity and theoretical maximum specific gravity, from which air voids content could be calculated for the PATB layer used in Michigan. Therefore these values had to be assumed to be similar to permeable asphalt treated base layer used in some other states under the same SPS-1 experiment. As stated earlier this makes the predictions also far less reliable.

Sections 123 and 124 also used PATB of 4 inch thickness but they had PATB layer below an additional 8 inches and 12.2 inches thick asphalt treated base layer. Figure 10.14 shows the pavement structures for these sections.

Later in the report we discuss the effect on performance of sections 120 and 121 when asphalt content and air voids values were assumed to be different from those used for preliminary analysis as reported here.

Layer No.	Layer Description
6	Original Surface Layer (Layer Type:AC)1.8 Inch
5	AC Layer Below Surface (Binder Course) (Layer Type:AC)2 Inch
4	AC Layer Below Surface (Binder Course) (Layer Type:AC)2.4 Inch
3	Base Layer (Layer Type:TB)8 Inch
2	Base Layer (Layer Type:TB)4 Inch
1	Subgrade (Layer Type:SS) Inch

Section 123

Layer No.	Layer Description
6	Original Surface Layer (Layer Type:AC)1.9 Inch
5	AC Layer Below Surface (Binder Course) (Layer Type:AC)1.9 Inch
4	AC Layer Below Surface (Binder Course) (Layer Type:AC)2.5 Inch
3	Base Layer (Layer Type:TB)12.2 Inch
2	Base Layer (Layer Type:TB)4 Inch
1	Subgrade (Layer Type:SS) Inch

Section 124

Figure 10.14. Pavement structure for sections 123 and 124

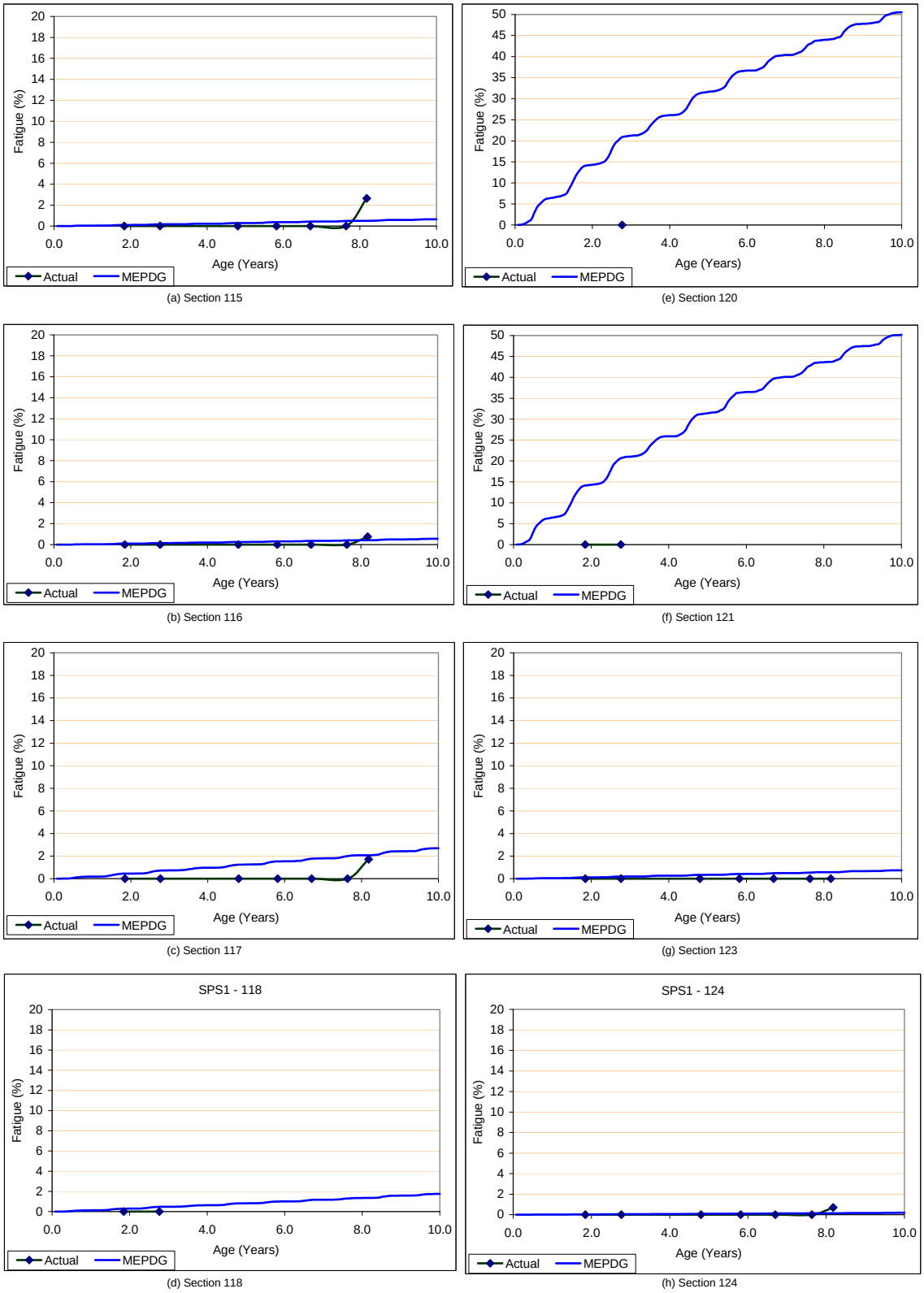

Figure 10.15. Observed fatigue cracking versus that predicted by M-E PDG for SPS-1 sections

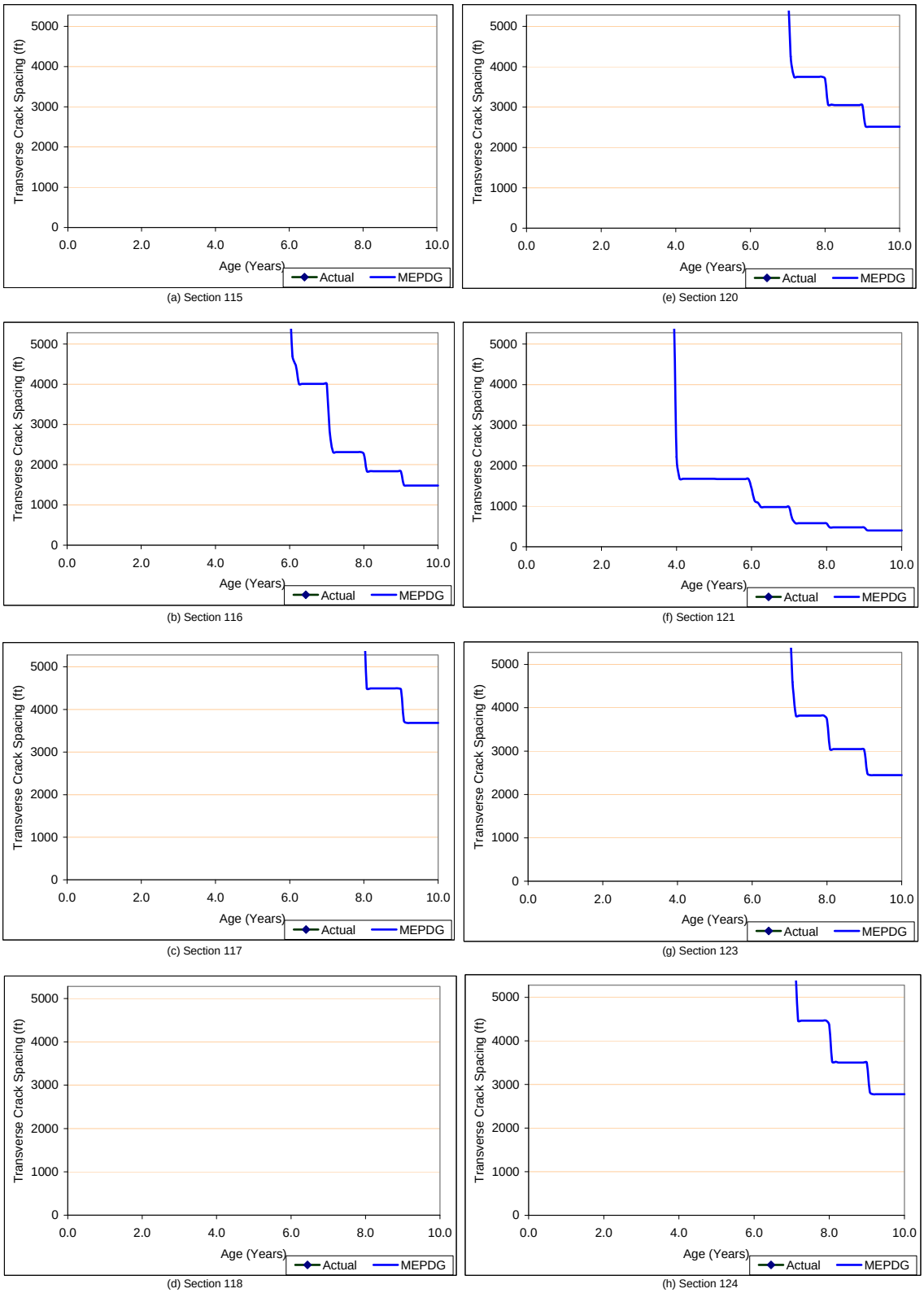

Figure 10.16. Observed transverse cracking versus that predicted by M-E PDG for SPS-1 sections

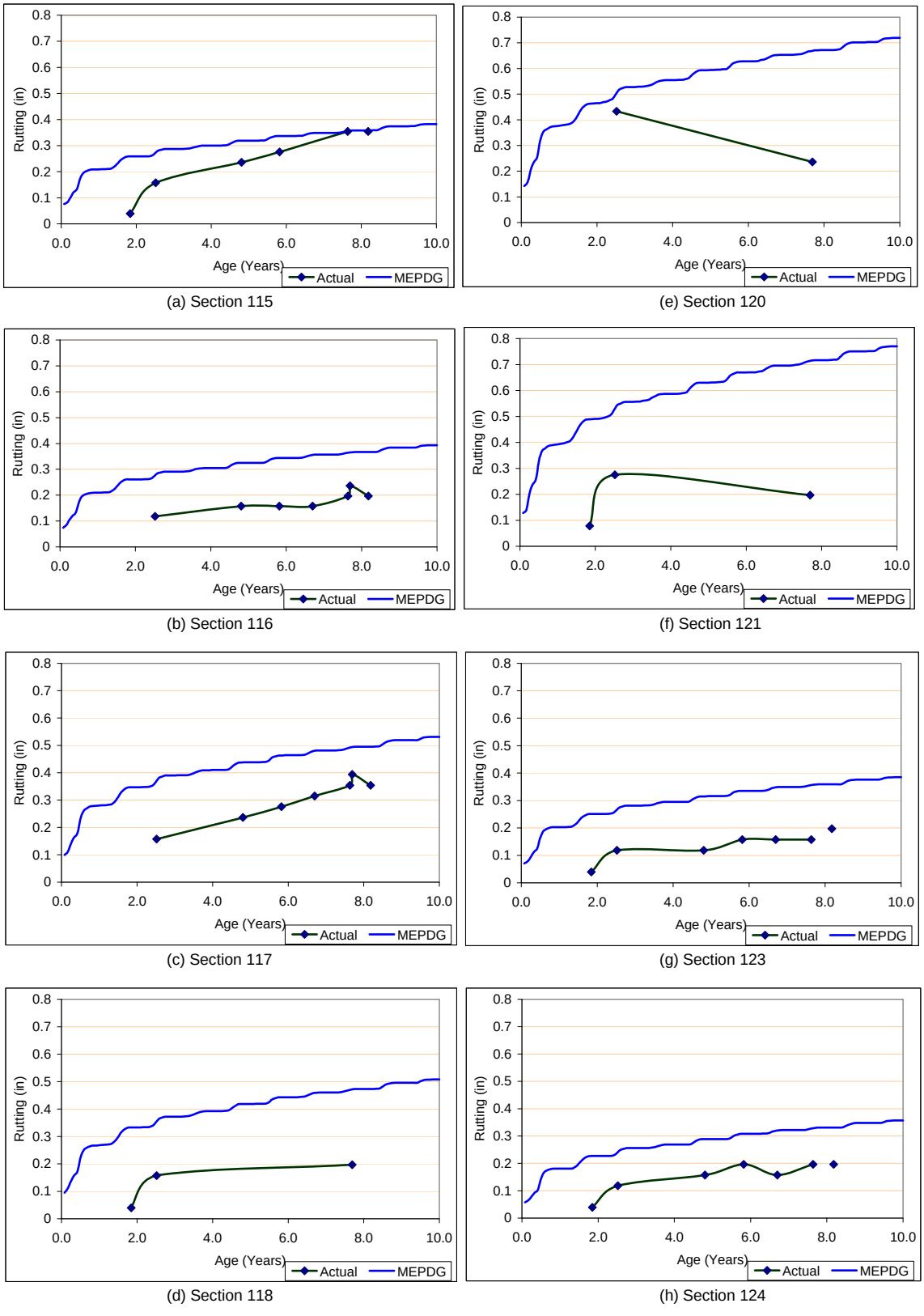

Figure 10.17. Observed rutting versus that predicted by M-E PDG for SPS-1 sections

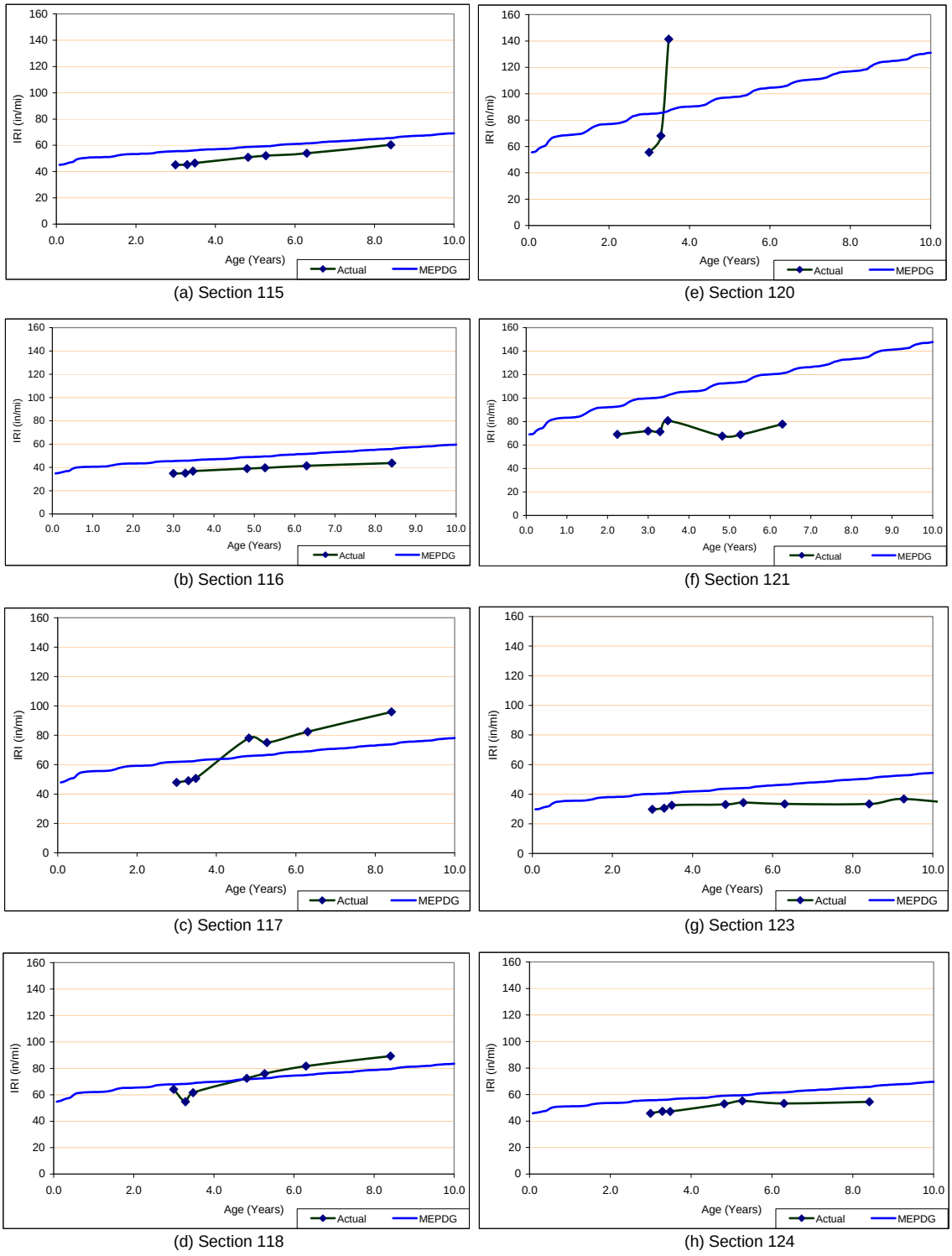

Figure 10.18. Observed IRI versus that predicted by M-E PDG for SPS-1 sections

Further analysis was conducted with sections 120 and 121 to verify the logical reasoning presented earlier for their particularly poor predicted performance. Figure 10.19 shows predicted performance for these sections when the asphalt content is raised from the initial assumption of 3 % to 4.5% percent. In-situ air voids content immediately after construction was also lowered from 12% to 8.5%. These two changes led to significantly better performance especially in fatigue. This exercise underlines the importance of correct inputs in the M-E PDG software. Therefore, it is recommended that site-specific data be used for all the inputs identified as significant inputs in preliminary and detailed sensitivity analyses.

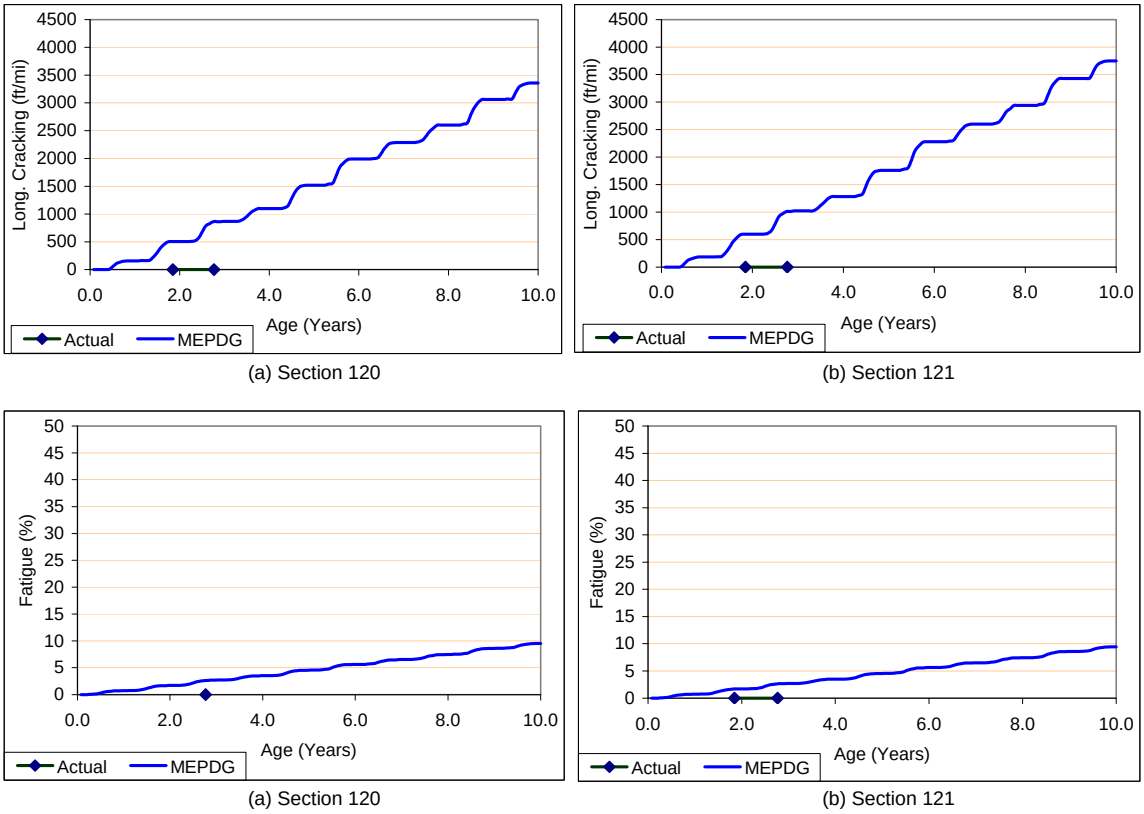

Figure 10.19.Longitudinal cracking and fatigue performance for sections 120 and 121 with higher asphalt content and lower air voids for PATB layer

10.5.1.4 Conclusions from SPS-1 Site Study

Table 10.8 summarizes how predicted performance compare with the observed performance for all the eight sections and for all the five performance measures, namely longitudinal cracking, fatigue cracking, transverse cracking, rutting and IRI.

It is interesting that except for sections 120 and 121 longitudinal cracking, fatigue cracking and IRI match reasonably well. In the case of transverse cracking and rutting M-E PDG seems to overpredict distress in most of the cases. This is consistent with what we have observed, in general, with the current version of the software.

Table 10.8. Comparison of predicted and observed asphalt pavement performance — SPS-1 Michigan Sections

Section	Longitudinal Cracking	Fatigue Cracking	Transverse Cracking	Rutting	IRI
26-0115	R	R	R	R	R
26-0116	R	R	O	O	R
26-0117	R	R	R	O	R
26-0118	R	R	R	O	R
26-0120	O	O	O	CC	U
26-0121	O	O	O	CC	O
26-0123	R	R	O	O	R
26-0124	R	R	O	O	R

R = Reasonable match between predicted and observed performance
O = Overestimate predicted performance
U = Underestimate predicted performance
CC = Can not Compare

10.5.2 MDOT Flexible Pavement Sections

This section gives details of verification performed using the 5 flexible pavement sections for which data was provided by MDOT (**Table 10.9**. These pavements were selected based on the service life i.e. at least 10 years of age so that sufficient distresses are manifested. The available pavement data required to execute M-E PDG was provided by MDOT. Level 3 input levels were adopted if appropriate or sufficient input data was unavailable. The respective weigh-in-motion (WIM) weigh station data was also used in the analyses to characterize the traffic loadings and repetitions for all these pavement sites. The traffic data used for the analysis is presented next.

Table 10.9. Details of selected MDOT flexible pavement sections

	Section 1	Section 2	Section 3	Section 4	Section 5
	17761N	20233N	29581E	29581W	18890N
Base/Subgrade Construction Year/Month	May-June 1983	Nov. 1985-April 1986	Jun-Aug 1994	May-Jun 1995	July-Sep 1988
Pavement Construction Year/Month	Jul-Nov 1983	Jun-Aug 1986	Aug-Oct 1994	Jul-Sep 1995	Aug-Sep 1989
Traffic Opening Year/Month	Jan. 1984	Oct. 1986	Nov. 1994	Oct. 1995	Nov. 1989
Project Location: County	Mecosta	Osceola	Eaton/Ingham	Eaton/Ingham	Mason
Project Location: City	Big Rapids	Reed City	Lansing	Lansing	Ludington
Ac Thickness (in)	7.25	7.25	14.25	11.75	7.5
Base Thickness (in)	4	4	7.75	7.75	4
Subbase Thickness (in)	18	18	10	10	18

10.5.2.1 Traffic Inputs

The closest WIM station to the pavement sites was used to acquire necessary traffic data. It should be noted that the closest WIM station was also at least 30 miles away from the site. Therefore, the actual traffic experienced by the sections may be somewhat different from those used in this verification exercise. Classification (Card 4) and truck weight (Card 7) data, for selected locations were analyzed using TrafLoad software to extract required traffic-related M-E PDG input data. Some of the weigh station sites have Piezo WIM sensors, which might cause

some concerns regarding temperature variations and calibration. However, the available traffic data was used in this analysis as no other representative information was available for these sites.

10.5.2.2 Material Inputs

Several material related inputs are required for various pavement layers, including; (a) layer thicknesses, (b) layer material types, (c) strength and index properties and (d) other structural details. These were provided by MDOT and were used in this analysis if available. In case, some material-related input was not available, level 3 inputs were assumed. Appendix B-4 shows all the inputs used in this analysis. Version 1.003 of the M-E PDG software was used in all the cases. Some of the important assumptions and considerations are as follows.

(1) One of the most important inputs for the unbound pavement layers is the modulus value of the material. For the crushed gravel base the modulus was assumed to be 25,000 psi in all the cases.
(2) Modulus for the sand subbase was assumed to be 13,500 psi for the three sections for which this input was not available.
(3) Gradation details for the sand subbase was available in the form of percent passing through #200, #100 and 1" sieves only. The gradation was input in the form only. To get better prediction a more detailed gradation should be input.
(4) Data in conventional penetration grade was given for the type of asphalt used in these projects. M-E PDG would calculate creep compliance, tensile strength as well as complex modulus based only on this information combined with aggregate gradation. Since penetration is based on penetration number at one temperature only it could lead to somewhat erroneous modulus and creep calculation through different seasons of the year.
(5) Effective binder content was also not available for any of the sections. Based on an empirical relationship it was estimated to be twice the binder content used.
(6) The air voids provided by MDOT is in the range of 2.5 to 4.5%. This is a strong indication that it was measured on lab compacted specimens and not from a field core immediately after compaction. In-situ air voids immediately after compaction should be much higher. Since there was no other way to estimate this it was decided that this value would be varied, within a feasible range to see the change in performance. To begin with, in-situ air voids was assumed to be twice as much as air voids in the plant compacted sample.
(7) Plasticity index and liquid limits for the subgrade were assumed to be 5% and 21%, respectively.

10.5.2.3 Climate

Two of the sites fall in Lansing and therefore, data from the Lansing weather station was used for those sections. Climatic data for the other three sections were interpolated using the nearest two or three weather station using actual latitude and longitude for the sites. Elevation of the sites had not been provided by MDOT. The mean elevation of the city in which the sections fell was used.

10.5.2.4 Discussion of Results for MDOT Sections

MDOT also provided the performance data available for the sections being studied in this exercise. However, it should be recognized that there seems to be some discrepancy in the performance data as discussed below.

(1) In several cases the distress goes down with time. This is possible only when there is some maintenance or repair activity on the pavement. For example in the case of longitudinal cracking, it was 7701 ft/mi in the 13th year and only 319 ft/mi in the fifteenth year. But M-E PDG does not account for such maintenance activity during the design life of the pavement. Therefore, it can not capture the improvement in pavement condition over time.
(2) In some cases pavement condition seems to be too good after even 15 years of service and then suddenly the distress increase sharply. This indicates that either there was some maintenance activity before the first performance survey was done or that the performance data may be erroneous. For example in the case of rutting for the pavement section 17761N rutting is only 0.06 inches in 15th year (the first year for which rutting performance is reported) and it rises to 0.26 inches within next two years.
(3) In the case of IRI estimates initial of IRI (immediately after construction) were not available which is an input in the software. In some case the first estimate of IRI reported was in the ninth year. For want of better data it was assumed that the initial IRI was same as the least value of IRI reported from actual survey. Therefore, care should be taken to rely more on the trend of IRI progression rather than the absolute value at any time during the design life of the pavement.

Figure 10.20 through Figure 10.24 show pavement performance as predicted by the M-E PDG software versus actual performance observed. Some of the salient points that can be derived from this comparison are presented below.

(1) M-E PDG software predicted no longitudinal cracking through the life of the pavements in all the five cases. However, actual performance data shows that section 17761N did see appreciable amount of longitudinal cracking. Pavement sections 20233N and 11890N experienced medium levels of longitudinal cracking. These three sections had only 7.25 or 7.5 inches of asphalt bound layer where as rest of the two pavements sections which are on I-96 had 14.25 and 11.75 inches of asphalt concrete layer. These two pavement sections saw very little of longitudinal cracking up to 11th year of service. But this trend was not captured by M-E PDG software.
(2) Fatigue performance for all the five pavement sections seems to be relatively more in agreement with those predicted by the M-E PDG software, as can be seen in Figure 10.21. In the case of section 20233N field performance shows no fatigue cracking till the 13th year. But within next two years fatigue cracking shoots to 18 percent. This seems to be an anomaly, which would need further study to be explained satisfactorily.
(3) Transverse cracking is predicted in terms of length of the cracks (in feet) per mile of the pavement. Based on the comment from the RAP during last quarterly meeting it was converted into crack spacing assuming 12 feet wide lane in all the cases. Therefore, unlike other distresses the crack spacing goes down with deteriorating pavement condition i.e. as the pavement gets more of transverse cracking. Before appearance of the first transverse cracks crack spacing is practically infinity. Therefore, this does not appear

in the plots in Figure 10.22. There is big difference in transverse crack spacing predicted by M-E PDG software and that actually observed in the field in pavement sections 17761N, 20233N and 18890N. Sections 29581E and 29581W, which both lie on I-96, seem to have much better agreement between predicted and actual performance.

(4) Figure 10.23 compares rutting performance for all the MI sections. Unfortunately actual rutting measurements provided for these all the sections have very few points and they also seem to be in error. M-E PDG software predictions show that the two interstate sections would have around 0.8 inches of rutting at the end of 20 years whereas rest of the three sections would have nearly or more than 1.0 inch of rutting by that time.

(5) As stated earlier for want of initial IRI for the pavements, particularly the three non-interstate sections absolute values of IRI should not be compared between the predicted and observed performance. In the case of the two interstate sections (29581E and 29581W) IRI was estimated in the first year. Accepting that as initial IRI would be a reasonable assumption. However for both of these sections and section 17761N IRI drops after 7^{th} and 12^{th} year respectively, which is not natural. Therefore, it is hard to compare the observed and predicted IRI performance. For rest of the two sections it can be said that they match to a reasonable degree.

These observations have been summarized in Table 10.10 below.

Table 10.10. Comparison of predicted and observed asphalt pavement performance —Michigan Sections

Section	Longitudinal Cracking	Fatigue Cracking	Transverse Cracking	Rutting	IRI
17761N	U	CC	U	CC	O
20233N	U	CC	U	CC	R
29581E	R	R	R	CC	CC
29581W	R	R	R	CC	CC
18890N	U	R	U	CC	R

R = Reasonable match between predicted and observed performance
O = Overestimate predicted performance
U = Underestimate predicted performance
CC = Can not Compare

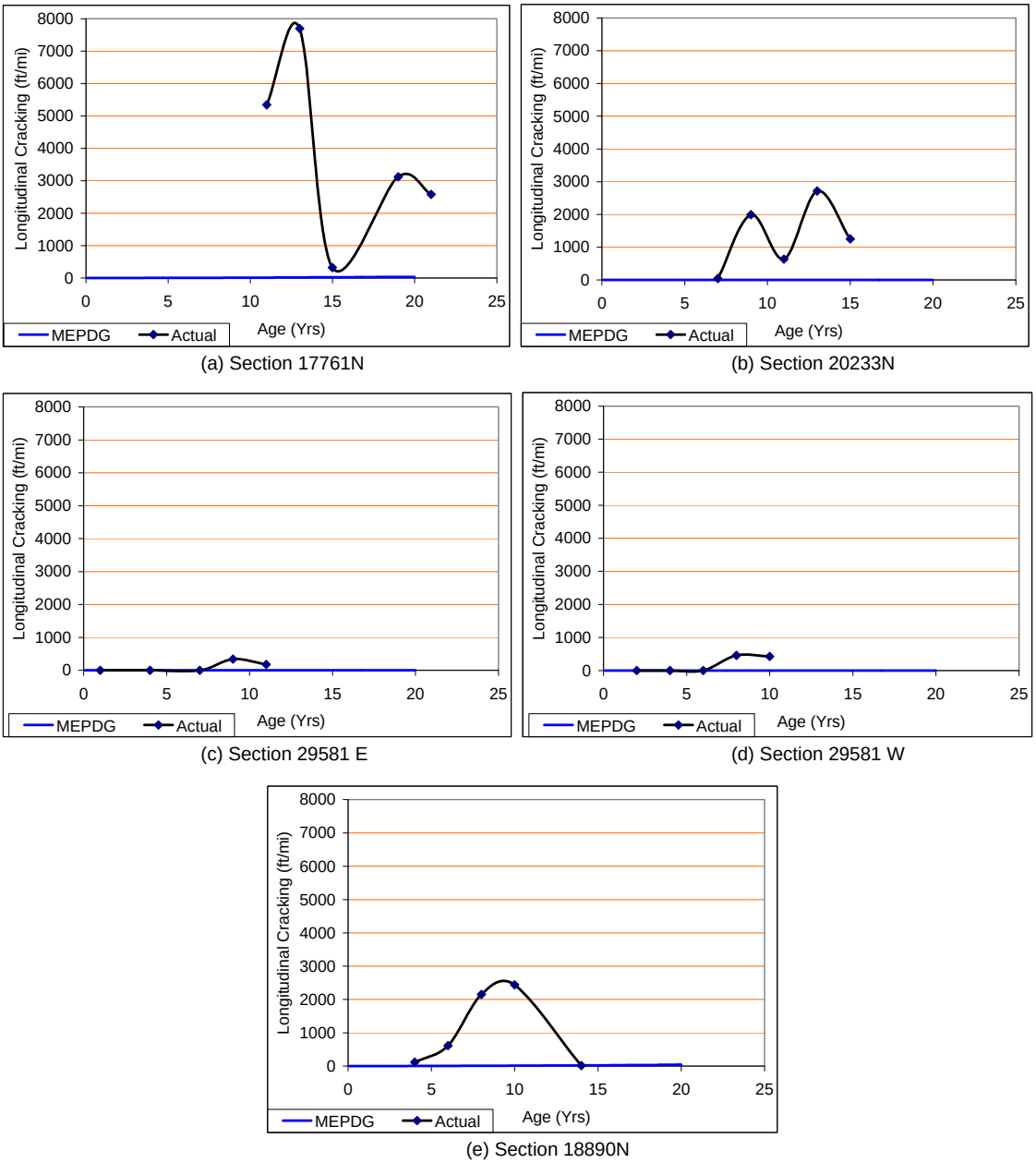

(a) Section 17761N

(b) Section 20233N

(c) Section 29581 E

(d) Section 29581 W

(e) Section 18890N

Figure 10.20. Observed longitudinal cracking versus that predicted by M-E PDG for SPS-1 sections

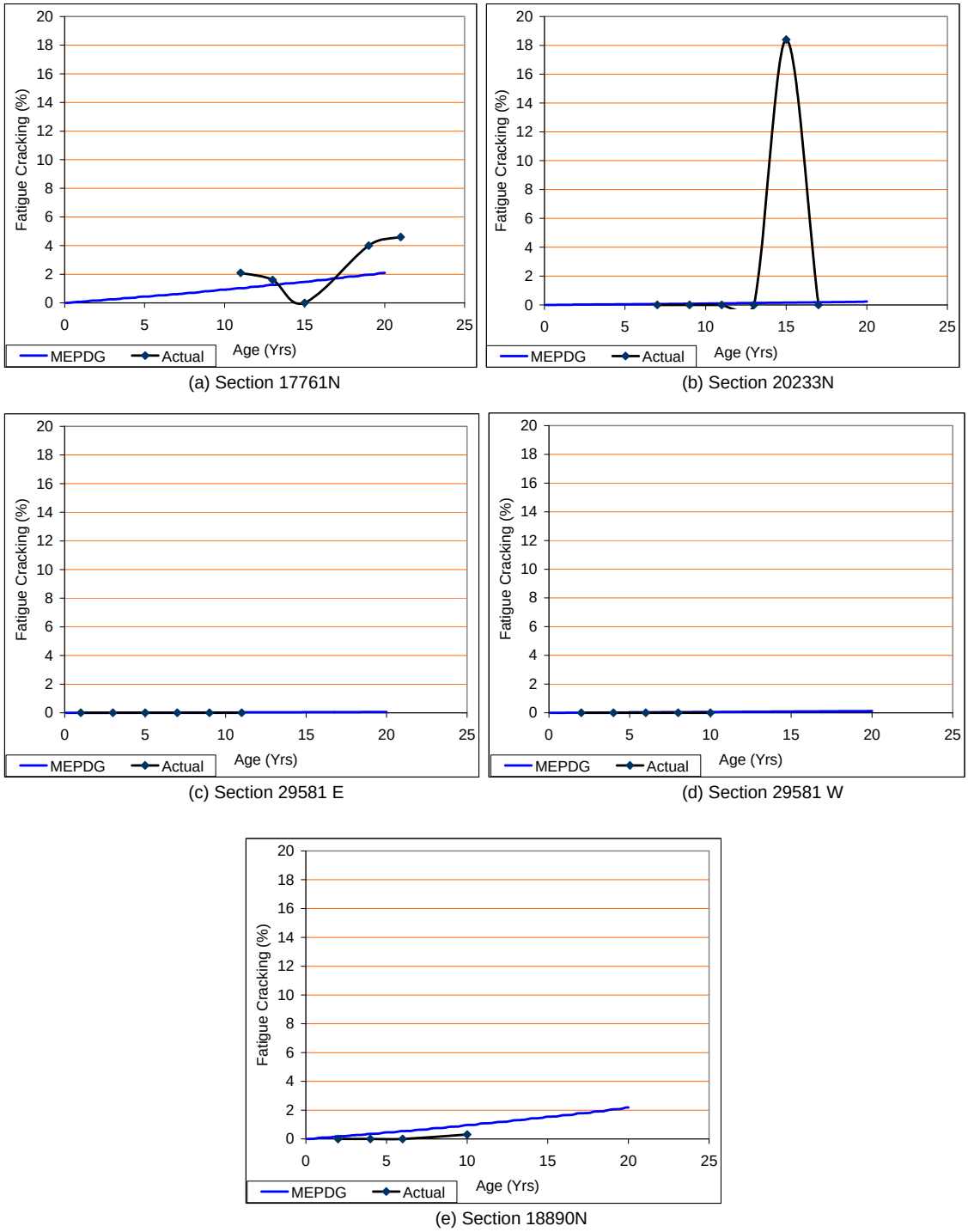

Figure 10.21. Observed fatigue cracking versus that predicted by M-E PDG for SPS-1 sections

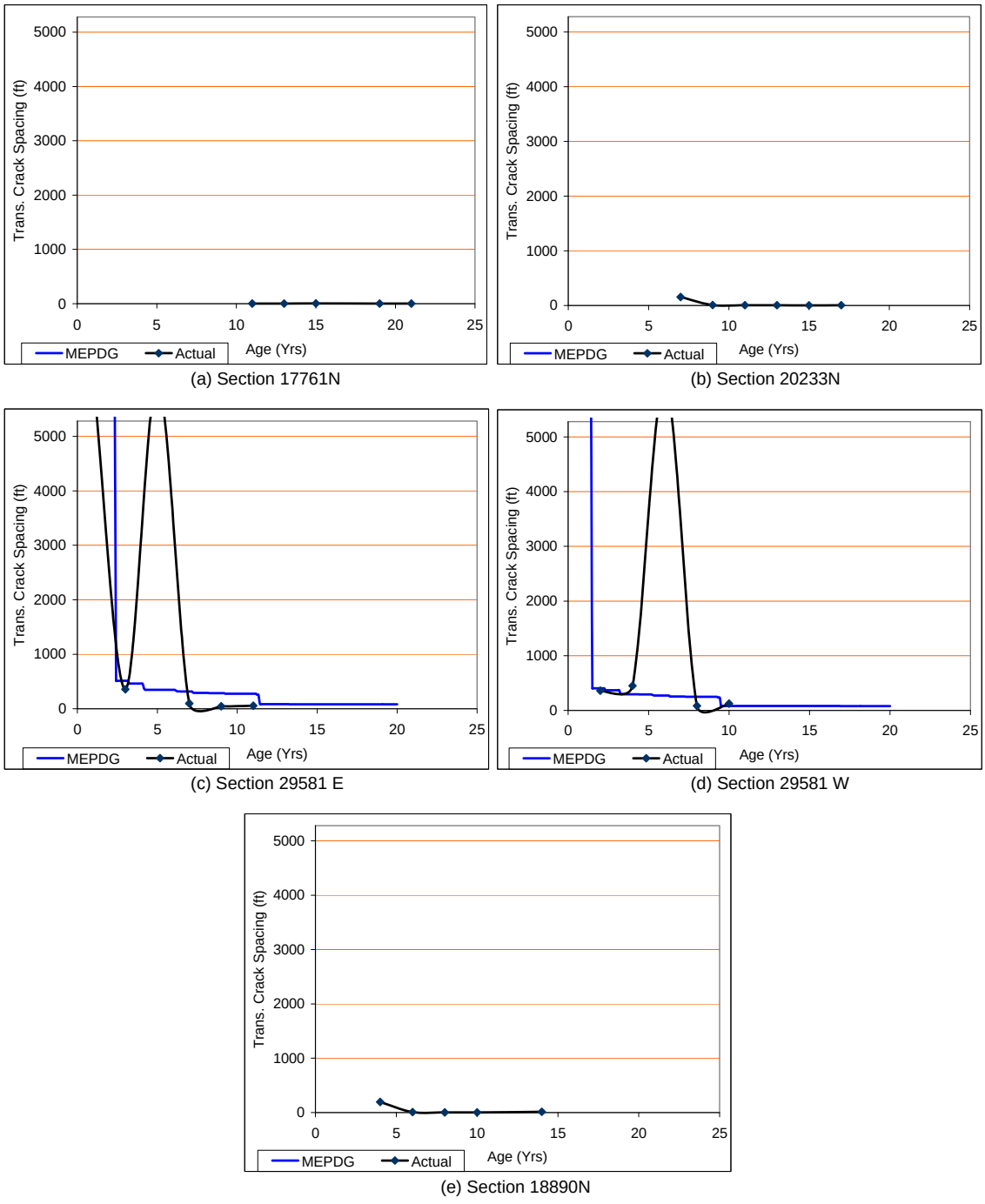

(a) Section 17761N

(b) Section 20233N

(c) Section 29581 E

(d) Section 29581 W

(e) Section 18890N

Figure 10.22. Observed transverse cracking versus that predicted by M-E PDG for SPS-1 sections

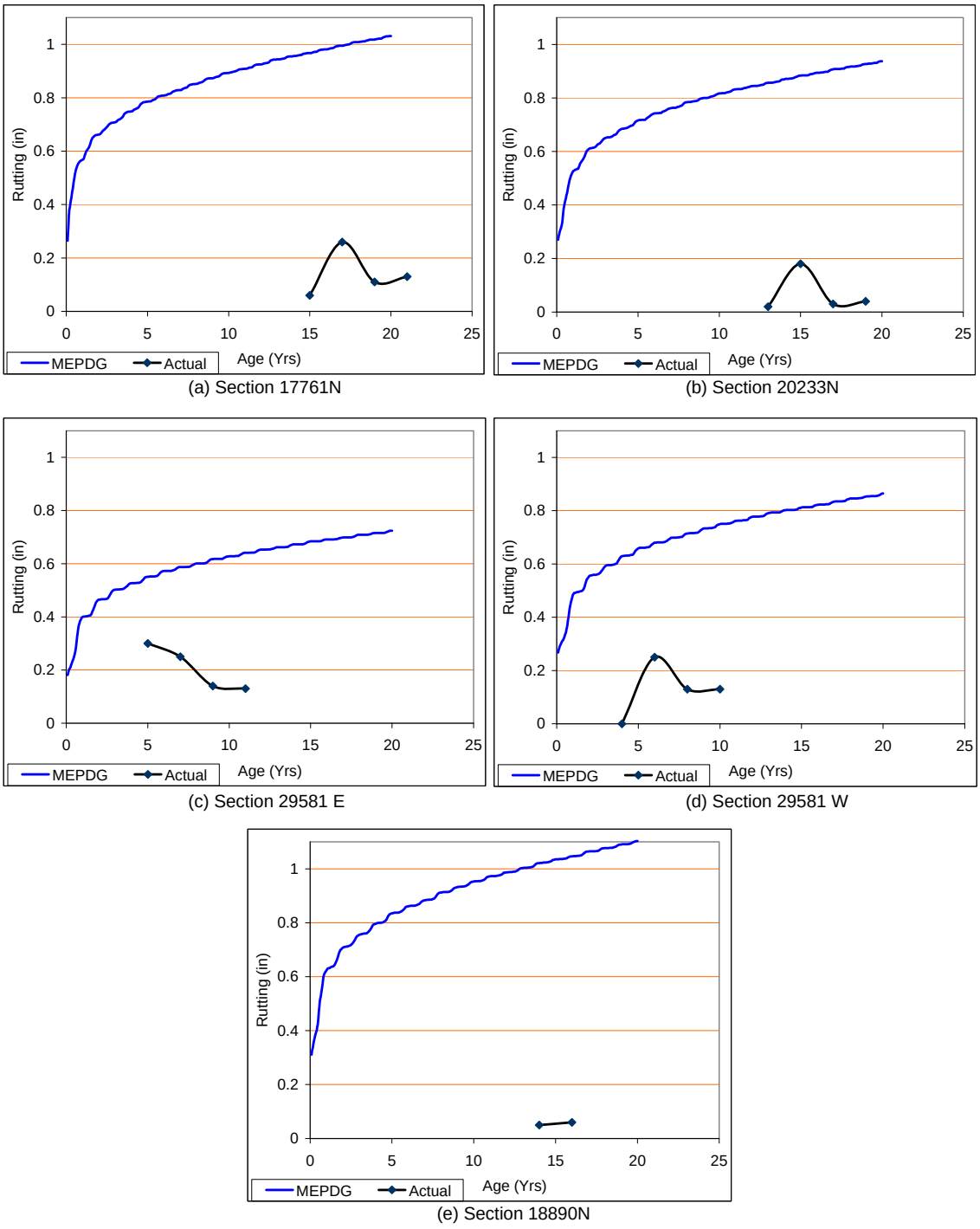

Figure 10.23. Observed rutting versus that predicted by M-E PDG for SPS-1 sections

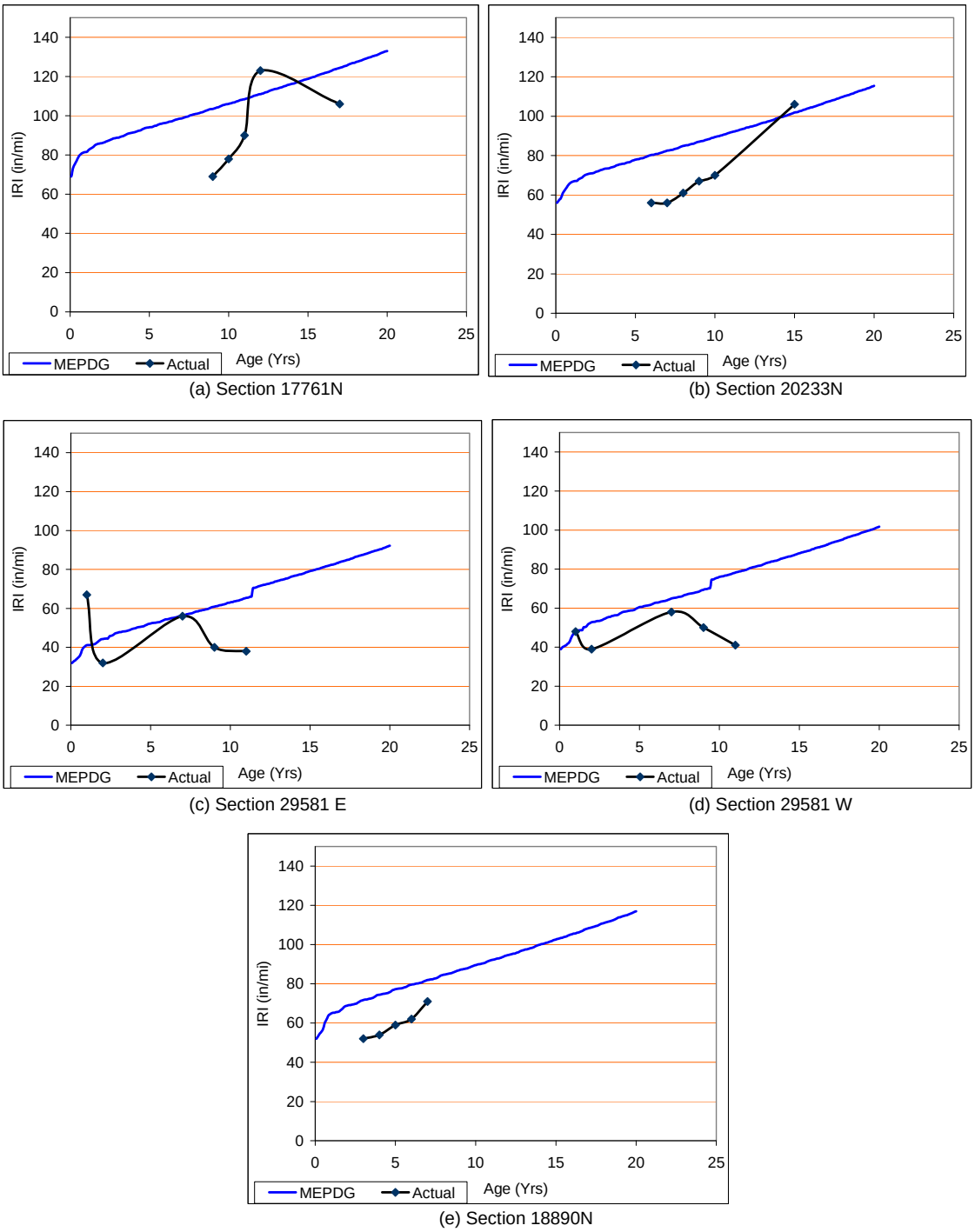

(a) Section 17761N

(b) Section 20233N

(c) Section 29581 E

(d) Section 29581 W

(e) Section 18890N

Figure 10.24. Observed IRI versus that predicted by M-E PDG for SPS-1 sections

CHAPTER 11 - DESIGN IMPLICATIONS - FLEXIBLE

11.1 INTRODUCTION

M-E PDG software uses different distress models to estimate distresses over the design life of the pavement for a given set of material, mix, traffic and environmental inputs. Therefore, M-E PDG can be used as a tool to analyze and compare different pavement designs. Such analysis would provide deeper insight into how different material or mix properties would affect performance of the pavement for a given expected traffic under certain climatic conditions. Although M-E PDG by itself is not a design software, it can be used by the pavement designer to come up with a design that would be bound by limiting values of expected distresses. This chapter presents strategies which can be used to achieve both these purposes, namely (1) analyze different possible designs and (2) come up with an optimal design for a given level of performance.

11.2 ANALYZING PAVEMENT DESIGNS

Analysis may be carried out for a specific design, a set of feasible designs or for a larger category. Analysis of individual designs is rather easily done using M-E PDG. One can input all the material, mix, traffic and environmental properties and see how the pavement is expected to perform. The same strategy can be applied even if there were more than one feasible design and pick the one which shows the best performance or best meets criteria based on cost, easy availability of materials, etc. Considering the fact that M-E PDG takes 30 to 50 minutes to analyze one case of HMA pavement with a design life of 20 years, analyzing a bigger category of designs would require substantial effort and time. However it is possible to develop strategies which can make such large scale analysis simpler as well as considerably more efficient and informative without sacrificing accuracy. In this section a possible strategy to achieve this objective is presented.

11.2.1 Pavement Design Analysis Strategy

In principal this strategy can be described in the following steps:

(1) Choose the design input variables that need to be studied for their effect on pavement performance.
(2) Choose the range of each design input variable.
(3) Choose two to five points spanning the entire range for each variable.
(4) Prepare a matrix with all possible combinations of all the variables. Fix other input variables that may be required for running the M-E PDG software.
(5) Run M-E PDG for each set of values of the design input variables.
(6) Develop n-dimensional response surfaces. (n-1) of those dimensions correspond to the design input variables and the last dimension would have distress predicted by M-E PDG.
(7) Suitable interpolation technique can be used to interpolate distress in the nth dimension corresponding to input values in between those which were identified in steps 1 through

3. In essence steps 1 through 7 provide pavement performance without running M-E PDG for as many cases as required.

(8) Such interpolation would give performance prediction for the entire design life of the pavement. Therefore, when comparing different designs the results obtained here can be used to determine the difference in service life which is a much more tangible parameter for state highway agencies in making their decisions.

11.2.2 Pavement Design Analysis Examples

Two examples are presented below to demonstrate the above strategy as well as highlight the uses and benefits of such an exercise.

Step 1: Two mix designs were chosen. These mix designs were selected from a set of mix designs used by MDOT on highway projects in the year 2007. The design input variables chosen for this example are given below. In all the cases a 1.5 inch thick surface course is assumed. Therefore, AC layer thickness would vary as the AC binder course thickness is varied.

(1) AC binder course thickness
(2) Base and subbase layer thicknesses
(3) Base modulus

Step 2: Range for each of the chosen variables

(1) AC binder course thickness: 4 in. to 12 in.
(2) Base and subbase layer thickness: (4 in. and 18 in.) or (8 in. and 10 in.)
(3) Base modulus: 18000 psi to 40000 psi

Step 3: Evaluation points

(1) AC binder course thickness: 4, 6, 8, 10, 12 in.
(2) Base and subbase thickness: (4 in. and 18 in.) and (8 in. and 10 in.)
(3) Base modulus: 18000, 25000, 32000 and 40,000 psi

Step 4: The matrix (see Table 11.1)

Step 5: M-E PDG was run for all the 40 cases shown in step 4 above for each of the two mix designs and the distress time histories were compiled.

Step 6: Since only a maximum of three dimensions can be plotted for visual inspection the plots below (Figure 11.1through Figure 11.4) show fatigue cracking and rutting at the end of 240 months (20 years) only. Also, since MDOT uses only two combinations of base and subbase thicknesses rather than varying them continuously, separate plots can be developed for the two levels.

Step 7: Piecewise cubic spline interpolation technique was used to determine pavement performance at intermediate levels. These intermediate levels can be chosen to be any combination of input variables as long as they fall within the range identified in step 2. It is possible to extrapolate to certain extent beyond this range using extrapolation techniques but that may lead to errors in the estimated performance.

Table 11.1. Combinations of all input variable values for M-E PDG run

Run Number	AC Binder Course Thickness	Base Modulus	Base & Subbase Thickness
1	4	18000	4, 18
2	4	18000	8, 10
3	4	25000	4, 18
4	4	25000	8, 10
5	4	32000	4, 18
6	4	32000	8, 10
7	4	40000	4, 18
8	4	40000	8, 10
9	6	18000	4, 18
10	6	18000	8, 10
11	6	25000	4, 18
12	6	25000	8, 10
13	6	32000	4, 18
14	6	32000	8, 10
15	6	40000	4, 18
16	6	40000	8, 10
17	8	18000	4, 18
18	8	18000	8, 10
19	8	25000	4, 18
20	8	25000	8, 10
21	8	32000	4, 18
22	8	32000	8, 10
23	8	40000	4, 18
24	8	40000	8, 10
25	10	18000	4, 18
26	10	18000	8, 10
27	10	25000	4, 18
28	10	25000	8, 10
29	10	32000	4, 18
30	10	32000	8, 10
31	10	40000	4, 18
32	10	40000	8, 10
33	12	18000	4, 18
34	12	18000	8, 10
35	12	25000	4, 18
36	12	25000	8, 10
37	12	32000	4, 18
38	12	32000	8, 10
39	12	40000	4, 18
40	12	40000	8, 10

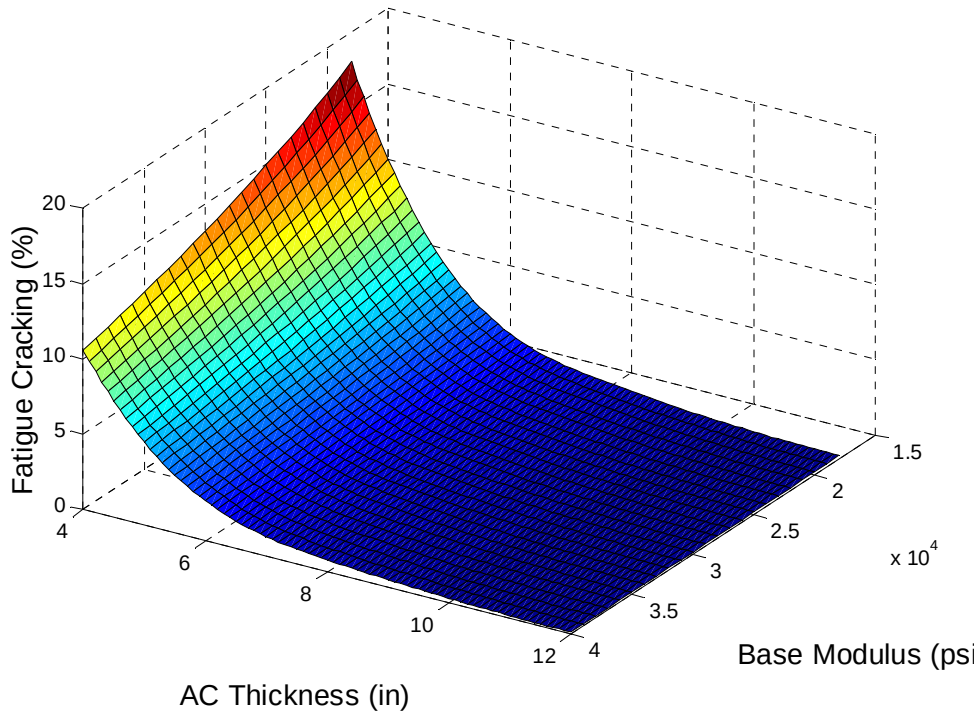

Figure 11.1. Interpolated fatigue cracking surface (at 20 years) for mix 1

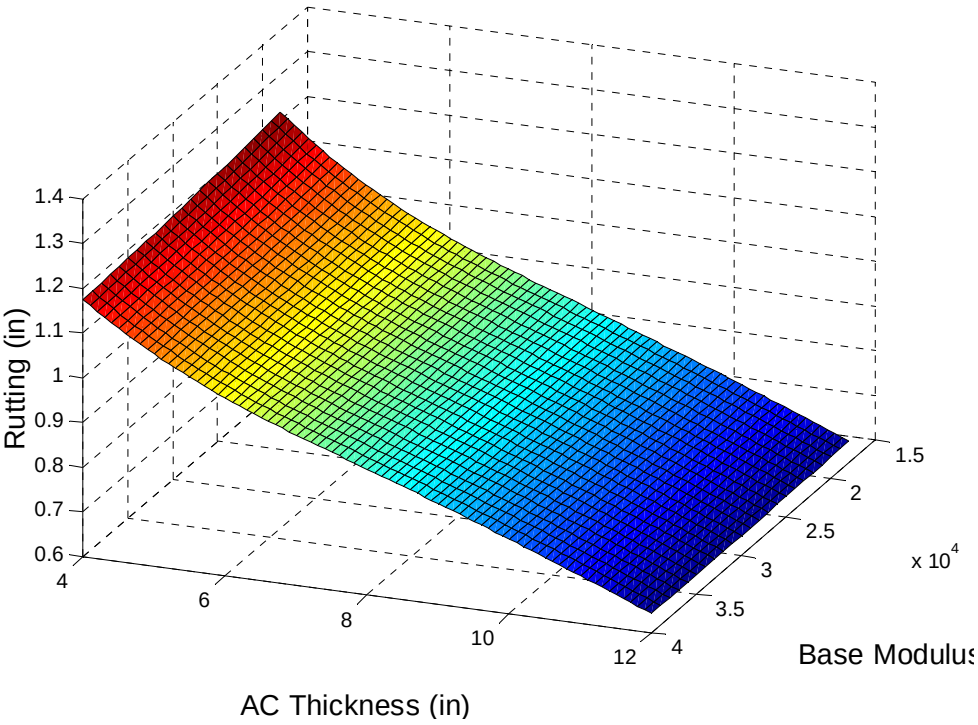

Figure 11.2. Interpolated rutting surface (at 20 years) for mix 1

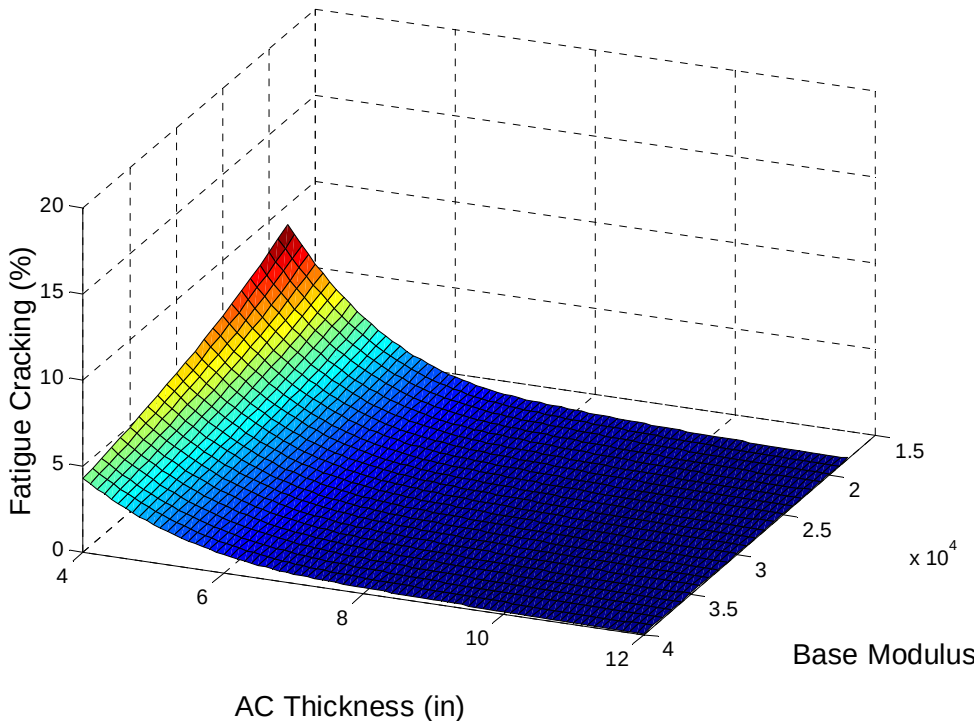

Figure 11.3. Interpolated fatigue cracking surface (at 20 years) for mix 2

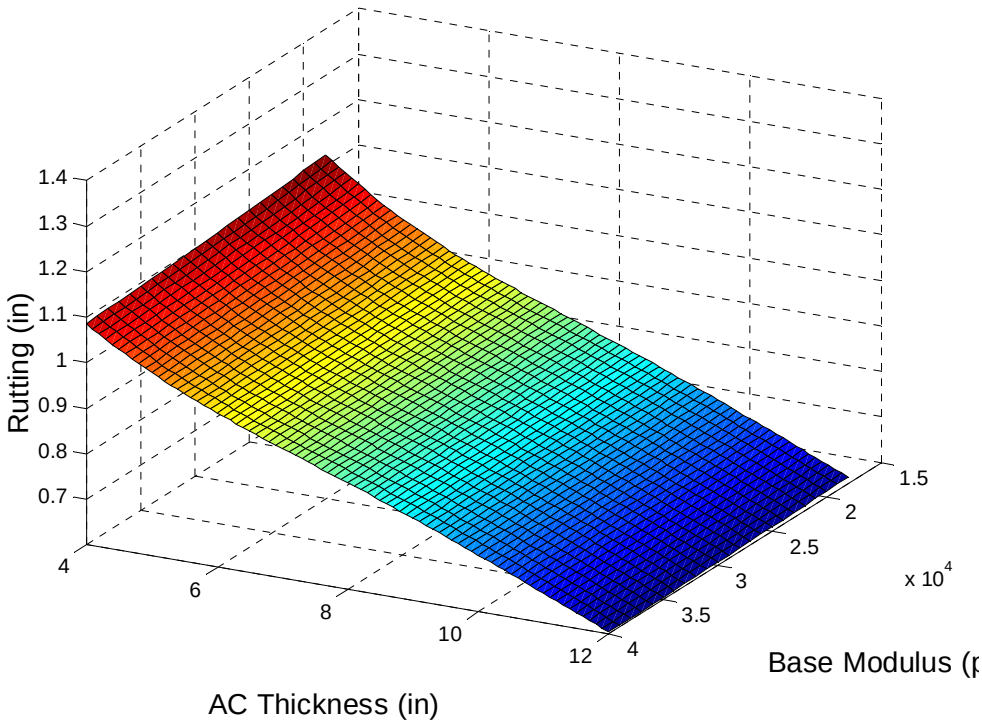

Figure 11.4. Interpolated rutting surface (at 20 years) for mix 2

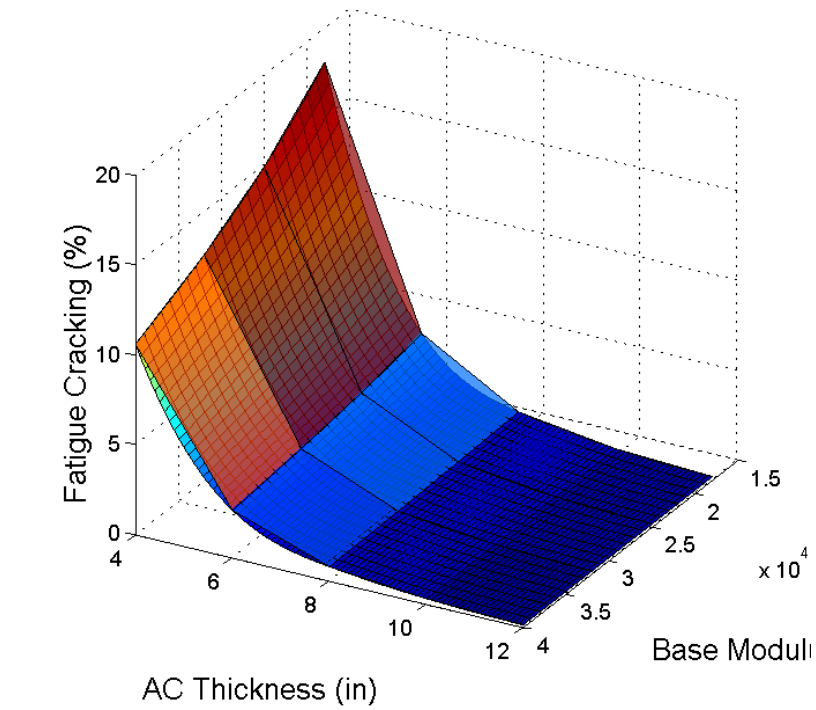

Figure 11.5. Fatigue cracking for mix 1: Original and interpolated surfaces (the original surface is translucent)

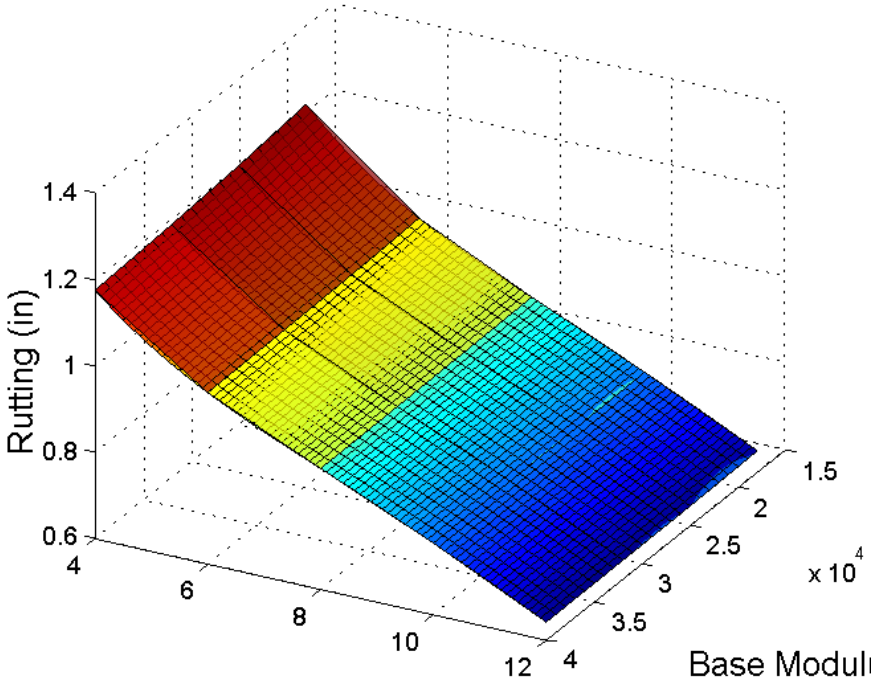

Figure 11.6. Rutting in mix 1: Original and interpolated surfaces (the original surface is translucent)

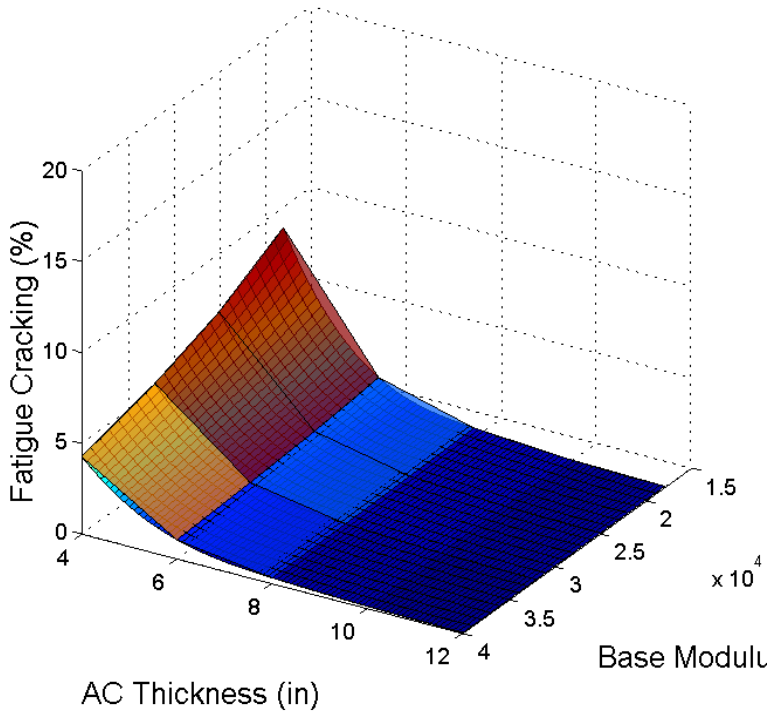

Figure 11.7. Fatigue cracking for mix 2: Original and interpolated surfaces

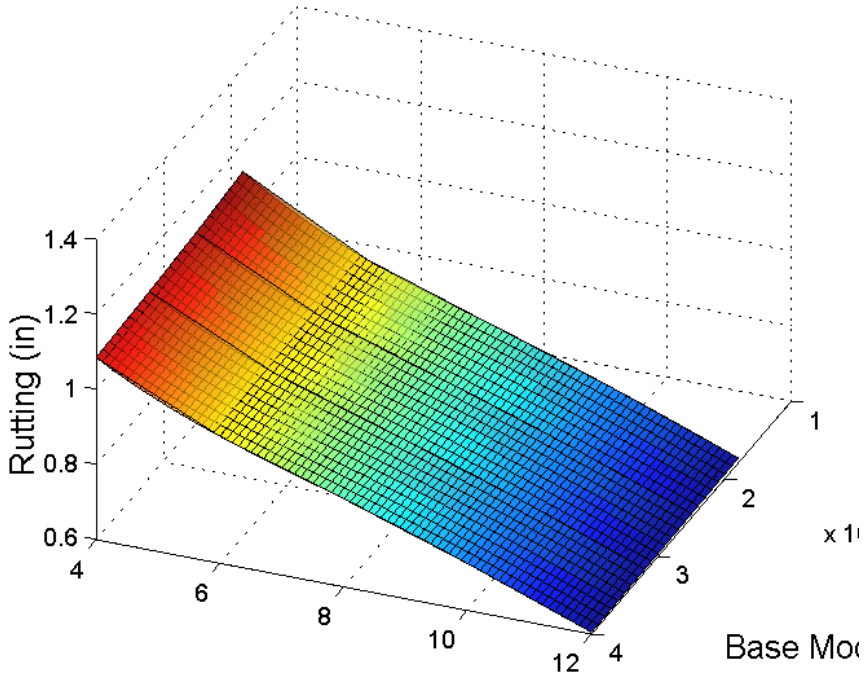

Figure 11.8. Rutting in mix 2: Original and interpolated surfaces (the original surface is translucent)

Figure 11.5 through Figure 11.8 show original fatigue cracking and rutting surfaces constructed directly from results obtained with M-E PDG runs as well as the surfaces constructed using the interpolated performance. The surface with solid face and translucent coloring represents the original results from M-E PDG and the surface with finer wire-mesh represents the interpolated results.

Step 8: Two sample pavement designs were chosen to show how the n-dimensional response surface developed above can be used for comparing designs and determining the difference in the expected life of the pavements constructed with those designs. Table 11.2 shows the main details of these two example designs. All other aspects of designs like subgrade, traffic, aggregate gradation etc. were kept the same. These two pavement designs were applied to both of the HMA mixes being considered.

Table 11.2. Details of two example designs

Design Variable	Design 1	Design 2
AC Surface Course Thickness (in)	1.5	1.5
AC Binder Course Thickness (in)	6.5	7.5
Base Thickness (in)	4	4
Subbase Thickness (in)	18	18
Base Modulus (psi)	23000	19000

11.2.3 Results from Pavement Design Analysis

Since all the values of the design variables chosen in the two example pavement designs fall within the range of the response surface generated in the previous steps we can directly estimate pavement performance from the surface. A MATLAB^{TM} program was written to generate these response surfaces and obtain responses for specific cases. Obtaining distresses for any possible combination of values of variables included in the response surface takes almost zero time. Figure 11.9 shows the expected fatigue performance for the two pavement designs when HMA mix 1 was used. The green horizontal line shows the maximum fatigue cracking for better performing pavement design, design 2 in this case.

Table 11.3 shows the amount of cracking and rutting at the end of 20 years for both the pavement designs and both the mixes. It also shows the difference in life that was determined using the interpolated response surface. A difference in life of 86 months between the two pavement designs for mix 1 means that pavements constructed using design 1 would have the same amount of fatigue cracking 86 months earlier than that in design 2 pavement at the end of a design life of 20 years. Although in this case the total amount of expected fatigue cracking is very low and, therefore, the difference may not seem to be of significant concern, the difference in life would be a concern when any of the pavement designs do show enough cracking to warrant major repair. Most important advantage of the strategy presented here is that it can be used to study all possible sceneries without running M-E PDG. The case presented here is just an example of one such scenario. The following section would demonstrate this further.

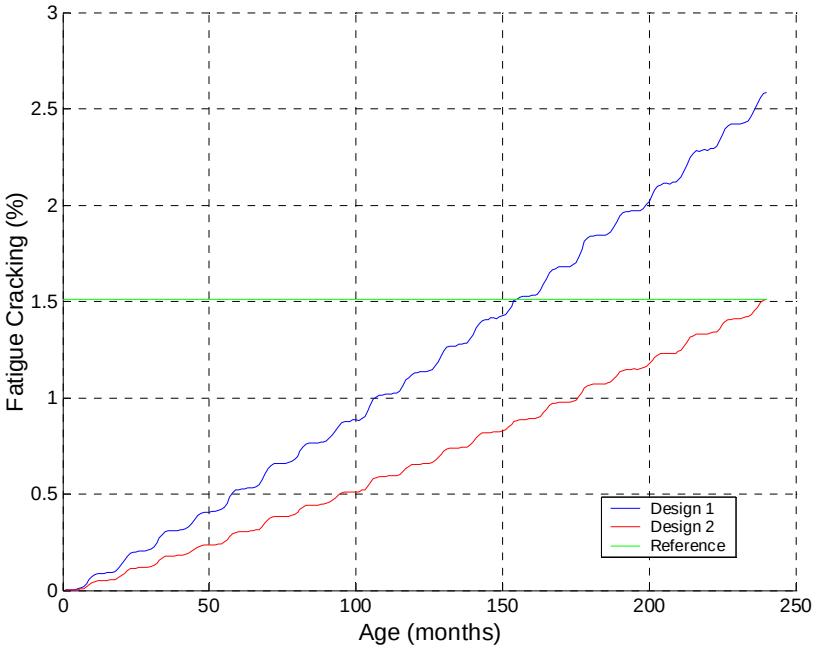

Figure 11.9. Fatigue cracking performance for the two designs (mix 1)

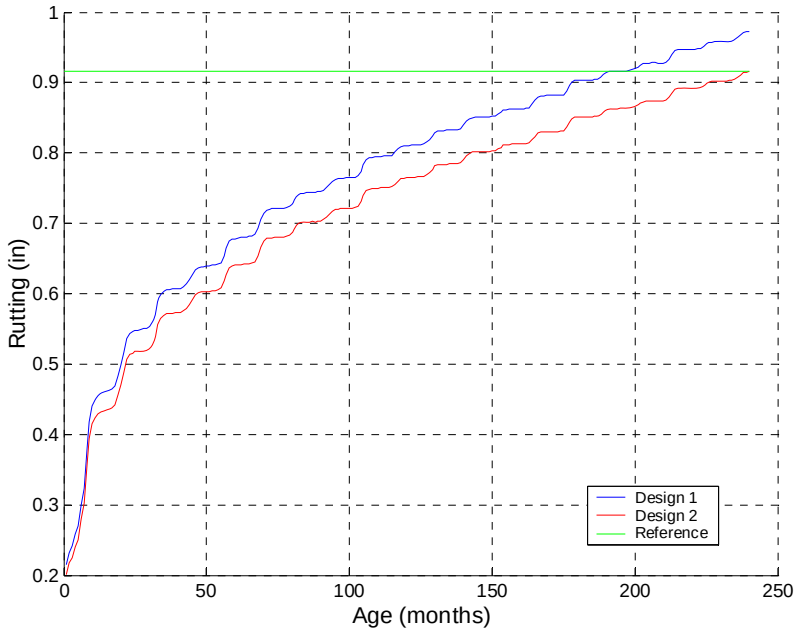

Figure 11.10. Rutting performance for the two designs (mix 1)

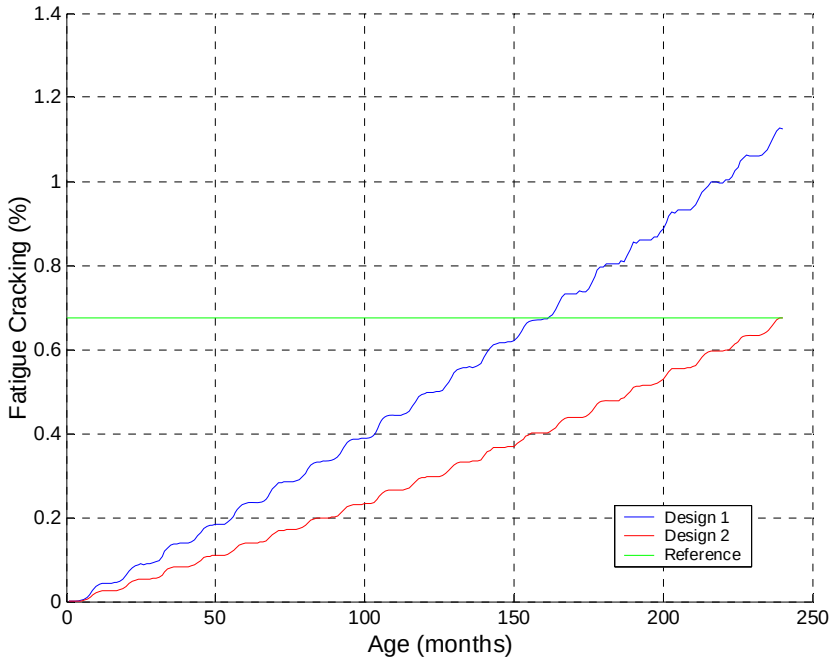

Figure 11.11. Fatigue cracking performance for the two designs (mix 2)

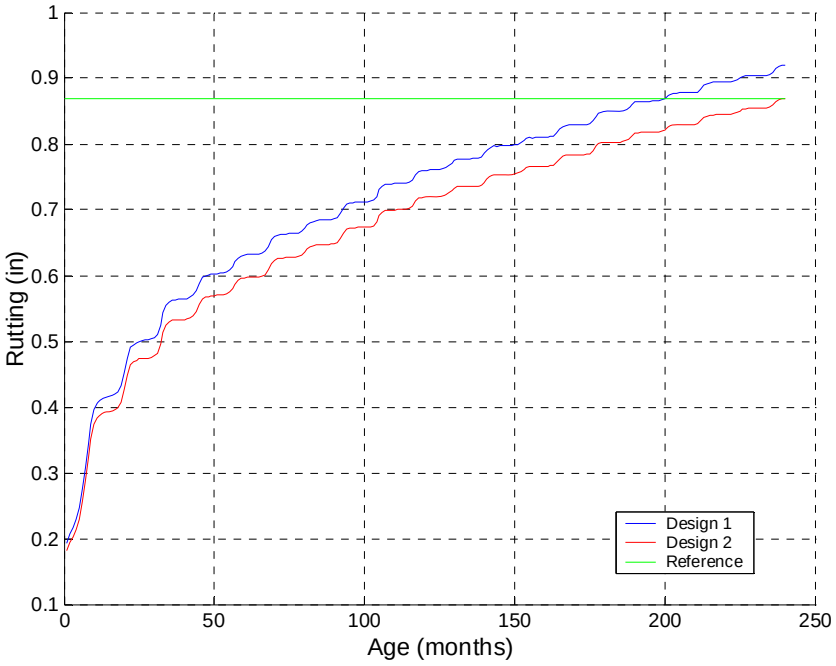

Figure 11.12. Rutting performance for the two designs (mix 2)

Table 11.3. Difference in performance and life (months) for the two pavement designs

Parameter	HMA Mix 1		HMA Mix 2	
	Design 1	Design 2	Design 1	Design 2
Fatigue cracking at 20 years (%)	2.6	1.52	1.14	0.68
Difference in fatigue life (months)	86		78	
Rutting at 20 years (in)	0.98	0.91	0.92	0.87
Difference in rutting life (months)	49		40	

11.3 DESIGN BASED ON PERFORMANCE

Most of the design procedures require a few critical inputs and provide thickness(s) of different pavement layers. A vast majority of them are empirical in nature and do not account for specifics of a particular design mix except for the few critical inputs. It is possible to use M-E PDG so that designs are finalized based on a particular threshold for maximum distress at the end of the design life. This section presents such a procedure followed by two examples.

11.3.1 Strategy for Design Based on Performance

Step1 through Step 7 in this strategy would be the same as that described in the earlier section on analyzing pavement designs. This would give us an n-dimensional response surface. The next step would be to obtain a relationship between performance and corresponding values of the design variable that needs to be determined. Then, based on the threshold desired for that performance/distress, the optimal values can be obtained from the relationship.

11.3.2 Examples of Design Based on Performance

There were two mixes analyzed in the earlier section. The same two mixes will be used to demonstrate this strategy. The response surface was prepared for the following set of variables and distress in the n^{th}-dimension.

(1) AC layer thickness: 4, 6, 8, 10, 12 in.
(2) Base and subbase layer thicknesses: (4 in. and 18 in.) and (8 in. and 10 in.)
(3) Base modulus: 18000, 25000, 32000 and 40,000 psi

The next step would be to set the threshold value for the distress(es). In this example the following thresholds were set.

Threshold for rutting at the end of 20 years = 0.8 inches
Threshold for fatigue cracking at the end of 20 years = 6%

The following values for the pavement design variables were set.

AC friction course Thickness = 1.5 inches
Base Thickness = 4 inches
Subbase Thickness = 18 inches
Base Modulus = 30000 psi

Therefore, the design problem will be to get the thickness of the AC layer so that the pavement would last for 20 years with less than 0.8 inches of rutting and 6% of fatigue cracking.

Using the response surface relationships, the design thickness for the HMA layer can be easily determined. Figure 11.13 shows the relationship between rutting and AC thickness for the given set of fixed design variables. According to the design requirement a maximum of 0.8 inches of rutting is allowable at 20 years. Therefore, as the figure shows design AC thickness should be 9.5 inches when using mix 1. Figure 11.14 shows the relationship between AC thickness and fatigue cracking after 20 years for mix 1. A threshold of 6% is used on fatigue cracking at the end of 20 years. To achieve that, the minimum thickness of AC required, as one can read from the plot in Figure 11.14, would be 5.2 inches. Considering the two thicknesses arrived at by imposing the criteria based on rutting and fatigue, AC layer thickness should be at least 9.5 inches. It is also possible to change other design variables which were fixed this far to see if the design AC thicknesses can be closer to each other when considering the two criteria and if any of those designs can be more cost effective.

To solve the same design problem with mix 2 one can generate plots as shown in Figure 11.15 and Figure 11.16. According to the rutting criteria the minimum AC thickness should be 8.8 inches. On the other hand, even if the AC layer was thinner than 4 inches it would still meet the criteria for fatigue cracking. Therefore, the design value for the AC layer should be 8.8 inches.

Table 11.4 presents the summary of designs obtained using the strategy proposed here.

Table 11.4. Results for pavement design examples

Design Variable	Based on Fatigue	Based on Rutting	Design Value
AC layer thickness using mix 1 (in)	5.2	9.5	9.5
AC layer thickness using mix 2 (in)	4.0	8.8	8.8

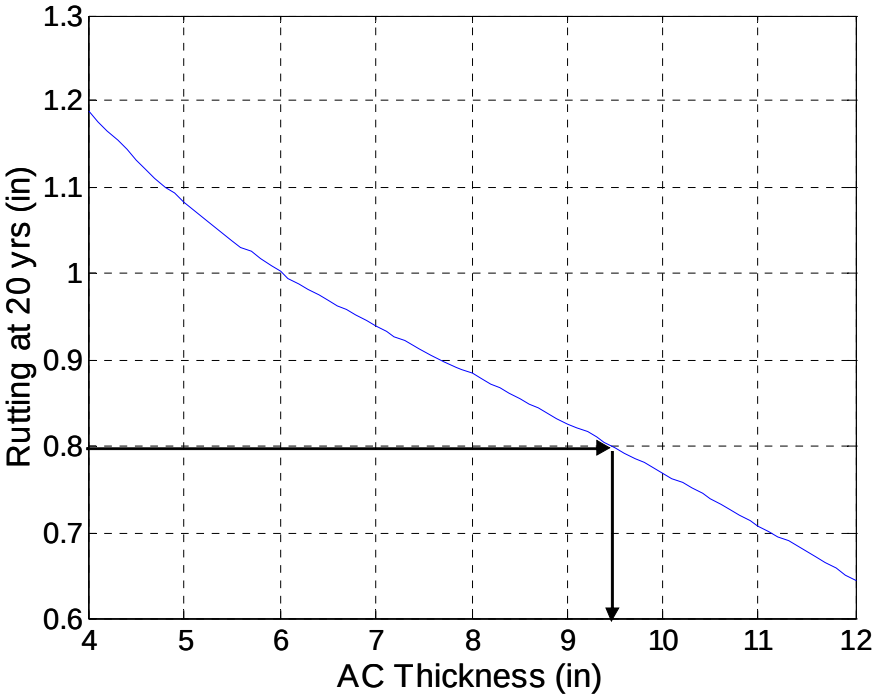

Figure 11.13. Relationship between AC thickness and rutting for pavement design with mix 1

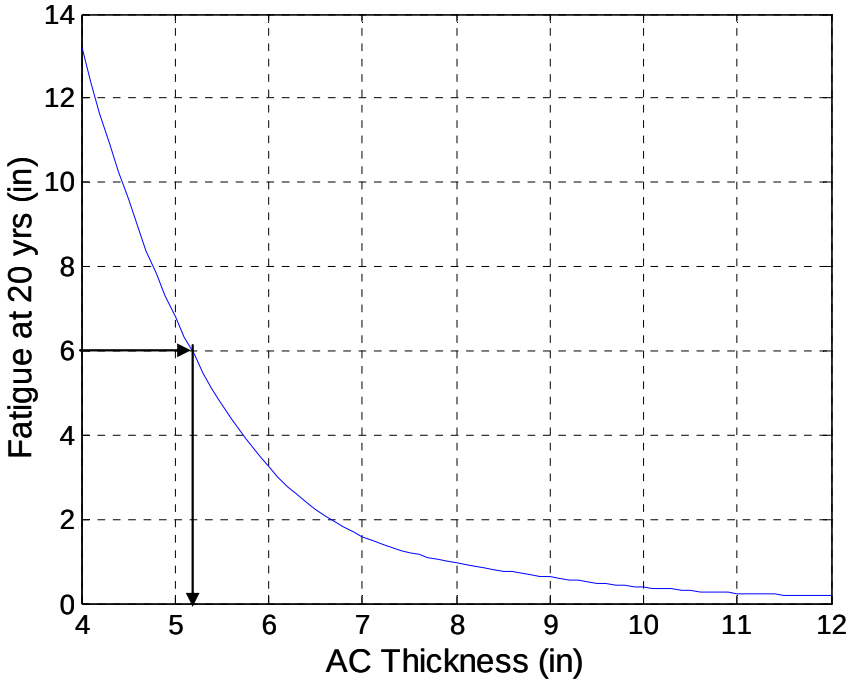

Figure 11.14. Relationship between AC thickness and fatigue for pavement design with mix 1

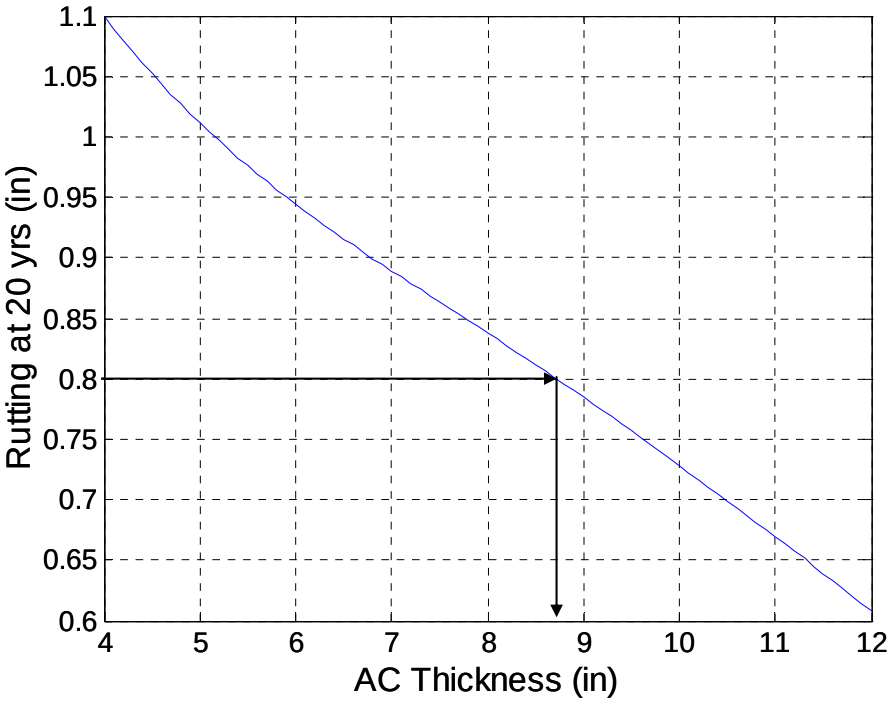

Figure 11.15. Relationship between AC thickness and rutting for pavement design with mix 2

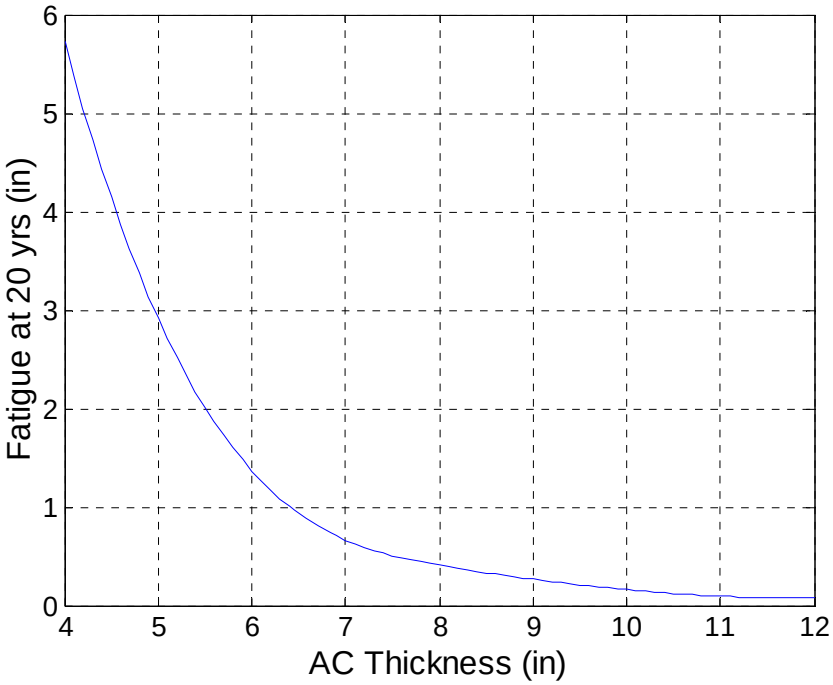

Figure 11.16. Relationship between AC thickness and fatigue for pavement design with mix 2

11.3.3 Advantages of Interpolation Method Used

The only stage at which approximation is used in either of the strategies presented in the preceding sections is when response surfaces are developed using interpolation methods. Localized (piece-wise) cubic spline method[1] was used for all interpolations. An important property of this method is that the interpolated values would definitely match the original values used for doing the interpolation. In other words, in Figure 11.5 through Figure 11.8 the interpolated response surface (shown with wire-mesh) would definitely pass through all the nodes in the original response surface (shown in solid faces with translucent colors). Also, at each of the nodes second derivatives of the local interpolation functions are matched for the surface, and continuity in the slope is met as well.

The interpolation method used here would in general be far more accurate than a regression equation that can be fit to the original data. The reason for this advantage is that the piece-wise cubic spline interpolation function fits itself to local variations in the slope of the surface in n-1 dimensions, while it would be extremely difficult to find a suitable function to model such slope changes at global levels and for such a wide range in the design input variables. This is because of the non-linear nature of relationships between the design input variables and pavement responses which get much more complicated because of interaction effects of the different design input variables.
For verifying the accuracy of the interpolation method the examples used in the preceding sections were used. Pavement responses for the optimal design obtained earlier were determined using the response surfaces as well as from M-E PDG. Figure 11.17 throughFigure 11.20 show the comparison of responses from the two sources. These figures clearly show that interpolated performances are quite accurate.

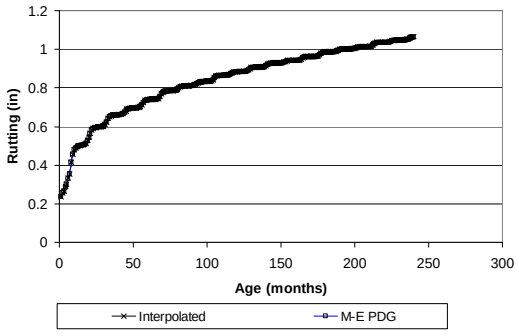

Rutting of Mix 1 and AC thickness = 5.2 in

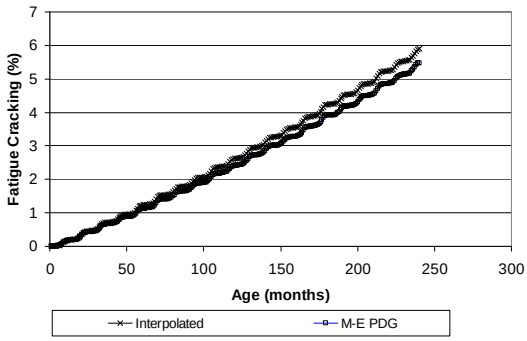

Fatigue of Mix 1 and AC thickness = 5.2 in

Figure 11.17. Comparison of interpolated and M-E PDG predicted performances – case 1

[1] Further details can be found at http://en.wikipedia.org/wiki/Spline_interpolation

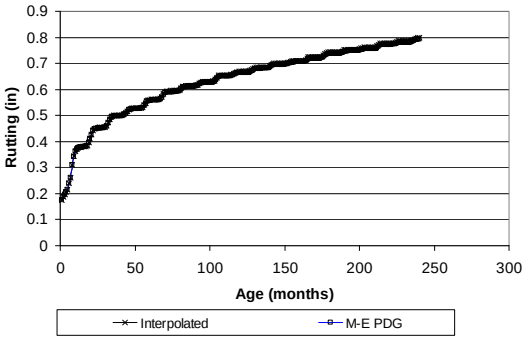

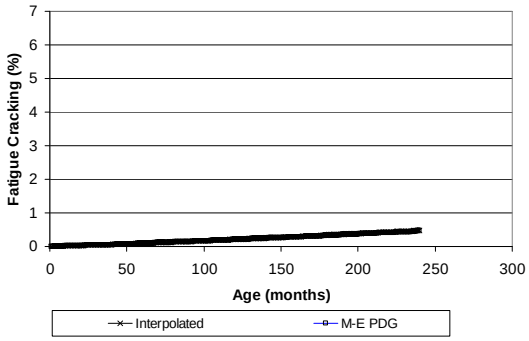

Rutting of Mix 1 and AC thickness = 9.5 in	Fatigue of Mix 1 and AC thickness = 9.5 in

Figure 11.18. Comparison of interpolated and M-E PDG predicted performances – case 2

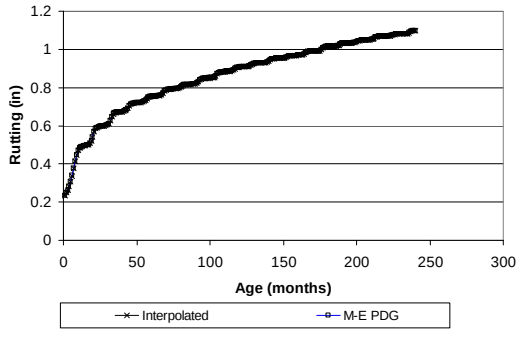

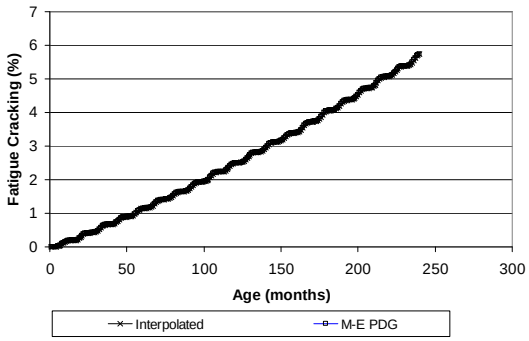

Rutting of Mix 2 and AC thickness = 4 in	Fatigue of Mix 2 andAC thickness = 4 in

Figure 11.19. Comparison of interpolated and M-E PDG predicted performances – case 3

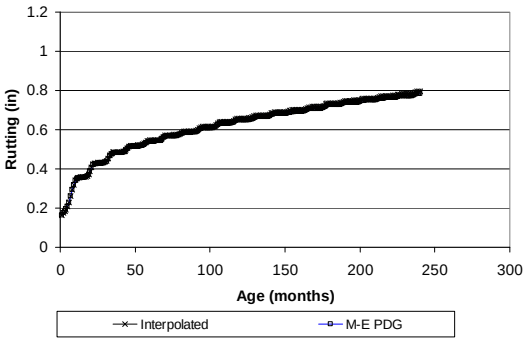

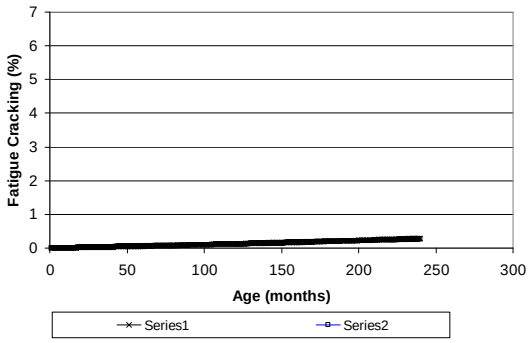

Rutting of Mix 2 and AC thickness = 8.8 in	Fatigue of Mix 2 and AC thickness = 8.8 in

Figure 11.20. Comparison of interpolated and M-E PDG predicted performances – case 4

11.4 CONCLUSION

It was demonstrated in this chapter that M-E PDG can be used efficiently as a pavement analysis and design tool by using strategies presented here. In the case of examples demonstrated, some specific design variables, namely HMA layer thickness, Base and subbase thicknesses and base modulus, were considered. Any other set of variables can be used instead of these as required. State highway agencies have a set of designs and materials that they use for their pavements. Once the response surfaces are developed for the variables that the state highway agency wishes to vary, the rest of the analysis and design would not take much time to conduct. Development of the original response surfaces and interpolated response surfaces and extracting distresses for design and analysis cases was done through a set of programs written in MATLAB.

It may appear that it will take much longer to get all the outputs from M-E PDG for developing response surfaces than running a few cases like the analysis examples that have been presented in section 12.2.2. However, it should be noted that the response surfaces can and should cover a very wide range of each design input variables. Therefore, once they are developed they can be used for many cases, which may vary widely in their inputs. The results are almost instantaneous unlike running M-E PDG which would take between 30 to 50 minutes to run one case. Also, there is no straightforward way to use M-E PDG for design. On the other hand, the strategy presented in section 12.3 gives simple plots for the pavement designer to pick design values for the variables considered. In addition, he/she can visually see the effect of digressing from the optimal design which would help him/her make decisions based on other constraints like material availability, equipment restraints, unexplained past anomalies in similar existing pavements etc. In other words the design strategy presented in this chapter gives optimal values of design variables for pavement which would be expected to have distresses only to acceptable threshold level at the end of design life. It should also be noted that the strategy can be used to get optimal values for other design variables as well. So, it is not restricted to use of a specific mix or specific variables only.

In summary, M-E PDG can be used for pavement analysis by running it to get distresses for specific pavement structures and materials. M-E PDG can also be used as a performance prediction tool for candidate designs in a design process. It is quite feasible to use M-E PDG directly if only a few runs are to be made either for analysis or design. However, every new case, even if only slightly different from the previous cases, would warrant a new run which takes 30 to 50 minutes for flexible pavements. The process proposed in this chapter requires some pre-work done to get pavement distresses by running M-E PDG for some specific combinations of input variable values which need to be studied in pavement analysis or are chosen as design variables. Then, interpolation techniques can be used to get distress predictions for any combination of values for those input variables without having to run M-E PDG. If the analysis or design variables are chosen wisely according to MDOT practices distress prediction can be quickly obtained for different projects through interpolation which would save valuable time. Examples presented in this chapter show how this can be achieved for pavement analysis and how this can be used for pavement design as well.

CHAPTER 12 - CONCLUSIONS – FLEXIBLE

Section III of this report is dedicated to the details of and results from the sensitivity analysis and satellite studies etc. performed for flexible pavements. Based on the analyses performed, several conclusions were made and are summarized in this chapter.

12.1 SENSITIVITY ANALYSES

The M-E PDG requires detailed information on several input variables. In order to identify the most important variables which significantly affect the performance prediction, sensitivity analyses were performed. The approach used to conduct the sensitivity analysis in this research contains: (1) one variable at a time to investigate the effect of individual input variables on performance (preliminary sensitivity analyses), and (2) full factorial design matrix to investigate the interaction effects of input variables on performance (detailed sensitivity analyses). The first task involves a preliminary analysis for each input variable to eliminate the less significant variables while the second task deals with detailed analyses including interaction between sensitive variables identified by the first task. The results from the above two tasks are presented below.

12.1.1 Preliminary Sensitivity

Considering all the factors the following list of input variables was deemed to have significant effect on flexible pavement performance. The variables have been categorized based on different layers in the pavement. Base/Subbase layers have been categorized together. However, their individual material types and thicknesses are required. So, the actual number of significant variables is more than 11 and depends on the pavement structure.

Table 12.1. Final List of selected significant input variables

Cluster	Category	Variable
Asphalt Material Properties	General	Layer thickness
		Aggregate Gradation Characteristics
	Asphalt Binder	Superpave PG Grade
	Asphalt General	Effective binder content
		Air voids
Base/Subbase	General	Unbound Material
		Thickness

Cluster	Category	Variable
Subgrade	General	Unbound Material
Thermal Cracking	Average tensile strength at 14^{o} F	
	Creep Compliance (Level 2)	
Climate	Climatic Regions	

12.1.2 Detailed Sensitivity

A reduced list of variables was prepared, based on engineering judgment, MDOT practice, and RAP feedback to decrease the number of runs within an achievable practical limit. The factorial consisted of 10 variables at two levels and the environment had three levels. This combination results in a full factorial with 192 runs ($2^6 \times 3$). The key objective for the detailed sensitivity by employing a full factorial design was to establish the statistical and the practical significance of main and interactive effects among input variables. The statistical significance was established from the results of analysis of variance (ANOVA), i.e., a *p-value* less than 0.05 (a confidence level of 95%) while the practical significance was established by comparing the mean differences between the levels of input variables and comparing them with a threshold for a particular distress at a given age.

12.1.2.1 Fatigue Cracking

Main Effects

AC Thickness: As expected, AC thickness has a significant effect on fatigue cracking. It is also notable in this case that fatigue damage is very significant from early stages in the case of thin pavements. This is primarily because such a thin structure cannot withstand heavy traffic applied in this case.

AC Aggregate Gradation: The effect of asphalt concrete aggregate gradation may not be so significant. However it should be noted that in this analysis the two levels of aggregates used did not have markedly different gradations.

AC Effective Binder Content: Effective binder content of the top AC layer has a significant impact on fatigue performance of the pavement. As would be expected pavement with higher effective binder content has less fatigue cracking. However the rate of fatigue cracking is somewhat similar after about 6 years of age.

AC Binder Grade: The two binder grades chosen for this analysis were the ones that are most commonly used in Michigan. The results show that there may be very little difference in fatigue performance of these two binder grades.

AC Air Avoids: Air voids in the top layer asphalt concrete has significant impact on fatigue performance. Lower air voids translate into a densely packed pavement layer leading to a greater fatigue resistance.

Base Thickness: The vast majority of pavements in Michigan have either 4 inch or 6 inch bases. The difference in thickness is not significant and therefore, the results also show that the difference in fatigue performance is not significant.

Base Material Type: The two types selected for the sensitivity study were the materials that are most commonly used in the state of Michigan. The results show significant impact of the material type on fatigue performance of the pavement.

Subbase Thickness: Subbase thicknesses chosen for the sensitivity analysis represent the extreme cases which would be used for Michigan pavements. There is marginal difference in the fatigue performance of pavements with 8 inch subbase as compared to those with 30 inch subbase.

Subbase Material: The two materials chosen in this study do show some difference in fatigue performance.

Subgrade Material: Subgrade layer is the farthest layer from the surface course which is directly subjected to traffic loads. The results show that the difference in fatigue performance is minimal.

Interaction Effects

Interaction effects are very important in such analysis since the main effect of one variable can be dependent on the value of one or more other variables. Interaction effects which are significant for fatigue cracking performance are listed below in order of their relative significance:

(i) AC layer thickness and AC air voids
(ii) AC layer thickness and AC effective binder content
(iii) AC layer thickness and base material
(iv) AC layer thickness and subbase material

12.1.2.2 Longitudinal Cracking

Main Effects

The pavements did not show extensive longitudinal cracking in almost all cases. Relatively speaking AC thickness and AC air voids have maximum impact on longitudinal cracking performance of the pavements. AC binder content, base, subbase and subgrade material also seem to have appreciable impact on longitudinal cracking performance. The differences in performance for the chosen ranges of AC aggregate gradation, asphalt grade, base and subbase thickness is not significant at all. However it should be noted that the two levels chosen for some of these variables were quite close to each other. Therefore, nothing conclusive can be said about these four variables in general. However, since the values chosen in the analysis was in

compliance with MDOT practices they may be categorized as not-significant for MDOT purposes.

Interaction Effects

Interaction effects which are significant for longitudinal cracking performance are listed below in order of their relative significance:

(i) AC layer thickness and AC air voids
(ii) AC layer thickness and subgrade material
(iii) AC layer thickness and base material
(iv) AC layer thickness and subbase material

12.1.2.3 Transverse Cracking

Main Effects

As would be expected binder grade has significant impact on transverse cracking performance of the pavements analyzed. AC thickness, AC binder content and AC air voids also significantly affect transverse cracking performance, although to a lesser degree than asphalt grade. Aggregate gradation of asphalt layer also has some significance in this regard but to a much lesser degree. As expected base and subbase thickness and material for these layers do not seem to affect transverse cracking performance to any significant degree. Subgrade material also does not have any affect.

Interaction Effects

Interaction effects which are significant for transverse cracking performance are listed below in order of their relative significance:

(i) Binder grade and AC air voids
(ii) Binder grade and AC aggregate gradation
(iii) Binder grade and effective binder content

12.1.2.4 Rutting

Main Effects

Rutting predictions from M-E PDG program are very high in all the cases. It has also been observed in other M-E PDG validation runs that the rutting model used in M-E PDG over-predicts rutting. However, the results do show expected trends in relative terms for various input parameters analyzed. Thickness of the asphalt layer and subgrade material combined with subgrade modulus, have maximum influence on rutting performance of the pavements studied. AC binder content, AC air voids, base and subbase material and their thicknesses also have appreciable influence on the amount of expected rutting in asphalt pavements. From the analysis it appears that asphalt layer aggregate gradation, binder grade and base thickness do not have

much influence. But it should be noted, once again, that these inputs were varied to a much smaller degree in this sensitivity analysis than other inputs.

Interaction Effects

Interaction effects which are significant for rutting performance are listed below in order of their relative significance:

(i) Subgrade material and subbase thickness
(ii) Subgrade material and asphalt layer thickness
(iii) AC layer thickness and subbase material
(iv) AC layer thickness and base material
(v) AC layer thickness and subbase thickness

12.1.2.5 IRI

Main Effects

Almost all the ten input variables being studied except for asphalt grade and base thickness have significant influence on IRI. The two levels used for asphalt grade were PG 58-22 and PG 64-34. Therefore, there was only one grade difference in the high temperature of these two grades. Base thickness was also only varied from 4 inches to 6 inches; hence, the small difference in performance.

Interaction Effects

Interaction effects which are significant for IRI performance are listed below in order of their relative significance:

(i) AC layer thickness and AC air voids
(ii) AC layer thickness and AC effective binder content
(iii) AC layer thickness and base material
(iv) AC layer thickness and subbase material
(v) AC effective binder content and base material

12.2 SATELLITE STUDIES

Several separate analyses were conducted as satellite studies; these evaluations included (a) studying the effect of thermal cracking inputs (b) studying the effects of E* and (c) verifying (at a very preliminary level) M-E PDG performance prediction for Michigan pavements. The results of analyses from these evaluations are presented briefly in the following sections.

12.2.1 Thermal Cracking Analysis

The projects analyzed in this satellite study had quite varied characteristics. The goal of this mini-study was to see how Michigan mixes are expected to perform from a thermal cracking point of view.

Almost all of the mixtures were predicted to perform very well in thermal cracking. There are only few projects which show some minimal cracking. It is significant to note that a change of air voids from 6 to 9% leads to nearly four times higher thermal cracking in most of the cases. In those cases where there was no thermal cracking with 6% air voids this difference is not visible because the mix may have much higher compliance than the threshold. Therefore, even with the higher air voids of 9% they have no thermal cracking.

It was also observed that if asphalt content in the mix is 0.5% lower than the optimal value thermal cracking increases significantly. If asphalt content is 1.0% lower than the optimal value amount of thermal cracking can be four times higher than that with optimal asphalt content.

12.2.2 Complex Modulus Satellite Study

Rutting and fatigue cracking performance were used to compare the effect of complex modulus for the various mixtures and different values of quality characteristics. At level 3 run in M-E PDG complex modulus is automatically calculated using mix characteristic like in-situ air voids, AC to dust ratio etc. In the present analysis values of these variables were varied to get difference in complex modulus and assess the effect of this change in E* on pavement performance.

Comparing the rutting levels for pavements with 9% versus 6% in-situ air voids, the ratio is quite constant and close to 1.07 in all the cases. This ratio was found to be close to 1.10 for the 10 million ESAL projects. This can be explained by the observation (from the M-E PDG output files) that most of the rutting was due to the unbound layers.

The ratio of fatigue cracking for 9% air voids to that for 6% air voids is about 4 in almost all the cases. The same ratio was observed in the case of 10 million ESALs projects as well.

The ratio of the AC moduli, i.e. for 9% versus 6%, is close to 0.8 (i.e., 20% reduction) in all the four cases studied. This shows that the complex modulus is very sensitive to in-situ air voids. Earlier it was noted that fatigue cracking was 4 times higher for mixes with 9% air voids as compared to those with 6% air voids. This can be explained by the 20% reduction in asphalt modulus. Recall from the discussion above that the same decrease in AC moduli leads to only 7 to 11 percent increase in rutting over 20 years for the same pavements. So rutting does not seem to be very sensitive to asphalt layer modulus.

12.2.3 Verification (Preliminary) of M-E PDG Performance Prediction for Michigan

The main objectives of this task were to (a) verify the M-E PDG performance predictions in Michigan, and (b) identify the suitability needs for calibration of M-E PDG performance models in Michigan. To accomplish these objectives, the LTPP SPS-1 flexible pavement sections in Michigan and selected MDOT sections were analyzed using M-E PDG software (version 1.0).

12.2.3.1 SPS-1 Sections

All the sections had none or very little longitudinal cracking. Performance predicted by the M-E PDG software is also similar except for two out of eight sections. In both of these pavement structures the asphalt concrete surface and binder layers together were only 3.6 inches and 3.9 inches thick, respectively. These two layers were constructed directly on open graded permeable asphalt treated base (PATB) layer. PATB is expected to have lower asphalt content and relatively higher air voids content. These conditions make it especially vulnerable to bottom up alligator cracking as well as longitudinal cracking. In essence even slight differences in asphalt content and air voids, therefore, would lead to vastly different performance prediction.

Table 12.2 summarizes how predicted performance compare with the observed performance for all the eight sections It is interesting that except for sections 120 and 121 longitudinal cracking, fatigue cracking and IRI match reasonably well. In the case of transverse cracking and rutting M-E PDG seems to over predict distress in most of the cases. This is consistent with what we have observed, in general, with the current version of the software.

Table 12.2. Comparison of predicted and observed asphalt pavement performance — SPS-1 Michigan Sections

Section	Longitudinal Cracking	Fatigue Cracking	Transverse Cracking	Rutting	IRI
26-0115	R	R	R	R	R
26-0116	R	R	O	O	R
26-0117	R	R	R	O	R
26-0118	R	R	R	O	R
26-0120	O	O	O	CC	U
26-0121	O	O	O	CC	O
26-0123	R	R	O	O	R
26-0124	R	R	O	O	R

R = Reasonable match between predicted and observed performance
O = Overestimate predicted performance
U = Underestimate predicted performance
CC = Can not Compare

12.2.3.2 MDOT Sections

Longitudinal cracking performance predicted by M-E PDG did not match well with that actually observed in the field on the sections being studied. The field data seems to have some anomalies like sudden rise in cracking and reduction in cracking at other times.

Fatigue performance for all the five pavement sections seems to be relatively more in agreement with those predicted by the M-E PDG software.

There is a large difference in transverse crack spacing predicted by M-E PDG software and that actually observed in the field in the case of three sections which had somewhat thinner (7.5 inches) HMA layer. The remaining two sections which had thicker HMA layer there was much better agreement between predicted and actual performance.

Unfortunately actual rutting measurements provided for these sections had very few points and they also seem to be in error. M-E PDG software predictions show that the two thicker HMA layer sections would have around 0.8 inches of rutting at the end of 20 years whereas the other three sections would have about 1.0 inch or more of rutting by that time.

In the case of IRI two sections had reasonable agreement between observed and predicted performance. Because of seeming anomalies in the observed IRI trends for the other three sections no definite conclusions could be drawn.

12.3 PAVEMENT DESIGN IMPLICATIONS

M-E PDG can be used as an efficient pavement analysis and design tool by using strategies presented in chapter 12. For the purpose of demonstration, some specific design variables, namely HMA layer thickness, base and subbase thicknesses and base modulus, were considered. Any other set of variables can be used as required. State highway agencies have a set of designs and materials that they use for their pavements. Once the response surfaces are developed for the variables that the state highway agency is interested in, the rest of the analysis and design would not take much time.

It may appear that it will take much longer to get all the outputs from M-E PDG for developing response surfaces than running a few cases like the analysis examples that have been presented in section 12.2.2. However, it should be noted that the response surfaces can and should cover a very wide range for each design input variable. Therefore, once they are developed they can be used for many cases, and these may vary widely in their inputs. Results are almost instantaneous unlike running M-E PDG which would take between 30 to 50 minutes to run for one case. Also, there is no straightforward way to use M-E PDG for design. In contrast, the strategy presented in section 12.3 gives simple plots for the pavement designer to pick design variable values from. In addition, he/she can visually see the effect of digressing from the optimal design which would help him/her make decisions based on other constraints like material availability, equipment restraints, unexplained past anomalies in similar existing pavements etc.

CHAPTER 13 - RECOMMENDATIONS

This chapter highlights the needs and the potential benefits of implementing the M-E PDG in Michigan. A systematic approach for the implementation of the M-E PDG along with the required resources to accomplish a successful adoption is also discussed. Finally, recommendations are made for future research to support a full adoption of the new design process in Michigan.

13.1 THE 1993 AASHTO GUIDE VERSUS THE M-E PDG DESIGN PROCESS

There are several important operational differences between 1993 AASHTO and M-E PDG procedures. As mentioned in the introduction chapter, the most important differences include:

- The 1993 AASHTO guide designs pavements to a single performance criterion, PSI, while the M-E PDG approach simultaneously considers multiple performance criteria (e.g., rutting, cracking, and roughness for flexible pavements). Appropriate design limits must be specified for each performance measure.
- The list of input variables required in the M-E PDG procedure is extensive, especially environmental, and material properties. It also employs a hierarchical input quality levels, depending upon the level of information, resources available, and the importance of the project.
- The 1993 AASHTO guide incorporates strength-related material variables; interaction between environment- and material-related variables is not addressed directly. The AASHTO guide was developed based on limited field test data from only one location (Ottawa, IL). Seasonal adjustment of subgrade resilient modulus and selection of appropriate layer drainage coefficients are the only ways of incorporating environmental influences on pavement deterioration. The M-E PDG procedure utilizes a set of project-specific climate data (i.e., air temperature, precipitation, wind speed, relative humidity, etc.) and the Enhanced Integrated Climate Model (EICM) to determine the material properties for different environmental condition throughout the year (i.e., temperature-adjusted asphalt concrete dynamic modulus and moisture-adjusted resilient modulus of unbound materials).
- The 1993 AASHTO guide uses the concept of equivalent single axle load (ESAL) to define traffic levels, while the M-E PDG approach uses traffic in terms of axle load spectra.
- The 1993 AASHTO design procedure outputs pavement layer thicknesses given the loss in serviceability, traffic, and subgrade modulus. The M-E PDG analysis procedure yields predicted performance (cracking, rutting, faulting and IRI) for a given pavement cross-section depending on pavement type.

All of these differences between the design procedures make a direct comparison more intricate. Most of the evaluations of the M-E PDG procedure to date have focused on sensitivity studies and tests of “engineering reasonableness.” However, direct comparisons

are essential to gain confidence in the newer mechanistic-empirical approach as a potential replacement for the existing empirical procedure. At the very least, the mechanistic-empirical approach should give designs and/or predicted performance that are broadly similar to those from the 1993 AASHTO Guide for "standard" types of design scenarios.

13.2 NEED FOR ADOPTING THE M-E PDG DESIGN PROCESS

There are several justifications and benefits for adopting the new design process, some important ones are mentioned below:

- The M-E PDG analysis and design process is based on a systems approach. The design process in this approach integrates materials properties, climatic variables, traffic inputs, and cross-section design to expected pavement performance.
- The integration of various inputs to expected performance is helpful in connecting construction practices to pavement performance. Combining material and construction variability with structural design allows for quantifying these effects on pavement performance. This can be useful in the context of performance-based specifications and in directly assessing the design reliability.
- A rational performance prediction can assist in improved planning for future maintenance and rehabilitation needs. This information is useful in performing a more authenticated life cycle cost analysis (LCCA) for making decisions by comparing different available alternatives.

13.3 ADOPTION OF THE M-E PDG IN MICHIGAN

Considering the required resources and current practice, it is recommended that MDOT may adopt the M-E PDG design procedure in two stages: (a) short-term adoption, and (b) long-term implementation. In short-term MDOT may use the M-E PDG as evaluation tool while in future, when certain important requirements are met, a full implementation should be adopted.

13.3.1 Short-term Plan

Currently MDOT's practice involves using the 1993 AASHTO pavement design guide for designing new pavements. It is recommended that in the short-term, the pavement thickness designed by the AASHTO guide may be verified using current version of the M-E PDG. This verification will certainly help MDOT designers in gaining more confidence in the new design procedure. The most influential variables, as identified in this study, can be reasonably estimated at various input levels considering the on-going research efforts at MDOT. Several research projects related to determination of material properties and traffic characterization in the state of Michigan have been completed or are in progress. These studies will help MDOT in obtaining several input variables at the highest input level for the M-E PDG adoption. These studies include:

1. Quantifying coefficient of thermal expansion (CTE) values of typical hydraulic cement concrete paving mixtures in Michigan (Completed in 2008)

2. Characterization of traffic for the new M-E pavement design guide in Michigan (On-going, expected to complete in 2009)
3. Pavement subgrade MR design values for Michigan's seasonal changes (On-going, expected to complete in 2009)
4. Resilient modulus at the limits of gradation and varying degrees of saturation (Completed in 2007)
5. Backcalculation of resilient modulus values for unbound pavement materials in Michigan (Staring in November, 2008)

While a crucial question regarding the rationale of current performance models in the M-E PDG can be raised, these models can provide a reasonable prediction in the present form.

13.3.2 Long-term Plan

In anticipation of current limitations of the performance models with regards to the observed field pavement performance, it is strongly recommended that the performance models should be validated for Michigan. If the need is felt, the models need to be calibrated for the local conditions, construction practices and frequently observed distresses. Once the models are validated and calibrated, MDOT should adopt the M-E PDG in its full spirit.

13.4 RECOMMENDATIONS FOR THE FUTURE RESEARCH

The calibration and validation of M-E PDG performance models were achieved by utilizing the pavements sections in the LTPP database. These test sections are distributed geographically all over the US. Thus, the coefficients in the current form are termed as "National" calibration coefficients. In addition, the current calibration of performance models may not reflect the local construction materials and practices, climate and subsequent manifestation of the common distress types despite the mechanistic aspects of the guide.

Several states have found that current calibrated distress prediction models do not validate with their pavement behavior. Although recently, the M-E PDG models for rigid pavements were recalibrated using additional and more recent data from the LTPP, an objective and more practical review of the prediction models in M-E PDG revealed several important aspects which will help the states to customize the distress prediction models to their local needs using local experience. For example, in Michigan, the following aspects need attention while considering the local calibration of JPCP distress models to reflect the local requirements:

- The negative temperature gradients cause curling stresses to produce top-down cracking. The effect of permanent curling that occurs during concrete hardening, and the curling resulting from climatic changes during the pavement service life. These combined effects produce a critical tensile stress and the influence of creep during the initial hardening stage should be considered in Michigan.
- The M-E PDG recommends using a value of −10°F for the effective temperature to determine permanent curl/warp. However, this value is affected by time of placement,

joint spacing, and load transfer at joints and base/slab interface conditions, some of which cannot be predicted at the design stage.
- The cracking model for JPCP assumes that shrinkage warping can be accounted for by use of an equivalent negative temperature profile that produces a concave upward curling of the slab. In Michigan, the interaction of this type of built-in curling, typical joint spacing (15-ft) and specific axle configuration seems to be critical in determining the expected cracking of JPCP.

In general, to locally calibrate M-E PDG performance models for rigid and flexible pavements in Michigan, the following is recommended:

- Calibration process should involve a wide spectrum of pavements within the state. The pavement sections with outlying performance should not be included in the database for calibration. However, the determination of unusual performance should be based on sound engineering judgment coupled with local experience.
- The selection of test sections should be based on sound experiment design considering several important attributes affecting pavement performance. For example, slab thickness, traffic, CTE, negative gradient to address built-in curling and concrete strength, etc. In addition, any particular construction practice should be included in the test matrix.
- The use of PMS performance data may include distress measurement variability which is another source of error in addition to model error. There is a need to quantify such errors in the calibration process to improve model predictions.
- The current rutting model predicts permanent deformation in all pavement layers (HMA, base, subbase, and subgrade). However, it was observed that about 80% of the total predicted surface rutting is attributed to the lower pavement layers. In general, the total surface rutting is over-predicted for pavements in Michigan. Thus, the M-E PDG models to account for rutting in lower layers specifically needs local calibration to represent Michigan materials and climate.
- The longitudinal cracking prediction for flexible pavements should be used with caution. This is because the assumptions used in the model remain unsubstantiated.
- The HMA mixtures used in Michigan needs to be characterized using fundamental mechanical testing such as E*, creep compliance and tensile strength. These inputs have significant influence on predicted fatigue and thermal cracking.
- Another very important but mostly ignored aspect for empirical modeling is the compromise between bias and prediction variability. Bias represents a systematic error in the model prediction; therefore, it is crucial to minimize the model bias while keeping the variance within acceptable limits. Several modern statistical techniques, such as bootstrapping and jackknifing, based on random sampling from a sample can be used to validate and improve the empirical models.

REFERENCES

1. NCHRP[1-37], "Guide for Mechanistic-Empirical Design of New and Rehabilitated Pavement structures," National Cooperative Research Program (NCHRP), Washington D.C Final Report, 2004.
2. Carvalho, R. L. and C. W. Schwartz, "Comparisons of Flexible Pavement Designs: AASHTO Empirical vs. NCHRP 1-37A Mechanistic-Empirical," *Transportation Research Record, CD-ROM*, 2006.
3. Galal, K. A. and G. R. Chehab, "Consideration for Implementing the 2002 M-E Design Guide Procedure Using a HMA Rehabilitation Pavement Section in Indiana," *Transportation Research Record, CD-ROM*, 2005.
4. Guclu, A. and H. Ceylan, "Sensitivity Analysis of Rigid Pavement Systems Using Mechanistic-Empirical Pavement Design Guide," presented at Proceedings of the 2005 Mid-Continent Transportation Research Symposium, Ames, Iowa, 2005, pp.
5. Hall, K. D. and S. Beam, "Estimation of the Sensitivity of Design Input Variables For Rigid Pavement Analysis Using the Mechanistic-Empirical Design Guide," *Transportation Research Record, CD-ROM*, 2005.
6. Kannekanti, V. and J. Harvey, "Sensitivity Analysis of 2002 Design Guide Rigid Pavement Distress Prediction Models," Pavement Research Center, University of California, Davis, University of California, Berkeley 2005.
7. Khanum, T., M. Hossain, S. A. Romanoschi, and R. Barezinsky, "Concrete Pavement Design in Kansas Following the Mechanistic-Empirical Pavement Design Guide," presented at Proceedings of the 2005 Mid-Continent Transportation Research Symposium, Ames, Iowa, , 2005, pp.
8. Uzan, J., T. J. Freeman, and G. S. Cleveland, "Development of a Strategic Plan for Implementation of the NCHRP 1-37A Pavement Design Guide for TxDOT Operations," *Transportation Research Record CD-ROM*, 2005.
9. Nantung, T., G. Chehab, S. Newbolds, K. Galal, S. Li, and D. H. Kim, "Implementation Initiatives of the Mechanistic-Empirical Pavement Design Guides in Indiana," *Transportation Research Record 2005 CD-ROM*, 2005.
10. Tran, N. H. and K. D. Hall, "Development and Significance of Statewide Volume Adjustment Factors om Mechanistic-Empirical Pavement Design Guide," *Transportation Research Record (2037)*, pp. 97-105, 2007.
11. Tran, N. H. and K. D. Hall, "Development and Influence of Statewide Axle Load Spectra on Flexible Pavement Performance," *Transportation Research Record (2037)*, pp. 160-114, 2007.
12. Kim, S. and H. Ceylan, "Sensitivity Study of Design Input Parameters for Two Flexible Pavement Systems Using Mechanistic-Empirical Pavement Design Guide," presented at Proceedings of the 2005 Mid-Continent Transportation Research Symposium, Ames, Iowa, , 2005, pp.

13. Kim, S., H. Ceylan, K. Gopalakrishnan, and M. Heitzman, "Sensitivity Study of Iowa Flexible Pavements Using the Mechanistic-Empirical Pavement Design Guide," *Transportation Research Record, CD-ROM*, 2006.

14. Zeghal, M., Y. E. Adam, O. Ali, and E. H. Mohamed, "Review of the new mechanistic-empirical pavement design guide – a material characterization perspective," presented at TAC Annual Conference, Calgary, Alberta, 2005, pp. 1-18.

15. Beam, S., "2002 Pavement Design Guide-Design Input Evaluation: JCP Pavements," Department of Civil Engineering, University of Arkansas, 2003.

16. Pomerantz, M., B. Pon, H. Akbari, and S.-C. Chang, "The Effect of Pavements' Temperatures on Air Temperatures in Large Cities," Heat Island Group, Lawrence Berkeley National Laboratory, Berkeley, CA 94720 2000.

17. Kannekanti, V. and J. Harvey, "Sensitivity Analysis of 2002 Design Guide JPCP Distress Prediction Models," *Transportation Research Record , CD-ROM*, 2006.

18. Khazanovich, L., D. M, B. R, and M. T, "Common Characteristics of Good and Poorly Performing PCC Pavements," Federal Highway Administration, FHWA-RD-97-131, 1998.

19. Rauhut, J. B., A. Eltahan, and A. L. Simpson, "Common Characteristics of Good and Poorly Performing AC Pavements," Federal Highway Administration, FHWA-RD-99-193, December 1999.

20. Hanna, A. N., S. D. Tayabji., and J. S. Miller, "SHRP-LTPP Specific Pavement Studies: Five-Year Report," Strategic Highway Research Program, National Research Council, SHRP-P-395, April 1994.

21. Haider, S. W., K. Chatti, N. Buch, R. W. Lyles, A. Pulipaka, and D. Gilliland, "Statistical Analysis of In-Service Pavement Performance Data for LTPP SPS-1 and SPS-2 Experiments,," *ASCE Journal of Transportation Engineering* vol. 133 (6), pp. 378-388, 2006.

22. SHRP, "Specific Pavement Studies Experimental Design and Research Plan for Experiment SPS-2, Strategic Study of Structural Factors for Rigid Pavements," National Research Council, Washington DC. April 1990.

23. Hansen, W., D. Smiley, Y. Peng, and E. A. Jensen, "Validating Top-Down Premature Transverse Slab Cracking in Jointed Plain Concrete Pavement (JPCP)," *Transportation Research Record, CD-ROM*, 2002.

24. NCHRP Project 1-37A, "Guide for Mechanistic-Empirical Design of New and Rehabilitated Pavement structures," National Cooperative Research Program (NCHRP), Washington D.C. Final Report, 2004.

25. NCHRP Project 1-40B, "User Manual and Local Calibration Guide for the Mechanistic-Empirical Pavement Design Guide and Software " NCHRP In Progress, 2007.

26. Quintus, H. V., C. Schwartz, R. H. McCuen, and D. Andrei, "Refine Model Calibration and Validation of Hot Mix Asphalt Performance Models: An Experiment Plan and Database," NCHRP Research Results Digest 284, 2003.

27. Quintus, H. V., C. Schwartz, R. H. McCuen, and D. Andrei, "Jackknife Testing - An Experiment Approach to Refine Model Calibration and Validation," NCHRP Research Results Digest 283, 2003.

28. Ceylan, H., K. Gopalakrishnan, and B. Coree, "A Strategic Plan for Implementing the Mechanistic-Empirical Pavement Design Guide in Iowa," *Transportation Research Record, CD-ROM*, 2006.

29. Li, J., S. T. Muench, J. P. Mahoney, and N. Sivaneswaran, "Calibration of the Rigid Pavement Portion of the NCHRP 1-37A Software for Use by the Washington State Department of Transportation," *Transportation Research Record, CD-ROM*, 2006.

30. Schram, S. and M. Abdelrahman, "Improving Prediction Accuracy in the Mechanistic-Empirical Pavement Design Guide," *Transportation Research Record, CD-ROM*, 2006.

31. Gramajo, C. R., G. W. Flintsch, and A. Loulizi, "Verification of Mechanistic-Empirical Pavement Deterioration Models Based on Field Evaluation of In-service High-priority Pavements," *Transportation Research Record, CD-ROM*, 2007.

32. Darter, M. M., J. Mallela, L. Titus-Glover, C. Rao, G. Larson, A. Gotlif, H. V. Quintus, L. Kazanovich, M. Witczak, M. El-Basyouny, S. El-Badawy, A. Zborowski, and C. Zapata, "Changes to the Mechanistic-Empirical Pavement Design Guide Software Through Version 0.900," NCHRP Research Results Digest 308, 2006.

33. Thompson, M., E. Barenberg, S. Brown, M. M. Darter, G. Larson, M. Witczak, and M. El-Basyouny, "Independent Review of the Mechanistic-Empirical Pavement Design Guide and Software," NCHRP Research Results Digest 307, September 2006.

34. Schwartz, C. W., "Implications of Distress Measurement Uncertainty for M-E Performance Model Calibration," *Transportation Research Record, CD-ROM*, 2007.

35. FHWA, "HPMS Key Inputs with a Moderate to High Influence on M-E PDG Predicted Distress/IRI," Office of Policy, Federal Highway Administration, Washington, D.C. Technical Memorandum #6, August 29 2006.

36. NCHRP Project 1-37A, "Appendix PP: Smoothness Prediction for Rigid Pavements," ARA, inc., ERES division, 505 west University Avenue, Champaign, Illinois 61820, 2004 Final Report: Guide for Mechanistic-Empirical Design of New and Rehabilitated Pavement Structures, 2001.

37. NCHRP Project 1-37A, "Appendix KK: Transverse Cracking of JPCP," ARA, inc., ERES division, 505 west University Avenue, Champaign, Illinois 61820, 2004 Final Report: Guide for Mechanistic-Empirical Design of New and Rehabilitated Pavement Structures, 2003.

38. NCHRP Project 1-37A, "Appendix JJ: Transverse Joint Faulting Model," ARA, inc., ERES division, 505 west University Avenue, Champaign, Illinois 61820, 2004 Final Report: Guide for Mechanistic-Empirical Design of New and Rehabilitated Pavement Structures, 2003.

39. NCHRP Project 1-37A, "Guide for Mechanistic-Empirical Design of New and Rehabilitated Pavement structures," National Cooperative Research Program (NCHRP), Washington D.C. Final Report, 2004.

40. FHWA, "Development of Simplified Rigid Pavement Performance Models Using M-E PDG for HERS/NAPCOM," Office of Policy, Federal Highway Administration, Washington, D.C. Technical Memorandum, May 15 2007.

41. FHWA, "Development of Procedures and Criteria for Evaluating Pavement Asset Management Systems for Use in HERS," Office of Policy, Federal Highway Administration, Washington, D.C. Technical Memorandum #2, March 11 2004.

42. FHWA, "Pavement Performance Model Needs For Highway Policy Analysis and Cost Allocation (HERS & HCAS)," Office of Policy, Federal Highway Administration, Washington, D.C. Technical Memorandum #1, March 11 2004.

43. FHWA, "State Pavement Management Survey," Office of Policy, Federal Highway Administration, Washington, D.C. Technical Memorandum #3, March 11 2004.

44. FHWA, "Technical Review of Pavement Models used in Software Program for Highway Cost Allocation," Office of Policy, Federal Highway Administration, Washington, D.C. Technical Memorandum #4, May 2004.

45. FHWA, "Data Requirements for Implementing the New M-E PDG Pavement Performance Prediction Models in HERS and NAPCOM," Office of Policy, Federal Highway Administration, Washington, D.C. Technical Memorandum #5, February 10 2006.

46. FHWA, "Implementing the M-E PDG Pavement Models Developed Under NCHRP Project 1-37A into HERS AND NAPCOM," Office of Policy, Federal Highway Administration, Washington, D.C. Technical Memorandum #7, February 17 2006.

47. Huang, Y. H., *Pavement Analysis and Design*, 2nd ed. Upper Saddle River, NJ 07458: Pearson Prentice Hall, 2004.

48. Deacon, J. A., "Load Equivalency in Flexible Pavements," *Proceedings of the Association of Asphalt Paving Technologists*, vol. 38, pp. 465-494, 1969.

49. Carey Jr., W. N. and P. E. Irick, "The pavement Serviceability-Performance Concept," *Highway Research Board*, vol. Bulletin 250, pp. 40-58, 1960.

50. Deacon, J. A. and R. C. Deen, "Equivalent Axle Loads for Pavement Design," *Highway Research Record*, vol. 291, pp. 133-143, 1969.

51. Huang, Y. H., "Computation of Equivalent Single-Wheel Loads using Layered Theory," *Highway Research Record*, vol. 291, pp. 144-155, 1969.

52. Ioannides, A. M., R. K. Karanth, and K. Sanjeevirao, "Mechanistic-Empirical Approach to Assessing Relative Pavement Damage," *Transportation Research Record*, vol. 1639, pp. 112-119, 1998.

53. AASHTO, "AASHTO Guide for Design of Pavement Structures," American Association of State Highway and Transportation Officials, Washington, D.C. 1993.

54. NCHRP Project 1-37A, "Appendix AA: Traffic Loading," ARA, inc., ERES division, 505 west University Avenue, Champaign, Illinois 61820, 2004 Final Report: Guide for Mechanistic-Empirical Design of New and Rehabilitated Pavement Structures, 2004.

55. Haider, S. W. and R. S. Harichandran, "Characterizing Axle Load Spectra by Using Gross Vehicle Weights and Truck Traffic Volumes," *CD ROM, 86th Annual Meeting of Transportation Research Record*, 2007.

56. Hong, F., F. M. Pereira, and J. A. Prozzi, "Comparison of Equivalent Single Axle Loads from Empirical and Mechanistic-Empirical Approaches," *CD ROM 85th Annual Meeting Transportation Research Record*, 2006.

57. Prozzi, J. A., F. Hong, and J. Leidy, "Optimum Statistical Characterization of WIM Data Based on Pavement Impact," *CD ROM 85th Annual Meeting Transportation Research Record*, 2006.

58. Timm, D. H., S. M. Tisdale, and R. E. Turochy, "Axle Load Spectra Characterization by Mixed Distribution Modeling," *ASCE Journal of Transportation Engineering* vol. 131, pp. 83-88, 2005.

59. Mohammadi, J. and N. Shah, "Statistical Evaluation of Truck Overloads," *ASCE Journal of Transportation Engineering* vol. 118, pp. 651-665, 1992.

60. Haider, S. W. and R. S. Harichandran, "Quantifying the Effects of Truck Weights on Axle Load Spectra of Single and Tandem Axle Configurations," presented at the Fifth International Conference on Maintenance and Rehabilitation of Pavements and Technological Control, Park City, Utah, USA, 2007, pp. 73-78.

61. Haider, S. W. and R. S. Harichandran, "Relating Axle Load Spectra to Truck Gross Vehicle Weights and Volumes," *ASCE Journal of Transportation Engineering*, vol. 133, pp. 696-705, 2007.

62. Haider, S. W., R. S. Harichandran, and M. B. Dwaikat, "Estimating Bimodal Distribution Parameters and Traffic Levels from Axle Load Spectra," *CD ROM, 87th Annual Meeting of Transportation Research Record*, 2008.